A study of the global effects of Apolipoprotein E using lipidomics.

Jade Hawksworth

A thesis submitted to Cardiff University in accordance with the requirements for the degree of

DOCTOR OF PHILOSOPHY

Systems Immunity Research Institute

School of Medicine

Cardiff University

March 2019

STATEMENT 1 This thesis is being submitted in partial fulfilment of the requirements for the degree of PhD

Signed _____ Date _____

STATEMENT 2 This work has not been submitted in substance for any other degree or award at this or any other university or place of learning, nor is it being submitted concurrently for any other degree or award (outside of any formal collaboration agreement between the University and a partner organisation)

Signed _____ Date _____

STATEMENT 3 I hereby give consent for my thesis, if accepted, to be available in the University's Open Access repository (or, where approved, to be available in the University's library and for inter-library loan), and for the title and summary to be made available to outside organisations, subject to the expiry of a University-approved bar on access if applicable.

Signed _____ Date _____

DECLARATION This thesis is the result of my own independent work, except where otherwise stated, and the views expressed are my own. Other sources are acknowledged by explicit references. The thesis has not been edited by a third party beyond what is permitted by Cardiff University's Use of Third Party Editors by Research Degree Students Procedure.

Signed _____ Date _____

WORD COUNT 46,387

(Excluding summary, acknowledgements, declarations, contents pages, appendices, tables, diagrams and figures, references, bibliography, footnotes and endnotes)

Acknowledgements

First and foremost, thank you to my supervisor, Professor Valerie O'Donnell for all of your support and wisdom over the last four years. I have enjoyed working for you very much. Thank you to Professor Julie Williams, my co-supervisor, for all of your help. I am grateful to everyone in the Cardiff Lipidomics Group for their good company, advice and the occasional shoulder to cry on. I will miss you all very much!

I am grateful to my funding body, the European Research Council, who made this work and my further study possible. Also, Professor Steve E. Humphries, Jackie Cooper, Jacquie Mitchell and the Northwick Park Heart Study II for access to precious *APOE* homozygote plasma samples. Professor Mark Goode and his lovely lab in Biosciences supported me through the data collection in Chapter 7.

Thank you to everyone in Cardiff who made it such a great four years, and especially Javier, who brought joy to us all. Thanks to Tolu, Dimple, Salma, Kate, Natalie and Becki, for being such wonderful and supportive friends, despite time and distance. Paul, I appreciate you so much. Thanks for everything over the last year, I hope we have many more together. I am very grateful to my wonderful parents, brother and grandma for supporting me through this process. I would not have finished (or even started) without you. Lastly, thank you to my wonderful uncle Andrew Hawksworth, who taught me to love nature, and who is sorely missed.

Published works

O'Connor, A., Brasher, C. J., Slatter, D. A., Meckelmann, S. W., Hawksworth, J. I., Allen, S. M. and O'Donnell, V. B. (2017) 'LipidFinder: A computational workflow for discovery of lipids identifies eicosanoid-phosphoinositides in platelets', JCI Insight, 2(7), e91634.

Fahy, E., Alvarez-Jarreta, J., Brasher, C. J., Nguyen, A., Hawksworth, J. I., Rodrigues, P., Meckelmann, S., Allen, S. M. and O'Donnell, V. B. (2018) 'LipidFinder on LIPID MAPS: peak filtering, MS searching and statistical analysis for lipidomics', Bioinformatics.

Meckelmann*, S.W., Hawksworth*, J.I., White, D., Andrews, R., Rodrigues, P., O`Connor, A., Brasher, C.J., Alvarez-Jarreta, J., Tyrrell, V.J., Hinz, C., Slatter, D.A., Allen, S., Acharya, J., Mitchell, J., Cooper, J., Aoki, J., Kano, K., Humphries, S.E. and O`Donnell, V.B. The lysophospholipid/autotaxin axis is dysregulated in Chromosome 9p21 gene variant (rs10757274), but not other cardiovascular risk modifying SNPs. *Under submission.*

Contents

List of Figures **Page**

List of tables

List of Abbreviations

-d(number)	Number of deuterium atoms attached to lipid
11-dehydro TxB2-d4	11-dehydro thromboxane B2-d4
3D	three-dimensional
3xTG mouse	Triple transgenic mouse model of Alzheimer's disease, with mutations on the *APP*, *Psen1* and *Mapt* genes
4ME 16:0 Diether PE	1,2-di-O-phytanyl-sn-glycero-3-phosphoethanolamine
AA	arachidonic acid
ABCA1	ATP-binding cassette transporter 1
ACN	acetonitrile
AD	Alzheimer's disease
ADAS-Cog	Alzheimer's Disease Assessment Scale Cognitive subscale
ADCS-CGIC	Alzheimer's Disease Cooperative Study Clinical Global Impression of Change
AICD	amyloid precursor protein intracellular domain
ALOX12/15	human 12/15 lipoxygenase gene
Alox12/15	murine 12/15 lipoxygenase gene
amu	atomic mass units
APOE	human apolipoprotein E
ApoE	murine apolipoprotein E
APP	amyloid precursor protein
Aβ	amyloid-beta
BACE1	beta-secretase 1
BBB	blood brain barrier
BH critical value	Benjamini-Hochberg critical value
BHT	butylated hydroxytoluene
CE	cholesteryl ester
CNS	central nervous system
cps	counts per second
CSF	cerebrospinal fluid

CVD	cardiovascular disease
CXP	collision cell exit potential
Da	Daltons
DAG	diacylglyceride
DHA	docosahexaenoic acid
DMPC	1,2-dimyristoylglycero-3-phosphocholine
DMPE	1,2-dimyristoylglycero-3-phosphoethanolamine
DTPA	diethylenetriaminepentaacetic acid
EDTA	ethylenediaminetetraacetic acid
EOAD	early-onset Alzheimer's disease
ESI	electrospray ionisation
FC	fold change
FDR	false discovery rate
GC-MS	gas chromatography – mass spectrometry
GL	glycerolipid
hAPP	human APP
HDL	high density lipoprotein
HDOHE	hydroxydocosahexaenoic
HETE	hydroxyleicosatetraenoic acid
hexCer	hexylceramide
HODE	hydroxyoctadecadienoic acid
HPETE	hydroperoxyeicosatetraenoic acid
i	rank in Benjamini-Hochberg correction
ID	identity
IPA	isopropanol
LC-MS	liquid chromatography-mass spectrometry
LC-MS/MS	liquid chromatography-mass spectrometry/mass spectrometry
LDL	low density lipoprotein
LDLR	low density lipoprotein receptor
LOAD	late onset Alzheimer's disease

LOX	lipoxygenase enzyme
LPC	lysophosphatidylcholine
LPE	lysophosphatidylethanolamine
LRP	lipoprotein receptor-related protein
LTP	long term potentiation
m	total number of lipids in Benjamini-Hochberg correction
MAG	monoacylglyceride
MAP2	microtubule-associated protein 2
MCI	mild cognitive impairment
MCT	medium chain triglyceride
MeOH	methanol
MMSE	mini mental state exam
MS	mass spectrometry
MWM	Morris Water Maze
N2A cell	murine neuroblastoma cell line
NPHSII	Northwick Park Heart Study II
oxPL	oxidised phospholipid
PBS	phosphate buffered saline
PC	phosphatidylcholine
PC	principal component
PCA	principal component analysis
PE	phosphatidylethanolamine
PGE2-d4	prostaglandin E2-d4
PHF	paired helical filaments
PI	phosphatidylinositol
PL	phospholipid
PLS-DA	partial least squares-discrimination analysis
PPP	platelet-poor-plasma
PR	Prenol lipids
PS	phosphatidylserine
PSEN1/2	presenilin-1 or 2

p-tau	phosphorylated tau
Q	false discovery rate in Benjamini-Hochberg correction
QC	quality control
ROC	receiver operating characteristics
RSD	relative standard deviation
RT	RT
SD	standard deviation
SL	Sterol lipids
SMpc	sphingomyelin
SP	sphingolipids
TAG	triacylglyceride
Tg2576	APP mutant mouse model of Alzheimer's disease
TIC	total ion count
TREM2	triggering receptor expressed on myeloid cells 2
TxB2-d4	thromboxane B2-d4

Abstract

Apolipoprotein E (*APOE*) has been widely studied, as common gene variants can predispose towards a range of conditions, including late-onset Alzheimer's disease (LOAD). The rarest variant, *APOE* ε2, lowers risk of LOAD, whilst *APOE* ε4 raises the risk of developing this disorder. *APOE* ε3, which is the most common variant, does not alter risk of LOAD. Plasma from human homozygotes for all 3 common *APOE* alleles (described herein as *APOE 22*, *APOE 33* and *APOE 44*) was analysed using lipidomics for the first time. Initial method optimisation and testing of methods investigated extraction efficiency, which is the recovery efficiency of the total lipid in the sample. Also, coefficient of variation (CV) was tested, which is variation within the method of measurement when identical samples are injected. Optimisation demonstrates that extraction efficiency is high and CV low, and both are in accordance with other publications.

In the first experiment, LC-MS analysis of plasma from *APOE* homozygotes revealed sphingolipids and glycerophospholipids are reduced in *APOE 22*, both before and after Benjamini-Hochberg (BH) correction. Multivariant analysis can separate *APOE 22* plasma from *APOE 33* . There are very few differences between *APOE 44* plasma and *APOE 33*, and BH correction removes all significant differences between alleles. Multivariate analysis can separate both *APOE 22* and *APOE 44* from *APOE 33* plasma. Targeted LC-MS/MS analysis of cholesterol and select cholesterol ester and triacylglycerol species demonstrates few species which differ between the alleles. Unexpectedly, some cholesterol esters are higher in *APOE* 33 participants, however, total cholesterol was also unexpectedly high in this group.

In a second experiment, the effect of *ApoE* and 12/15-lipoxygenase (12/15-LOX) deficiency (*ApoE*$^{-/-}$ and *Alox12/15*$^{-/-}$, respectively) was tested in two behavioural models, the "novel object test" and the "object-in-place test". The "novel object test" measures recognition memory, which is the ability to distinguish a novel object from a known object. The "object-

in-place test" measures recollection memory, which is a test of spatial memory. *ApoE*$^{-/-}$ is not associated with a deficit in recognition memory but does cause impairment of recollection memory, as measured by the above tests. In line with previous research, these data indicate that ApoE supports recollection memory. A protective effect of 12/15-LOX inhibition has been observed in mouse models of Alzheimer's disease, however, variability in the *ApoE*$^{-/-}$*/Alox12/15*$^{-/-}$ double knock out mouse data prevents any conclusions being drawn about this group. Some 12/15-LOX esterified products are significantly higher in the *ApoE*$^{-/-}$ mice, and these may correlate with recollection memory. Further experiments are needed to confirm this finding.

Chapter 1: Introduction

1.1 An introduction to lipidomics

Lipids are a large and diverse group of hydrophobic molecules, which are highly conserved between species (Fahy et al., 2005, Khrameeva et al., 2018). Lipids play a wide range of biological roles, but are less well characterised than either genes or proteins (Lander et al., 2001, Kim et al., 2014). The lipidome is therefore the sum of all lipids contained within a tissue or cell. The lipidome varies across tissue or cell types, and between subjects (Sales et al., 2016, Slatter et al., 2016, Pradas et al., 2018, Grzybek et al., 2019, Leuthold et al., 2017, Wood and Woltjer, 2018, Ishikawa et al., 2014). Lipid metabolism is tightly regulated, and many lipids are conserved across species, due to their functional roles in homeostasis (Drin, 2014, Khrameeva et al., 2018).

Lipidomics is the study of all of the lipidome, commonly coupling analytical chemistry and mass spectrometry to separate and identify lipids (Yang and Han, 2016). Lipidomics is distinguished from lipid measurements such as total cholesterol or total triglycerides by (i) the separation of lipids, (ii) the identification of individual species and (iii) the techniques used.

1.1.1 LIPID MAPS lipid classification system

In this thesis, I used the LIPID MAPS lipid classification system (Fahy et al., 2005, Fahy et al., 2009), which describes 8 lipid categories, each of which is divided into lipid classes and subclasses (Table 1.1). Lipids are defined as small molecules, which are soluble in nonpolar solvents and which may be amphipathic or hydrophobic (McNaught and Wilkinson, 1997, Fahy et al., 2009). Throughout this thesis, I have categorised lipids according to LIPID MAPS categories, which build upon previous guidelines, and are assigned according to lipid backbone, fatty acyl groups and presence of functional groups (Fahy et al., 2005, 1978). Each category contains several classes and subclasses of lipid. Below are brief descriptions of each

Lipid categories in the LIPID MAPS lipid classification system

Category (abbreviation)	Classes (abbreviation)
Fatty acyls (FA)	Fatty Acids and Conjugates Octadecanoids Eicosanoids Docosanoids Fatty alcohols Fatty aldehydes Fatty esters Fatty amides Fatty nitriles Fatty ethers Hydrocarbons Oxygenated hydrocarbons Fatty acyl glycosides Other Fatty Acyls
Glycerolipids (GL)	Monoradylglycerols (MAG) Diradylglycerols (DAG) Triradylglycerols (TAG) Glycosylmonoradylglycerols Glycosyldiradylglycerols Other Glycerolipids
Glycerophospholipids (GP)	Glycerophosphocholines (PC) Glycerophosphoethanolamines (PE) Glycerophosphoserines (PS) Glycerophosphoglycerols (PG) Glycerophosphoglycerophosphates Glycerophosphoinositols (PI) Glycerophosphoinositol monophosphates Glycerophosphoinositol bisphosphates Glycerophosphoinositol trisphosphates Glycerophosphates Glyceropyrophosphates Glycerophosphoglycerophosphoglycerols CDP-Glycerols Glycosylglycerophospholipids Glycerophosphoinositolglycans Glycerophosphonocholines Glycerophosphonoethanolamines Di-glycerol tetraether phospholipids (caldarchaeols) Glycerol-nonitol tetraether phospholipids Oxidized glycerophospholipids Other Glycerophospholipids
Prenol lipids (PR)	Isoprenoids Quinones and hydroquinones Polyprenols Hopanoids Other Prenol lipids
Sphingolipids (SP)	Sphingoid bases Ceramides Phosphosphingolipids Phosphonosphingolipids Neutral glycosphingolipids Acidic glycosphingolipids Basic glycosphingolipids Amphoteric glycosphingolipids Arsenosphingolipids Other Sphingolipids
Sterol lipids (ST)	Sterols Steroids Secosteroids Bile acids and derivatives Steroid conjugates Other Sterol lipids

Table 1.1: LIPID MAPS lipid categories. There are 8 categories in the LIPID MAPS lipid classification system, 6 of which are listed above. The 2 categories not listed are polyketides and saccharolipids, which are not found physiologically in humans under normal circumstances. Categories are then

split into classes, which are based on lipid structure. Examples of structure from each category are found later on.

category, and exemplar lipids are shown (Figure 1.1). Fatty acyls comprise of a methyl group, repeating methylene groups and carboxylic acid (Figure 1.1A). Fatty acyls tend to have low molecular weight and are a component of many other lipids. Glycerolipids are made up of a glycerol headgroup and one to three fatty acyls Figure 1.1B). Glycerophospholipids (GPs) are comprised of a glycerol headgroup, phosphate group, and one or two fatty acyl chains (Figure 1.1C). Prenol lipids are products of the mevalonic acid pathway and contain several or many C5 units (Figure 1.1D). Sphingolipids contain a sphingosine headgroup and two fatty acyl chains (Figure 1.1E). Sterol lipids all contain four C5 units (Figure 1.1F). The last two LIPID MAPS lipid categories, polyketides and saccharolipids, are produced exclusively by plants and bacteria (Figure 1.1G and Figure 1.1H, respectively) (Fahy et al., 2009).

1.1.2 The plasma lipidome is dependent on many factors

As previously mentioned, many studies have profiled lipids from tissues and plasma or serum (Table 1.2). The studies selected have been chosen to illustrate the diversity of lipid species and the lipidome. For example, gender and use of contraceptives are both associated with changes in the plasma lipidome (Sales et al., 2016). The platelet lipidome is highly variable between individual donors and across tissue types (Slatter et al., 2016, Leuthold et al., 2017, Pradas et al., 2018, Grzybek et al., 2019, Wood and Woltjer, 2018, Ishikawa et al., 2014).

1.1.3 Mass Spectrometry for lipidomics

1.1.3.1 Principals of mass spectrometry

There are three principal steps in mass spectrometry (MS) (Figure 1.8). The first is ionisation, the second is analysis, and the final stage is detection. There are varying methods which can be employed to complete each stage. Below, the principals of each stage are discussed, alongside alternative methods.

An overview of selected lipidomics studies which investigated tissue lipid profiles

Study	Participant demographics	Sample type	Relevant findings
Sales et al., 2016	71 healthy Caucasian subjects Male (36) and female (35)	Plasma	→ 112 of 281 lipids measured differ between males and females → PEs higher in females → Hormonal contraceptives change plasma lipidome
Slatter et al., 2016	3 healthy subjects Male (2) and female (1)	Platelets	→ Great diversity between individuals → Roughly half of lipids were not found in lipid databases
Leuthold et al., 2017	Human and porcine	Kidney	→ Over 1,000 lipids measured → SPs, GPs, DAGs and TAGs measured in kidney
Pradas et al., 2018	Adult rat	Kidney, skeletal muscle, heart, white adipose tissue and liver	→ 1,916 lipids measured in total → Tissue-specific patterns in lipid levels → E.g. PG is the predominate GPL in heart muscle → High concentration of SP and cholesterol in kidney
Grzybek et al., 2019	Lean and obese adult mice	White (WAT) and brown (BAT) adipose tissue	→ Approximately 99 % of adipose tissue lipids are TAGs → DAGs and GPs detectable in BAT but not WAT → Obese mice demonstrate higher cholesterol in BAT but lower in WAT than lean mice
Wood et al., 2018	Human	Cerebrospinal fluid (CSF)	→ Numerous lipids in CSF, from categories including fatty acyls, GPLs and SPs
Ishikawa et al., 2014	Human	Plasma and serum	→ Levels of polyunsaturated fatty acyls, PCs, DAGs and TAGs are significantly changed between plasma and serum

Table 1.2: Lipidomics studies profiling a range of tissue types. A select number of studies were included above to demonstrate the variability between tissues, individuals and genders.

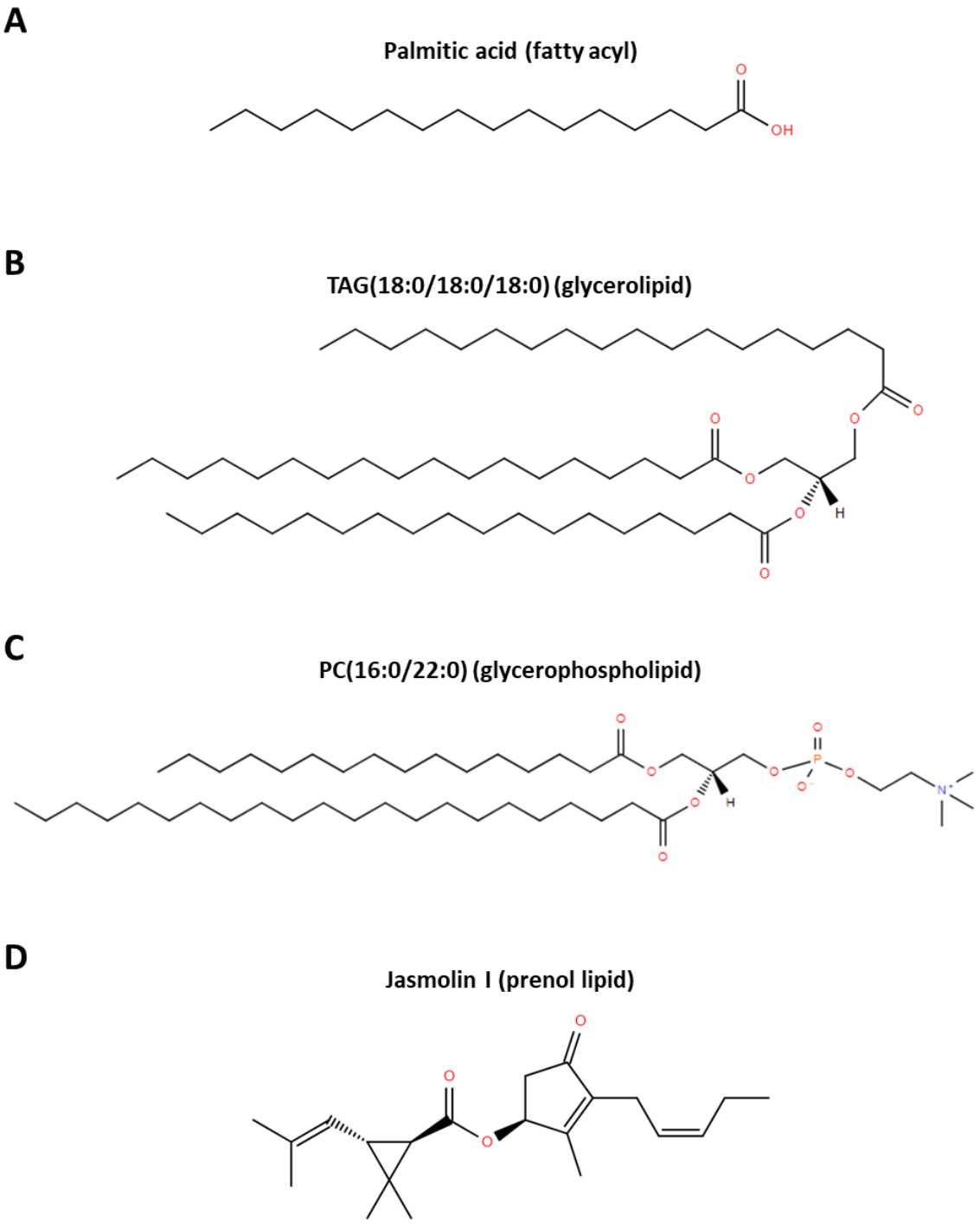

Figure 1.1: Lipids from each LIPID MAPS category. Exemplar lipids from the (A) fatty acyl, (B) glycerolipid, (C) glycerophospholipid and (D) prenol lipid categories. **A.** Fatty acyls are comprised of a methyl group, followed by one or more methylene groups and a carboxylic acid. Fatty acyls are also a constituent of lipids from other categories. **B.** Glycerolipids contain glycerol headgroups, from

which they derive their name, attached to up to three fatty acyls. **C.** Glycerophospholipids are comprised of glycerol, with a phosphate group at sn3, and one or two fatty acyl groups. **D.** Prenol lipids contain one or more C5 units, which are supplied by the mevalonic acid pathway as prescursors isopentenyl diphosphate and dimethylallyl diphosphate.

E

Cer(d18:1/16:0)(sphingolipid)

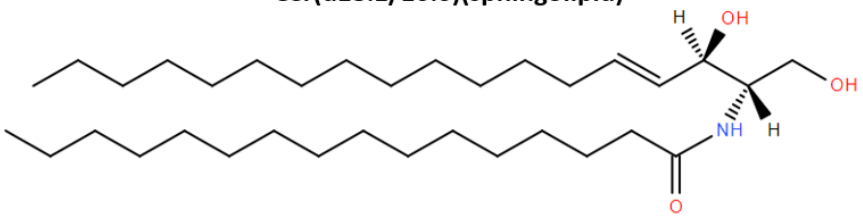

F

Cholesterol (sterol lipid)

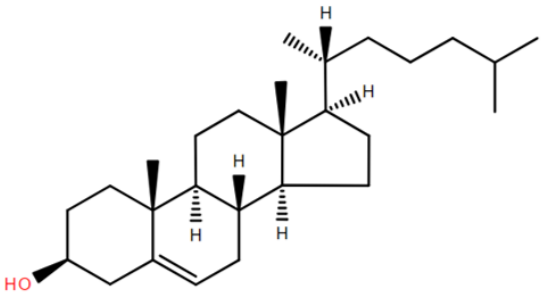

G

Laurenenyne A (polyketide)

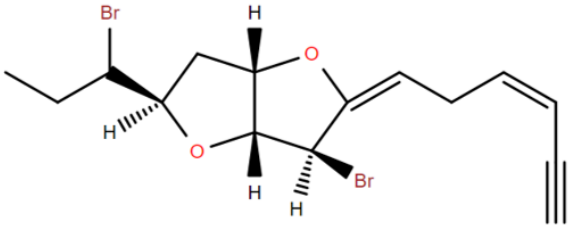

H

2,3-bis-(3R-hydroxy-tetradecanoyl)-αD-glucosamine-1-phosphate(saccharolipids)

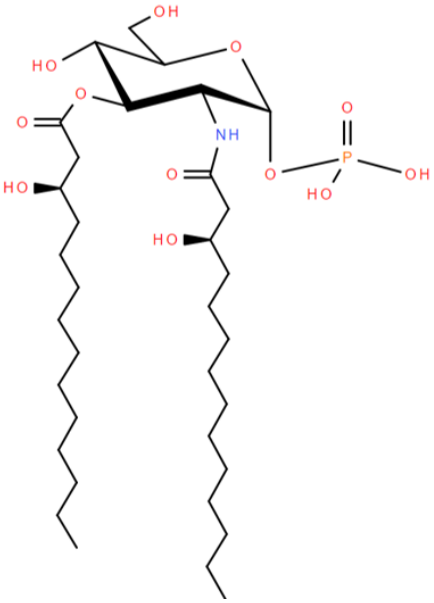

Figure 1.1(cont.): Lipids from each LIPID MAPS category. Lipids from the (E) sphingolipid, (F) sterol lipid, (G) polyketide and (H) saccharolipids categories. **E.** Sphingolipids contain two fatty acyl chains, esterified to a sphingosine headgroup. **F.** Sterol lipids all contain four C5 unit, with one oxygen molecule attached as OH. **G.** Polyketides are diverse in structure and contain (or are derived from) species with alternating methylene and carbonyl groups. **H.** Saccharolipids are comprised of a sugar backbone and one or more fatty acyl groups.

1.1.3.1.1 Ionisation

Prior to analysis using MS, lipids can be ionised using a variety of different techniques, and the most commonly used are discussed below. Ionisation techniques can be 'hard' or 'soft' depending on the amount of energy used. Hard ionisation techniques confer a large amount of energy to the analyte, and therefore result in more fragmentation. Soft ionisation uses less energy and yields fewer fragments. Soft ionisation makes data easier to analyse later on, as 'parent' mass (i.e. the mass of the ionised lipid) can be compared directly to lipid databases, without first matching fragments to produce a complete molecule. Data analysis for soft ionisation is simpler, and absolute quantification is more accurate.

Electrospray ionisation (ESI) is an ionisation technique in which mist of electrically charged liquid droplets, containing the analyte and solvent, is released from a charged capillary. (Whitehouse et al., 1985) (Figure 1.2). The solvent containing the analyte is evaporated by heat on the source and flowing nitrogen gas, then when the droplet is small enough, it reaches the Rayleigh limit and splits into smaller droplets, each of which contains one analyte molecule and one charge. The remaining solvent is evaporated, and the charged lipids are drawn into the aperture, which is also charged. If ionisation mode is positive, then lipids are positively ionised, and the sweep cone is negatively ionised to draw ions towards the inlet. If ionisation mode is negative then lipids are negatively charged, and the sweep cone is positively charged. ESI is a soft ionisation technique, and little or no lipid fragmentation takes place (Table 1.3). However, matrix effects can occur in ESI, during which lipids and matrix molecules compete for ionisation (Taylor, 2005). Matrix effects in biological samples can enhance or reduce lipid ionisation (King et al., 2000).

Another possible ionisation method is matrix-assisted laser desorption (MALDI) (Karas et al., 1987) (Table 1.3). A lipid is mixed with an abundance of matrix, which normally consists of small organic molecules. A laser is used to vaporise the matrix and analyte, which exchange H^+ and other ions to form charged particles, which are then injected into the MS. MALDI is commonly linked to a time of flight (TOF) analyser (Fuchs et al., 2010).

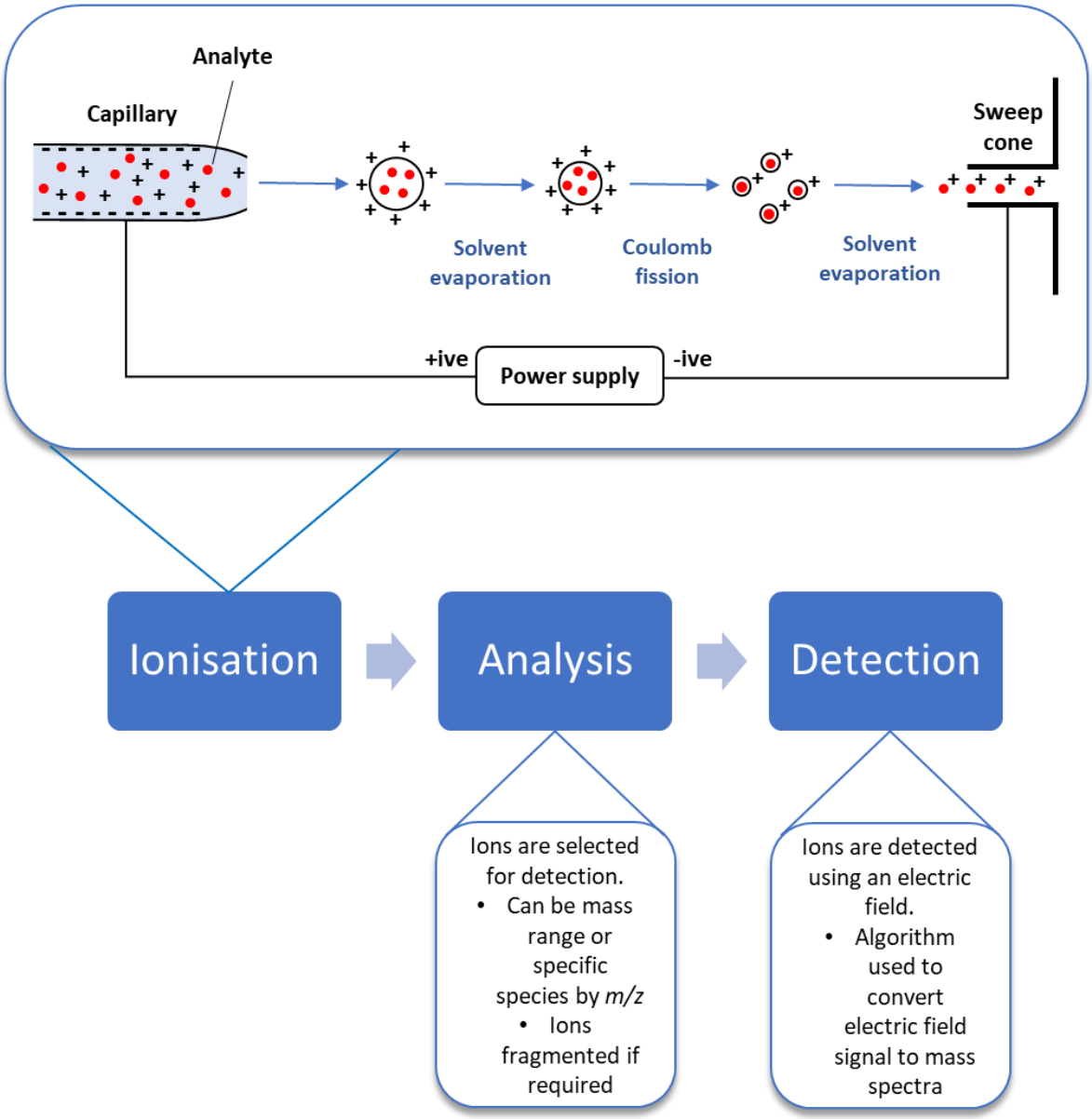

Figure 1.2: The 3 stages of electrospray ionisation mass spectrometry (ESI-MS). Electrospray ionisation in the source is pictured in positive mode. A positive charge on the spray capillary attracts negative ions, leaving positive ions to be ejected into the source. Solvent is then evaporated using heat and source gases, before Coulomb fission occurs and the remaining solvent is evaporated. Positive ions are drawn into the negatively charged aperture. In negative mode, the current is reversed. Positively charged ions are attracted to the electrospray probe and negative ions are drawn towards the positively charged aperture. After ionisation, ions are selected (and fragmented if applicable) and sent to the detector for analysis.

Ionisation method	Advantages	Disadvantages	References
Electrospray ionisation (ESI)	• Soft ionisation method with little/no fragmentation of lipids • Ion signal proportional to lipid concentration	• Matrix effects • Some doubly or triply charged ions produced	(Whitehouse et al., 1985, Ho et al., 2003, Taylor, 2005, King et al., 2000)
Matrix-assisted laser desorption (MALDI)	• Not as vulnerable to matrix effects as ESI • Most ions produced are singly charged • Can analyse solid state samples and provide spatial information	• Rapid in source fragmentation of PLs and TAGs can make it difficult to quantify individual species • Separation into lipid classes aids study of complex mixtures • Less sensitive to negative ions	(Karas et al., 1987, Harvey, 1995, Al-Saad et al., 2002, Fuchs et al., 2010)
Desorption electrospray ionization (DESI)	• Can analyse solid state samples and provide spatial information • No matrix needed • Can give spatial information	• Less reproducible than ESI • Lower spatial resolution than MALDI	(Takáts et al., 2004, Abbassi-Ghadi et al., 2016, Ifa et al., 2010)
APCI	• Soft ionisation method	• Relative intensity of ions related to lipid saturation as well as concentration • Some insource/near source fragmentation	(Horning, 1973, Byrdwell, 2001)

Table 1.3: Advantages and disadvantages of varying ionisation techniques. Ionisation techniques prepare ions for injection into the MS. The most appropriate technique should be chosen according to the qualities of the analyte.

Desorption electrospray ionization (DESI) is also commonly used to study lipids (Table 1.3). A spray of charged droplets, shot directly onto a sample, ionises analytes on the surface (Takáts et al., 2004). Droplets are aqueous and exert electrostatic and pneumatic forces upon the sample to desorb ions from the surface.

Finally, in atmospheric-pressure chemical ionisation (APCI), a heated vaporiser tube desorbs lipid molecules from a sample, which are then ionised by a discharge needle and collected using a vacuum behind a pinhole entrance (Horning, 1973). APCI is also a soft ionisation method, although more fragmentation takes place than when using ESI (Byrdwell, 2001).

ESI was used throughout this thesis as (i) the soft ionisation yields fewer fragments of lipid molecules, aiding identification, (ii) relative intensity is directly related to lipid concentration and (iii) ESI is highly reproducible (Whitehouse et al., 1985, Ho et al., 2003, Abbassi-Ghadi et al., 2016).

1.1.3.1.2 Analysis

The second step of MS is analysis, in which ions are selected and accelerated by electrical currents. Two MS systems were used in this thesis (untargeted and targeted) and analysis differs between the two. In the Orbitrap (ThermoFisher), ions are selected by an ion trap for analysis. The ion trap contains a high-pressure cell for ion selection (mass range or specific masses for fragmentation) and a low-pressure cell for ion ejection further into the MS. The ions move into a rotated quadrupole (C trap), which is charged and affects ion trajectory, causing the ions to move around the C Trap and neutral atoms to fly directly into a central block. Ions are concentrated within the C Trap and then forced into the Orbitrap for detection. Separately, a QTrap 4000 (Sciex) was used for targeted MS methods. The Qtrap 4000 contains three quarupoles, known as quadrupole 1 (Q1), quadrupole 2 (Q2) and quadrupole 3 (Q3). Q2 can be used as a collision cell, depending on which method of analysis is used. After passing through Q1-3, ions are injected into the detector.

During the analysis portion of MS, there are various methods for selecting which ions are measured. In an untargeted analysis, an upper and lower mass limit are chosen, and all ions

present in this range are detected. Whilst this method is suitable to analyse complex samples, and samples of an unknown composition, untargeted methods are less sensitive as the number of ions which can be trapped in the detector is finite. Therefore, low concentration lipids may be missed in a complex sample. Also, more post-acquisition data analysis is required to filter the data and identify lipids.

Information-dependant acquisition (IDA) cycles through masses or a mass range several or many times over a MS analysis, selecting ions in Q1. If a specified mass is found, it is fragmented in Q2 and fragments are collected in Q3. IDA is useful if a smaller group of lipids are being targeted, but fragmentation patterns and retention time are unknown. Sensitivity of IDA is dependent on the total cycle time, with a smaller cycle time providing a more sensitive analysis.

Selected reaction monitoring (SRM) is a suitable MS method when you already have extensive information on lipids of interest (Liebler and Zimmerman, 2013). A 'parent' mass is selected in Q1, ions collected in Q2, and a 'daughter' mass is then selected in Q3.
The 'parent' mass is the mass of the ionised lipid, whilst the 'daughter' mass is the mass of an expected fragment. If both 'parent' and 'daughter' mass are present, you can be reasonably confident that you are measuring the lipid of interest. A retention time window is also required, during which the MS will scan for the 'parent' and 'daughter' masses. SRM becomes multiple reaction monitoring (MRM) when multiple windows are used to scan for multiple 'parent' and 'daughter' ions. MRM provides an increased sensitivity compared to untargeted methods, as only chosen species are passed along to the detector. However, MRM cannot be used when the fragmentation pattern and retention time of the lipid are unknown.

If lipids being analysed are similar in structure, for example if only the position of a double bond differs, further fragmentation of the lipid can aid identification. In MS/MS, the 'parent' and 'daughter' ion are monitored, alongside the 'product' ion, which is a fragment of the 'daughter' ion. In this case, the 'parent' ion is selected in Q1, the 'daughter' ion in Q2 and the 'product' ion in Q3.

An alternative to the ion trap and triple quadrupole MS systems detailed above would be a TOF analyser/detector, which was first developed in the 1950s (Wolff and Stephens, 1953). In TOF analysis, ions are released into a flight tube, each with an equal amount of kinetic energy. TOF uses the relationship between kinetic energy and velocity to calculate exact mass. TOF is commonly linked to MALDI (Fuchs et al., 2010). MALDI-TOF has a faster acquisition rate than liquid chromatography coupled to ESI-MS and a low limit of detection (Schiller et al., 2004). However, MALDI-TOF is associated with more lipid fragmentation, which complicates the analysis of complicated mixtures such as plasma (Al-Saad et al., 2002). The use of two analysis systems was deemed most appropriate for this work, the ion trap and Orbitrap for untargeted and accurate mass measurements, and the triple quadrupole for to follow up with targeted MS/MS experiments.

1.1.3.1.3 Detection

The final step is detection. Collision of ions with the detector causes an electron pulse, which is converted into a spectrum by attached software. In the Orbitrap Elite, lipids enter the titular Orbitrap and oscillate around a highly charged inner electrode. Current is measured across split outer electrodes, the signal amplified and Fourier Transformation (FT) is used to change the amplified signal into a frequency spectrum and then a mass spectrum is produced. FT is an extremely accurate method of mass detection (ref). Detection in the QTrap relies on one electric field, into which ions are propelled. Mass detection is less accurate than the Orbitrap (ref).

1.1.3.3 Liquid chromatography coupled with MS allows the detection of more species

The methods to be used in this work separate lipids using reverse phase LC and analyse them using MS and bioinformatics tools (Section 2.5) to allocate an accurate mass and retention time (RT). Coupling MS with liquid chromatography (LC) allows more species to be profiled than just using MS alone. The analyser and detector within the MS both have a finite volume, in which a certain number of ions can be stored. An injection of lipids extracted from the whole sample could cause the detector to be swamped, which could prevent lower abundance ions from being measured as few ions would enter the detector. Separating the

sample over time using LC causes fewer ions to enter the MS at any one time, therefore reducing the risk of swamping the analyser/detector and missing lower abundance species (ion suppression). Also, lipids are separated due to their intrinsic physical properties and therefore exit the LC column with other lipids with similar characteristics in a predictable pattern, aiding identification. Therefore, retention time (RT) can be a useful tool in assigning putative lipid identifications.

The RT at which lipids come off the LC column to be analysed by the mass spectrometer is modulated by the interaction of the lipid with the stationary and mobile phases (Figure 1.3). The stationary phase in the global analysis method is silica beads, 2.6 µm in diameter, with C18 carbon chains projecting from the outside. Lipids can interact with the beads in several ways. Non-polar lipids remain longer in the non-polar C18 chain matrix around the silica beads. Hydrophilic polar lipids move along the LC column faster and enter the MS sooner and have earlier RTs. As solvent A (aqueous) decreases and B (organic) is ramped, the non-polar lipids are drawn off the column for analysis. Also, lipids with longer chain fatty acyls are more likely to interact with the C18 chains, slowing their progress along the LC column (ref). Therefore, lipids are separated according to polarity and m/z.

Lipid chromatography/mass spectrometry (LC/MS) provides a powerful tool for accurate lipid analysis due to its ability to read extremely accurate mass and due to its high sensitivity. Further analysis of LOAD using 'omics' technologies such as lipidomics could provide important mechanistic insights and allow the development of novel preventative treatments (Orešič et al., 2009, Lista et al., 2016).

1.1.4 Using bioinformatics to analyse MS data

Bioinformatics is the development of software methods or tools which allow analysis of biological data. The field uses coding, maths and statistics to treat data and mine results.
The field of lipidomics requires the analysis of complex and large-scale data, therefore automated systems of data processing prevent manual errors and facilitate in depth data mining (Pauling and Klipp, 2016). Bioinformatics tools for lipid analysis can have many

functions, including statistical analysis, lipid classification, data visualisation or biological pathway mapping (Fahy et al., 2007).

In this thesis, an in-house-built software called LipidFinder, which uses the Python programming language, was used to extract lipid data from raw, untargeted MS output (Section 1.1.4.1) (O'Connor et al., 2017, Van Rossum and Drake Jr, 1995). Lipid Finder combines mass spectra into lipid peaks using complex algorithms and allows the user to define and optimise parameters for their own data (O'Connor et al., 2017, Fahy et al., 2018).

After data treatment using XCMS, followed by LipidFinder, statistics and figures will be produced in the coding language R using RStudio (Smith et al., 2006). Targeted MS data is smaller and simpler than untargeted MS data. In this thesis, targeted data was analysed manually.

1.1.4.1 Using Lipid Finder to process MS data

Lipid Finder is a package of open access software, available in Python and on the Lipid Maps website (Van Rossum and Drake Jr, 1995, O'Connor et al., 2017). Python is a free and open source programming language with a huge library of readily available functions and code. It is considered easy to learn and is embeddable in other code such as html. Lipid Finder is written in Python and transforms raw MS data frames into peaks. Each peak represents a lipid, with an intensity value and retention time for each. Lipid finder can then perform optional data analysis and data visualisation. The program contains several modules to support these functions. Firstly, the PeakFilter module creates peaks from the raw data. After removing background ions, which are present in extracted blanks or throughout the analysis, data frames are clustered according to mass, using a mass window set by the user. Peaks are produced by combining frames within set mass and retention time windows. Contaminants and adducts from a preset list are removed and retention times aligned across samples. Where there are small differences in recorded mass between samples, mass is taken to be the mean mass recorded. PeakFilter output is a peak list, produced in either positive or negative mode. The Amalgamator module then combines positive and negative analyses by

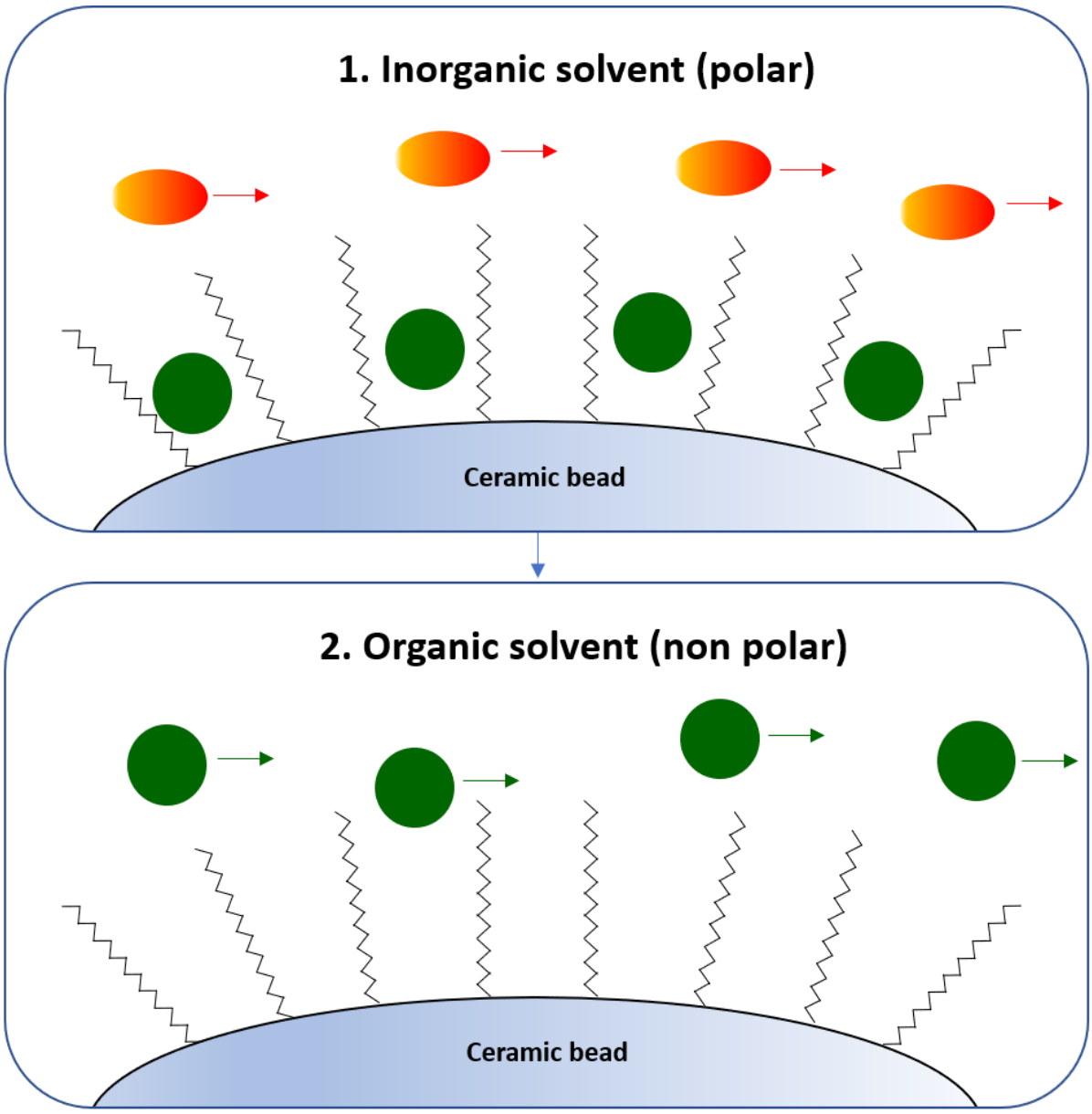

Figure 1.3: Liquid chromatography separates lipids through interaction with C18 carbon chains which are attached to ceramic beads. 1. The polar starting conditions encourage polar lipids to move along the column, whilst non polar lipids are sequestered amongst the C18 chains. The polar lipids are drawn along the column and enter the MS. **2.** Once organic solvent is introduced, the less polar lipids disassociate from the C18 matrix and are pushed along the column to enter the MS.

using accurate mass differences to predict which ions are from the same species. The output is a list of peaks, with replicates removed where lipids were measured in both modes. WebSearch then compares recorded mass for each lipid to online lipid databases. If a match is found, putative lipid identity is recorded, as well as lipid category and subcategory (Fahy et al., 2009). Finally, the FileProcessing module combines searches from different lipid databases to standardise lipid nomenclature and file layout. Any duplicates or database matches with a mass error (difference between database mass and recorded mass) larger than a set value are removed. There is also an optional module to optimise peak finding parameters, but this was not used for data contained within this thesis.

1.1.4.2 Univariate and multivariate analysis as tools to analyse complex datasets

Data analysis using statistics reduces the likelihood of errors in study conclusions. Errors are broadly split into two groups; a type I error is an incorrect rejection of the null hypothesis, and a type II error is when the null hypothesis is incorrectly accepted. Statistical tests should be chosen during study design, and the most appropriate tests depend on the data being collected. Paired data, which originates from one subject at different timepoints, should be treated by different tests than unpaired data, which comes from separate subjects. Univariate analysis techniques are appropriate when few variables are being tested, or when variables are independent of one another. Selection of the univariate test will depend on the way the data is distributed (Figure 1.4). Normally distributed data is tested using parametric tests, for example, t test, one-way analysis of variance (ANOVA). Abnormally distributed data is tested using nonparametric tests like the Wilcoxon Rank sum test, Mann-Whitney U test or Spearman correlation.

Normally distributed data sits on a frequency histogram in a symmetrical bell-shaped curve (Figure 1.5). To evaluate distribution, you must first calculate the mean and standard deviation of the data. Standard deviation is calculated by first taking the mean from each value, and then squaring the differences from the mean individually. The mean of the squared differences is calculated and finally the square root of the mean of the squared differences. If 68 % of the data falls within one standard deviation of the mean, 95 % within two standard deviations and 99.7 % between three standard deviations, then data is normally distributed

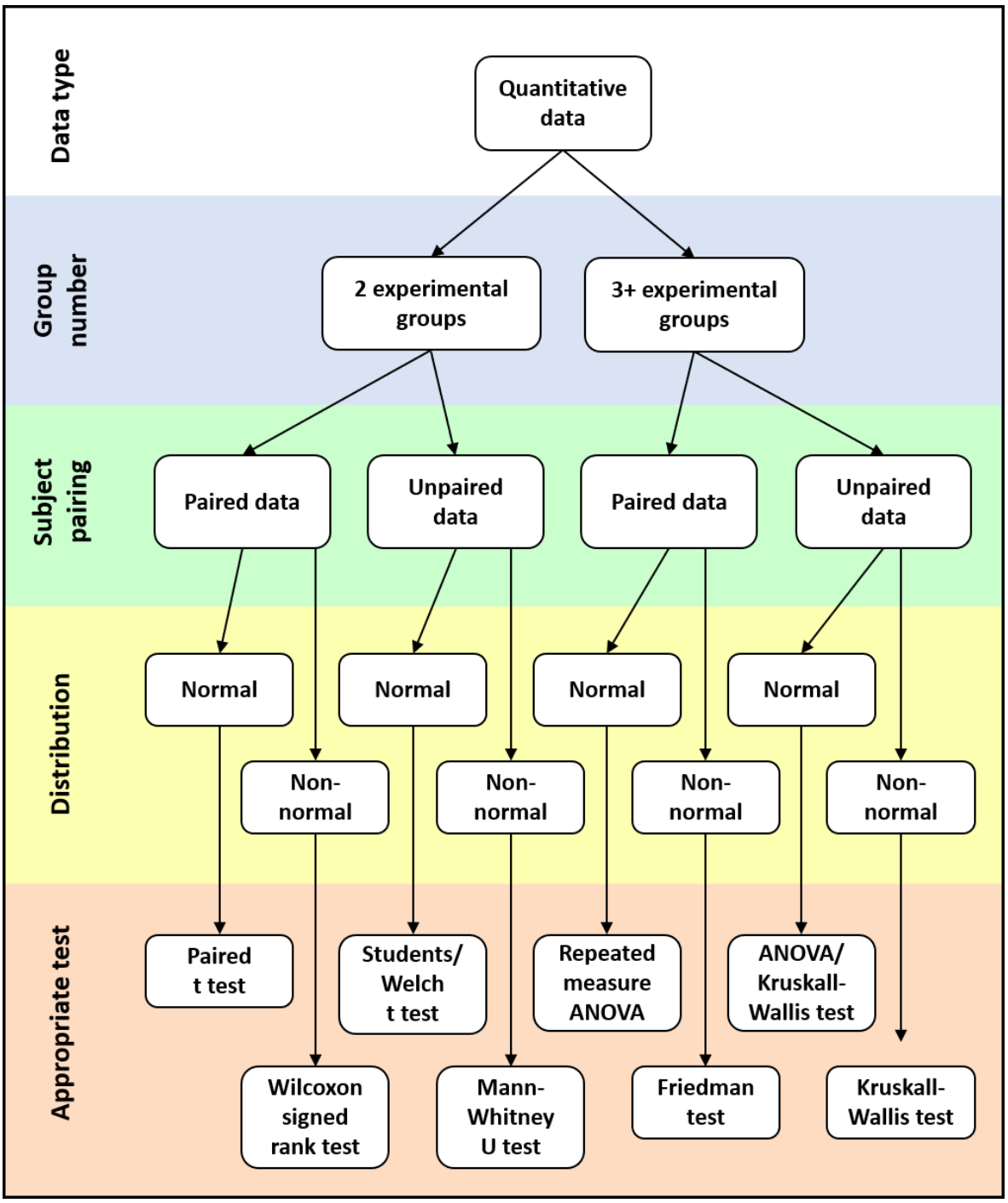

Figure 1.4: Data analysis techniques should be chosen according to data type. A flowchart depicting the correct univariate tests for different types of quantitative data. Quantitative data analysis depends on the number of experimental groups (blue), whether data is paired (green) and the distribution of the data (yellow). Multivariate tests could be used to supplement or replace tests when multiple experimental groups or variables are present.

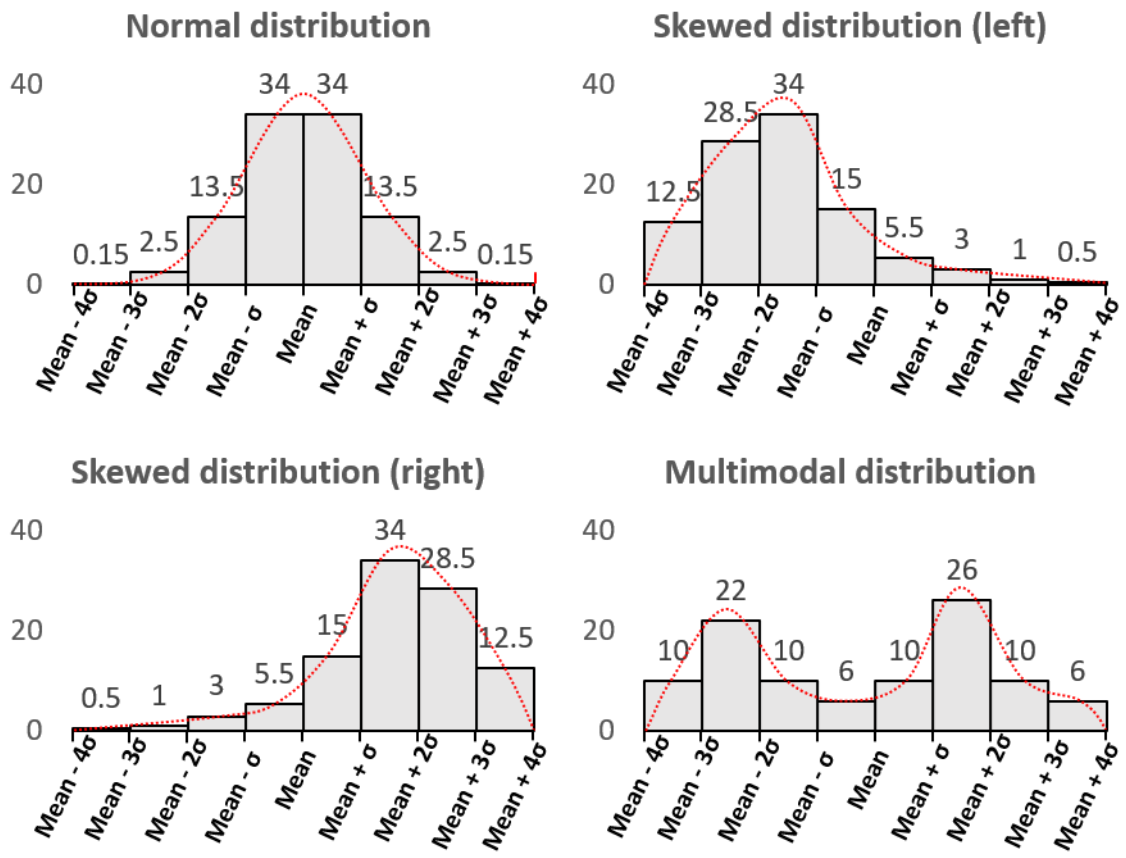

Figure 1.5: Data distribution is described according to how data is clustered around the mean. i) Normally distributed data. σ = standard deviation. Numbers above bars are percentages of data falling within each bracket. **ii)** Data which is skewed to the left of the mean. More data points fall below the mean than above. **iii)** Data which is skewed to the right of the mean. More data points fall above the mean than below. **iv)** Data with a multimodal distribution. Data falls in two or more groups, which may be above and below the mean (when two groups present) or above, below and on the mean (when more than groups are present).

(Figure 15i). Alternatively, data can be skewed, and the majority of data points sit above or below the mean (Figure 1.5ii-iii) or multimodal, where data is clustered into groups (Figure 1.5iv).

Univariate tests can be one-way or two-way (McDonald, 2014). One-way tests are used if the direction of deviation in the data is known, e.g. the null hypothesis is that 'genotype A does not have significantly higher cholesterol than genotype B', and the alternative hypothesis is that 'plasma from genotype A will have significantly higher cholesterol than plasma from genotype B'. If the deviation of the data is unknown, a two-way hypothesis should be used. An example of this would be a null hypothesis of 'plasma from genotype A will contain as much cholesterol as plasma from genotype B' and an alternative hypothesis of 'plasma from genotype A will contain a significantly different amount of cholesterol to plasma from genotype B'. I have used two-way tests throughout, as the direction of data deviation is unknown.

There are two possible approaches to analysing multiple variables. Firstly, a multiple comparison correction can be applied to the results of a univariate analysis. Two commonly used examples of multiple comparison corrections would be the Bonferroni correction and the Benjamini-Hochberg correction (Neyman and Pearson, 1928, Benjamini and Hochberg, 1995, McDonald, 2014). Multiple comparison corrections adjust p values obtained from univariate tests to consider the number of variables tested, by multiplying p value by the number of tests. These procedures reduce the likelihood of a type I error.

The second approach when analysing multiple variables would be the use of multivariate analysis tools, such as multivariate analysis of variance (MANOVA), principal component analysis (PCA) and partial-least-squares discrimination analysis (PLS-DA). Multivariate analysis should be used when data includes many variables. Multivariate analysis is a valuable tool in the analysis of lipidomic datasets as data tends to be large and complex (Checa et al., 2015). Using multivariate analysis is preferable to multiple univariate analyses in determining the weighting of individual lipids towards total result (Huberty and Morris, 1989). Multivariate analysis can compare more than two experimental groups. Also, when variables are not independent, multiple univariate analyses may provide redundancy in the results, as each

lipid which significantly differs between groups is not a new finding if lipids are linked. Multivariate analysis tools were used within this thesis to study untargeted lipidomics data, because (i) many lipids were measured, which were not independent of one another, (ii) to determine which lipids e and (iii) to determine if multivariate analysis and univariate analysis defined the same lipids as having the most effect on the dataset.

PCA and PLS-DA are often used alongside each other in multivariate data analysis. A function of PCA and PLS-DA is to simplify complicated multi-level datasets into an easily-visualised one-dimensional (1D) graph (Pearson, 1901, Worley and Powers, 2013). Input for PCA requires enough variables (i.e. axes) to be transformed into a three-dimensional (3D) matrix, for example, here axes were sample, lipid name and lipid intensity. Briefly, to produce a normalised 3D data matrix, values are normalised around the origin. An ellipsoid is fitted onto the 3D matrix, with each diagonal across the ellipsoid being a principal component (PC). Variance for each lipid is then calculated as the distance from the principal component to the lipid and variance contained by a PC is the sum of the variances of all lipids in relation to that PC. Thus, PC1 is the PC which contains the most variance and PC2 is orthogonal (at a right angle) to PC1.

PLS-DA is, unlike PCA, a supervised algorithm, where group ID (e.g. genotype, disease or control) is inputted alongside other data. After the data matrix is produced, the matrix is rotated to provide the best separation of the alleles. PC1 and PC2 are the first two PCs optimised to separate *APOE* 22 and control. Loadings plots for both PCA and PLS-DA models demonstrate the contribution of each lipid to variation, with a higher PC score on the loadings plot indicating that an individual lipid was more different in *APOE* 22. Positively correlated lipids are grouped, whereas highly negatively correlated lipids sit diagonally opposite. PC1 and PC2 are the first two PCs optimised to separate groups by group ID. PCA and PLS-DA can be visualised on scores plots, which represent how samples are grouped, and loadings plots, which display information on lipid concentrations and grouping of lipids (Checa et al., 2015). LC-MS coupled with the multivariate analysis techniques PCA and PLS-DA have been used to separate plasma type-2 diabetes mellitus and control using lipids, as well as to identify biomarkers of disease (Wang et al., 2005).

Receiver operating characteristic (ROC) analysis is also useful in lipidomic analysis (Checa et al., 2015). An ROC analysis is another supervised analysis, in which an algorithm attempts to predict which experimental group individual samples originate from (Metz, 1978). If area under the curve (AUC) is 1, the algorithm has taken each sample from the remainder and correctly predicted which group that sample came from. When trialling a clinical diagnostic test, the minimum acceptable AUC is 0.70 but 0.9 or higher is preferable (Mandrekar, 2010). Migraine patients can be separated from control using serum lipids and ROC analysis (Ren et al., 2018).

Some studies combine different types of multivariate data analysis to validate results. PLS-DA and ROC curves can be used to differentiate non-small cell lung cancer from control and benign lung disease using plasma lipids (Chen et al., 2018). Also, PCA, PLS-DA and ROC of serum lipids can distinguish coronary heart disease from control (Liu et al., 2018). To conclude, univariate and multivariate analysis techniques should be chosen during experimental planning. Techniques will differ according to how data is distributed. Multiple comparison procedures can be used to correct p values when many variables are being measured, whilst multivariate analysis can be used when there are many variables or more than two experimental groups. A combination of univariate and multivariate data analysis tools have been used to analyse lipidomics data.

1.2 Genetically modified mice as a tool to study disease

Genetically modified mice have been used for decades as a tool to study human disease. Mice have been genetically engineered to express gene variants of interest for the study of many disorders, such as Alzheimer's disease or heart disease (Sturchler-Pierrat et al., 1997, Webster et al., 2014, Geisterfer-Lowrance et al., 1996, Musunuru et al., 2005). The murine genome can be edited using either pronuclear injection or embryonic stem cell editing. In pronuclear injection, plasmids are microinjected into fertilised oocytes, which are then implanted into a female mouse to develop (Gordon et al., 1980). As the transgene integrates randomly into the genome, the endogenous variant of the gene will also be expressed, and the transgene may be overexpressed. During embryonic stem cell editing, embryonic stem cells are selected

and transfected with genes of interest (Gossler et al., 1986). This is known as gene targeting, as endogenous genes are replaced with gene variants of interest. Cells which have been successfully transfected are reintroduced into blastocytes, and blastocytes implanted into female mouse. Gene targeting can be used to produce knock out mice, which do not express a gene, or knock in mice, which express a modified gene.

Like humans, mice are diploid, i.e. cells (except for gametes) contain a maternal and paternal copy of each chromosome. Therefore, after genetic modification though gene targeting, mice can be homozygous or heterozygous for a gene of interest. Homozygous mice have two copies of a gene which match, whilst heterozygous mice have two gene variants. Offspring must be genotyped to see if (i) gene modification has been effective, and (ii) if offspring are homozygous or heterozygous for gene variant (Figure 1.6). Homozygosity of some recessive gene variants or complete knock out of some proteins can be fatal, and heterozygous mice should be used in this circumstance (Castle and Little, 1910, Ioffe and Stanley, 1994, Coleman et al., 1995).

The C57BL6 mouse is commonly used as 'wild-type' and as a background onto which gene editing takes place, and have been extensively phenotyped (Bryant, 2011, Waterston et al., 2002). There are several substrains of C57BL/6 mouse, all of which originate from the C57BL/6J, created at the Jackson Laboratory. C57BL/6N was created after breeders were taken to the National Institute for Health (NIH) in 1951. Other substrains include C57BL/6C, and C57BL/6NCrl (Charles River), C57BL/6NTac (Taconic), and C57BL/6NHsd (Harlan Sprague Dawley), all of which originate from C57BL/6N. Substrains developed when breeding mice were isolated in a new facility, and small genetic changes occurred. Whilst there are many similarities between the substrains, there are some genotypic and phenotypic differences (Simon et al., 2013, Matsuo et al., 2010). For example, the startle response in C57BL/6N is smaller than C57BL/6J and resting heart rate is higher (Simon et al., 2013). C57BL/6N has a shorter latency to fall from a suspended wire, all substrains behave significantly differently from each other in the light/dark transition test, and distance travelled in social tests and forced swim differs between some substrains (Matsuo et al., 2010). Therefore, it is imperative that all genetically modified mice being compared are from the same substrain, and some substrains may be more appropriate for some experiments than others.

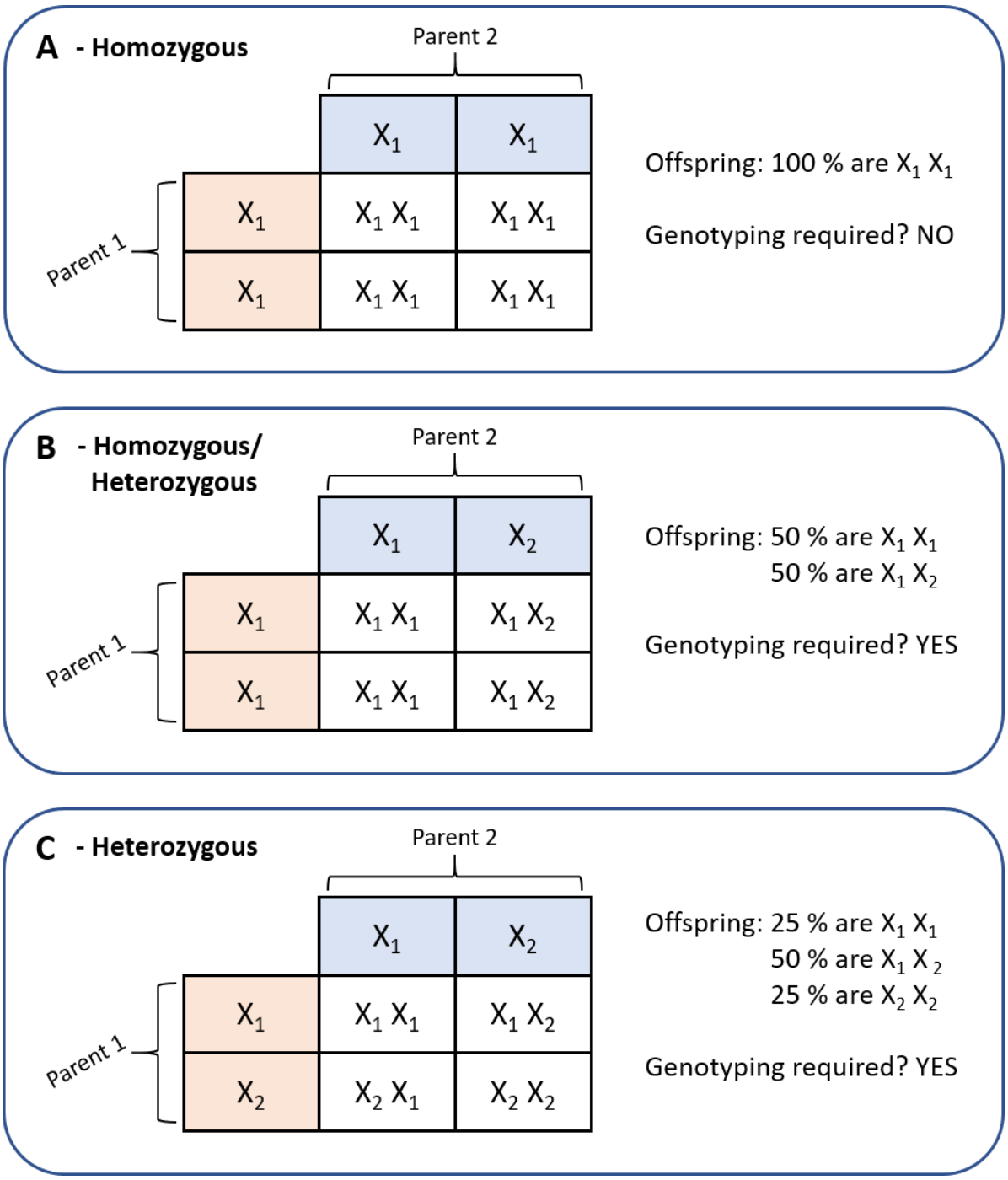

Figure 1.6: Homozygous and heterozygous mice, and their offspring, visualised in Punnett Squares. Two variants of the same gene (X) are represented as X_1 and X_2. In this example, X_1 is the gene variant of interest. Parent mice are either homozygous (A) or heterozygous (B,C) for variants of X. **A.** Mating two mice which are homozygous for X_1 produces offspring which are homozygous for X_1. **B.** Mating two mice, when one parent is homozygous for X_1, and one parent is heterozygous (X_1 X_2), produces offspring who are 50 % X_1 X_1 and 50 % X_1 X_2. Therefore, offspring must be genotyped. **C.** Mating two mice, both of which are heterozygous for gene X, produces a mix of offspring. 25 % are homozygous for X_1, 50 % are X_1 X_1 , and the last 25 % are homozygous for X_2 X_2.

Genetically modified mice are a valuable tool for the study of neurological disease. Tissue from the brain is not readily available and tends to come only from post-mortem, with the exception of tissue collected during neurosurgery (ref). Genetically modified mice can be used to study the time course of neurological disease, especially when risk genes have been identified and pathology can be reproduced. There are many mouse models of Alzheimer's disease, which have been used to study pathology and trial treatments (Sterniczuk et al., 2010, Leissring et al., 2003, Marr et al., 2003, Iwata et al., 2004, Poirier et al., 2006, El-Amouri et al., 2008, Santacruz et al., 2005, Elder et al., 2010). Some of the more widely used mouse models of Alzheimer's disease are described in Table 1.4.

Mice are also a useful model organism in the field of lipidomics. Lipids and lipid-associating proteins are highly conserved between many species, including humans and mice (Birsoy et al., 2013, Kaabia et al., 2018, Jha et al., 2018, Frieden, 2015, Bashtovyy et al., 2011, Segrest et al., 1998, Brash, 1999). Whilst lipids cannot be directly modified by gene editing, lipid-related proteins and enzymes can be targeted. Several diseases related to lipid metabolism have been modelled in mice (Table 1.4) (Sango et al., 1995, Zhang et al., 1992, Maue et al., 2012, Sullivan et al., 1998).

1.3 APOE and Lipid Transport

The apolipoprotein E (*APOE*) gene encodes the ApoE protein, which plays an important role in lipid homeostasis in humans, as well as in many other species (Mahley et al., 2009, Holtzman et al., 2012, Huang and Mahley, 2014, Frieden, 2015). The function of apoE is determined by its structure (Figure 1.7) (Mahley et al., 2009). ApoE binds to several receptors to facilitate lipid movement between cells and in the circulation (Sections 1.3.1 and 1.3.2) (Mahley, 1988, Attie et al., 2001, Krimbou et al., 2004, Getz and Reardon, 2009, Koldamova et al., 2014). For example, apoE can bind to the low-density lipoprotein receptor (LDLR), facilitating the influx of cholesterol and TAGs from lipoproteins into cells (Mahley, 1988). ApoE also binds to the ATP-binding cassette transporter 1 (ABCA1) receptor on cell surfaces, triggering ABCA1-dependant cholesterol efflux (Attie et al., 2001).

Reference	Gene(s) targeted	Gene modification	Outcome	Disease modelled
Sterniczuk et al., 2010	Amyloid precursor protein (*APP*) Microtubule associated protein (*MAPT*) Presenilin 1 (*PSEN1*)	Knock in of human risk variants	Protein accumulation in brain	Alzheimer's disease
Mucke et al., 2000	*APP*	Amino acid substitution	Protein accumulation in brain	Alzheimer's disease
Masliah et al., 1996	*APP*	Knock in and overexpression of human risk variant	Protein accumulation in brain	Alzheimer's disease
Hsiao et al., 1996	*APP*	Knock in and overexpression of human risk variant	Protein accumulation in brain	Alzheimer's disease
SantaCruz et al., 2005	Microtubule associated protein tau (*MAPT*)	Knock in of human risk variant	Protein accumulation in brain	Alzheimer's disease
Yoshiyama et al., 2007	*MAPT*	Knock in of human risk variant	Protein accumulation in brain	Alzheimer's disease
Zhang et al., 1992	Apolipoprotein E (*APOE*)	Knock out	Failure to clear lipids from blood	Atherosclerosis
Sullivan et al., 1998	Apolipoprotein E (*APOE*)	Knock in of human risk variant	Failure to clear lipids from blood	Type III hyperlipoproteinemia, leading to atherosclerosis
Sango et al., 1995	Hexosaminidase subunit beta (*HEXB*)	Gene editing – introduction of multiple gene fragments	Lipid accumulation in intracellular compartments	Sandhoff disease
Maue et al., 2012	Niemann-Pick type c1 (*NPC1*)	Amino acid substitution	Abnormal cholesterol storage and metabolism, altered glycolipid profile	Niemann-Pick C1 disease

Table 1.4: Mouse models used in Alzheimer's disease and lipidomics experiments. Mice have been used to model many diseases, including Alzheimer's disease and lipid-related disorders. Some of the widely used models are summarised above, including the original piece of research describing the model, the gene targeted for mutation, its protein product and the disease being modelled. All of these mouse models have been used in multiple publications.

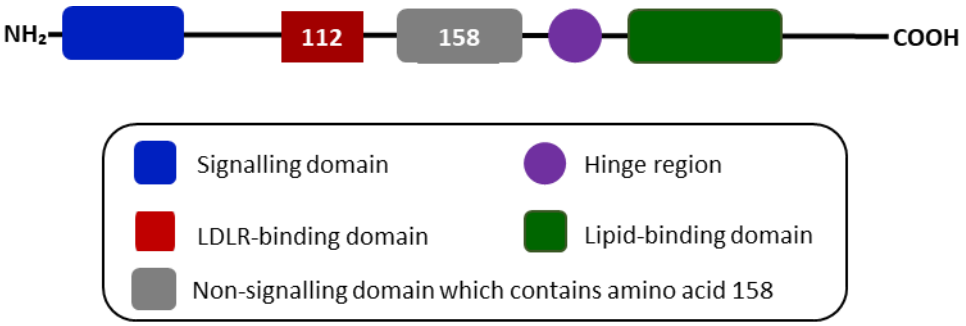

Figure 1.7: A representation of the primary structure of apoE. The N-terminus of the apoE protein contains the signalling domain and the low-density lipoprotein receptor (LDLR) binding domain, whilst the C-terminus contains the lipid binding domain. The two domains are separated by a hinge region.

***APOE* allele distribution and character**

	ε3	ε2	ε4
Frequency*	**0.79**	**0.07**	**0.14**
Defining amino acids†	**Cys-112 Arg-158**	**Cys-112 Cys-158**	**Arg-112 Arg-158**
LDLR binding ability (%)	**100**	**<2**	**100**
Lipid binding ability	**Normal**	**Normal**	**Decreased**
Risk of late-onset Alzheimer's disease (LOAD)	**Average**	**Decreased**	**Increased**

Table 1.5: APOE allele frequencies and traits. *Frequency of each *APOE* allele in a 38 population meta analysis, where 1 is the whole population (ALZGENE, 2010). †Amino acids present at position 112 and 158 in the apoE protein produced from the 3 common *APOE* alleles. These amino acid substitutions can alter the structure and function of the apoE protein. LDLR binding ability is the affinity of the protein isoform for the LDLR, in comparison to the apoE ε3 protein. Lipid binding ability refers to be availability of the lipid-binding active site. Risk of LOAD refers to the relative risk of LOAD, taking *APOE* ε3 carriers as the norm.

There are three common *APOE* alleles, known as ε2, ε3 and ε4. The protein products of these three alleles have amino acid substitutions at two possible locations, amino acids 112 and 158 (Table 1.5) (Weisgraber et al., 1981). Amino acid 112 is in the LDLR binding domain of apoE, whilst amino acid 158 is in a non-signalling region of the molecule (Figure 1.7). *APOE* ε2 carriers produce an apoE protein which contains cysteine in both positions. *APOE* ε3 carriers produce apoE with cysteine at position 112 and arginine at amino acid 158. *APOE ε*4 carriers produce apoE with arginine at both 112 and 158. Both substitutions alter apoE function because apoE forms a globular structure in plasma, with many interactions between the C- and N-terminal domains (Mahley et al., 2009, Chen et al., 2011). The apoE ε2 isoform demonstrates a deficit in LDLR binding compared to the other two alleles, and this deficit can cause hypercholesterolemia due to reduced clearance of lipoproteins and lipoprotein remnants from the circulation (Mahley et al., 1999, Weisgraber et al., 1982). Both apoE ε3 and apoE ε4 protein isoforms demonstrate normal LDLR binding. Whilst *APOE* allele determines the ability of the protein to bind to the LDLR, all three alleles induce cholesterol efflux through ABCA1 with the same efficiency (Krimbou et al., 2004). Whilst the basis of lipids binding to apoE is not yet fully understood, it is likely that lipids bind to apoE between the hinge region and C-terminus, but that binding is influenced by residues from both N- and C-terminus domains (Frieden et al., 2017, Chen et al., 2011).

Humans have a diploid genome and therefore each individual is either homozygous or heterozygous for *APOE*. Throughout this work, when samples are described as *APOE 22*, *APOE33* or *APOE 44*, these samples originated from homozygotes. When participants are described as *APOE* ε2, *APOE* ε3 or *APOE* ε4 carriers, the study has not distinguished between homozygotes and heterozygotes. The word *APOE* capitalised refers to the gene, whilst apoE refers to the protein product.

1.3.1 ApoE acts as a cholesterol transporter in the brain

To consider how *APOE* allele could be affecting LOAD risk, we must first discuss the role of *APOE* in the CNS, where it acts as the principal lipid transporter, providing cholesterol, cholesterol esters and other lipids to neurons. The blood-brain barrier (BBB) prevents lipoprotein exchange between the brain and the body, therefore the brain must produce most

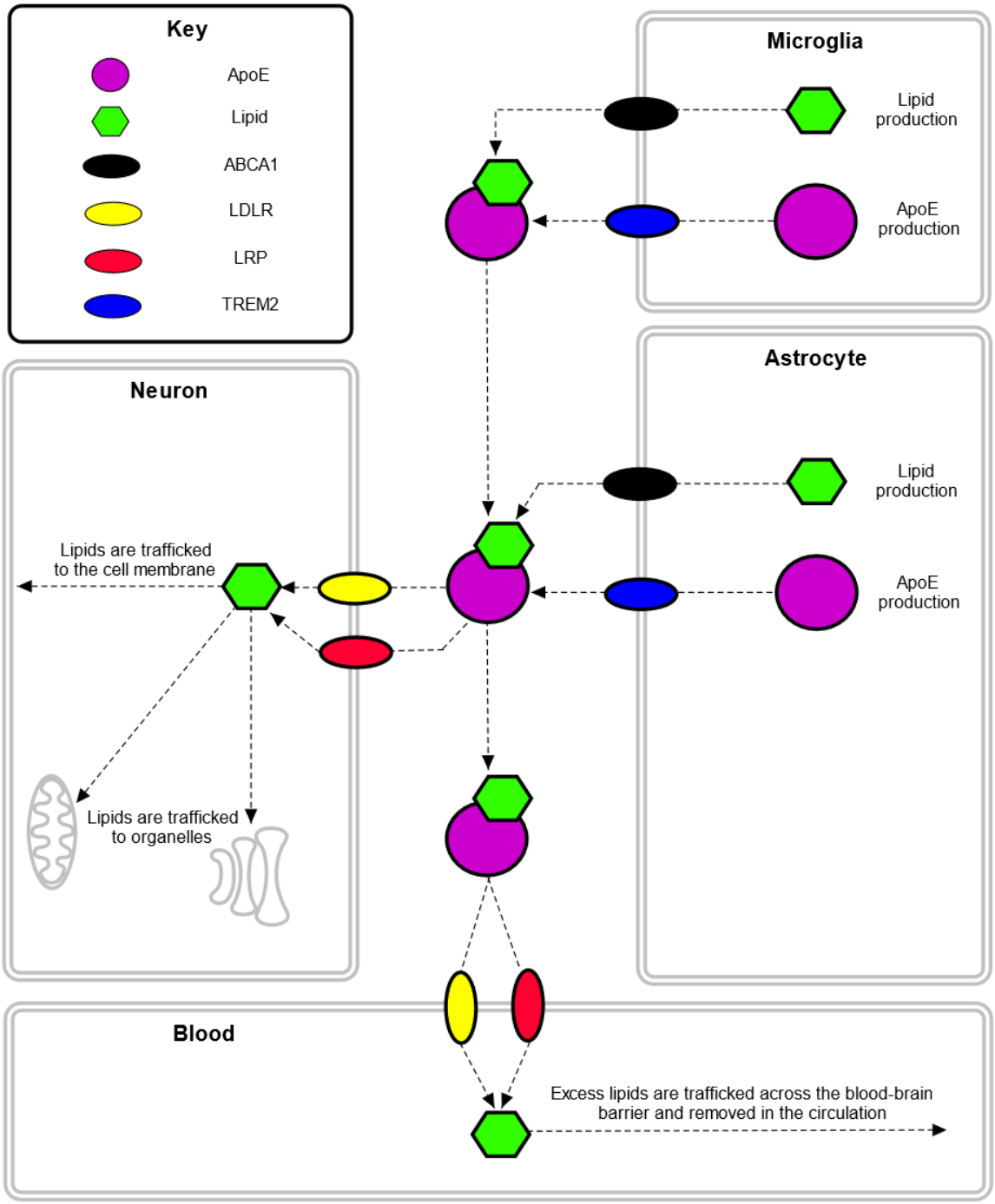

Figure 1.8: ApoE function and trafficking within the central nervous system. ApoE is produced in the glial cells and enters the extracellular space through TREM2. ApoE is lipidated by the ABCA1 receptor, creating a lipoprotein. This lipoprotein interacts with the LDLR and LRP receptor in an apoE-mediated manner, allowing lipids to enter neurons, where they are used primarily as a fuel source.

of the lipids needed (Zlokovic, 2008). Neurons produce significantly less cholesterol than astrocytes, so cholesterol and phospholipids are released from astrocytes and microglia in an apoE-dependent manner to provide neurons with the lipids needed (Nieweg et al., 2009, Gong et al., 2002). The apoE protein acts as the main lipid transporter in the brain (Boyles et al., 1985, Pitas et al., 1987b) (Figure 1.8). ApoE is produced by glial cells and released into the extracellular space through triggering receptor expressed on myeloid cells 2 (TREM2) (Pitas et al., 1987a). ApoE in the extracellular space can also be lipidated by astrocytic ABCA1 receptors, which bind apoE and externalise cholesterol and phospholipids to form a HDL-like lipoprotein particle (Attie et al., 2001, Koldamova et al., 2014). These lipoproteins can be trafficked to neurons to maintain synaptic transmission and allow synaptogenesis (Zhang and Liu, 2015). The lipoprotein particles associate with neural low density lipoprotein (LDL) and low density lipoprotein receptor-related protein (LRP) receptors, which bind to apoE and are endocytosed along with the lipoprotein to facilitate lipid transport across the plasma membrane (Bu, 2009). Excess lipids are removed across the BBB into the bloodstream via LRP receptors. ApoE can bind to the microglial triggering receptor expressed on myeloid cells-2 (TREM2), which modulates the neural circuit by facilitating synapse elimination (Atagi et al., 2015, Bailey et al., 2015, Filipello et al., 2018). Synapse elimination is a key step in synaptic plasticity.

1.3.2 ApoE acts as a lipid transporter and lipoprotein constituent in the periphery

Lipids within the body derive from two sources, the diet and *de novo synthesis*. Cells can synthesise a range of lipids, and the remainder are provided through lipoprotein-mediated transport (Drin, 2014). ApoE plays an important role in lipid transport and metabolism in the periphery. The apoE protein is an amino acid glycoprotein, which acts as a component of the LDL, VLDL and HDL lipoprotein complexes and facilitates the transport of lipids between the intestine, liver and other cells within the body (Getz and Reardon, 2009). *APOE* allele regulates circulating levels of total cholesterol and triglycerides, probably due to amino acid substitutions which affect the ability of apoE to bind to receptors and lipids (Sing and Davignon, 1985, Dallongeville et al., 1992, Weisgraber et al., 1982, Saito et al., 2003). However, the effect of *APOE* allele on the rest of the plasma lipidome is unknown.

1.3.3 Genetic ablation of APOE causes cognitive deficit in mice

The roles of apoE in the brain have already been discussed (Section 1.2.1) and its importance is further demonstrated by knock-out studies in mice. There is less acetylcholine (ACh) activity in the hippocampus and frontal cortex of the *APOE* knock out mouse, and this is associated with a deficit in working memory, as measured by the Morris Water Maze (Gordon et al., 1995). Also, neurodegeneration has been described in the *APOE* knock out mouse (*ApoE*$^{-/-}$), and immunoreactivity of synaptic markers was up to 40 % lower in the neocortex and hippocampus, when compared to control mice (Masliah et al., 1995). Not all studies are in accordance, one did not find neurodegeneration or cognitive deficit after *ApoE*$^{-/-}$, although it did stress the presence of cardiovascular disease (Moghadasian et al., 2001). Cardiovascular disease is one of several factors which predisposes towards LOAD, as well as towards other forms of dementia (Whitmer et al., 2005, Newman et al., 2005). Therefore, neurodegeneration seen in the *ApoE*$^{-/-}$ mouse could be caused by two factors, apoE deficiency or vascular disease, or a combination thereof.

1.4 Alzheimer's Disease is a growing global burden with a complex pathology

As the population of the world increases and people live longer, the number of people suffering from age-related disease is rising. It's estimated that by 2050, 131.5 million people worldwide will be suffering from some form of dementia (Prince et al., 2015). The most common is Alzheimer's disease (AD), which accounts for 54 - 78 % of cases (Lobo et al., 2000, Barker et al., 2002), therefore representing a huge number of patients worldwide. Neurodegeneration, progressive cognitive deficit and behavioural changes are characteristic of AD, resulting in diminished short-term memory and reasoning, impairment of language, loss of visuospatial memory, and eventually death (Weintraub et al., 2012). The disease process takes place over decades, pathology is advanced before cognitive deficit occurs, and the long-term care needed is expensive (Braak and Braak, 1991, Morris et al., 1996, Souêtre et al., 1999). AD will put an increasing burden on healthcare worldwide unless an effective treatment is developed. Currently, licenced medications like Donepezil, Rivastigmine and

Galantamine alleviate symptoms and may slow neurodegeneration, but no cure has been found.

Early onset Alzheimer's disease (EOAD) makes up around 5 % of AD cases and is caused by autosomal dominant mutations in the genes apolipoprotein precursor protein (*APP)*, presenilin-1 (*PSEN1)* or presenilin-2 (*PSEN2)* (Zhu et al., 2015, Goate et al., 1991, Sherrington et al., 1995, Rogaev et al., 1995, Group, 1995). The APP, PSEN1 and PSEN2 mutations which cause EOAD cause an upregulation in production of the amyloid-β (Aβ) protein, causing a toxic build up of Aβ within the brain (Scheuner et al., 1996, Kumar-Singh et al., 2006, De Strooper et al., 1998). Disease-associated PSEN1 and PSEN2 mutations upregulate the activity of the γ-secretase enzyme, leading to increased Aβ in cell culture and CSF (De Strooper et al., 1998, Wolfe et al., 1999, Tomita et al., 1997). The pathology of EOAD can be explained fully by these genetic mutations. However, the aetiology of late-onset Alzheimer's disease (LOAD) is less well understood.

The largest genetic risk factor for LOAD is *APOE* (Table 1.5). The *APOE* ε4 allele raises risk of LOAD by 3 times if you carry one allele and 8 times if you carry two, and the presence of 1 or more ε4 alleles is associated with an earlier age of disease onset (Corder et al., 1993). On the other hand, the ε2 allele is protective; each copy lowers risk of LOAD by 4 times (Corder et al., 1994). The cumulative increase or decrease in risk is because each individual translates both *APOE* alleles into protein, therefore deficits in one apoE isoform can be partially restored by the presence of another isoform of the protein. The presence of an *APOE* ε4 allele is associated with an earlier age of disease onset and more amyloid deposits in the brains of LOAD patients (Corder et al., 1993, Drzezga et al., 2009). *APOE* ε2 is associated with a lower rate of amyloid and tau deposition and a lesser chance of developing LOAD (Tiraboschi et al., 2004, ALZGENE, 2010). The manner with which *APOE* confers disease risk is unknown, although there are several theories as to the role of *APOE* in neurodegeneration, which will be discussed below.

The delay between the start of LOAD pathology, cognitive deficit and diagnosis makes the study of the primary disease process difficult. The most well documented neuropathological hallmarks of Alzheimer's disease are extracellular amyloid plaques and intracellular tau

tangles. Alois Alzheimer also initially described a third pathology (lipid droplets) when defining AD, while other pathologies since discovered include neuroinflammation and synapse loss (Heneka et al., 2015, Sheng et al., 2012). The principal theories as to how LOAD progresses are discussed below, alongside evidence for lipid dysregulation in LOAD. It is worth noting that these theories do not stand alone, and pathologies are interlinked.

Developments in mass spectrometry (MS) have facilitated the study of lipidomics, which is the study of all lipids contained within a cell, tissue or organism (Shevchenko and Simons, 2010). Unlike the genome or the proteome, the human lipidome is poorly characterised, however lipids are tightly regulated, and many are bioactive (Drin, 2014). Thus, identification of lipid mediators could elucidate mechanisms both of homeostasis and disease. MS can be coupled with liquid chromatography (LC) to facilitate the study of a larger number of species. LC/MS lipidomics methods produce large amounts of data, which must be carefully processed. Bioinformatic tools, such as coding languages, allow the analysis of thousands of lines of data simultaneously. Herein, LC/MS has been combined with bioinformatics tools to study genes related to LOAD in both human and murine samples.

1.4.1 The amyloid hypothesis

The most well-known and long-standing theory behind the cause of AD is the amyloid hypothesis. In AD, amyloid proteins called amyloid-beta (Aβ), especially those 40 to 42 amino acid in length, accumulate in the extracellular space to form β-pleated sheets (Glenner and Wong, 1984, Wong et al., 1985, Joachim et al., 1988). These discoveries led to the hypothesis that LOAD pathology is instigated by deposition of amyloid in extracellular plaques in the brain (Glenner and Wong, 1984, Hardy and Allsop, 1991, Beyreuther and Masters, 1991).

Aβ is produced by sequential cleavage of APP (Chow et al., 2010). Cleavage can first occur at two sites along APP (Figure 1.9A), depending on which enzyme is present. Cleavage by α-secretase produces the neuroprotective sAPPα and c83, then cleavage of c83 by γ-secretase produces c3 and AICD (Furukawa et al., 1996). 'Amyloidogenic' cleavage of APP by β-secretase produces sAPPβ and c99, then cleavage of c99 by γ-secretase produces Aβ and AICD. Aβ may have several physiological roles (Pearson and Peers, 2006). For example, Aβ could regulate

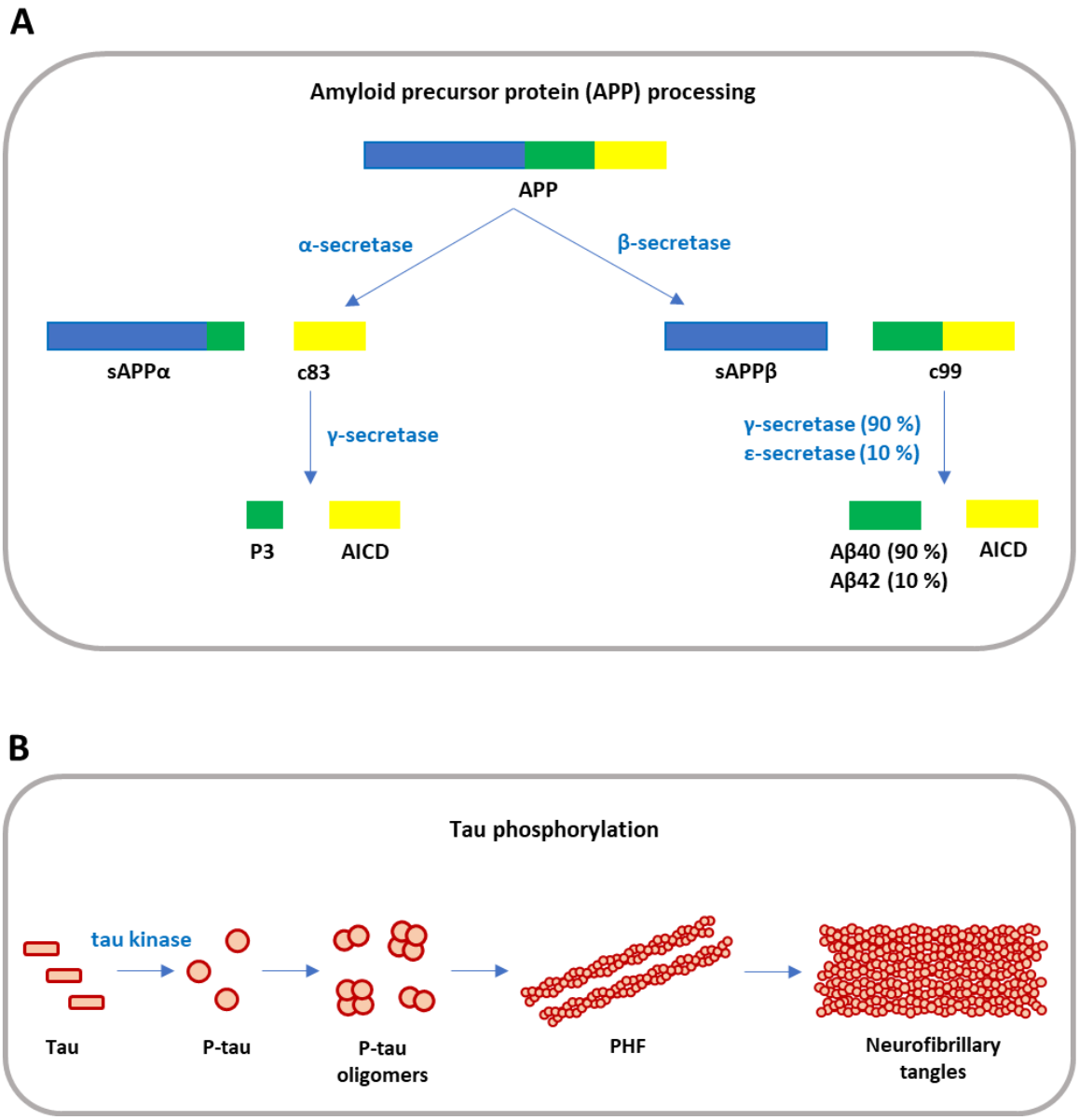

Figure 1.9: In LOAD, amyloid and tau proteins aggregate. A. Products of amyloid precursor protein (APP) cleavage are dependant on the secretase enzyme(s) present. Cleavage by α-secretase produces soluble APPα (sAPPα) and c83, which is subsequently cleaved by γ-secretase into P3 and amyloid precursor protein intracellular cytoplasmic/C-terminal domain (AICD). Cleavage by β-secretase produces sAPPβ and c99. c99 is cleaved preferentially by γ-secretase, producing AICD and the amyloidogenic species Aβ40. Around 10% of sAPPβ is cleaved by ε-secretase instead of γ-secretase, forming AICD and Aβ42. **B**. Tau phosphorylation leads to the build up of tau microtubules inside neurons (p-tau = phosphorylated tau, PHF = paired helical filiments). Tau is phosphorylated by tau kinases under normal circumstances to act as a molecular switch, however, aberrant phosphorylation allows p-tau to form oligomers, which can then form PHF and eventually, neurofibrillary tangles.

neurotransmission in the hippocampus, and it is present in the CSF of non-demented controls, as well as LOAD patients (Kamenetz et al., 2003, Tamaoka et al., 1997).

In LOAD, APP is preferentially cleaved along the amyloidogenic route (Fukumoto et al., 2002), causing soluble Aβ in the brain to rise and extracellular plaques of Aβ to form in a location and time-specific manner (Fukumoto et al., 2002, Braak and Braak, 1991). Amyloid pathology is associated with cognitive deficit and more extensive Aβ plaques tend to correlate with worsened cognition. However, the presence of one or two *APOE* ε2 alleles can partially negate this relationship, i.e. post-mortem samples have indicated that, whilst most *APOE* ε2 carriers are protected against amyloid deposition in the brain, some carriers have Aβ neuropathology but appear to have been protected against cognitive deficit prior to death (Nagy et al., 1995, Berlau et al., 2009). Also, other pathologies such as tau deposition are more correlated with cognitive deficit than Aβ (Barber, 2010). These data suggest *APOE* allele may affect cognition separately from Aβ. A global lipidomic analysis of *APOE* homozygote plasma could identify lipids which provide a cognitive benefit in *APOE* 2 plasma.

The amyloid hypothesis suggests that prevention or removal of amyloid plaques should prevent cognitive deficit. *In vivo* experiments have suggested that clearing amyloid plaques through Aβ-degrading enzymes is effective at reducing amyloid load, neurodegeneration and cognitive deficit (Marr et al., 2003, Leissring et al., 2003, Iwata et al., 2004, Poirier et al., 2006, El-Amouri et al., 2008). Clinical trials demonstrate that Aβ immunisation is effective at reducing amyloid plaque load in the brain (Nicoll et al., 2003, Nicoll et al., 2006, Bombois et al., 2007, Delnomdedieu et al., 2016). However, except for one phase I clinical trial, anti-amyloid treatment is not associated with a significant improvement in cognitive symptoms (Sevigny et al., 2016, Gilman et al., 2005, Holmes et al., 2008, Salloway et al., 2009, Farlow et al., 2012, Doody et al., 2014, Salloway et al., 2014). Trials have suggested that Aβ immunisation may have serious side effects. A phase II clinical trial of Aβ immunisation was halted after 6 % of participants developed meningoencephalitis (Orgogozo et al., 2003). Amyloid plaques cause structural disruption; however, *in vitro* and *in vivo* models suggest that soluble Aβ (sAβ) aggregates may be more neurotoxic (Kuo et al., 1996, Gong et al., 2003, Shankar et al., 2008). Aβ deposits could begin as a neuroprotective mechanism to sequester toxic soluble species (Brody et al., 2017). Failure of Aβ-clearing drugs to improve cognitive

symptoms could be due to treatment occurring too late in the disease process, as amyloid pathology is advanced when diagnosis occurs (Morris et al., 1996). Alternatively, it could be because soluble Aβ, or another factor such as lipid changes is driving cognitive deficit.

Lipids can modulate how APP is processed and the amount of amyloid deposited in the brain, as discussed later (Section 1.1.5.1). I suggest that a more complete disease model is needed which can explain amyloid and tau pathology, lipid changes, neuroinflammation and synaptic dysfunction. An investigation of the *APOE* plasma lipidome, as detailed in Chapter 5, could further the disease model by identifying lipids which could be affecting risk of LOAD. These lipids could be acting through the amyloid pathway or through another mechanism.

1.4.2 Tau phosphorylation leads to intracellular tangles

Neurofibrillary tau tangles are the second major neuropathology in LOAD (Brion et al., 1985, Braak et al., 1986). The tau protein, which is encoded by the microtubule-associated protein tau gene (*MAPT)*, is widely distributed around the nervous system and has several physiological functions (Andreadis et al., 1992, Trojanowski et al., 1989). For example, tau facilitates transport of vesicles along microtubules, as well as maintaining spacing between microtubules and other cell elements (Magnani et al., 2007, Chen et al., 1992). Tau has multiple potential binding partners, including the lipids phosphatidylinositol (PI) and PI bisphosphate and, therefore, could influence multiple signalling pathways (Morris et al., 2011, Surridge and Burns, 1994, Flanagan et al., 1997). Phosphorylation of tau is used as a molecular switch. For example, several phosphorylation sites have been identified which reduce the association of tau with microtubules (Drewes et al., 1995, Ksiezak-Reding et al., 2003, Sengupta et al., 1998).

In Alzheimer's disease (Figure 1.9B), tau is hyperphosphorylated, and accumulates in fibrils and paired helical filaments (PHF) inside neurons (Ksiezak-Reding et al., 1992, Köpke et al., 1993, Brion et al., 1985, Braak et al., 1986). Soluble p-tau aggregates into neurofibrils (NFs) and then neurofibrillary tangles (NFTs) (Alonso et al., 1996). Severity of tau pathology is associated with severity of Aβ deposition. Tau pathology develops after amyloid pathology and is more closely associated with cognitive deficit than amyloid (Braak and Braak, 1991).

Evidence suggests that the presence of large amounts of p-tau can disrupt normal cell functions. For example, p-tau filaments prevent kinesis-based neural axonal transport and cause synaptic dysfunction (Kanaan et al., 2011, Hoover et al., 2010). In fact, it has been suggested that, like amyloid, soluble p-tau is the most neurotoxic form (Kopeikina et al., 2012).

In vivo models suggest that targeting p-tau could improve neuropathology and reduce memory deficits. In a mouse model of tau-mediated neurodegeneration, pharmacological tau suppression restores spatial memory and brain weight (Santacruz et al., 2005). Interestingly, NFT formation continued after tau suppression, supporting the idea that NFTs are forming to sequester harmful soluble p-tau. Immunotherapy against p-tau reduces tau deposition and improves motor skills in a mouse model of tauopathy (Asuni et al., 2007). Also, *APOE* allele could modulate amount of p-tau produced and deposited within the brain. An *APOE* ε4 knock in mouse demonstrates more total tau in brain, more p-tau and more tau deposition than an *APOE* ε3 knock in (Shi et al., 2017). Therefore, lipidomic analysis of *APOE* homozygote plasma could suggest a lipid or set of lipids which could predispose towards higher tau deposition. Known interactions of lipids and tau are reviewed in Section 1.1.5.2.

Results from a recent phase III clinical trial suggest that treatment with a compound designed to prevent tau aggregation was effective at reducing cognitive deficit and slowing atrophy, but only when used alone (without currently licensed LOAD-treating medication) (Wilcock et al., 2018). Tau-directed therapies for LOAD merit further research. Statins, which are cholesterol lowering drugs, may reduce tau phosphorylation and deposition in LOAD (Section 1.1.5.2).

1.4.3 Inflammation in the central nervous system in LOAD

In LOAD, glial cells such as microglia and astrocytes are activated, promoting the release of inflammatory mediators such as cytokines (Griffin et al., 1989, Griffin et al., 1995). Also, some inflammatory genes are upregulated in a region-specific manner (Cribbs et al., 2012, Sudduth et al., 2013). This upregulation of inflammatory genes, activation of glial cells and production of inflammatory mediators is known as ‘neuroinflammation’. Activation of glial cells is

correlated with both amyloid and tau pathology (Sheng et al., 1997a, Sheng et al., 1997b). Neuroinflammation is mediated mainly by microglia, and to a lesser extent, astrocytes. Amyloid plaques contain microglia and astrocytes, and activation of these cells is also correlated with severity of tau pathology (Dickson et al., 1988, Sheng et al., 1997a).

1.4.3.1 Microglia

Astrocytes and neurons in the CNS are protected by microglial cells, which remain in state of active surveillance, patrolling the brain to search for threats (Nimmerjahn et al., 2005). During their resting phase, cell bodies remain in a fixed position whilst processes are mobile, extending, retracting and reforming repeatedly. Indeed, microglial processes could survey the extracellular space in the brain as often as every four hours. Microglia activate in response to threats or after damage to BBB, upon which they develop an amoeboid structure, thickening processes and increasing the volume of the cell body (Nimmerjahn et al., 2005, Cho et al., 2006).

There are two microglial phenotypes, distinguished by how activation occurs. These are designated as 'M1' or 'M2' microglia and can be distinguished by surface markers (Tang and Le, 2016, Colton, 2009). M1 microglia are classically activated microglia, characterised by the release of proinflammatory mediators such as interleukin-1 (IL-1), interleukin-6 (IL-6), tumour necrosis factor-α (TNF-α) and reactive oxygen species, as well as phagocytosis of nearby neurons (Upender and Naegele, 1999, Block et al., 2007, Smith et al., 2012). M2 microglia are in a state of either alternative activation or acquired deactivation (Tang and Le, 2016). The alternative activation M2 phenotype is characterised by release of interleukin-4 (IL-4) and interleukin-13, which activate genes preventing inflammation and promoting cell proliferation (Ponomarev et al., 2007, Pepe et al., 2017, Colton et al., 2006). Microglia exposed to interleukin-10 signals enter an anti-inflammatory state of acquired deactivation (Sawada et al., 1999, Tang and Le, 2016). Microglial phenotype depends on external signals and microglia exist along an activation scale, rather than in discrete and set groups (Boche et al., 2013). Examination of post-mortem tissue from LOAD patients suggests that patients demonstrate either predominantly M1 or M2 phenotype (Sudduth et al., 2013). However, in that small study, neither phenotype was protective.

During neuroinflammation, microglial activation is multifactorial. Microglia can be activated directly by Aβ, which is upregulated and aggregates in the brain of LOAD patients (Section 1.4.1). For example, Aβ can associate with CD36 receptors, Aβ scavenger receptor A (SRA), or toll-like receptors (TLR) 2 or 4 alongside their coreceptor CD14 (El Khoury et al., 2003, Reed-Geaghan et al., 2009, Walter et al., 2007, Stewart et al., 2010). These receptors then instigate the release of inflammatory mediators. IL-1 releasing M1 microglia are present at highest concentration in and around diffuse non-neural amyloid plaques (Griffin et al., 1995). Over half (55%) of enlarged microglia are associated with plaques, as are 91 % of phagocytotic microglia (Sheng et al., 1997b). Also, the number of IL-1α presenting microglia is positively correlated with the number of number of tau tangles (Sheng et al., 1997a).

Microglial activation mechanisms aim to clear aggregated protein and dying cells from the brain. For example, dying neurons externalise TREM2-L, which dimerises with microglial TREM2 to initiate phagocytosis (Hsieh et al., 2009). Human leukocyte antigen – DR isotype (HLA-DR) is upregulated in post-mortem AD brain, especially in amyloid plaques (McGeer et al., 1987). HLA-DR is an antigen presenting protein, which presents anti-Aβ antigens to trigger the protease-mediated degradation of soluble Aβ (Lee and Landreth, 2010). However, in neuroinflammation, chronic inflammation of glial cells becomes a secondary pathology, which causes further damage to the surrounding tissues (Hensley, 2010, Santiago et al., 2017). During activation by peripheral neural injury or cerebral ischemia, microglia surrounding the damaged area express APP, possibly exacerbating amyloid pathology in LOAD (Banati et al., 1993, Banati et al., 1995, Raivich et al., 1999, Griffin et al., 1995). In a transgenic mouse model of Alzheimer's disease, increasing inflammatory mediators is associated with a decrease in Aβ-binding receptors such as scavenger receptor A (Hickman et al., 2008).

1.4.3.2 Astrocytes

Astrocytes perform a range of functions, including lipoprotein release and immune functions such as antigen presentation (Dong and Benveniste, 2001, Nieweg et al., 2009, Gong et al., 2002). In LOAD, astrocytes are activated and immunoreactive for interleukin-1 and S-100 (Griffin et al., 1989). The number of S-100β-presenting astrocytes is also positively correlated with the number of tau tangles (Sheng et al., 1997a). Reactive astrocytes from LOAD brain

demonstrate increased APP, BACE-1 and γ-secretase, and release Aβ in a manner which could exacerbate amyloid pathology (Frost and Li, 2017).

1.4.4 Neurotransmitter hypothesis

There are many neurotransmitters within the human brain, with the prevalent excitatory neurotransmitters in the CNS being acetylcholine (ACh), glutamate and aspartate, and the main inhibitory neurotransmitter being GABA (Bear et al., 2006). Presynaptic neural activity stimulates neurotransmitter release from presynaptic membranes by exocytosis (Figure 1.10) (Fon and Edwards, 2001). Neurotransmitters defuse across the synapse and interact with postsynaptic receptors to initiate a post synaptic potential.

To treat LOAD, NICE only recommends drugs based on the neurotransmitter hypotheses described below. Three of these drugs (donepezil, galantamine, and rivastigmine) are ACh inhibitors and memantine is an N-methyl-D-aspartate (NMDA) antagonist. These four licensed drugs treat symptoms and slow neurotransmitter-related neurodegeneration, thereby slowing cognitive decline. They are not targeted towards preventing amyloid or tau pathology, do not halt or reverse neuropathology and are not effective throughout the disease process.

1.4.4.1 Acetylcholine hypothesis

ACh is an excitatory neurotransmitter, which is widely distributed around the brain and is a ligand for many receptor types (Macintosh, 1941, Ishii and Kurachi, 2006, Dani, 2015). ACh activity in LOAD is reduced in the hippocampus and cerebral cortex, causing loss of cholinergic neurons and memory loss (Drachman, 1974, Bowen et al., 1976, Perry et al., 1977, Perry, 1978, Whitehouse, 1982, Rylett, 1983). The basal nucleus of Meynert is the source of cholinergic innervation for most of the forebrain, and it is the first region from which cholinergic neurons are lost (Mesulam, 1976, Whitehouse et al., 1981, Sassin et al., 2000). Cytoskeletal changes in this region in the early stages of LOAD are followed by loss of downstream cholinergic neurons. Choline acetyltransferase (ACh producing enzyme) activity

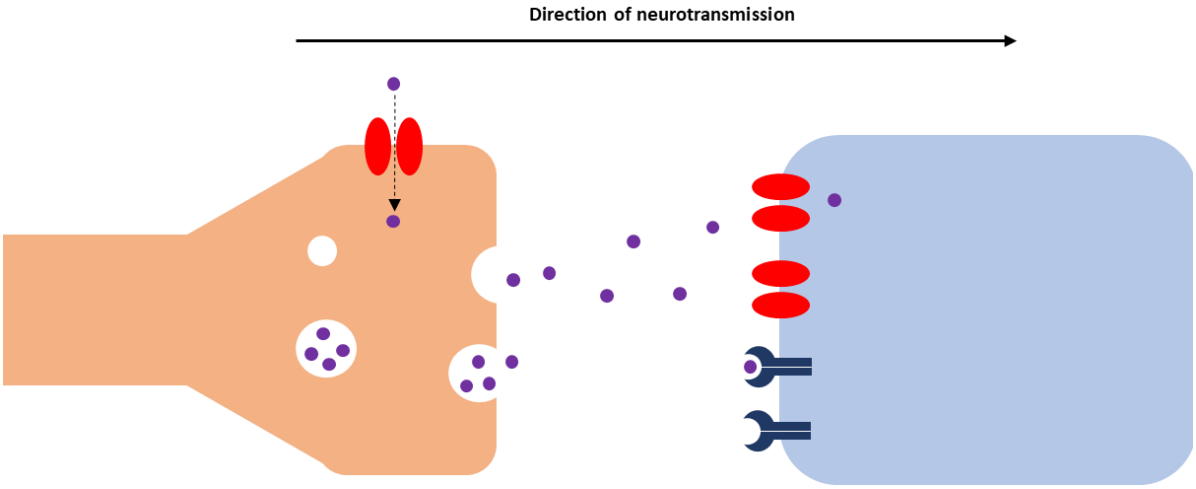

Figure 1.10: Neurotransmission is regulated presynaptically by neurotransmitter release and postsynaptically by dendritic receptors. Neurotransmitters are produced in the presynaptic cell, or trafficked from the synapse back into the synaptic bouton. Neurotransmitters are packaged into vesicles, which are released when stimulated by a change in the membrane potential (due to the arrival of an action potential). Neurotransmitters defuse across the synapse and interact with post synaptic receptors, which can be ionotrophic (red) or metabotrophic (dark blue). Post synaptic receptors then trigger an action potential in the post-synaptic cell if a threshold signal is reached,

is negatively correlated with Aβ deposition and neurofibrillary tangles (Perry et al., 1978, Geula et al., 1998). Aβ oligomers in post mortem brain are associated with a reduction in ACh receptors (Bao et al., 2012).

Three of the four drugs licensed to treat LOAD act on the cholinergic system and prevent the cholinesterase-mediated degradation of ACh (Hansen et al., 2008). This increases the amount of ACh available at the synapse, preventing synaptic pruning and reducing neurodegeneration related to the loss of ACh-releasing neurons. Donezepil, galantamine and rivastigmine all prevent degradation of ACh by cholinesterase, whilst galantamine also acts allosterically on the ACh receptor and rivastigmine also inhibits butyrlcholinesterase, another ACh-cleaving enzyme (Lilienfeld, 2002, Mesulam et al., 2002). All of these drugs can slow brain atrophy and rate of cognitive decline (Summers et al., 1986, Hashimoto et al., 2005, Cavedo et al., 2016, Cavedo et al., 2017, Giacobini, 2001, Prins et al., 2014, Wilcock et al., 2000, Tariot et al., 2000, Lilienfeld and Parys, 2000, Corey-Bloom et al., 1998, Rösler et al., 1999). There are mixed results with regard to if the effects of galantamine can be modulated by *APOE* genotype. Whilst one study found that galantamine treatment improved cognition regardless of *APOE* genotype (Wilcock et al., 2000), MRI suggests that galantamine slows the rate of brain atrophy in patients with mild cognitive impairment, but only in *APOE* ε4 carriers (Wilcock et al., 2000, Prins et al., 2014).

1.4.4.2 Glutamate hypothesis

The final drug licensed to treat LOAD is memantine, which is an NMDA receptor antagonist (Johnson and Kotermanski, 2006). In LOAD, the number of glutamate receptors in the cortex is significantly reduced, especially in the hippocampus, while glycine and glutamine (glutamate precursors) are lower in CSF (Greenamyre et al., 1985, Cowburn et al., 1988, Smith et al., 1985). High levels of glutamate are neurotoxic and cause excitotoxicity through an influx of Ca^{2+} (Olney and Sharpe, 1969, Olney, 1969, Manev et al., 1989). The glutamate hypothesis is that cell death in LOAD is caused by an excess of extracellular glutamate, due to either excess production, excess release, or a decrease in reuptake (Maragos et al., 1987). Glutamate receptor density is preferentially lost as glutaminergic receptors are concentrated

in dendrites which are surrounding areas of excess glutamate release. Memantine blocks the effects of excess glutamate by partially preventing NMDA-R activity through its activity as an NMDA receptor antagonist (Johnson and Kotermanski, 2006).

Clinical trials of memantine have mixed results. Memantine provides a significant cognitive benefit in moderate to severe AD patients and adding memantine to donezepil treatment improves score in the Mini-Mental State Examination compared to donezepil alone (Howard, 2011, Tariot et al., 2004). However, several trials have also concluded that memantine has no significant effect on LOAD symptoms (Ballard et al., 2013, Schneider et al., 2011). In contrast to Tariot et al. (2004), other studies concluded that combination treatment with memantine is not any more effective than treatment with donezepil alone (Porsteinsson et al., 2008, Howard et al., 2012).

1.4.5 A strong body of evidence links lipids with cognitive deficit

The least studied of the Alzheimer's disease pathologies is the 'lipid droplet' described by Alois Alzheimer in 1901. There is a growing body of evidence implicating lipids in LOAD pathology. In fact, a Pubmed search for "lipid" plus "Alzheimer's disease" gave 14,559 results as of the 31st of October, 2018. A search for "lipidomics" and "Alzheimer's disease" provided 89 results and relevant studies are discussed below, as well as papers found whilst considering the literature. It should be noted that this search only flagged papers with lipidomics in the title or abstract. Therefore, this method will have underestimated the true number of lipidomics papers available.

Results from cell culture suggest that the composition of the plasma membrane regulates γ-secretase activity. The lipids around the membrane-bound γ-secretase complex are important to enzyme function and some phospholipids will abolish activity if present in microdomain around the γ-secretase complex (Aycirіex et al., 2016). For example, the presence of charged lipids in cell membrane reduces γ-secretase activity, as hydrogen bonds form between charged lipid and γ-secretase, which prevent its activity (Aguayo-Ortiz et al., 2018). These data raise the possibility of targeting cell membrane composition to modulate Aβ pathology. Drugs targeting cell membrane composition are already being trialled to treat some forms of cancer.

For example, NaCHOleate alters cell membrane levels of sphingomyelin, DAG and phospholipids through inhibition of sphingomyelin synthase (Lladó et al., 2014). Therefore, this could provide a novel anti-amyloid therapy in the future.

Lipidomic analyses have described differences in plasma or serum relating to LOAD; these are diverse and occur across several lipid categories. Several eicosanoids have been described as changing in the circulation in LOAD. Linoleic acid decreases and mead acid increases in LOAD patients, and changes are correlated with disease stage (Iuliano et al., 2013). Also, there is an increase in the ratio of arachidonic acid to docosahexaenoic acid ratio in plasma of converters (from control to disease) prior to conversion, but only in the presence of an *APOE* ε4 allele (Abdullah et al., 2017). Cholesterol esters (sterol lipids) have been implicated as circulating markers of LOAD. Lipidomics of plasma suggests that putatively identified long-chain cholesterol esters are reduced in MCI and AD (Proitsi et al., 2015). A follow up concludes that a panel of 24 lipids can be used to distinguish AD participants from control with over 70 % accuracy, and masses of many of these lipids match CE and TAG (glycerolipid) species (Proitsi et al., 2017). Another comparison in serum found TAGs and phospholipids are significantly altered in AD compared to control and these were confirmed in second sample group (Anand et al., 2017). Phospholipids have also been implicated as altered in LOAD. Of four serum biomarkers of LOAD, identified in a screening and confirmed in a second sample group, 3 were phosphatidylcholines (PCs) (Shah et al., 2016). A lipidomic analysis, also of serum, using multivariate analysis revealed a panel of lipids which could distinguish AD from control (González-Domínguez et al., 2014). This panel included PCs, DAGs, an eicosanoid and several proteins. DAGs and ethanolamine plasmalogens were measured and used to stratify patients into three groups which were present both in MCI and AD, suggesting heterogeneity within disease groups (Wood et al., 2016). Finally, sphingolipids are also disrupted in LOAD. Sulfatides and PE plasmalogens are reduced in plasma of LOAD patients and ceramides are increased (Han, 2010). Another study found ceramides were again increased, and 8 plasma sphingomyelins were decreased (Han et al., 2011).

Lipidomic analyses of post-mortem brain samples confirm lipids, particularly sphingolipids, phospholipids and glycerolipids, are altered in regions of neurodegeneration. Amyloid plaques dissected from post-mortem brain of LOAD patients demonstrate significantly higher

levels of Cer(d18:1/18:0) and Cer(d18:1/20:0) (Panchal et al., 2014). Mining of existing neurolipidomics datasets reveals alterations in phospholipids, oxidised phospholipids and ether lipids, which suggest membrane remodelling (Bennett et al., 2013). This is in contrast with normal aging, during which the phospholipids in the entorhinal cortex remain fairly stable (Hancock et al., 2017).

Sulfatide levels are lower in brain of preclinical LOAD patients (some pathology but no cognitive symptoms) compared to controls, which mirrors changes seen in animal models (Cheng et al., 2013, Cheng et al., 2010). Lipidomics suggests that the sulfatide reduction in human and animal brain in LOAD/EOAD is due to alterations in apoE-mediated transport (Han, 2007, Cheng et al., 2010). Also, gangliosides containing ceramide are reduced in hippocampal grey matter in AD (Taki, 2012). In prefrontal cortex in LOAD patients, sphingolipids and DAGs are increased, whilst in entorhinal cortex, sphingomyelin, CEs, lysobisphosphatidic acid and ganglioside GM3 are increased (Chan et al., 2012). Changes in CEs and GM3 were also confirmed in mouse model of EOAD. MAGs and DAGs (glycerolipids) are increased in frontal cortex, grey matter, plasma and CSF in MCI, suggesting a possible staging mechanism for LOAD (Wood et al., 2015b, Wood et al., 2015a). Also, PEs are reduced in grey matter in both MCI and LOAD (Wood et al., 2015a). The increase in DAGs has been suggested to reflect immune activation (Wood et al., 2018). Finally, fatty acyls, which are eicosanoids, are increased in parietal lobe of moderate but not severe AD, suggesting that lipidomics changes are not linear throughout the disease process. (Nasaruddin et al., 2018).

Animal models also implicate lipids in neurodegeneration. Metabolism of the eicosanoids, linoleic acid and arachidonic acid, as well as sphingolipids, is altered in serum in a murine model of EOAD (Gao et al., 2018). Sixteen lipid markers of LOAD were identified, which included eicosanoids and sphingolipids. Also, an endocannabinoid (lipid neurotransmitter), which increases with age, is significantly decreased in the striatum in EOAD, as well as CEs (Maroof et al., 2014). Lipids are also altered in brain samples in EOAD models. Inhibiting hippocampal sphingomyelin synthase 1, which catalyses the conversion of ceramide using a modified adenovirus reduces amyloid plaque density, synaptic loss and cognitive deficit as measured by the novel object recognition test and Morris Water Maze (MWM) (Lu et al., 2019). This seems in contrast with data from studies of plasma, as in both animal and human

studies, ceramides have been increased and sphingomyelin decreased. Several studies have also described alterations in phospholipids in the murine brain during EOAD. Mice with human APP (hAPP) knocked in and phospholipase A2 knocked out (enzyme which cleaves fatty acyl from sn2 position of phospholipids) perform better at tests of memory than mice which have hAPP knocked in alone (Sanchez-Mejia et al., 2008). Moreover, Aβ oligomers added to cell culture are neurotoxic in a phospholipase A2-dependant manner. There is also a plaque-specific increase in PIs which contain arachidonic acid and lyso-PIs (PI degradation products) (Michno et al., 2018). In 3 x TG mouse brain PCs and ethanolamine plasmalogens are increased (Monteiro-Cardoso et al., 2015). These phospholipid changes could be due to Lands cycle changes, seen in the cortex in two animal models of AD, which cause alterations in PCs, lyso-PCs and PAF (Granger et al., 2018). Taken all together, investigations of human and animal models, using both brain and plasma or serum, suggest that metabolism of sterol lipids, GPs, glycerolipids and sphingolipids is perturbed in AD, and that some of these changes may be mechanistic (Figure 1.11).

It is currently unknown how risk factors for LOAD like *APOE* affect the lipidome of the brain and blood. I investigated the *APOE* homozygote plasma lipidome to identify which circulating lipids could be associated with a change in risk of LOAD and theorise how this process could be occurring. This is the first such analysis of human *APOE* homozygote plasma and as such could identify novel or risk-associated lipids.

1.4.5.1 Circulating cholesterol may regulate Aβ deposition

In vitro, *in vivo* and longitudinal studies have suggested that long-term statin use may be protective against amyloid pathology. Statins are drugs, currently licenced to lower cholesterol, which inhibit 3-hydroxy-3-methylglutaryl-coenzyme A (HMG-CoA) reductase and the mevalonate pathway, reducing cholesterol production (Stancu and Sima, 2001). Cholesterol accumulates in the amyloid plaque and investigations in neural cell culture suggest that cholesterol could regulate APP processing (Mori et al., 2001). Solubilising membrane cholesterol reduces α-secretase cleavage of APP, therefore APP is preferentially metabolised by BACE1 and γ-secretase, which produces the precursor of Aβ (Bodovitz and Klein, 1996). Supporting this, treatment of neurons with statins reduces cholesterol and

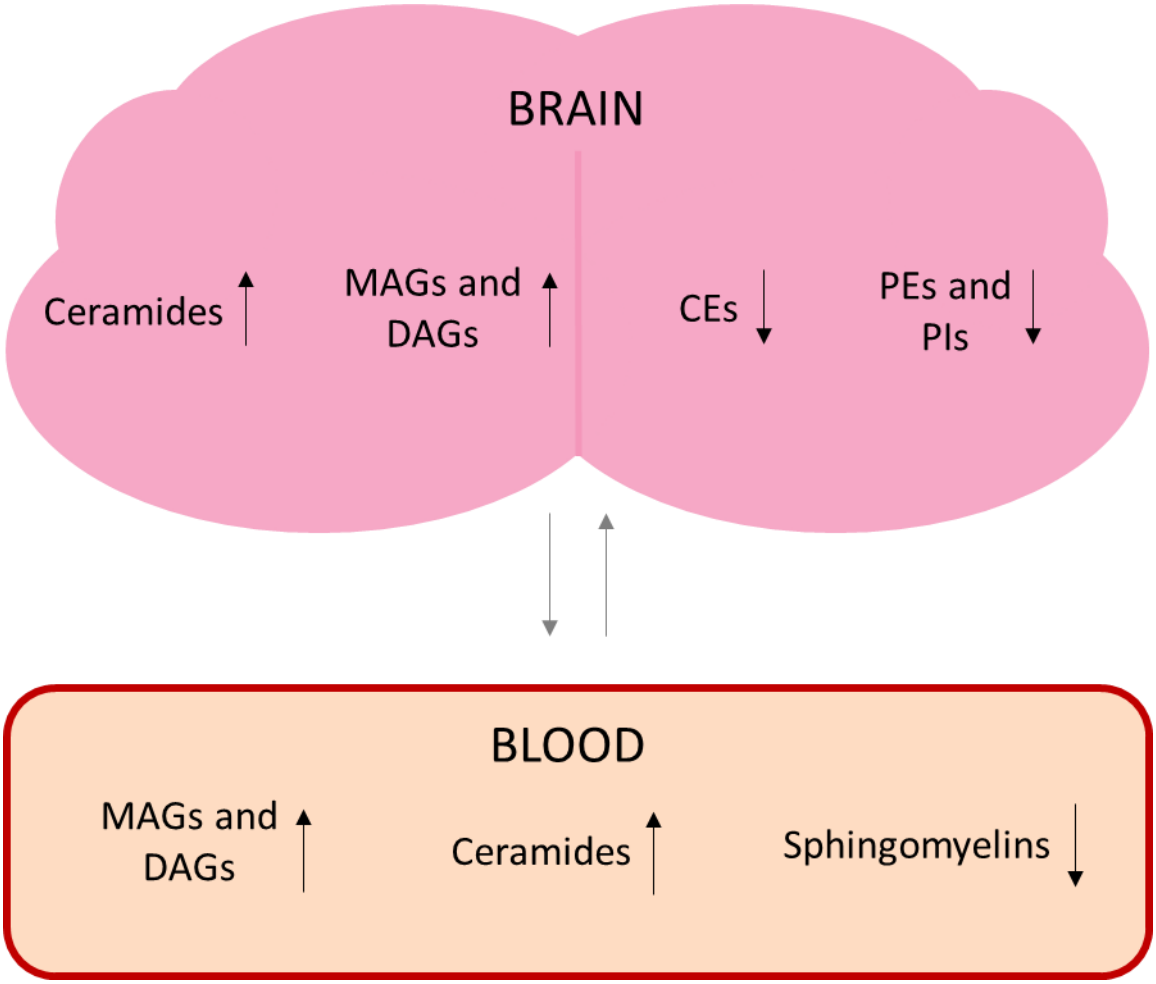

Figure 1.11 Lipid metabolism is altered in the plasma and brain of LOAD patients. All differences in lipid levels included in this figure have been described by at least two independent studies using human samples or have been recorded in both human samples and animal models. MAGs = monoacylglycerols, DAGs = diacylglycerols, CEs = cholesteryl esters, PEs = phsophatidylethanolamines, PIs = phosphatidylinositols.

therefore, Aβ production and release (Simons et al., 1998, Fassbender et al., 2001). Also, treatment of cultured neurons with cholesterol, which increases membrane cholesterol, reduces amyloid transport and increases endosome size in a manner similar to that seen in LOAD (Marquer et al., 2014).

Cholesterol lowering drugs could lower Aβ production through inhibition of formation of 'lipid raft' regions. Cholesterol is required for the formation of lipid rafts, which are phase ordered membrane segments consisting of central motifs of cholesterol and glycosylphosphatidylinositol (GPI), surrounded by sections rich in cholesterol, GPs and sphingolipids (de Almeida et al., 2003). Lipid rafts favour amyloidogenic processing of APP via BACE1 and γ-secretase, whilst a larger proportion of APP is processed by α-secretase in non-ordered membrane regions (Ehehalt et al., 2003). Also, in a macromolecular crowding environment which mimics the cell environment, Aβ accumulates in the lipid bilayer, but only in ordered lipid raft regions (Hirai et al., 2018). Thus, Aβ could accumulate faster in phase ordered membrane regions.

Evidence suggests Aβ could regulate lipid metabolism. Aβ40 inhibits hydroxymethylglutaryl-CoA reductase (HMGR) activity, therefore decreasing mevalonate pathway activity and reducing de novo synthesis of cholesterol in murine fibroblasts (Grimm et al., 2005). This could represent a negative feedback mechanism whereby cholesterol synthesis is reduced to slow the rate of Aβ production. Taken together, data from *in vitro* studies suggest that (i) cholesterol can regulate Aβ production through lipid raft stabilisation, (ii) amyloid can likewise moderate lipid production and (iii) a low cholesterol environment could be protective against amyloid pathology.

In vivo models also demonstrate that circulating cholesterol may regulate Aβ. In a double knock in mouse (hAPP and hPSEN1), a cholesterol lowering drug reduces absolute Aβ in brain immunostaining (Refolo et al., 2001). Simvastatin treatment of healthy guinea pigs reduced Aβ in CSF and brain tissue (Fassbender et al., 2001). Atorvastatin reduced Aβ deposition in rat brain, which was induced by a high fat diet (Lu et al., 2010). Treatment of the triple transgenic (3xTG) mouse model, which carries mutations in APP, PSEN1 and MAPT, with simvastatin reduced cognitive deficit and amyloid deposition (Zhou et al., 2016). Interestingly, the Tg2576

(APP mutant) murine model of AD demonstrates phospho-tau deposition within lipid rafts after accumulation of Aβ, suggesting that disrupting lipid rafts via lowering cholesterol could be a target to reduce tau pathology (Kawarabayashi et al., 2004).

In LOAD patients, plasma cholesterol metabolism is altered (Sittiwet et al., 2018). Clinical trials of statins in patients with AD have produced mixed results. Daily atorvastatin treatment is associated with significant improvement in three clinical measures of cognition at one year: Alzheimer's Disease Assessment Scale Cognitive subscale (ADAS-Cog), Alzheimer's Disease Cooperative Study Clinical Global Impression of Change (ADCS-CGIC) and Neuropsychiatric Inventory Scale after 12 months (Sparks et al., 2005). However, a trial of 72 weeks of atorvastatin in mild to moderate Alzheimer's disease patients found no positive effect on cognition as measured by ADAS-Cog and ADCS-CGIC, despite a significant reduction in circulating cholesterol (Feldman et al., 2010). It is worth noting that patients were weaned off statins prior to cognitive testing, therefore possibly negating a temporary effect of statin use on soluble Aβ, which is implicated in memory deficit (Lue et al., 1999). Twenty-four weeks treatment with simvastatin reduced cholesterol but did not improve ADAS-Cog scores (Sano et al., 2011). According to one piece of research, statins reduced circulating cholesterol and Aβ40 in CSF of mild AD but not in severe disease, suggesting that disease staging could be affecting the effectiveness of cholesterol treatment in some studies (Simons et al., 2002). Finally, a large study of over 1,000 healthy individuals found that long-term (5+ years) statin use did not significantly improve cerebral amyloid deposition, or prevent neurodegeneration or changesso in white matter intensity (Ramanan et al., 2018).

Reviews of the clinical trial literature differ on whether statins are providing a cognitive benefit, one reanalysed data to conclude that atorvastatin provides a small cognitive improvement in the form of the ADAS-Cog, whilst another found no significant change when comparing statins versus control (Geifman et al., 2017, McGuinness et al., 2014). Geifman et al. (2017) may have detected statistically significant improvement as atorvastatin alone (but not all statins combined) is associated with a reduction in AD risk. Longitudinal studies also provide some support for the use of statins to treat dementia. A large investigation of patient data suggests that statin use is associated with a 60 – 70 % reduced risk of LOAD compared to other CVD-treating medications (Wolozin et al., 2000). A recent meta-analysis of 25

populations using random effects models concluded that use of statins overall was associated with a reduced risk of dementia (Chu et al., 2018). However, it has been suggested that statin use only reduces risk of LOAD when other comorbidities were present (Zamrini et al., 2004).

To summarise, *in vivo* and *in vitro* work suggests that lowering cholesterol may be a viable route to reducing Aβ production in mild LOAD. Statins lower cholesterol and may prevent amyloid and tau pathology, however results from clinical trials are mixed on whether statins provide a cognitive benefit. Longitudinal studies suggest that effectiveness of statin treatment could be dependent on other factors such as concurrent disease. As such, more research is needed to determine if statin treatment is effective in treating a subset of LOAD patients.

1.4.5.2 Circulating cholesterol may regulate amounts of phosphorylated tau

Various investigations have linked statins with a reduction in p-tau, the hyperphosphorylated form of tau which aggregates in LOAD. In neural cell culture, arvostatin and lovastatin prevent tau phosphorylation, and pitavastatin reduces both total tau and p-tau by reducing the amount of membrane-associated Rho family G proteins (Sui et al., 2015, Li et al., 2015, Hamano et al., 2012). *In vivo*, treatment of mutant APP mice with atorvastatin and pitavastatin reduces p-tau in the brain and cognitive deficit, but only after a minimum of 10 months treatment (Kurata et al., 2011). Statins also reduce p-tau in high-fat-fed rats (Lu et al., 2010). A murine model of EOAD (knock in human pro-Alzheimer's APP/PSEN1) suggests that a week of statin treatment could reduce memory deficits in 2 behavioural tests and reduce tau phosphorylation though the AKT/GSK3β signalling pathway (Zhou et al., 2016). In a tauopathy model, treatment with simvastatin or atorvastatin reduces neurofibrillary tangle burden after 2 and 5 months, and authors suggested that this was through a reduction in neuroinflammation, as tau deposition is associated with the number of activated microglia (Boimel et al., 2009).

Analysis of post-mortem brain samples of LOAD patients demonstrates that statin use is associated with fewer NFTs (Li et al., 2007). Longitudinal studies and clinical trials have yielded mixed results. Biomarkers of LOAD such as total tau and p-tau do not significantly change in CSF of healthy adults after statin treatment (n = 25) (Li et al., 2017). Simvastatin for 12 weeks

reduced cholesterol production in the brain but did not reduce p-tau depositions (Serrano-Pozo et al., 2010). Also, 14 weeks of simvastatin (but not atorvastatin) reduced p-tau in CSF of AD patients but no other pathology was improved (Riekse et al., 2006). However, animal research suggests that statin treatment is effective long (but not short) term, which has implications for short term trials of statins for cognitive benefit (Kurata et al., 2011).

A 4-month treatment of the middle-aged children of LOAD patients with simvastatin lowered total tau (and Aβ) in CSF and also improved performance in some tests of cognition (Carlsson et al., 2008). Contrastingly, a large trial of over 1,000 participants using neuroimaging techniques suggests that 5 years or more of statin treatment did not prevent or reduce neurodegeneration, tau pathology, or other LOAD pathologies measured (Ramanan et al., 2018). The type of statin used could affect trial outcome; a comparison of 6 statins found that simvastatin improved cognitive performance over a number of tests and is the most likely candidate for neuroprotection as it can cross the BBB (Sierra et al., 2011).

The relationship between statin use and tau pathology is not yet elucidated. Trials have mixed results and outcomes could be affected by types of statin used and length of statin treatment. If high circulating cholesterol and CEs can cause tau pathology, quantifying cholesterol and CEs in *APOE* homozygote plasma could indicate if one allele is more or less predisposed towards tau pathology.

1.4.5.3 Dietary medium chain TAGs have been trialled as a treatment for LOAD

In Alzheimer's disease, hypometabolism of glucose occurs in the hippocampus, temporal lobe and parietal cortex, which is worsened by the presence of *APOE* ε4 (Small et al., 1995). This hypometabolism can be used to predict conversion from normal cognition to MCI or dementia (de Leon et al., 2001, Small et al., 1995). It has been suggested that medium chain triglycerides (MCTs) could act as a substitute energy source, providing a source of ketones, thereby improving cognition (Costantini et al., 2008). MCTs are TAGs with fatty acyl tails of 6 – 12 carbons in length, which are not found under physiological conditions. There have been several small clinical trials of medium chain TG (MCTs) in Alzheimer's disease.

MCTs with leucine and vit D improved MMSE scores by 30 % in elderly adults (n = 38) (Abe et al., 2017). Another small study (n = 28) found that 90 days of MCT supplement improves MMSE scores in LOAD patients with an entry MMSE score ≥15, but not in those with more severe mental impairment (Kimoto et al., 2017). However, a review of 3 earlier trials concluded that MCTs were useful in *APOE* ε4 patients only, and that as genetic profiling of patients is not routinely performed in a healthcare setting, MCTs are not currently a useful tool for treating LOAD (Sharma et al., 2014). In fact, it is unclear whether lipids within the brain are responsive to changes in dietary fat profile, and studies disagree on whether ingested fatty acyls are integrated into lipids within the CNS (Abbott et al., 2012, Bascoul-Colombo et al., 2016). More research is needed in this area, although this is beyond the remit of my thesis.

1.4.5.4 Lipids mediate the resolution of neuroinflammation

Lipids with anti-inflammatory properties, known as specialised pro-resolving mediators (SPMs), could aid the resolution of a pathological inflammatory state (Serhan et al., 2002, Wang et al., 2015, Lee et al., 2018). For example, resolvins, a subcategory of fatty acyls, inhibit microglial cytokine release and reduce inflammation peripherally (Serhan et al., 2002). A study of SPMs and their receptors in CSF and brain samples from LOAD patients demonstrates that the SPM lipoxin A4 is reduced in the CSF and hippocampus of LOAD patients (Wang et al., 2015). Lipoxin A4 and resolvin d1 in CSF both correlate with score in the MMSE. Also, 15-LOX-2 (a lipoxin a4 synthesising enzyme) and the SPM receptors lipoxin A4 receptor and ChemR23 are all elevated in brain tissue from LOAD patients. Together, this suggests a dysregulation in SPM homeostasis, possibly through SPM upregulation and exhaustion. SPMs are upregulated by elevated sphingosine kinase 1 (SphK1), and conversely, both SphK1 and SPMs are downregulated in the brain of an AD mouse model (Lee et al., 2018).

1.4.5.5 Lipids support synapse function

Lipids pay important and varied roles in the support of neural activity and synaptic function. For example, the insulating myelin sheath around neurons is made up of many layers of lipid bilayer (Horrocks, 1967). Neurons use lipids as an energy source and lipid metabolism is tightly

regulated (Tracey et al., 2018). Also, at the synapse, correct membrane composition is required alongside protein complexes to facilitate endocytosis and exocytosis (Mochel, 2018).

1.5 12/15-lipoxygenase has been implicated in pathology of LOAD

12/15-lipoxygenases (12/15-LOX) are a set of lipid-modifying enzymes, which have been implicated in LOAD through research into cell culture, animal models and human samples. 12/15-LOX catalyses the addition of oxygen to fatty acyls with double bonds on either the 12th or 15th carbon atom (Brash, 1999). Substrates are arachidonic acid and docosahexaenoic acid (DHA), which can be free or esterified, and LOX products (HETEs and HDOHEs) and their downstream effectors have a number of biological functions (Brash, 1999, Dobrian et al., 2011). Humans produce tissue-specific isoforms of 12/15-LOX, namely 12S-LOX (platelet type), 12R-LOX (epidermis type), 15-LOX-1 (reticulocyte and leukocyte type) and 15-LOX-2 (epidermis type) (Brash, 1999). Human LOX enzymes can form mixtures of products, for example, 15-LOX (reticulocyte type) can produce some 12-HPETE as well as preferentially producing 15-HPETE. Mice only express 12-LOX, however, the murine leukocyte-type 12-LOX preferentially produces 12-HPETE, but also can form small amounts of 15-HPETE (Chen et al., 1994). 12/15-LOX is found in murine neurons within the brain, especially under stress conditions (van Leyen et al., 2006). LOX enzymes are highly conserved across mammalian species (Kuhn et al., 2015). Within this thesis, human 12- and 15-LOX and murine 12-LOX will be referred to as 12/15-LOX to reflect their similar distribution and products. The primary 12/15-LOX products are HPETEs or HDOHEs, depending on whether the substrate is arachidonic acid or DHA (Figure 1.12). It should be noted that some downstream products of 12/15-LOX (lipoxins, hepoxilins, resolvins and protectins) are SPMs (Section 1.4.5.4) (Serhan and Petasis, 2011, Serhan, 2014).

Several studies in cell culture have suggested a role for 12/15-LOX in cell death. Initially, it was noted that glutathione depletion causes cell death through a 12/15-LOX-dependent mechanism, suggesting a role for the enzyme in Parkinson's-type neurodegeneration (Li et al., 1997). 12/15-LOX was then implicated in amyloid production, for example, pharmacological inhibition of 12/15-LOX in CHO and N2A cells reduces supernatant Aβ, sAPPβ and BACE1

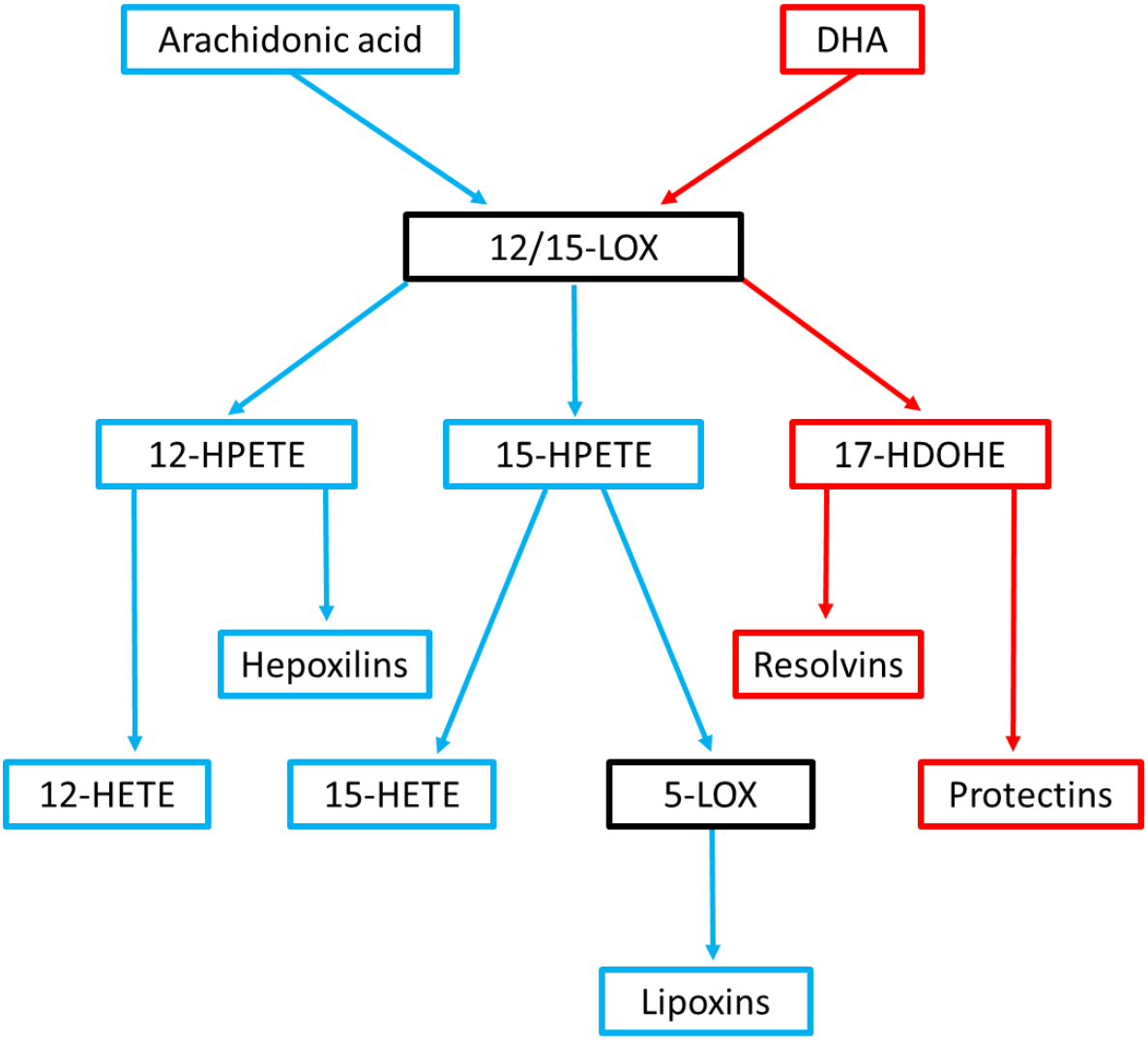

Figure 1.12: Products of 12/15-LOX and arachidonic acid or DHA. Possible substrates of 12/15-LOX include arachidonic acid and DHA. Immediate products of fatty acids and 12/15-LOX are HPETEs, which are then reduced to HETEs, hepoxilins, resolvins and protectins. 15-HPETE combined with 5-LOX can also produce lipoxins.

(Succol and Pratico, 2007). Also, 12-LOX inhibition in neural culture prevents Aβ-induced apoptosis and glutamate toxicity (Lebeau et al., 2004, Yao et al., 2005, van Leyen et al., 2008).

Both animal and human studies demonstrate that 12/15-LOX and its products are altered in LOAD (Figure 1.13). Inhibition of 12-LOX in murine models of AD also prevents neurodegeneration and associated cognitive effects. Genetic or pharmacological 12/15-LOX inhibition reverses cognitive impairment and Aβ and tau pathology in the 3xTg AD mouse model (Yang et al., 2010, Chu et al., 2015, Di Meco et al., 2017). Conversely, in the same mouse model, overexpressing 12-LOX is associated with higher levels of Aβ expression and deposition, as well as increased p-tau in the hippocampus and a reduction in synaptic marker density (Chu et al., 2012, (Giannopoulos et al., 2013). P-tau was not reduced by pharmacological inhibition of γ-secretase, suggesting that 12-LOX could modulate tau phosphorylation independently of Aβ.

However, one particular LOX product, lipoxin a4, is associated with improved cognition. Treatment of the 3xTG AD mouse model with lipoxin a4, a product of 12-HPETE, improves memory, reduces Aβ and reduces p-tau deposition (Dunn et al., 2015). This is supported by work in human brain, which demonstrates low lipoxin a4 in CSF and hippocampus in LOAD, as well as increased upregulated 15-LOX-2 in astrocytes and microglia (Wang et al., 2015).

Meanwhile, 12/15-LOX levels and other LOX products are increased in human brain samples in LOAD. 12/15-LOX enzyme is increased in frontal cortex and temporal cortex in brain samples of LOAD patients, as are the enzyme products 12- and 15-HETE (Praticò et al., 2004, Yao et al., 2005). These changes were associated with an increase in oxidative stress markers. Interestingly, this increase was more marked in Braak and Braak stage I-IV than stages V-VI, suggesting that 12/15-LOX increases may play a role in the early stages of LOAD pathogenesis. Together, these data suggest that dysregulation of 12/15-LOX signalling may take place in LOAD (Figure 1.6B).

As 12/15-LOX has been implicated in several types of neurodegeneration, and genetic ablation or pharmacological inhibition of 12/15-LOX reduces neurodegeneration and cognitive deficit in several mouse models, I postulated that knocking out 12/15-LOX will

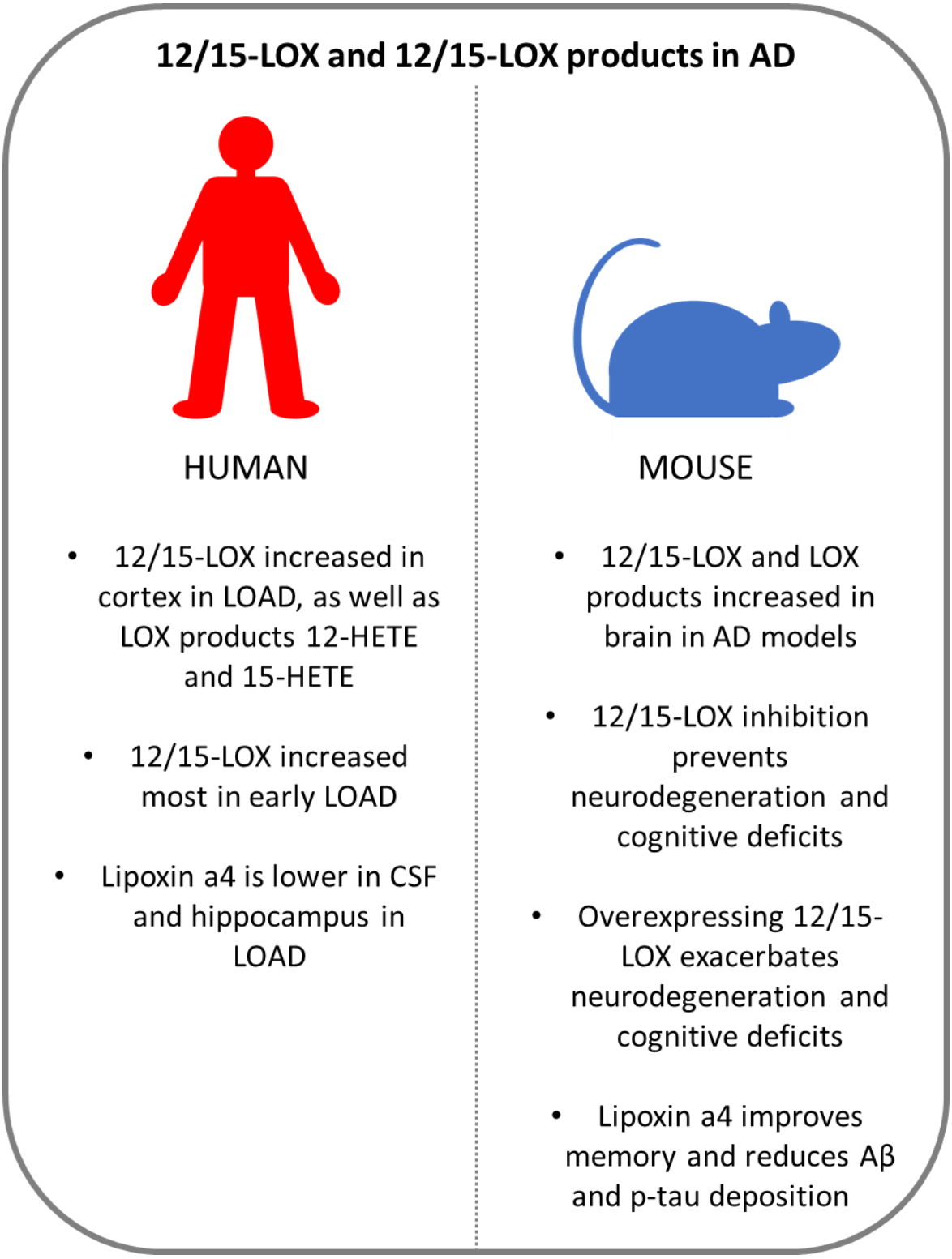

Figure 1.13: 12/15-LOX substrates, products and changes in 12/15-LOX activity in LOAD. 12/15-LOX protein, as well as 12/15-LOX substrates, are upregulated in human LOAD, as well as animal models of LOAD. The exception to this rule is lipoxin a4, which is reduced in the brain of LOAD patients.

reduce neurodegeneration and working memory deficit in the *ApoE*$^{-/-}$ mouse. This will be the first such investigation into the effect of knocking out both *APOE* and *12/15-LOX* together and I conducted behavioural tests and lipidomic analysis of brain regions to assess the effect of knocking out one and both of these genes. *APOE* and *12/15-LOX* knock out mice are described in this work as ApoE$^{-/-}$ and ALOX12/15$^{-/-}$. The double knock out mouse is described as ApoE$^{-/-}$/ALOX12/15$^{-/-}$.

1.6 Northwick Park Heart Study

The Northwick Park Heart Study II (NPHSII) was a longitudinal study of risk factors for CHD, during which blood and medical data was collected for several thousand middle aged British men (Humphries et al., 2007, Miller et al., 1995, Hawe et al., 2003, Miller et al., 1996). Samples were collected between 1989 and 1994 and participants were aged between 50 and 64 at time of entry (Miller et al., 1995). Smokers and those with a history of coronary heart disease (CHD) were excluded. There have been more than 70 papers published on data collected from the NPHSII and samples have been genotyped as part of this research (Robertson et al., 2003, Humphries et al., 2007). For example, a study found that genotyping was a useful tool alongside traditional measures of CHD risk (blood pressure, total circulating cholesterol, total circulating TAGs) and adding in status for several risk genes increased accuracy when predicting who would develop CHD (Humphries et al., 2007). Also, variants of the paraoxonase genes, which encode a protein which associates with HDL, can predict risk of CHD independently of traditional risk factors (Robertson et al., 2003, Shunmoogam et al., 2018).

Various studies have described and analysed the NPHSII plasma samples and data collected alongside plasma. An investigation of the data associated with 2,827 NPHSII participants confirmed that (i) family history is a good predictor of CHD, (ii) smoking raises risk of CHD and (iii) the presence of one or more *APOE* ε4 alleles raises risk of CHD (Hawe et al., 2003). Mean total cholesterol in individuals who did not go on to develop CHD was 5.69 ± 1.00 mmol/L^2 and mean total TAG in the same group was 1.77 ± 0.92 mmol/L^2 (Humphries et al., 2007). Meanwhile, an analysis of LDL-cholesterol found that LDL-cholesterol was lower in *APOE* ε2 carriers than *APOE* ε3 homozygotes, and highest in *APOE* ε4 carriers (Shahid et al., 2016).

However, no one has analysed NPHSII samples using untargeted lipidomics to date. I analysed a select set of 95 plasma samples collected during the NPHSII study as homozygotes for all 3 common *APOE* alleles were present.

1.7 Aims and hypotheses

This thesis aims to bridge several gaps in the literature. Firstly, no global lipidomic analysis of human *APOE* homozygote plasma has been performed which includes *APOE 22*, *APOE33*, and *APOE 44*. Total cholesterol and total TAGs are associated with risk of LOAD, however this measure includes either both cholesterol and CEs, or all TAG species (refs). It is currently unknown how individual CE and TAG species differ between *APOE* alleles.

ApoE$^{-/-}$ mice suffer from recollection memory loss, but the effect of *AloX12/15*$^{-/-}$ on memory is unknown. Also, pharmacological and genetic ablation of 12/15-LOX improves cognition and prevents neurodegeneration in AD model mice, however, this protective effect has never been tested in *APOE*$^{-/-}$ mice.

My aims were as follows:

1. To investigate the plasma lipidome of *APOE* allele homozygotes to determine if lipids are altered in a manner which affects risk of LOAD
2. To quantify cholesterol, CEs and TAGs in *APOE* homozygote plasma
3. To determine if genetic ablation of 12/15-LOX prevents loss of working memory seen in *APOE*$^{-/-}$ mice.
4. To determine how 12/15-LOX products change in regions of neurodegeneration and if lipids are correlated with memory deficits.

My null hypotheses were as follows:

- The global lipidome will not differ significantly between fresh and NPHSII plasma.
- *APOE* allele will not affect levels of either lipid categories or individual lipid species in human plasma.

- *APOE* allele will not be associated with an increase or decrease in cholesterol or any individual CE or TAG species.
- 12/15-LOX deletion will not rescue cognitive deficit in an *ApoE* $^{-/-}$ mouse.
- Performance of genetically modified mice in memory tests will not be associated with levels of 12/15-LOX products.

Chapter 2: Materials and methods

2.1 Materials

2.1.1 Antibodies and isotype controls

Primary antibodies anti-microtubule associated protein (MAP2) (ab5392) and anti-synaptophysin (ab32127) and secondary antibodies goat anti-chicken (ab150171) and goat anti-rabbit (ab150077) were all purchased from Abcam (UK). DAPI (564907) was purchased from BDBiosciences (CA, USA). Isotype controls monoclonal rabbit IgG (ab172730) and polyclonal chicken IgY (ab37382) were purchased from Abcam.

2.1.2 Buffers and solutions

Antigen retrieval buffer

1 mM ethylenediaminetetraacetic acid (EDTA) and 0.05 % Tween 20 in distilled deionised water (ddH_20).

Blocking buffer

0.3 % or 0.5 % Triton and 1 % goat serum (secondary antibody host species) in 0.1 M phosphate buffer.

Extraction buffer

Isopropanol (IPA)/hexane/acetic acid at 30:20:2 (v/v/v).

0.1 M phosphate buffered saline (PBS)

5 Oxoid phosphate buffered saline tablets (Thermo Fisher, MA, USA) dissolved in 500 mL of ddH_20.

Tissue buffer

Butylated hydroxytoluene (BHT) and diethylenetriaminepentaacetic acid (DTPA) in PBS at a concentration of 100 µM.

Washing buffer

0.3 % or 0.5 % Triton-X100 in 0.1 M phosphate buffer.

2.1.3 Chemicals and solvents

BHT, DTPA, EDTA, ethylene glycol, polyvinyl pyrrolidone, sucrose, Triton-X100 and Tween-20 were purchased from Sigma Aldrich (MO, USA).

The following were purchased from Thermo Fisher (MA, USA); glacial acetic acid, acetonitrile (ACN), ammonium ethanoate, chloroform, hexane, IPA, methanol (MeOH), Oxoid PBS tablets.

2.1.4 Consumables

The following consumables were purchased from Thermo Fisher (MA, USA); pipettes, pipette tips, Eppendorf plastic ware, glass extraction vials, plastic 30 mL Universals, gloves.
Centrifugal filters with an upper weight limit of 10 Kd were purchased from Merck Millipore (Herts, UK).

Greiner CELLSTAR 24-well plates were purchased from Sigma Aldrich (MO, USA).

2.1.5 Lipid standards

The following lipid standards were purchased from Avanti Polar Lipids (AL, USA); prostaglandin E2-d4 (PGE2-d4), thromboxane B2-d4 (TxB2-d4), 11-dehydro thromboxane B2-d4 (11-dehydro TxB2-d4), 13-hydroxyoctadecadienoic acid-d4 (13-HODE-d4), 12- and 15-hydroxyleicosatetraenoic-d8 acid (12- and 15-HETE-d8), 1,2-dimyristoylglycero-3-phosphoethanolamine (DMPE), arachidonic acid-d8, 1,2-di-O-phytanyl-sn-glycero-3-phosphoethanolamine (4ME 16:0 Diether PE), cholesterol ester (18:1)-d7 (CE (18:1)-d7) and triglyceride (51:1)-d5 (TAG (51:1)-d5).

2.1.5.1 Internal standard mix 1

Standard mix 1 included the standards PGE_2-d4, TxB_2-d4, 11-dehydro TxB_2-d4, 13-HODE-d4, 12- and 15-HETE-d8 and DMPE. Standards were prepared in serial dilutions from concentrations of 1 mg/mL to 0.5 µg/mL, diluted in MeOH. Each plasma sample, spiked with 10 µL of standards prior to extraction, contained 5 ng of each standard. This standard mix was used to check extraction efficiency of eicosanoids, which are of low abundance in plasma (Quehenberger et al., 2010).

2.1.5.2 Internal standard mix 2

Standard mix 2 was made up of arachidonic acid-d8 and 1,2-di-O-phytanyl-sn-glycero-3-phosphoethanolamine (4ME 16:0 Diether PE) in MeOH. Serial dilutions took place, decreasing the concentration from 1 mg/mL to a final concentration of 1 µg/mL. 10 µL of the mix, added before extraction to each sample, contains 10 ng of each lipid standard. Internal standard mix 2 was added to samples extracted for global lipidomic analysis.

2.1.5.3 Internal standard mix 3

Cholesterol ester (18:1)-d7 (CE (18:1)-d7) and triglyceride (51:1)-d5 (TAG (51:1)-d5) concentrations was reduced in serial dilutions from 1 mg/mL to 5.0 µg/mL and 0.5 µg/mL

respectively. 10 µL of standard was then added to each plasma sample to give 50 ng CE (18:1)-d7 and 5 ng TAG (51:1)-d5 per sample. This standard mix was used for quantitative analysis of cholesterol, cholesterol esters and triacylglycerides.

2.1.5.4 Internal standard mix 4

DMPC, DMPE and 15-HETE-d8 were serially diluted, in methanol, from 1 mg/mL to 0.5 µg/mL. 10 uL of standard mix 4 was added to each brain region to give 5 ng DMPC, 5 ng DMPE and 5 ng 15-HETE-d8 per sample. This standard mix was used for analysis of oxPLs, HETEs and HDOHEs.

2.1.6 Technology

An ELP megapixel USB camera (1080P+H.264) was used to record behavioural tests (Ailipu Technology, Guangdong, China).

An OMNI Bead Ruptor Elite was purchased from Omni-Inc (Cambridgeshire, UK).

An EVOS FL cell imaging system was purchased from Thermo Fisher and used with the kind permission of Professor Philip Taylor (Systems Immunity Research Institute, Cardiff University).

2.1.7 Software

Software used throughout this piece of work was supplied as follows; Analyst 1.6 (AB Sciex, Canada), Endnote Desktop (Clarivate Analytics, PA, USA), Graphpad Prism (Graphpad Software, CA, USA), LipidFinder (Cardiff Lipidomics Group, Wales), iSpy (developerinabox, WA, Australia), Microsoft Office (Microsoft, WA, USA), Multiquant 1.1 (AB Sciex, Canada), RStudio (MA, USA) and Sieve 2.2 (Thermo Fisher, MA, USA).

2.2 Plasma samples

2.2.1 Phlebotomy and preparation of platelet-poor-plasma

Blood was taken from healthy adult donors with informed consent and approval of the Cardiff University School of Medicine Ethics Committee (SMREC 12/13). 9 mL of blood was drawn from each donor and combined with 1 mL of trisodium citrate at 0.06 M. To prepare platelet-poor-plasma (PPP), whole blood was centrifuged at 724 g for 10 minutes at room temperature (RT). Plasma was pipetted off and centrifuged again at 724 g for 10 minutes at RT before PPP was collected and stored at -80 ˚C.

2.2.2 Northwick Park Heart Study II plasma

Plasma samples were kindly donated from the Northwick Park Heart Study II (NPHSII) by Prof Steve Humphries and team. NPHSII is a prospective CVD study of approximately 3000 men, described previously (Miller et al., 1995, Cooper et al., 2005). Briefly, subjects were middle-aged men, aged 50 - 64 at time of first sample collection. Exclusion criteria included smoking and previous diagnosis of diabetes or CVD (acute MI, silent MI or coronary surgery). Bloods collected into trisodium citrate, before being centrifuged twice and stored at – 80 ˚C until analysis. Samples were selected which had been genotyped and analysed for total cholesterol and triacylglycerides, as previously described (Humphries et al., 2007). 95 samples were chosen for analysis based on their status as *APOE* 2, 3 or 4 homozygotes.

2.3 Lipid Extraction

2.3.1 Plasma lipid extraction

Plasma lipids were extracted using a liquid-liquid extraction comprised of two steps. The first being a hexane/IPA extraction (Maskrey et al., 2007), and the second a modified Bligh and Dyer method (Bligh and Dyer, 1959). 100 µL of plasma was diluted up to 1 mL with water and acidified to pH 3 with 4 µL glacial acetic acid. 10 µL of internal standard mix 2 was added. 2.5 mL of extraction buffer (Section 2.1.2) was added. Samples were vortexed for 1 minutes at RT. 2.5 mL hexane was added and samples were vortexed again for 1 minute at RT before being centrifuged for 5 minutes at 300 g at 4˚C. The upper layer was collected using a glass pipette and 2.5 mL hexane was added to the lower layer. The lower layer and hexane were vortexed for 1 minute at RT and centrifuged for a further 5 minutes at 4 ˚C. The upper layer was collected and combined with the hexane extract, and evaporated under vacuum. A further 3.75 mL of a chloroform/MeOH mixture (1:2; v/v) was added to remaining aqueous layer before samples were vortexed for 1 minute. 1.25 mL chloroform was added and each sample vortexed for 30 sec at RT. Finally, 1.25 mL water was added before vortexing again and the mixture centrifuged for 5 minutes at 300 g at 4˚C. The bottom layer of each sample was aspirated using a glass Pasteur pipette and dried down under vacuum. Lipids were re-dissolved in 400 µL MeOH, spun through centrifuge filters with a 10 Kd cut off (Merck Millipore, Herts, UK) for 15 minutes at 400 g at 4˚C and stored at -80 ˚C until analysis.

2.3.2 Lipid extraction from brain samples

Brain regions, prepared as detailed (Section 2.6.4), were placed into 500 µL tissue buffer with 10 µL of 100 mM tin chloride (Section 2.1.2). Samples were homogenised using an OMNI Bead Ruptor Elite (Cambridgeshire, UK) for 20 secs at 4 m/s. Samples were placed into 2.5 mL of extraction buffer (Section 2.1.2) and 10 µL of standard mix 4 (Section 2.1.5.4). Homogenisation tubes were washed out with 500 µL tissue buffer, which was also added to the extraction buffer. Brain samples were then extracted as previously (Section 2.3.1). Brain

extracts were suspended into methanol, with the cerebellum in 600 µL, hippocampus in 300 µL, frontal cortex in 500 µL and cortex in 800 µL. Extracts were stored at -80°C until analysis.

2.4 LC/MS systems

2.4.1 Global lipidomic analysis

An Orbitrap Elite with an Accela 1250 Pump and an Accela Open Autosampler (Thermo Fisher Scientific, UK) was used for high-resolution reverse phase LC/MS analysis. Lipids were separated on an Accucore C18 column (2.6 µm, 150 x 2.1 mm) maintained at 30 ˚C by column sleeve. The gradient was 2 – 98 % mobile phase B (IPA/glacial acetic acid/ammonium ethanoate at 700:300:0.1:4, v/v/v/mM) in mobile phase A (H_2O/ACN/glacial acetic acid/ammonium ethanoate at 800:200:0.1:4, v/v/v/mM); 16 % B for 12 min, 60 % B for 7 min, 72 % B for 23 min, 98 % B for 9.5 minutes and finally 16 % B for 2.5 minutes. The flow rate was 400 µL/minute for 51 minutes followed by 425 µL/minute for 9 minutes. The Orbitrap Elite scan settings included resolution of 60,000 and mass range of 100-1,800 *m/z*. The source settings were source temp. 350 ˚C, sheath gas flow rate 37, auxiliary gas flow 15, sweep gas flow 2, spray voltage 3.5 kV, capillary temp. 320 ˚C and S-lens RF level 69 %. A lock mass was used to prevent mass accuracy drifting over the analysis, with sodium dodecyl sulfate (SDS) chosen in negative mode (*m/z* 265.1479) and the plasticiser ion disoctyl phthalate in positive mode (*m/z* 391.2842).

2.4.2 Quantification of cholesterol ester and triglyceride species

2.4.2.1 Cholesterol and CE method 1

This method was used to quantify CE species in Chapter 4. Free cholesterol and CE (Table 2.1A) were quantified using a Nexera liquid chromatography system (Shimadzu, Japan) coupled with a 4000 QTrap (AB Sciex, Canada). Lipids were separated on a Hypersil Gold column (1.9 µm, 100 x 2.1 mm column, Thermo Fisher Scientific) maintained at 30 ˚C. The

method was isocratic, and the mobile phase was ACN:IPA:ammonium ethanoate at 60:40:4 (v/v/mM). Flow rate was 100 µL/minute. MS conditions were as follows for all species except CE (18:1)-d5: ESI temperature 0 °C, N2 as drying gas, ion source gas1 25 psi, ion source gas2 50 psi, curtain gas 35 psi, ESI positive spray voltage 5.0 kV, declustering potential 91 V, entrance potential 10 V, collision energy 33 V, and collision cell exit potential 25 V. Dwell time for each transaction was 150 msec for and the total cycle time 1.12 sec. CE (18:1) d5 was set a declustering potential of 86 V and a collision energy of 19 V with all other conditions identical. Data from all 4000 QTrap methods (Section 2.4.2.1-2.4.2.4 and 2.4.3) were analysed using the Multiquant 1.1 software and species quantified relative to internal standards. This method was improved for use in Chapter 7 (Section 2.4.2.2); separation of species was improved by adding in a mobile phase gradient, contamination was reduced by adding heat to the ESI and more masses were monitored. The improved method has a higher sensitivity and gives more biological information as more lipids were quantified. This method is detailed below (Section 2.4.2.2).

2.4.2.2 Cholesterol and CE method 2

This method was used to analyse NPHSII samples in Chapters 6 and 7 and was developed from cholesterol and CE method 1. This method used a Nexera liquid chromatography system coupled with a 4000 QTrap and Hypersil Gold column (1.9 µm, 100 x 2.1 mm column) to quantify cholesterol and CE species (Table 2.2). Mobile phase A was H_2O:mobile phase B:ammonium ethanoate at 19:1:4 (v/v/mM) and mobile phase B was ACN:IPA:ammonium ethanoate at 40:60:4 (v/v/mM). The column was maintained at 40 °C and the following linear gradient for B (Section 2.1.3.3) was applied: 90 % for 1 min, 90 – 100 % from 1 to 5 minutes and held at 100 % for another 3 minutes followed by 3 minutes at initial condition for column re-equilibration. MS conditions were as follows: ESI temperature 150 °C, N2 as drying gas, ion source gas 1 25 psi, ion source gas 2 50 psi, curtain gas 35 psi, ESI positive spray voltage 5.0 kV, declustering potential 70 V, entrance potential 10 V, collision energy 20 V, and collision cell exit potential 25 V. Dwell time for each transition was 75 ms for and the total cycle time 1.12 sec.

A

Cholesterol and CE parent and daughter masses monitored by cholesterol and cholesterol ester method 1

Lipid	Q1 (Da*)	Q3 (Da)
CE(14:0)	614.6	369.1
CE(16:0)	642.6	369.1
CE(16:1)	640.6	369.1
CE(18:0)	670.7	369.1
CE(18:1)	668.5	369.1
CE(18:2)	666.5	369.1
CE(20:4)	690.6	369.1
CE(18:1)-d5	673.6	376.1

B

Triglyceride Q1 masses monitored during targeted analysis by triglyceride method 1

Lipid	Q1 (Da)
TG(50:0)	852.8
TG(50:1)	850.7
TG(50:2)	848.7
TG(50:3)	846.7
TG(52:2)	876.8
TG(52:3)	874.7
TG(52:4)	872.7
TG(54:3)	902.8
TG(54:4)	900.8
TG(54:5)	898.8

Table 2.1A & B. Masses monitored to measure (A) cholesterol, CEs and (B) TAGs using Cholesterol and CE method 1 and Triacylglycerides (TAG) method 1. All masses above are ammonium adducts monitored in positive mode using the 4000 Qtrap and Cholesterol and CE method 1 (Section 2.4.2.1) or Triacylglycerides (TAG) method 1 (Section 2.4.2.3). Q1 ion selection took place in the first quadrupole and Q3 in the second quadrupole. *Da = daltons.

Cholesterol and CE parent and daughter masses monitored by cholesterol and cholesterol ester method 2

	Q1 (Da*)	Q3 (Da)
Cholesterol	404.0	369.1
CE(14:0)	614.6	369.1
CE(16:0)	642.6	369.1
CE(16:1)	640.6	369.1
CE(18:0)	670.7	369.1
CE(18:1)	668.5	369.1
CE(18:2)	666.5	369.1
CE(18:3)	664.6	369.1
CE(20:4)	690.6	369.1
CE(22:6)	714.6	369.1
CE(18:1)-d7	675.6	376.1

Table 2.2. Masses monitored to measure cholesterol and CEs using Cholesterol and CE method 2. All masses above are ammonium adducts monitored in positive mode using the 4000 Qtrap and Cholesterol and CE method 2 (Section 2.4.2.2). Q1 ion selection took place in the first quadrupole and Q3 in the second quadrupole. *Da = daltons.

2.4.2.3 Triacylglycerides (TAG) method 1

This method was used to analyse TAGs for the data contained in Chapter 4. It used a Nexera liquid chromatography system coupled with a 4000 QTrap and Hypersil Gold column (1.9 µm, 100 x 2.1 mm column) to quantify TAG species (Table 2.1B). The column was maintained at 40 °C. Triglyceride species were quantified using Q1 in positive mode. The method was isocratic and the mobile solvent was ACN:IPA:ammonium ethanoate at 60:40:4 (v/v/mM).Flow rate was 100 µL/minute (Section 2.1.3.4). MS conditions were as follows: ESI temperature 0 °C, N2 as drying gas, ion source gas1 25 psi, ion source gas2 50 psi, curtain gas 35 psi, ESI positive spray voltage 5.0 kV, declustering potential 91 V, entrance potential 10 V, collision energy 33 V, and collision cell exit potential 25 V. Scan duration was 15.9 minutes, with a start mass of 800.00 amu and stop Mass of 950.00 amu. This method was also improved for use in Chapter 7 (Section 2.4.2.4). Temperature was added to the ESI, which reduces contaminants entering the MS. Separation of species was improved by adding in a mobile phase gradient and more masses were monitored. The improved method (TAG method 2) is more sensitive than this method and provides more biological insight as more species were monitored. This method is detailed below (Section 2.4.2.4).

2.4.2.4 TAG method 2

This method was used to analyse NPHSII samples in Chapters 6 and 7. Triglyceride species (Table 2.3) were quantified using a Nexera liquid chromatography system coupled with a 4000 QTrap and Hypersil Gold column (1.9 µm, 100 x 2.1 mm column). Mobile phase A was H_2O:mobile phase B:ammonium ethanoate at 19:1:4 (v/v/mM) and mobile phase B was ACN:IPA:ammonium ethanoate at 60:40:4 (v/v/mM). The column was maintained at 40 °C and the following linear gradient for B (Section 2.1.3.5) was applied: 90% for 1 min, 90 - 100% from 1 to 5 minutes and held at 100 % for another 3 minutes followed by 3 minutes at initial condition for column re-equilibration. MS conditions were as follows: ESI temperature 0 °C, N2 as drying gas, ion source gas1 25 psi, ion source gas2 50 psi, curtain gas 35 psi, ESI positive spray voltage 5.0 kV, declustering potential 91 V, entrance potential 10 V, collision energy 33 V, and collision cell exit potential 25 V. Triglyceride species were quantified using a Q1

Triglyceride Q1 masses monitored during targeted analysis by triglyceride method 2	
	Q1 (Da*)
TG(32:0)	600.5
TG(34:0)	628.5
TG(36:0)	656.6
TG(38:0)	684.6
TG(40:0)	712.6
TG(42:0)	740.7
TG(44:0)	768.7
TG(46:0)	796.7
TG(48:0)	824.8
TG(48:1)	822.8
TG(48:2)	820.7
TG(50:0)	852.8
TG(50:1)	850.8
TG(50:2)	848.8
TG(50:3)	846.8
TG(50:4)	844.7
TG(52:0)	880.8
TG(52:1)	878.8
TG(52:2)	876.8
TG(52:3)	874.7
TG(52:4)	872.8
TG(52:5)	870.8
TG(54:0)	908.9
TG(54:1)	906.8
TG(54:2)	904.8
TG(54:3)	902.8
TG(54:4)	900.8
TG(54:5)	898.8
TG(54:6)	896.8
TG(56:0)	936.9
TG(56:1)	934.9

Table 2.3. Masses monitored to measure TAGs using TAG method 2. All masses above are ammonium adducts monitored in positive mode using the 4000 Qtrap and TAG method 2 (Section 2.4.2.4). Q1 ion selection took place in the first quadrupole. *Da = daltons.

Triglyceride Q1 masses monitored during targeted analysis by triglyceride method 2	
	Q1 (Da*)
TG(56:2)	932.9
TG(56:3)	930.8
TG(56:4)	928.8
TG(56:5)	926.8
TG(56:6)	924.8
TG (51:1)d5	869.8

Table 2.3 (continued): Masses monitored to measure TAGs using TAG method 2. All masses above are ammonium adducts monitored in positive mode using the 4000 Qtrap and TAG method 2 (Section 2.4.2.4). Q1 ion selection took place in the first quadrupole. *Da = daltons.

Parent (Q1) and product (Q3) transitions monitored during analysis of oxPLs by oxPL method 1		
Species	**Q1 (Da*)**	**Q3 (Da)**
PC(O-35:4)/PE(O-38:4)/PS(O-35:5)	782.6	319.2
PC(O-39:4)/PE(O-42:4)/PS(O-35:5)	808.7	319.2
PC(O-37:4)/PE(O-40:4)/PS(O-37:5)	810.7	319.2
PC(O-37:0)/PE(O-40:0)/PS(O-37:0)	788.6	343.2
PC(O-39:6)/PE(O-42:6)/PS(O-39:7)	834.7	343.2

Table 2.4. Masses monitored to measure oxPLs using the Oxidised phospholipids (oxPLs) method. All masses above are ammonium adducts monitored in positive mode using the 4000 Qtrap and Oxidised phospholipids (oxPLs) method (Section 2.4.3). Q1 ion selection took place in the first quadrupole and Q3 in the second quadrupole. *Da = daltons

method in positive mode and scan duration was 10.9 minutes, with a start mass of 800.00 Da and stop Mass of 950.00 Da. A dwell time of 10 msec was used for all species.

2.4.3 Oxidised phospholipids (oxPLs) method

OxPLs were quantified using a Nexera liquid chromatography system coupled with a 6500 QTrap. Plasma samples were spiked using standard mix 4 (Section 2.1.5.4), which contains 5 ng each of DMPC, DMPE and 15-HETE-d8 per 10 µL addition. Samples were extracted as detailed (Section 2.3.2) and separated by LC on a LUNA column (Phenonenex, c18, 3 µm, 150 x 2 mm). OxPLs were monitored using an MS/MS method in negative mode (Table 2.4). The gradient was 50-100 % mobile phase B (methanol:ammonium ethanoate, 1:1, v/mM) in mobile phase A (methanol:acetonitrile (ACN):H_2O:ammonium ethanoate at 6:2:2:1, v/v/v/mM) over 50 min; 100 % B for 42 minutes and 50 % B for 8 minutes. The flow rate was 200 µL/minute. Dwell time for each species was 100 msec, declustering potential -140 V, entrance potential -10 V, collision energy -50 V and collision cell exit potential -10 V. Lipids were normalised to DMPE before analysis.

2.4.4 Eicosanoid method

Eicosanoids were quantified using a Nexera liquid chromatography system coupled with a 4000 QTrap. Plasma samples were spiked prior to extraction using standard mix 4 (Section 2.1.5.4), which contains 5 ng each of DMPC, DMPE and 15-HETE-d8 per 10 µL addition. Samples were extracted as previously detailed (Section 2.3.2) and separated by LC using a LUNA column (Phenomenex, c18, 3 µm, 150 x 2 mm). Eicosanoids were monitored using MS/MS in negative mode (Table 2.5). The gradient was 50-90 % mobile phase B (methanol:ACN:glacial acetic acid at 3:2:2, v/v/mM) in mobile phase A (water:ACN:glacial acetic acid at 3:1:2, v/v/mM) over 30 min; 50-90 % B for 20 min, 90 % B for 5 minutes and 50 % B for 5 minutes. The flow rate was 1 mL/minute. Dwell time for each lipid was 150 msec and source conditions are in Table 2.5. Ratio of 15-HETE-d8 internal standard and a curve of known concentrations were used to quantify eicosanoids.

Q1, Q3 and source conditions used during eicosanoid analysis

	Q1 (Da*)	Q3(Da)	Declustering potential (volts)	Collision energy (volts)	CXP† (volts)
5-HETE	319.2	281.2486	-80	-22	-6
8-HETE	319.2	255.233	-70	-22	-1
11-HETE	319.2	641.5115	-70	-30	-15
12-HETE	319.2	639.4959	-85	-20	-9
15-HETE	319.2	750.5443	-45	-20	-13
7-HDOHE	343.2	766.5392	-50	-21	-9
8-HDOHE	343.2	478.2928	-50	-19	-9
10-HDOHE	343.2	772.585625	-51	-21	-5
11-HDOHE	343.2	480.309025	-60	-18	-10
13-HDOHE	343.2	790.5604	-55	-19	-9
14-HDOHE	343.2	775.5495	-45	-17	-9
16-HDOHE	343.2	675.497	-55	-17	-10
17-HDOHE	343.2	885.5499	-70	-15	-10
20-HDOHE	343.2	687.5441	-70	-22	-10
15-HETE-d8	327.2	863.6912	-65	-16	-5

Table 2.5: Masses monitored and source conditions when analysing eicosanoids using the 4000 Qtrap. All masses above are in positive mode using the 4000 Qtrap and Eicosanoid method (Section 2.4.4). Q1 ion selection took place in the first quadrupole and Q3 in the second quadrupole. * Da = daltons. † CXP = collision cell exit potential.

2 .5 Analysis of Orbitrap Elite data

2.5.1 Sieve-LipidFinder workflow

Raw global lipidomics data obtained as in 2.4.1 was analysed using Sieve 2.2 software using a small molecule, single non-differential analysis. Quality control sample 1 was used as the reference sample, with a retention time window of 01.00 – 57.00 mins, frame width of 0.70 mins, *m/z* minimum of 100 amu, *m/z* maximum of 1800 amu and an *m/z* width of 10 parts per million (ppm). Frame selection parameters were; max number of frames of 1,000,000, peak intensity threshold of 50,000 and a minimum alignment threshold of 10,000. Tile size was set to 300 and max retention time shift was 0.70 minutes. The output was exported to a csv file and filtered to exclude any frames with a PRElement of over 0, a PRSize of under 1 and/or a charge of over 1. The csv file was analysed using a custom in-house generated software, LipidFinder, which removes solvents and contamination ions, removes isotopes and searches for matches for each mass in three online databases (O'Connor et al., 2017). LipidFinder designates a putative identification and lipid category based on accurate mass. Significance was calculated for each feature using the non-parametric Mann-Whitney test and fold-change was calculated for each feature as below.

Fold-change (FC) = (intensity of rare allele) ÷ (intensity of common allele)

2.5.2 XCMS-LipidFinder workflow

Raw global lipidomics data obtained as in 2.4.1 was processed through MSConvert and transformed to the XCMS file format before using the XCMS module in RStudio to align the data and identify peaks, each of which represents a lipid species. Data was then exported to a Microsoft Excel (Microsoft, WA, USA) comma separated csv file for further processing. The output csv file was analysed using LipidFinder and a putative identity and lipid category was assigned for each *m/z* value (Section 2.5.3) (O'Connor et al., 2017). Significance and fold-change were calculated for each feature as above (Section 2.6.1). Volcano plots, box plots, heatmaps, principal component analysis (PCA) plots and orthogonal projections to latent structures discriminant analysis (PLS-DA) plots were created in RStudio using the pheatmap,

RColorBrewer, colorRamps, car and devEMF libraries. After the data was visualised post-LipidFinder, lipids were filtered for peak quality using the QC peaks. Lipids with a fold-change of over 2 and/or a significance value below 0.075 were identified and QC peaks for each mass gathered into a pdf file for visual analysis. Peaks were visually checked using Microsoft Edge (Microsoft, WA, USA) and lipids discarded if peaks fell under one of the following four criteria; (i) peaks were absent in more than 66% of the genotype samples plus all the QC samples, (ii) peaks were irreproducible across QC samples, either by shape or an area change of more than 100 %, ion suppression removed any part of the peak in one or more QC samples, (iv) peaks were lipids containing one or two C^{13} isotopes. Finally, all lipids remaining in the dataset were confirmed to ensure that QC RSD (the relative standard deviation of a lipid in multiple QC samples) was less than 50 % and that QC mean was under 1,000,000.

2.5.3 Assigning putative lipid ID

The m/z and RT assigned to each lipid were checked against two sources, firstly, the LIPID MAPS curated lipid database for matches on accurate mass and secondly, an in-house generated database of RTs for this LC method. This in-house generated database contains expected RTs for lipids, putatively identified by global lipidomics, using the Orbitrap Elite and solvent systems detailed in this thesis. The in-house generated database was produced from previous analyses of plasma and standards using the global lipidomics method and identifications are putative, therefore this database informs our putative IDs but a match is not a definitive ID. If a lipid matched both databases, the lipid was assigned a putative ID, i.e. a species name. If no match in the RT database was found but one or more matches was found in the LIPID MAPS database, the lipid was assigned the category with the most mass matches. If a match was found in neither, the lipid was assigned an ID in the style 'Accurate mass/RT/Unknown'.

2.5.4 Visualising processed Orbitrap Elite data

Boxplots were drawn in Graphpad Prism, and all other plots using RStudio. Scatter plots, volcano plots, PCA, PLS-DA and ROC curves were produced using the devEMF library.

Heatmaps were produced using the readxl, tidyverse, data.table, pheatmap and RColorBrewer libraries.

2.5.5 A Benjamini-Hochberg correction for multiple comparisons

Orbitrap Elite data analysed in Chapter 5 was treated using the Benjamini-Hochberg procedure for multiple comparisons (Benjamini and Hochberg, 1995). Benjamini-Hochberg is less stringent than Bonferroni and allows the addition of a False Discovery Rate (FDR), which can be adjusted to suit experimental design (Benjamini and Hochberg, 1995, McDonald, 2014). A higher FDR will give more false positives, whilst a lower FDR could provide false negatives. Therefore, the cost of each to your experiment should be evaluated. Significance was calculated using a students two-tailed t test, assuming unequal variance. Lipids were then ranked on p value, with the smallest p value given a rank of "1", then next smallest a rank of "2" and so on. The Benjamini-Hochberg critical value (BH critical value) was calculated as below, where i is rank, m is total number of lipids measured and Q is the chosen FDR:

$$BH\ critical\ value = \left(\frac{i}{m}\right)Q$$

BH critical value was then compared to the t test p value. The lipid with the largest p value which is smaller than the BH critical is then significant, as are all the lipids with smaller p values than this lipid, even if their p value is bigger than their BH critical value.

2.6 Mouse models

2.6.1 Mouse strains and numbers

Mice from four genetically altered strains were used, all of which were on the C57BL/6NCrl background, purchased from Charles River (Charles River Laboratories, UK) at 8 weeks old. *C57BL/6NCrl* mice were used as controls and *ALOX12*$^{-/-}$, *APOE*$^{-/-}$ and double knock outs (*ALOX12*$^{-/-}$ and *APOE*$^{-/-}$) were bred in-house under the Home Office Licence 30/3150, by Dr Allen-Redpath and others at the Heath Park Campus Animal Facility, Joint Biological Services, Cardiff University (Lauder et al., 2017). All animals were bred and housed under Home Office-

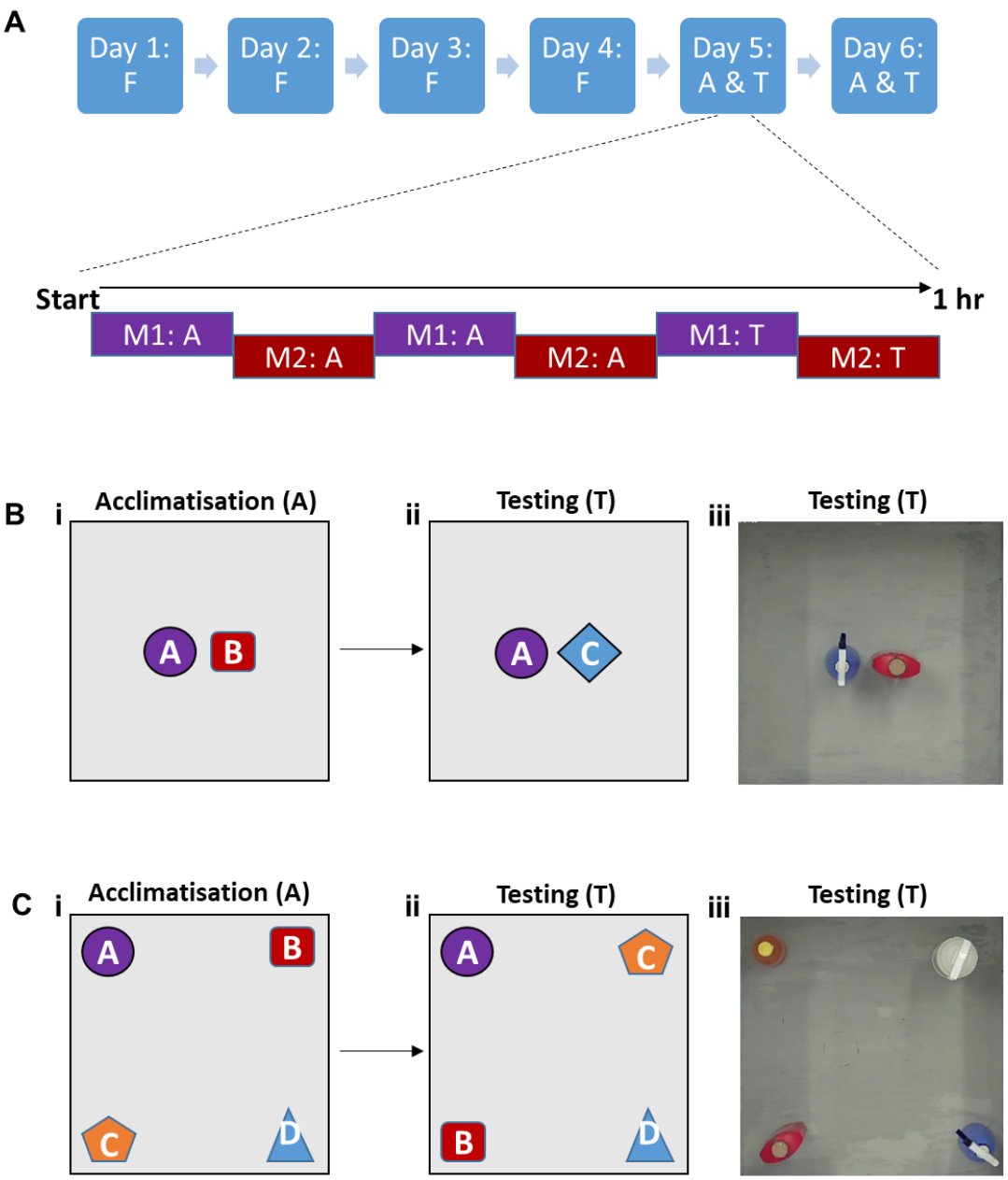

Figure 2.1: Behavioural tests used to assess object and spatial memory in mice. A. Mice were familiarised (F) to the arena for four days before testing began. The first two days consisted of 10 minutes familiarisation time per mouse in the empty arena. The following two days consisted of 10 minutes familiarisation per mouse, in the arena with two objects not used for testing. During testing days, two mice (mouse 1, M1, and mouse 2, M2) were acclimatised (A) and tested (T) per hour. The arena in the novel object test during acclimatisation and testing stages. **B.** The arena in the novel object test during (i) acclimatisation and (ii) testing stages. A photograph of the testing phase (iii) is also included. **C.** The arena in the object-in-place test during (i) acclimatisation and (ii) testing stages. A photograph of the testing phase (iii) is also included.

approved conditions with a 12-hour sleep wake cycle, a constant temperature of 20 – 22˚C and free access to standard chow and water. Behavioural tests were performed as an unlicensed procedure. A total of 20 (10 male and 10 female) mice were used from each genotype.

2.6.2 Novel object test

A total of 20 (10 male and 10 female) mice were used from each genotype. This behavioural test assesses whether an animal can distinguish between new and familiar objects (Antunes and Biala, 2012). Testing was conducted in a 60 cm x 60 cm arena, with visual cues placed on the walls of the room housing the arena and a camera suspended above. Behavioural testing was performed at 28 weeks old (± 3). Prior to the beginning of testing, each mouse was familiarised with the arena over four days to reduce anxiety during the testing paradigm (Figure 2.1A). Each familiarisation session was 10 minutes, the first two sessions were held in the empty arena and the second two sessions in the presence of two garden gnomes. After four days of familiarisation, mice then underwent two days of testing. Half the mice of each genotype underwent the novel object test first, and half the object-in-place test first. On a testing day, mice were first acclimatised to the arena and two objects in two periods of 10 minutes (Figure 2.1C). Between each acclimatisation stage, mice were returned to their home cages for 10 min, allowing two mice to be acclimatised and tested alternatively. The objects and arena were wiped with IPA between each mouse to prevent an olfactory trail. After the second acclimatisation, one familiar object was removed from the arena and replaced with a novel object in the same location . For the 10 minutes testing phase, mice were put back into the arena and filmed using the ELF webcam, with videos anonymised for genotype to prevent bias. Videos were blinded prior to analysis. Using iSpy software to watch the videos, the time an animal spent interacting with both the familiar and novel object was measured in sec, with interaction defined as the animal facing the object whilst being within 2 cm of it. The discrimination ratio was then calculated as time spent interacting with the novel object divided by time spent interacting with both objects.

2.6.3 Object-in-place test

The object-in-place test assesses spatial memory i.e. whether a mouse recognises that an object has moved (Lesburgueres et al., 2017). The arena was in a room as described previously, with visual cues around the room and a camera suspended above the arena (Section 2.6.2). Four objects, distinct in shape, size and colour, were placed in the arena, with one in each corner (Figure 2.1C). Mice were familiarised to the arena as stated previously (Section 2.6.1) before testing. During the testing days, mice were acclimatised twice to the arena and objects for 10 minutes intervals, with 10 minutes in the home cage between each interval. The objects and arena were wiped with IPA between each mouse to prevent an olfactory trail. After the second acclimatisation phase, objects from opposing corners were swapped. Mice were then placed in the arena for the final 10 minutes testing phase whilst being filmed. Videos were blinded, and time spent interacting with objects which moved and objects which stayed in the same position was recorded. The discrimination ratio was again calculated as time spent interacting with the novel object divided by time spent interacting with both objects. Mice were culled, and tissue samples collected 4/5 days after the second day of testing.

2.6.4 Culling and tissue preparation

2.6.4.1 Culling, perfusion and dissection

Animals were culled using a Schedule 1 method, specifically rising concentration of CO_2 followed by confirmation of death using palpation. A cardiac puncture was performed, with 500 µL of blood drawn from each animal. Cadavers were opened, and a needle was inserted into the left ventricle. They were then perfused with phosphate-buffered saline (PBS) using a gravity system until the liver was clear and lungs white.

Once perfusion was complete, the animal was decapitated using dissection scissors and the brain removed. The right hemisphere was dissected into cortex, frontal cortex (taken as

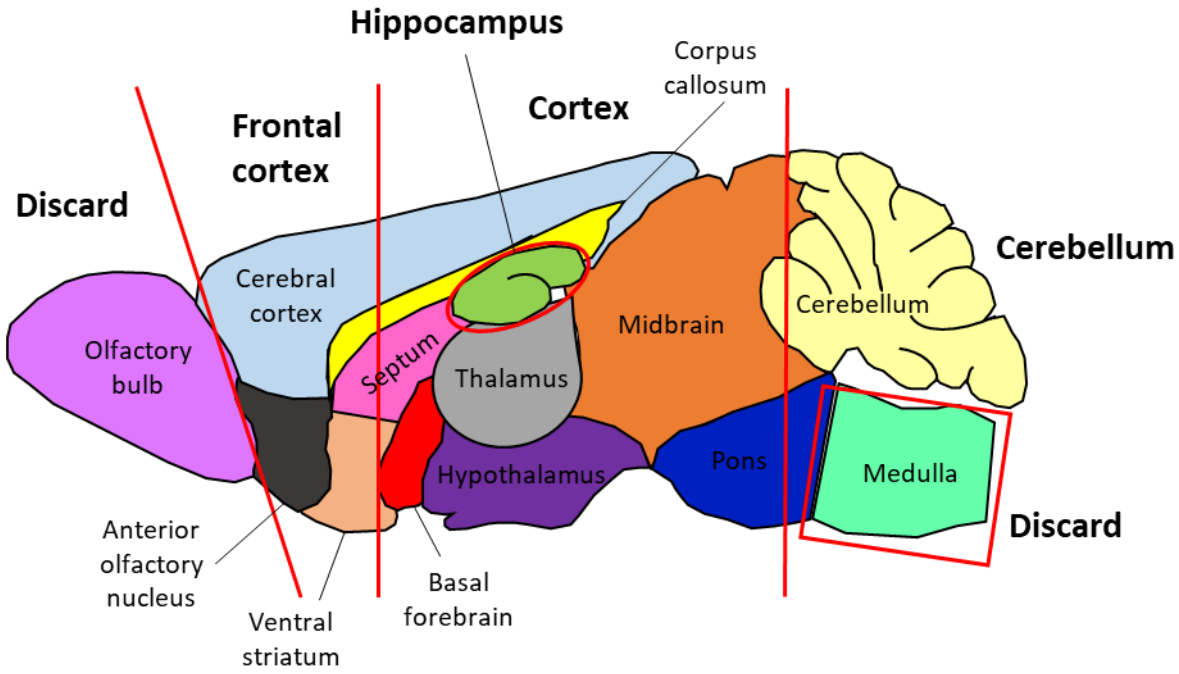

Figure 2.2: The four brain regions collected and analysed for lipids and synapse density. Each red line represents where the brain was dissected, with the olfactory bulb and medulla being discarded. Brains were therefore dissected into four rough regions, the frontal cortex, cortex, hippocampus, and cerebellum.

anterior third of cortex), hippocampus and cerebellum (Figure 2.2). These dissected regions were snap-frozen in liquid nitrogen and stored at -80 ˚C until analysis.

2.6.5 Lipid extraction and analysis

Each brain region was weighed and placed into a 1.5 mL Eppendorph with twelve 1.4 mm ceramic beads and 1 mL tissue buffer (Section 2.1.2). Tissue was homogenised using an OMNI Bead Ruptor Elite for 20 sec at temperature 4 ˚C and speed 4 msec. The homogenised tissue and beads were transferred into an extraction tube, where tissue was chemically reduced for 10 minutes using 10 µL 0.1 M $SnCl_2$ at room temperature (RT). 10 ng each of 1,2-dimyristoyl-sn-glycero-3-phosphocholine (DMPC) and 1,2-dimyristoyl-sn-glycero-3-phosphoethanolamine (DMPE) was added to each sample. 2.5 mL of extraction solution (IPA/hexane/1 M acetic acid; 150:100:1; v/v/v) was added to each sample before it was vortexed for 1 minute at RT. A further 2.5 mL hexane was added. This was vortexed again for 1 minute at RT before being centrifuged for 5 minutes at 300 g and 4 ˚C. The upper phase was collected with a glass Pasteur pipette and 2.5 mL hexane added to the lower layer. Finally, this was vortexed for 1 minutes at RT and centrifuged for 5 minutes at 300 g and 4 ˚C. The upper layer was combined with the first layer collected and layers were dried under vacuum at 30 °C. Extracted lipids were suspended in 200 µL MeOH and analysed on the 4000 QTrap (Section 2.4.3) Oxidised phospholipids were quantified using the internal standard mix 4 (Section 1.2.5.4).

Chapter 3: Optimisation of Lipid Extraction and Mass Spectrometry

3.1 Introduction and aims

I optimised extraction, MS analysis and data treatment methods prior to analysis of the NPHSII cohort samples. Extraction methods were tested for extraction efficiency using standard mix 1 (Section 2.1.5.1), which is an in-house-made mix of bioactive lipids, which are present at low concentrations in plasma (Quehenberger et al., 2010). To preserve sample and prevent clogging or overloading the HPLC column, differing volumes of plasma were extracted to determine the lowest volume at which endogenous species can be measured. To ensure the solubility of lipids when extracts are re-suspended, I tested three solvents, considering peak area and shape. Lastly, to save machine time, I trialled a combination of high and low mass ranges, which were previously performed as two separate analyses.

3.1.1 Aims

The extraction efficiency, coefficient of variation (CV) and effect of reducing plasma volume extracted on number of lipids measured have not been tested for these optimised extraction and MS methods. Also, the effect of combining high and low mass analyses on the lipids detected is unknown.

Therefore, my aims were as follows:

- To determine extraction efficiency and coefficient of variation
- To minimise volume of plasma extracted
- To test three solvents for re-suspending lipid extracts
- To determine if combining high and low mass analyses into one MS method causes fewer lipids to be measured

3.2 Results

3.2.1 Lipid extraction efficiency is high, and CV is low

To determine the extraction efficiency of a range of lipids found endogenously in plasma, I spiked plasma with standard mix 1, which is a mix of deuterated lipids which are found in their undeuterated form in plasma (Section 2.1.5.1). I extracted lipids using a hexane extraction followed by a modified Bligh and Dyer extraction (Section 2.3), and then compared standard peak areas to peak areas in an injection of unextracted standard mix 1 (Bligh and Dyer, 1959). Extraction efficiencies ranged from 61.23 % to 104.23 %, with an average extraction efficiency of 91.63 % (Table 3.1).

Coefficient of variation (CV) was calculated for both unextracted standards and standards in plasma, as standard deviation divided by mean, and then multiplied by 100. CV ranged from 0.97 % to 5.84 % for unextracted standards, and from 1.68 % to 5.98 % for standards in plasma (Table 3.2).

3.2.2 Volume of Plasma Extracted

I determined if the volume of plasma being extracted could be reduced to conserve sample and lengthen column life. I extracted 100 µL, 50 µL, 20 µL and 10 µL of plasma, and searched for 35 endogenous species, known to be present in plasma, using accurate mass in Lipidfinder output data (Quehenberger et al., 2010). Exemplar chromatograms of some species found in the 100 µL plasma extraction are in Figure 3.1. Clear peaks are present for five fatty acids and four out of five eicosanoids.

Accurate masses matching 23 of the 35 endogenous species can be found in 100 µL and 50 µL extractions of NPHSII plasma, and 22 in 20 µL and 10 µL extractions (Figure 3.2). As expected, intensity of most lipids declines as plasma extraction volume becomes smaller. However, a few species, such as PC(30:1) and PC(32:1), increase in peak area as extraction volume decreases.

Extraction efficiency of six standards in plasma						
	PGE_2-d4	**TxB_2-d4**	**11-dehydro-TxB_2-d4**	**13-HODE-d4**	**12/15-HETE d8**	**DMPE**
Plasma 1.1	92.83	64.88	92.66	105.66	108.43	104.18
Plasma 1.2	93.75	60.62	87.71	105.24	114.50	95.99
Plasma 1.3	92.15	60.76	87.54	104.28	94.62	104.53
Plasma 1.4	88.82	58.65	84.71	101.76	83.56	111.18
Mean	91.89	61.23	88.16	104.23	100.28	103.97

Table 3.1: Extraction efficiency of 6 standards in plasma after a liquid-liquid phase lipid extraction and analysis via LC/MS/MS on the QTrap 4000. Extraction efficiency was calculated as intensity in unextracted standard, divided by intensity in extracted sample, and multiplied by 100.

A

CV of unextracted standards					
	PGE_2-d4	**TxB_2-d4**	**11-dehydro TxB_2-d4**	**13-HODE-d4**	**DMPE**
Stnd 1.1	4.34E+05	7.96E+04	1.08E+05	3.33E+05	2.90E+05
Stnd 1.2	4.49E+05	8.13E+04	1.02E+05	3.37E+05	3.26E+05
Stnd 1.3	4.49E+05	8.21E+04	1.07E+05	3.39E+05	3.30E+05
Stnd 1.4	4.48E+05	8.09E+04	1.11E+05	3.40E+05	3.25E+05
Mean of raw data	4.45E+05	8.10E+04	1.07E+05	3.37E+05	3.18E+05
SD	7.45E+03	1.07E+03	3.89E+03	3.28E+03	1.85E+04
CV	1.67	1.32	3.64	0.97	5.84

B

CV of extracted standards in plasma					
	PGE_2-d4	TxB_2-d4	11dehydro TxB_2-d4	13-HODE d4	DMPE
Plasma 1.1	4.13E+05	5.25E+04	9.90E+04	3.56E+05	3.31E+05
Plasma 1.2	4.17E+05	4.91E+04	9.37E+04	3.55E+05	3.05E+05
Plasma 1.3	4.10E+05	4.92E+04	9.35E+04	3.52E+05	3.32E+05
Plasma 1.4	3.95E+05	4.75E+04	9.05E+04	3.43E+05	3.53E+05
Mean of raw data	4.09E+05	4.96E+04	9.42E+04	3.52E+05	3.30E+05
SD	9.55E+03	2.12E+03	3.53E+03	5.89E+03	1.98E+04
CV	2.34	4.28	3.75	1.68	5.98

Table 3.2A and B: Coefficient of variation (CV) of 6 lipid standards. CV in both **(A)** unextracted and **(B**) in plasma, after a liquid-liquid phase lipid extraction and analysis via LC/MS/MS on the QTrap 4000. CV calculated as standard deviation (SD) divided by mean and multiplied by 100.

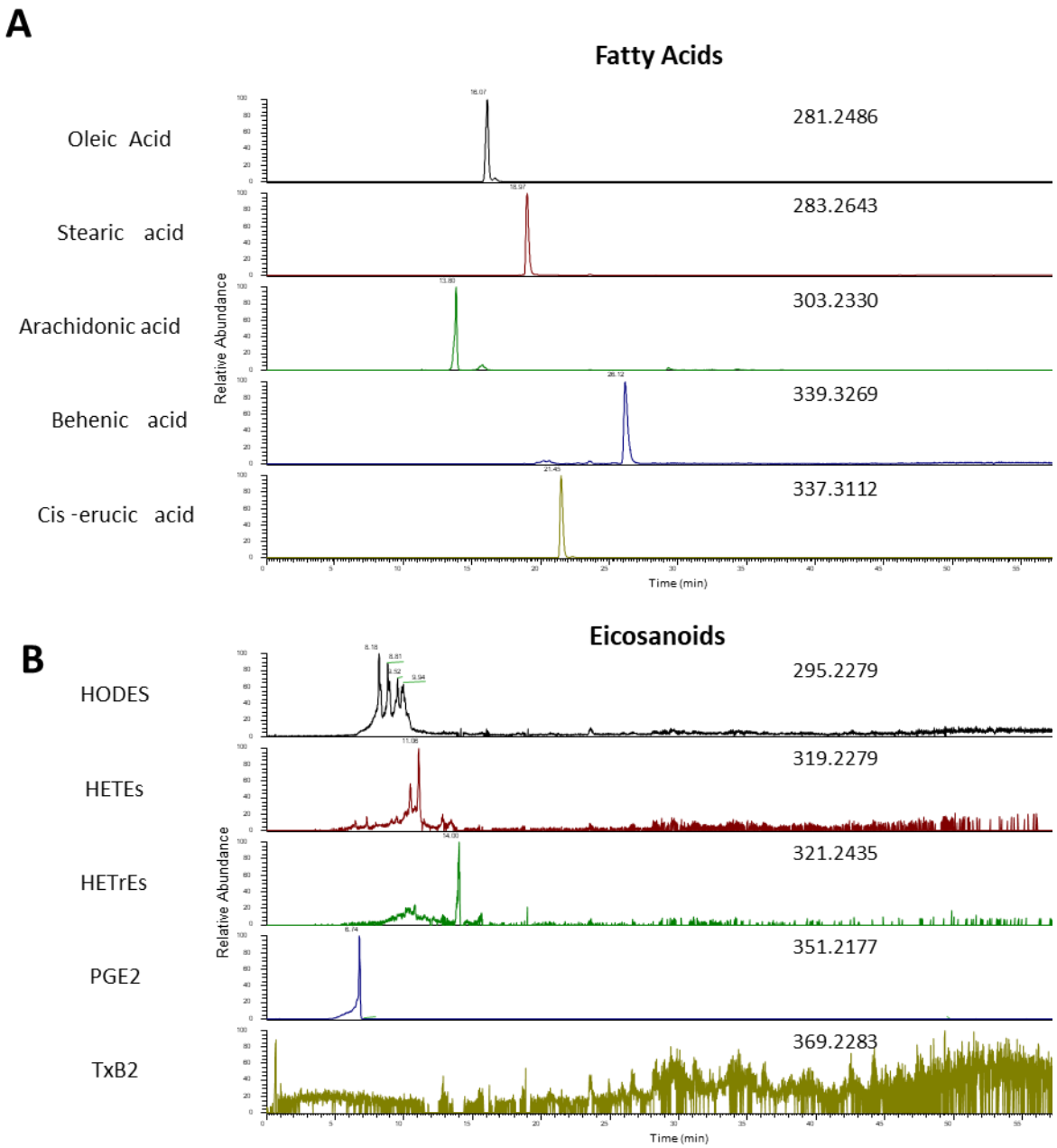

Figure 3.1: Exemplar chromatograms of endogenous lipids extracted from plasma. Chromatograms of endogenous (a) fatty acids and (b) eicosanoids in plasma, analysed on the Orbitrap Elite in negative mode. Species found using accurate mass for [M-H]- in Orbitrap raw data, ion accurate mass is noted on each chromatogram.

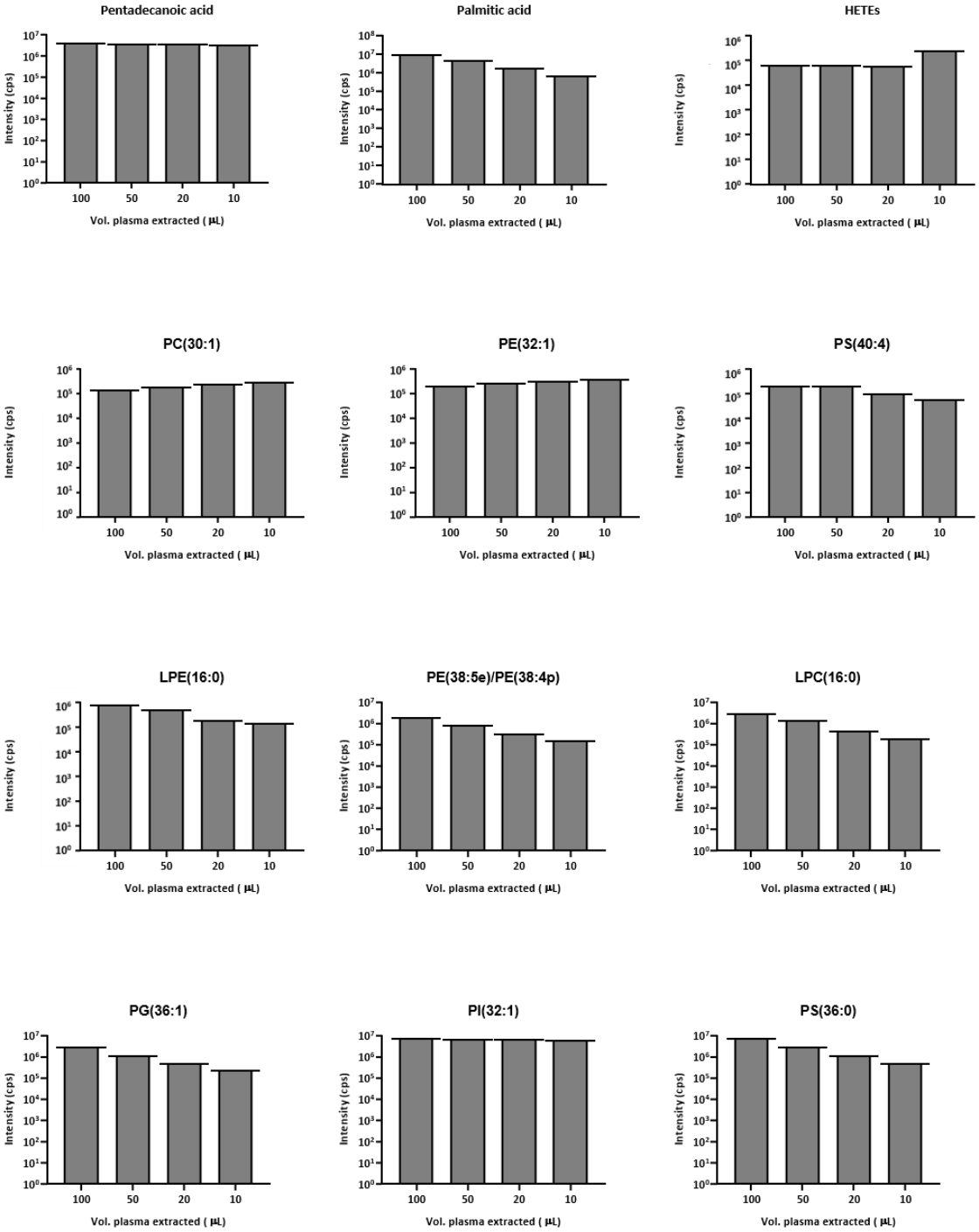

Figure 3.2: Recovery of endogenous PLs in extractions of four volumes of plasma, analysed on the Orbitrap Elite. Volumes of plasma extracted were 100 µL, 50 µL, 20 µL and 10 µL, and intensity is stated in counts per second (cps). Lipids identified using accurate mass, as calculated on LIPID MAPS, in Lipid Finder output files.

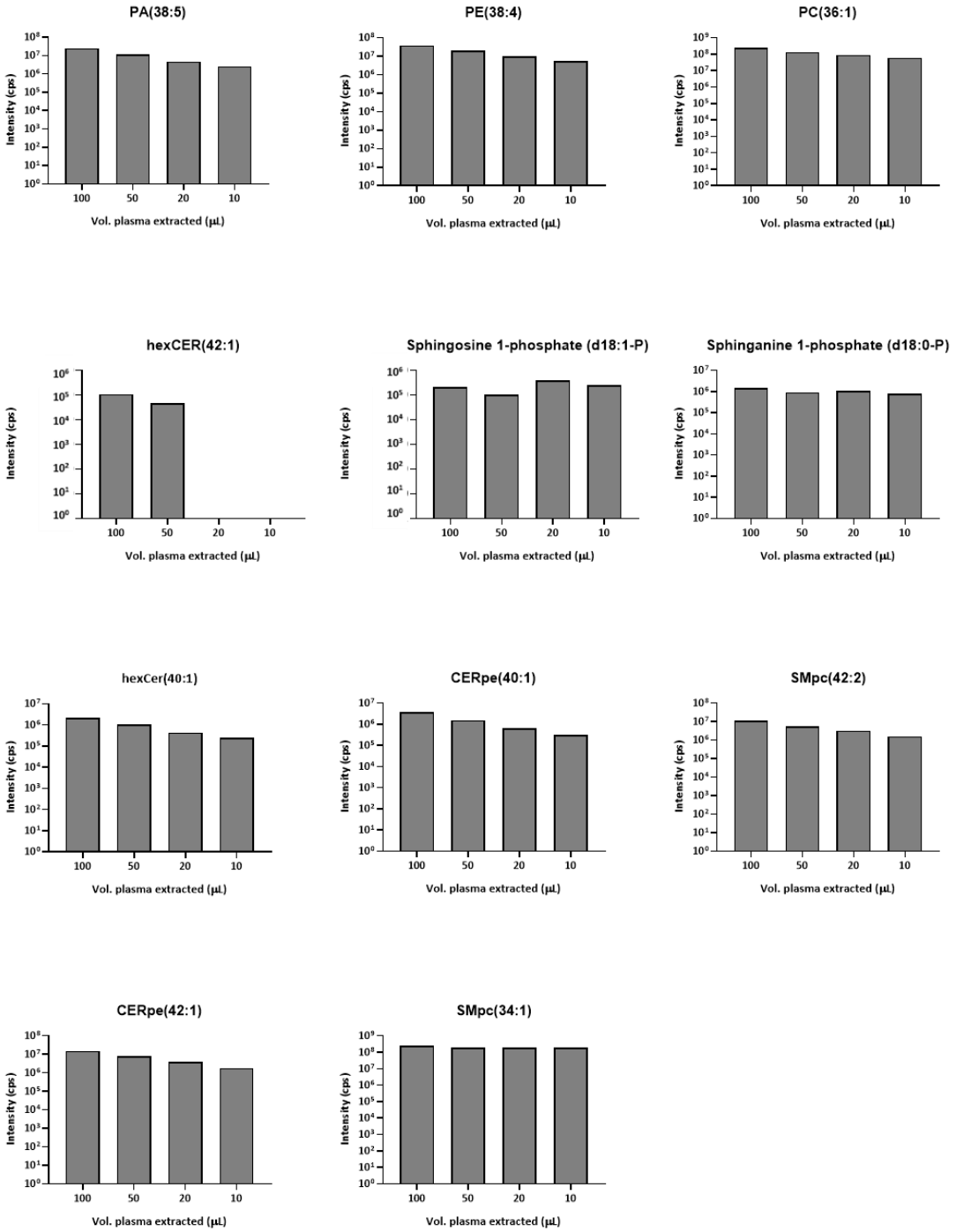

Figure 3.2(cont.): Recovery of endogenous lipid species in extractions of four volumes of plasma, analysed on the Orbitrap Elite. Volumes of plasma extracted were 100 µL, 50 µL, 20 µL and 10 µL, and intensity is stated in counts per second (cps). Lipids identified using accurate mass, as calculated on LIPID MAPS, in Lipid Finder output files.

3.2.3 Solvent for suspension of extracted lipids

Chloroform is recommended for storage of lipids and some studies use a methanol/chloroform mixture to resuspend lipid extracts after extraction and before LC/MS/MS analysis (Bligh and Dyer, 1959, Reis et al., 2013). To determine if changing the solvent used to suspend lipid extracts would increase lipid solubility or improve chromatography, I resuspended a range of lipids in three solvents and compared the results. Lipids were suspended in either methanol or a methanol/chloroform mixture at 2:1 or 1:1 (v/v). Peak area of standards is reduced when resuspending in a methanol/chloroform mix, suggesting that lipid extracts are less soluble in a chloroform methanol mix than in methanol alone (Table 3.3). Chromatography is also negatively impacted by the addition of chloroform, as peaks become wider and less defined (Figure 3.3).

3.2.4 Combining High and Low Mass Analysis on the Orbitrap Elite

I tested to see if the high and low mass analyses, which were previously performed separately, could be combined into a single run. Lipid categories all changed in size after the two analyses were combined, however, these changes were under 15 % (Figure 3.4). The glycerolipids category actually increased in size by 3.9 %, whilst the unknown category lost the most lipids (14.6 %).

3.3 Discussion

3.3.1 Extraction efficiency and CV are within acceptable limits

Some extraction efficiencies were slightly above 100 %, indicating that matrix effects may be taking place (Table 3.1). These occur in mixed samples when some species alter the ionisation of others, probably due to competition between analytes and matrix molecules for ionisation (Tang and Kebarle, 1993). Matrix effects are believed to originate from competition between analytes and matrix molecules for ionisation (Taylor, 2005). Only a limited number of

	PGE_2-d4	TxB_2-d4	11dehydro TxB2-d4	13-HODE d4	12/15 HETE d8	DMPE
Standard*	4.45E+05	8.10E+04	1.07E+05	3.37E+05	2.23E+05	3.18E+05
Methanol	4.13E+05	5.25E+04	9.90E+04	3.56E+05	2.42E+05	3.31E+05
Methanol/ Chloroform 2:1 (v/v)	2.54E+05	3.20E+04	6.60E+04	2.61E+05	2.20E+05	2.21E+05
Methanol/ Chloroform 1:1 (v/v)	3.19E+05	4.46E+04	7.81E+04	3.26E+05	1.44E+05	3.89E+05
Lipid recovery (%):						
Methanol	92.83	64.88	92.66	105.66	108.43	104.18
Methanol/ Chloroform 2:1 (v/v)	57.02	39.57	61.75	77.40	98.74	69.52
Methanol/ Chloroform 1:1 (v/v)	71.64	55.08	73.12	96.74	64.40	122.45

Table 3.3: Recovery of 6 lipid standards with three suspension solvents. *Standard denotes the peak area in an unextracted standard. The three suspension solvents were methanol, methanol:chloroform at 2:1 and methanol:chloroform at 1:1. Lipid recovery calculated as peak area in unextracted standard, divided by peak area in extracted standard, and multiplied by 100.

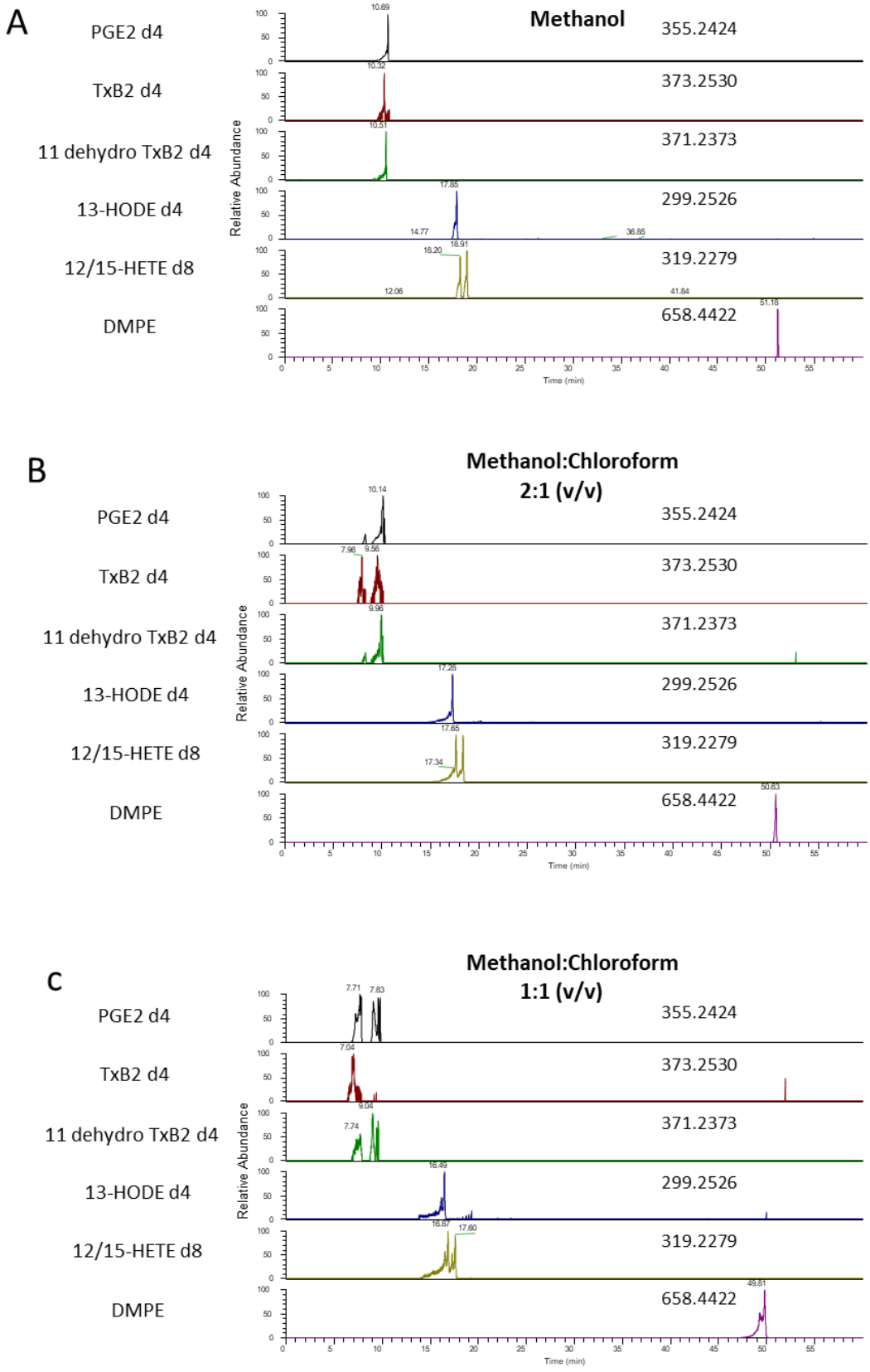

Figure 3.3: Chromatography with differing lipid suspension solvents. Chromatograms of deuterated eicosanoid standards with three suspension solvents, **(a)** Methanol, **(b)** Methanol:chloroform at 2:1 and **(c)** Methanol:chloroform at 1:1. All species found in negative mode ([M-H]-) except for DMPE, which was seen in positive mode ([M+Na]+). Transitions are noted on each chromatogram.

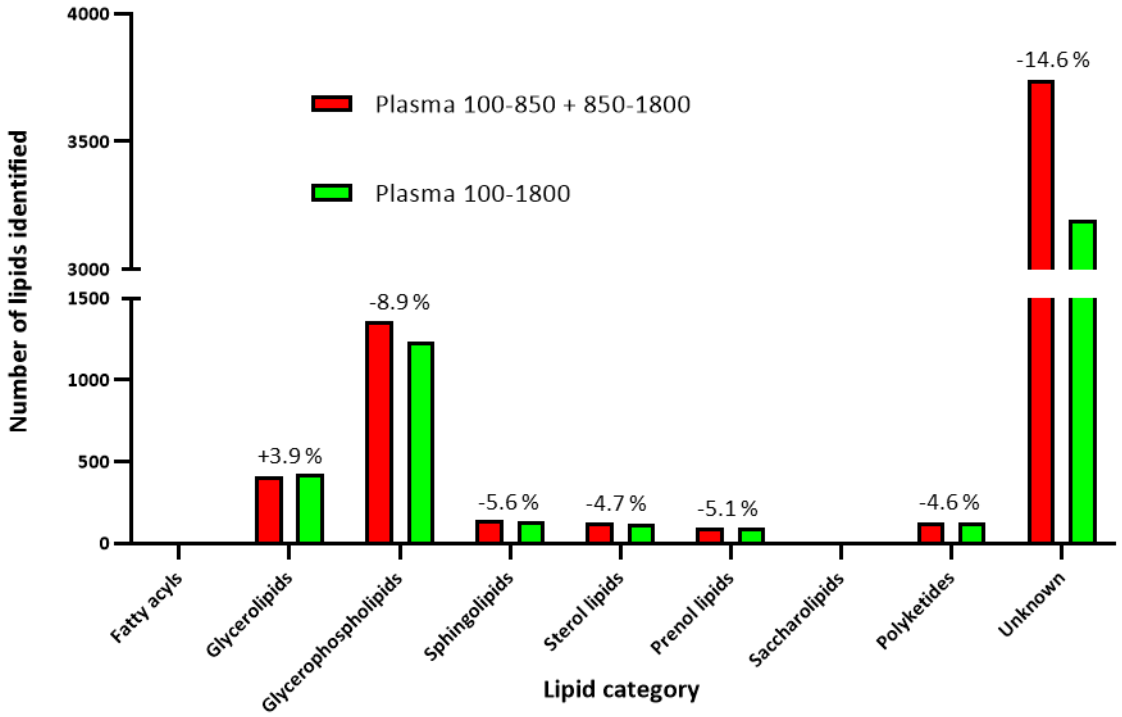

Figure 3.4: Lipid category counts across differing mass range analyses. The numbers represented above are lipids found per category per analysis. Plasma 100-850 and 850-1800 are the low and high mass analyses, which have been combined post LipidFinder. Plasma 100-1800 is the full mass range, completed in one analysis. Numbers above columns represent the percentage change in the size of the lipid category, calculated as the number of lipids in separate analyses, divided by the number of lipids in combined analyses, and multiplied by 100.

molecules can be present at the surface of the droplet during ionisation in an electrospray ion source, and background ions which elute at the same time as an lipid can prevent or enhance lipid ionisation (King et al., 2000). Separating analytes from the initial injection peak reduces matrix effects, and this is achieved by LC in methods used in this thesis (Taylor, 2005) (Sections 2.4.1 and 2.4.2). Mean extraction efficiency is 91 %, which is comparable to published methods of lipid extraction (Bligh and Dyer, 1959, McDonald et al., 2012, Alshehry et al., 2015). Also, whilst some extraction efficiencies are slightly over 100 %, this falls within the measured method variability of 1-6 % (Table 3.2).

Some studies remove lipids with a CV above a specific cut off, for example, 30 %, whilst others report a CV of 4-15 % (Maile et al., 2018, Li et al., 2013, Surma et al., 2015). Taylor et al., 2005 defines an acceptable CV to be below 15 % (Taylor, 2005). In this chapter, I demonstrate CV of 1-6 % for five standards in plasma, which compares favourably with the literature. As CV is low and because I have over 20 biological replicates, I will analyse each sample once in each mode on the Orbitrap Elite. This will save both machine time and sample.

3.3.2 Lipid extraction and MS analysis was modified to optimise lipid recovery and chromatography

Previous research has extracted varying volumes of plasma, for example, Quehenberger et al. extracted between 1 and 200 µL, depending on the lipid category being analysed, and recorded over 500 species in total (Quehenberger et al., 2010). Tests of differing extraction volumes suggested that some endogenous species will be lost at lower extraction volumes. However, investigation of the endogenous lipids suggests that some species are present at higher abundance in smaller extraction volumes (Figure 3.1). This suggests that matrix effects in more concentrated samples could be reducing ionisation efficiency of some lipids. In an effort to find as many lipids as possible, while minimising matrix effects which could alter quantification, I am reducing plasma volume to 50 µL. Few lipid species are lost and this may reduce matrix effects compared to a 100 µL extraction. I extracted 50 µL throughout the rest of this thesis, as no endogenous species will be lost in extraction and analysis when compared to a 100 µL extraction, and this saves sample analysed by 50 %. Reducing volume of sample

extracted also reduces the likelihood of overloading or clogging the column during lengthy analyses.

The solvent test results indicate that resuspending in a methanol/chloroform solution does not improve lipid solubility and negatively impacts chromatography. Therefore, I will continue re-suspending dried lipid extracts in methanol after the extraction procedure. I also determined I will combine the high and low mass analyses, as few lipids are lost in the process. The mass combination analysis clarified that polyketides and saccharolipids are being putatively identified in the dataset as they are present in the LIPID MAPS Structure Database (Sud et al., 2007). However, polyketides and saccharolipids originate from bacteria, fungi and plant sources, and lipids identified as either of these categories will be assigned as unknowns (Fahy et al., 2009).

3.3.3 Conclusions

Lipid extraction and analysis were optimised for lipidomic analysis of plasma. Extraction efficiency was high, and was similar to extraction efficiency in publication (Bligh and Dyer, 1959, McDonald et al., 2012, Alshehry et al., 2015). CoV was low, and similar to CoV of other targeted methods (Taylor, 2005, Maile et al., 2018, Li et al., 2013, Surma et al., 2015). The volume of plasma extracted was reduced from 100 µL to 50 µL, as investigation of a panel of endogenous lipids suggested that lipids can be measured in 50 µL, and that matrix effects occur during LC/MS analysis of the more concentrated plasma samples. Addition of chloroform when suspending lipid extracts caused peak splitting, therefore lipid extracts were suspended in methanol throughout this thesis. High and low mass analyses were combined to half machine time and use of sample and mobile phases. Also, the search parameters for lipid identification were narrowed to include only curated results.

Chapter 4: An LC/MS comparison of the lipidome of fresh and NPHSII plasma reveals minimal storage effects

4.1 Introduction

The NPHSII plasma samples I analysed in Chapters 5 and 6 were collected between 1989 and 1994, meaning samples were at least 21 years old at time of analysis (Miller et al., 1995). Once blood has been drawn and plasma isolated, it is imperative that storage conditions minimise in-sample changes to prevent degradation or oxidation of lipids. Pooled or cohort plasma is often used as a material for LC/MS, but many papers do not detail plasma storage conditions (Reitz et al., 2004, Liu et al., 2016).

Little is known about changes in lipid composition of plasma or serum during long term storage. Most studies have so far only considered only total cholesterol and TAGs, and results are disputed. For example, studies have variously suggested total cholesterol and total TAGs increase in long-term storage, total TAGs increase in storage but total cholesterol does not, or that neither are altered after a year or more at -70° (Kronenberg et al., 1994, Nanjee and Miller, 1990, Evans et al., 1997). Another investigation of over 100 serum lipids, this time by GC/MS, found that long-term storage and freeze-thaw cycles had little effect on lipids from all lipid classes (Zivkovic et al., 2009). These studies suggest that total cholesterol and TAGs in plasma or serum may undergo minimal change during storage.

The effect of long-term storage at -70°C or below on individual CE and TAG species has never been tested, and the longest duration that any samples spent in storage prior to analysis was 24 months, far shorter than the 25 years in storage for NPHSII samples being used herein (Kronenberg et al., 1994). To investigate whether a longer storage period had effects on lipid levels in NPHSII samples, I compared relative levels of a number of endogenous lipids in a subset of NPHSII plasma samples with fresh plasma. Ten NPHSII samples were randomly chosen and, for comparison, venous blood was drawn from 10 healthy volunteers then plasma isolated. Lipids from 'fresh' plasma were extracted alongside 10 NPSHII plasma samples on the same day as fresh blood was drawn.

4.1.1 Aims and hypothesis

The effect of storage for over 20 years at -70°C on plasma lipids is unknown.

My aims were as follows:

- To determine if the global lipidome of NPHSII plasma samples is altered by long term storage using LC/MS.

The null hypothesis is that the global lipidome will not differ significantly between fresh and NPHSII plasma.

4.2 Results

4.2.1 The total ion counts of NPHSII plasma samples are similar to total ion counts of fresh plasma samples

Before analysis, it was important to determine if lipids in NPHSII samples had altered during 20 years storage at – 70˚C. I compared 10 randomly chosen samples from the NPHSII cohort with 10 freshly drawn plasma samples taken from healthy volunteers. 10 fresh and 10 NPHSII samples were analysed using the global lipidomics method (Section 2.4.1) and Sieve-LipidFinder workflow (Section 2.5.1). Total ion count (TIC) for each sample was retrieved and means for fresh and NPHSII samples compared. TICs for the positive mode analysis of fresh and NPHSII plasma are not statistically significantly different when tested using a students t test (two-tailed, unequal variance), with means of 5.82 x 10^8 in fresh plasma and 4.87 x 10 in NPHSII plasma ($p = 0.0525$, $n = 10$) (Table 4.1). TICs did not differ significantly in negative mode, with means of 2.78 x 10^8 and 2.89 x 10^8 respectively in fresh and NPHSII plasma mode ($p = 0.31$, $n = 10$) (Table 4.2). A visual examination of TIC chromatograms for both positive and negative mode demonstrated a similar overall profile in terms of peak elution for fresh and NPHSII plasma samples, although there are several peaks at RT 10 – 17 min which are higher

A

Table 4.1A: TIC of fresh and NPHSII plasma in positive mode

Sample	TIC fresh (cps)	TIC NPHSII (cps)
1	3.89e+008	6.16e+008
2	4.27e+008	4.59e+008
3	7.23e+008	6.1e+008
4	5.36e+008	4.79e+008
5	4.41e+008	6.38e+008
6	5.15e+008	7.42e+008
7	3.68e+008	6.67e+008
8	4.84e+008	6.13e+008
9	5.59e+008	5.74e+008
10	4.37e+008	4.24e+008
Mean	4.88E+008	5.82E+008

B

Table 4.1B: TIC of fresh and NPHSII plasma in negative mode

Sample	TIC fresh (cps)	TIC NPHSII (cps)
1	2.88e+008	2.98e+008
2	2.56e+008	2.82e+008
3	3.22e+008	2.84e+008
4	2.78e+008	2.98e+008
5	2.8e+008	2.79e+008
6	2.67e+008	2.85e+008
7	2.72e+008	2.97e+008
8	2.62e+008	2.88e+008
9	2.97e+008	2.47e+008
10	2.55e+008	3.04e+008
Mean	2.78E+008	2.86E+008

Table 4.1A & B: Comparison of total ion counts (TIC). TIC represents all ionisable species in plasma, in **(A)** positive and **(B)** negative mode for 10 fresh plasma samples and 10 plasma samples from NPHSII cohort. TIC is measured in counts per second (cps).

in the NPHSII samples in negative mode (Figure 4.1, Figure 4.2). MS spectra from lipids eluting between RT 10 – 17 min revealed a group of ions that were generally higher in the NPHSII plasma (Figure 4.2B, black box). There are 2,457 peaks with a retention time of 10-17 minutes, 733 of which are significantly increased in NPHSII plasma. Of these, 30 are putatively identified as fatty acyls, 91 are glycerophospholipids, 1 is a glycerolipid, 1 is a prenol lipid, 3 are sterol lipids are the remainder (606) are unknown.

4.2.2 Fourteen of seventeen endogenous lipid species were not significantly different between fresh and NPHSII plasma

I decided to look at a panel of lipids, from which I can ascertain whether any large scale decomposition has taken place. I chose to analyse the dataset in this way rather than compare all the lipids contained within for two reasons. Firstly, 10 samples per group is a very small number when considering that thousands of lipids are found in the analysis. Thus, false positives and negatives would occur. Secondly, the differences between the plasma lipidome of individuals is not yet fully understood, but LC-MS/MS suggests that age may contribute to variation in the lipidome, and it would not be possible to determine if global changes in the lipidome were caused by participant demographics (Sanderson et al., 1995). Using accurate *m/z* according to LIPID MAPS, lipids were identified in NPHSII and fresh plasma (Sud et al., 2007). A 17 lipid panel was chosen from species quantified previously, with two chosen from each lipid category except phospholipids (GPLs) (Quehenberger et al., 2010). In that case, one GPL was chosen to represent each class (choline, ethanolamine, inositol, serine), as well as a lyso-phosphotidycholine (LPC), a lysophosphotidylcholine (LPE) and a plasmalogen or ether (plasmalogen and ether species cannot be resolved with accurate mass alone). Fold change was calculated as mean peak area in NPHSII plasma, divided by mean peak area in fresh plasma. All 17 of the lipid panel can be found in the fresh and NPHSII plasma using accurate *m/z* (mass error less than 5 ppm). All lipids putatively identified in this manner fell within the expected retention times for the category. None of the 9 fatty acyls, SPs and sterol lipids are statistically increased or decreased in NPHSII plasma compared to fresh (Figure 4.4). LPC(16:0) is significantly higher in NPHSII plasma with a fold change of 1.83, whilst PE(38:4) and PI(38:4) are both lower in NPHSII plasma, with fold changes of 0.50 and 0.77 respectively. PE(38:4)

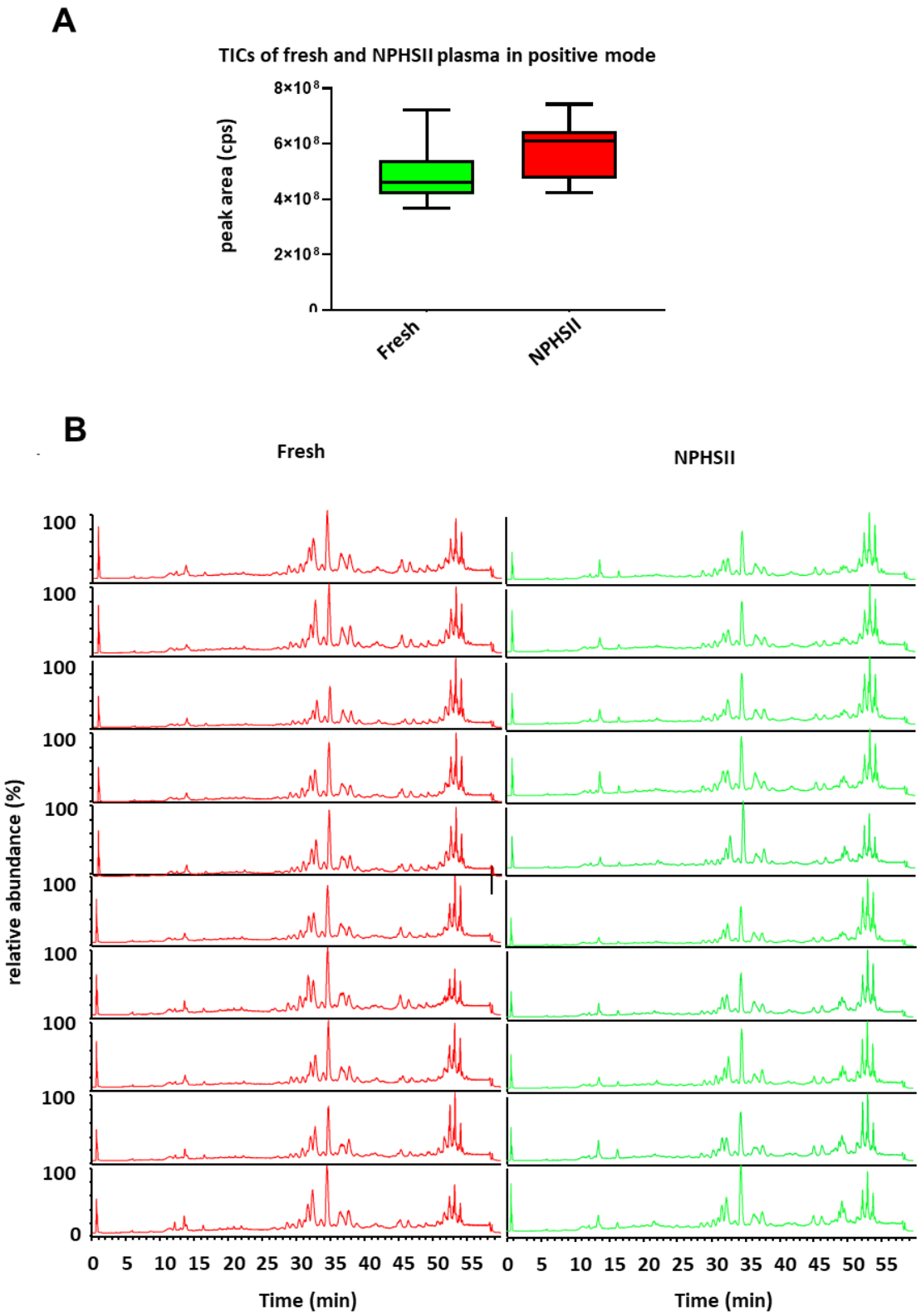

Figure 4.1: TICs of 10 NPHSII and 10 fresh plasma samples in positive mode do not differ visually or using a students t test. A: Boxplot of TICs from 10 fresh and 10 NPHSII plasma samples analysed on the Orbitrap Elite coupled to a Hypersil Gold column. Lower fence of boxplot represents the data point which is the lowest value greater than the 25th percentile minus 1.5 times the IQR. The upper fence represents the data point which is the greatest value lower than the 75th percentile pus 1.5 times the IQR. p = 0.0525, two-tailed unpaired t test (n = 10). **B:** Visual comparison of the TICs from freshly-drawn plasma samples (red) and NPHSII (green) (n = 10).

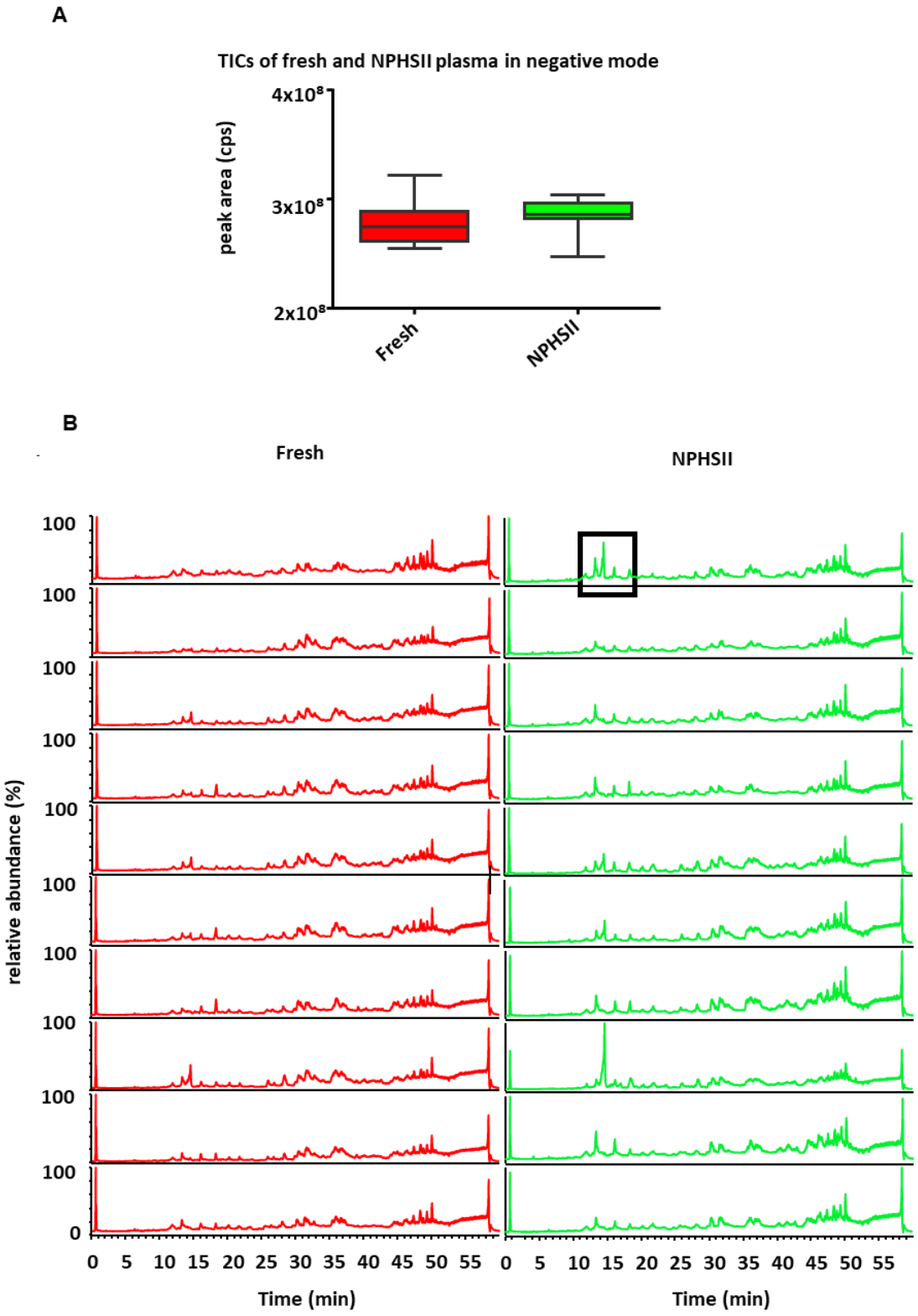

Figure 4.2: TICs of 10 NPHSII and 10 fresh plasma samples in negative mode do not differ visually or using student's t test. A: Tukey boxplot of TICs from 10 fresh and 10 NPHSII plasma samples analysed on the Orbitrap Elite coupled to a Hypersil Gold column. Lower fence of boxplot represents the data point which is the lowest value greater than the 25th percentile minus 1.5 times the IQR. The upper fence represents the data point which is the greatest value lower than the 75th percentile pus 1.5 times the IQR. p = 0.32, two-tailed unpaired t test (n = 10). **B:** Visual comparison of the TICs from freshly-drawn plasma samples (red) and NPHSII (green) (n = 10). The black box denotes several peaks with a higher relative abundance in the NHSII plasma.

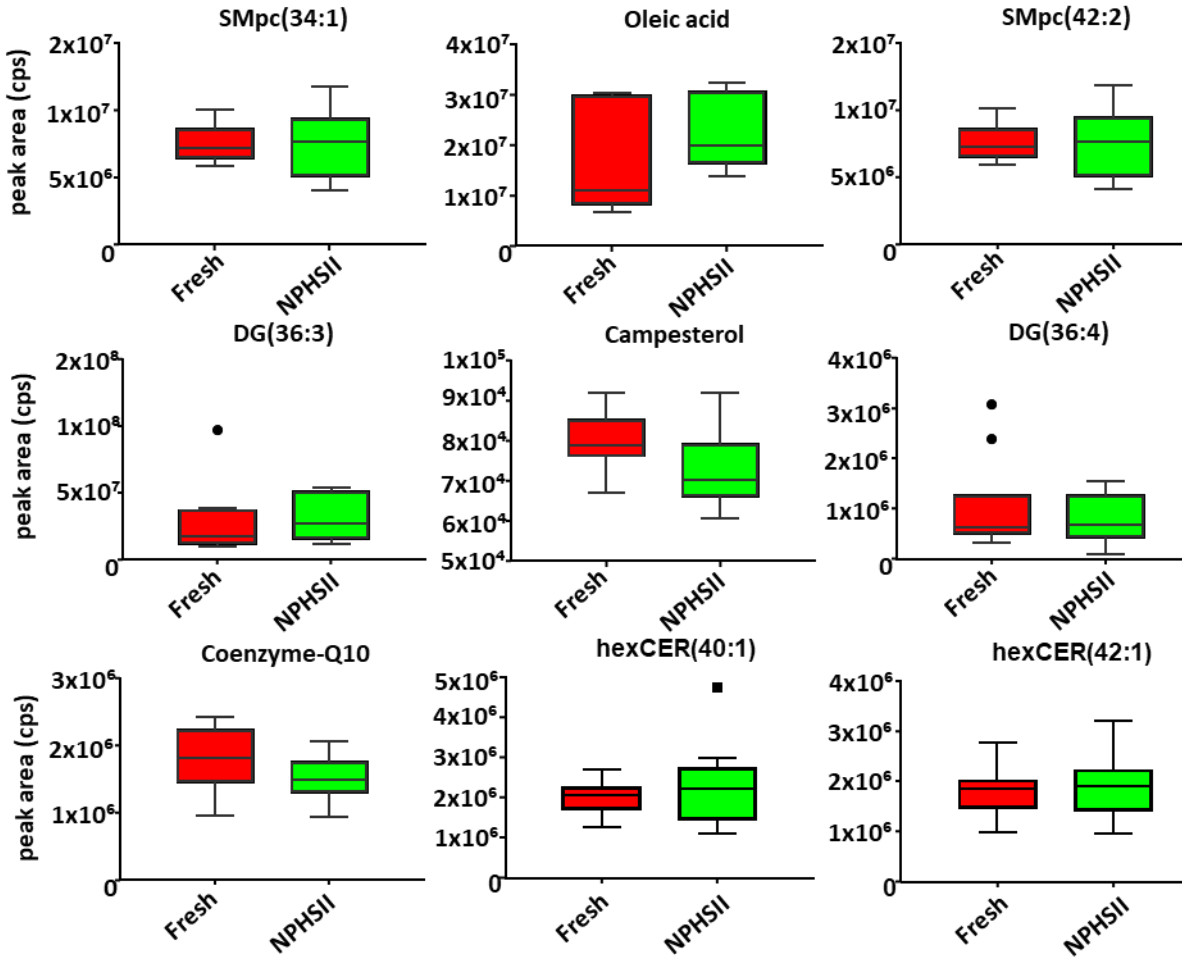

Figure 4.3: Nine lipids were identified by accurate mass, of which none were significantly altered in NPHSII plasma. Tukey boxplots comparing peak area of 9 lipid species, found by global lipidomics, in fresh prepared human plasma and in plasma samples from the NPHSII study (n=10). Significance was calculated using a t test with Benjamini-Hochberg multiple comparisons test, where Q = 10%. Lower fence of boxplots represent the data point which is the lowest value greater than the 25th percentile minus 1.5 times the IQR. The upper fence represents the data point which is the greatest value lower than the 75th percentile pus 1.5 times the IQR.

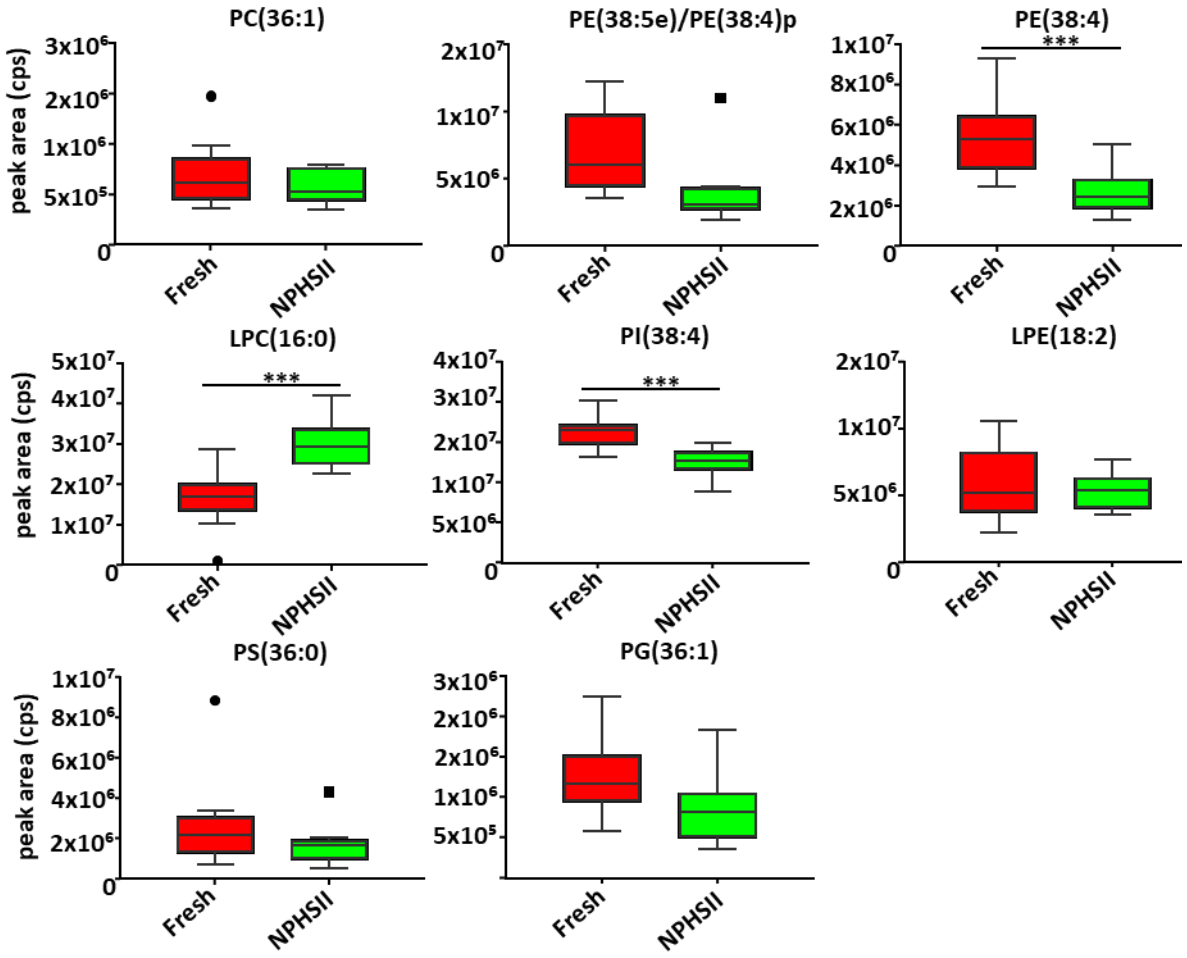

Figure 4.4: Polyunsaturated PL species were reduced in NPHSII plasma. Tukey boxplots comparing of peak area of 18 lipid species, found by global lipidomics, in fresh prepared human plasma and in plasma samples from the NPHSII study (n=10). Significance was calculated using a t test with Benjamini-Hochberg multiple comparisons test, where Q = 10%. Lower fence of boxplots represent the data point which is the lowest value greater than the 25th percentile minus 1.5 times the IQR. The upper fence represents the data point which is the greatest value lower than the 75th percentile pus 1.5 times the IQR.

.

and PI(38:4) are both easily oxidised due to the presence of two double bonds, thus, I also analysed four oxidised GPLs (oxPLs), below.

4.2.3 Oxidation measured by oxPLs is higher in NPHSII plasma than fresh

Non-enzymatic oxidation of lipids is a common problem and could in theory occur during long term storage of plasma. There were a number of lipids, including GPLs, which were increased in NPHSII plasma between 10 and 17 mins. It is possible that these GPLs are oxidized, as they elute earlier than expected for this lipid category under my analysis conditions. Therefore, I analysed four oxPLs via LC-MS/MS to determine if NPHSII samples contain more oxidised species (Section 2.4.3). OxPL peak area was normalised to DMPC (internal standard) to account for extraction efficiency. NPHSII and fresh samples were analysed using a targeted LC/MS/MS method (Section 2.4.3). All four oxPL species were detected and peak areas compared using a students t test (two-tailed, unequal variance) (Figure 4.5). Two of these are significantly higher in the NPHSII plasma, PE(18:0a/9`-oxo-nonanoyl) with a fold change of 1.86 and PC(18:0a/9`-oxo-nonanoyl) with fold change of 2.52. The other two oxPLs are higher in the NPHSII plasma, although this did not reach significance.

4.2.3 Quantitative analysis of triacylglyceride and cholesterol ester species reveals few changes between fresh and NPHSII plasma

4.2.3.1 Cholesterol esters

Seven CEs were quantified using a targeted LC-MS/MS and concentration curve (Section 2.4.2.1). A students t test (two-tailed, unequal distribution) used to distinguish if concentration in fresh plasma samples differed significantly from concentration in NPHSII plasma (n = 10). Six of the seven species measured are present at statistically similar levels in fresh and NPHSII plasma, whilst one, CE(20:4), is significantly lower in the NPHSII plasma than fresh, with a fold change of 0.61 (Figure 4.6). Absolute amounts of most CE species quantified were not significantly different between NPHSII and fresh plasma.

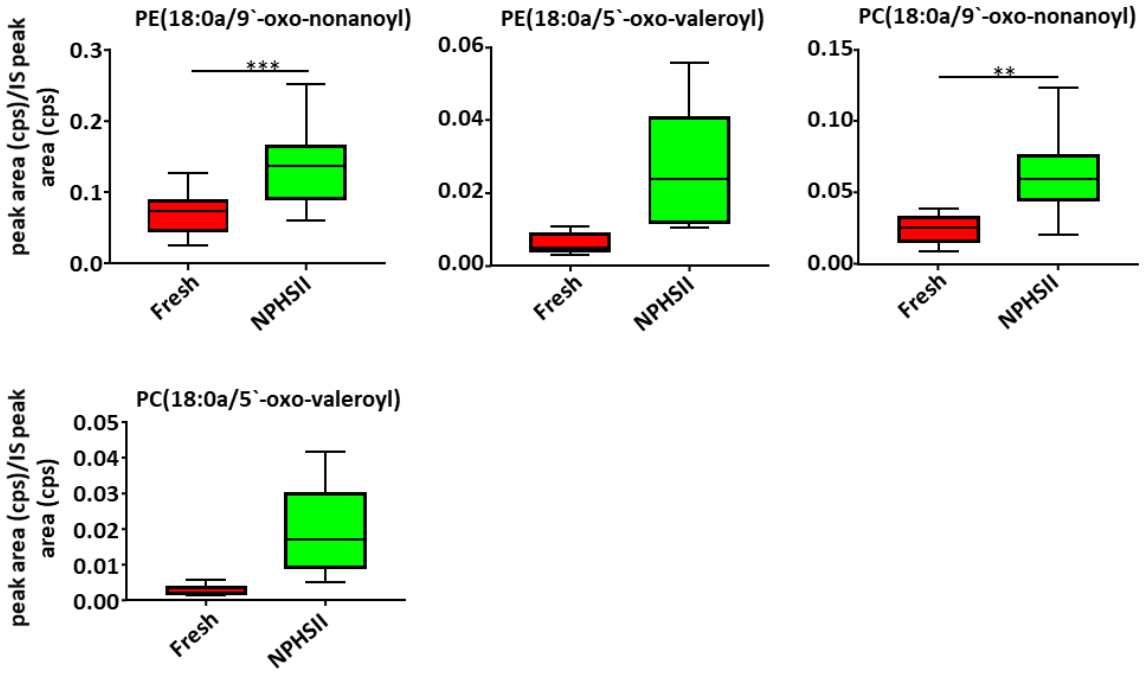

Figure 4.5: oxPLs are increased in NPHSII plasma. Tukey boxplots comparing oxPLs, analysed on the 4000QTrap coupled to a Shimadzu LC system and Luna column (n = 10). Data analysed by two-way anova with Sidak's multiple comparisons test. Lower fence of boxplots represent the data point which is the lowest value greater than the 25th percentile minus 1.5 times the IQR. The upper fence represents the data point which is the greatest value lower than the 75th percentile pus 1.5 times the IQR.

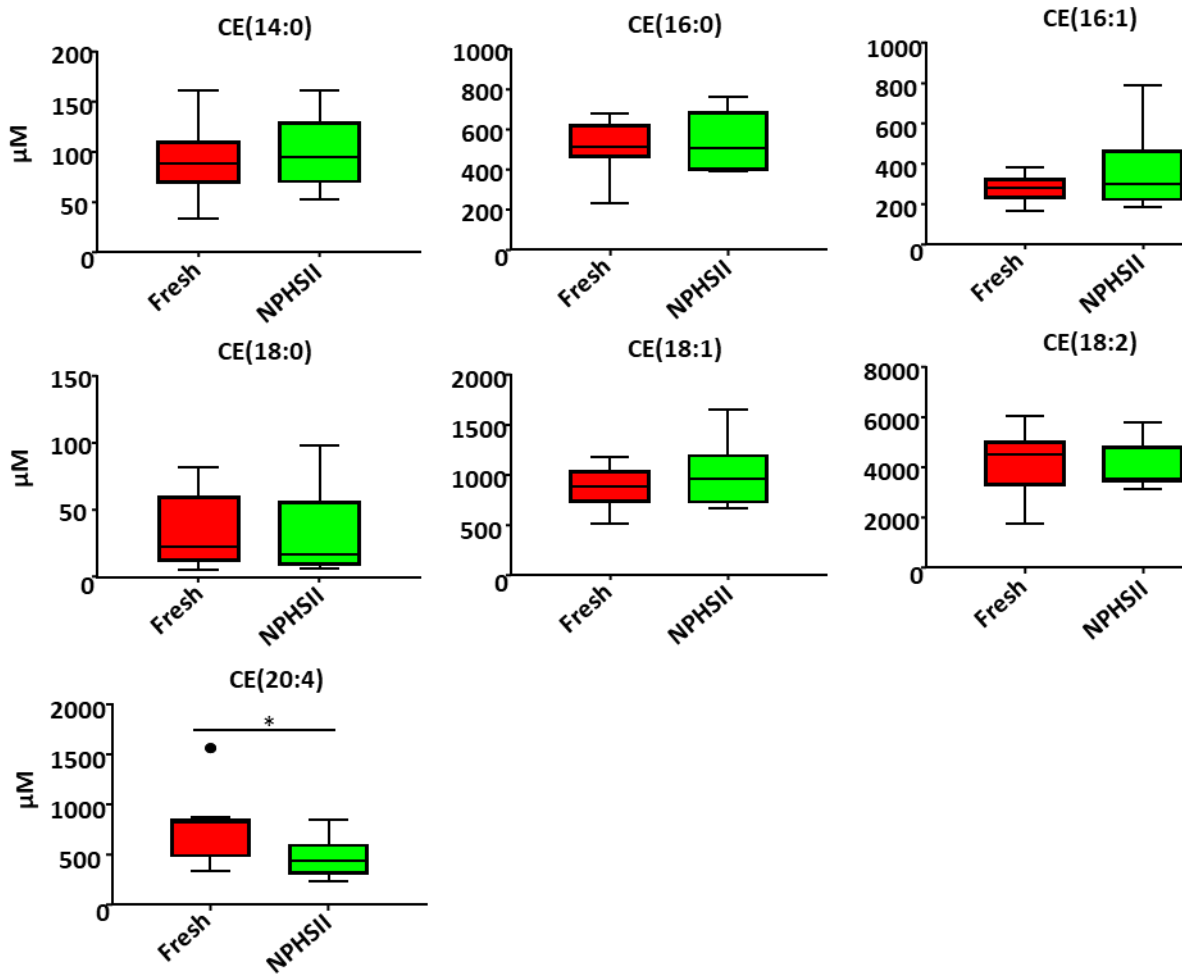

Figure 4.6: CE(20:4) is decreased in NPHSII plasma. Cholesterol and cholesterol esters concentrations (µM) in fresh and NPHSII plasma after targeted analysis (n = 10). CEs were quantified on a 4000 Qtrap coupled to a Shimadzu LC system and Hypersil Gold column. Significance was calculated using a t test with Benjamini-Hochberg multiple comparisons test, where Q = 10%. Lower fence of boxplots represent the data point which is the lowest value greater than the 25th percentile minus 1.5 times the IQR. The upper fence represents the data point which is the greatest value lower than the 75th percentile pus 1.5 times the IQR.

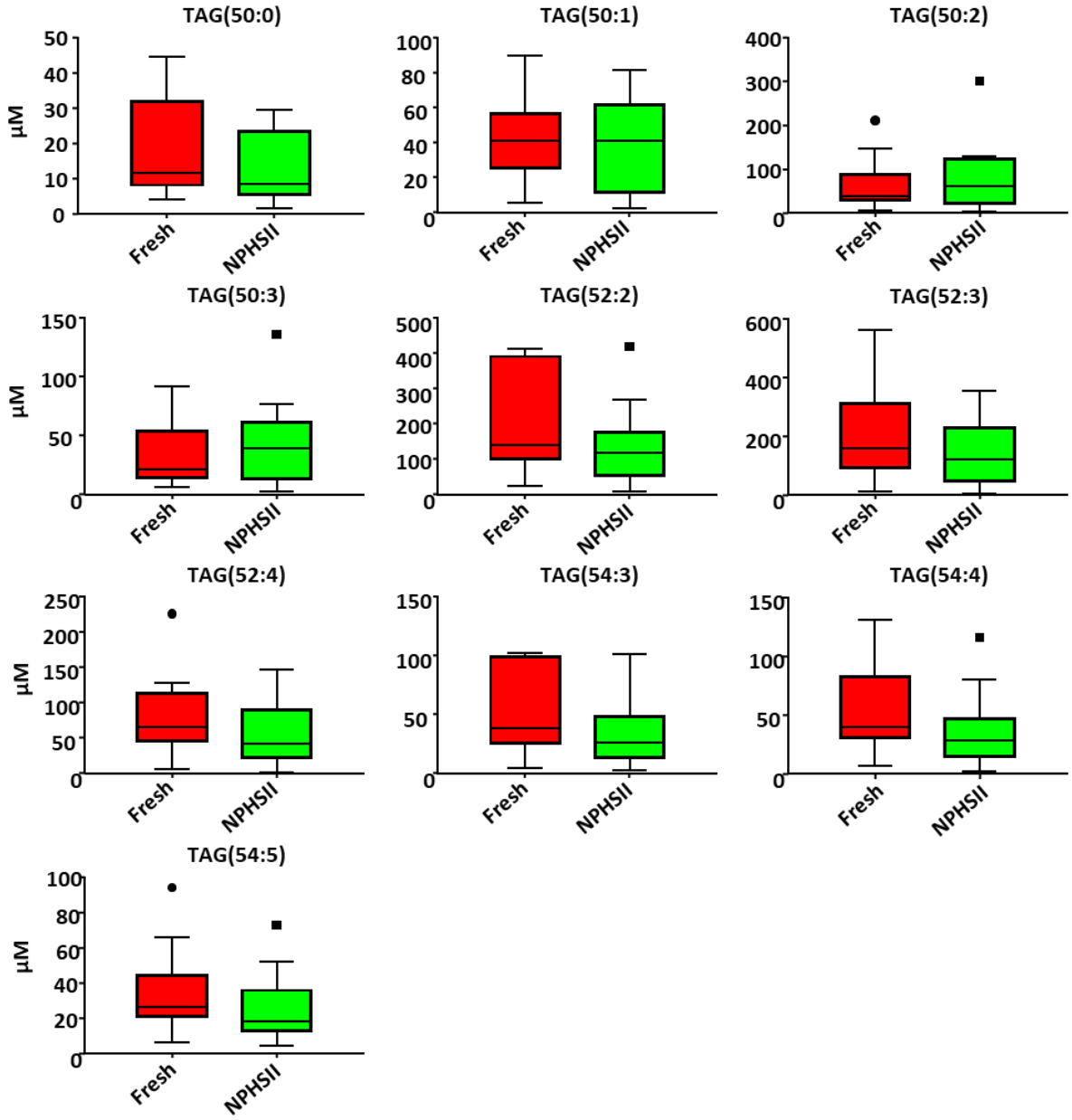

Figure 4.7: Absolute amounts of TAG species did not differ between fresh and NPHSII plasma. Tukey boxplots comparing triglyceride concentrations (µM) in fresh and NPHSII plasma after targeted analysis (n = 10). TAGs were quantified on a 4000 Qtrap coupled to a Shimadzu LC system and Hypersil Gold column. Significance was calculated using a t test with Benjamini-Hochberg multiple comparisons test, where Q = 10%. Lower fence of boxplots represent the data point which is the lowest value greater than the 25th percentile minus 1.5 times the IQR. The upper fence represents the data point which is the greatest value lower than the 75th percentile pus 1.5 times the IQR.

4.2.3.2 Triacylgylcerides

TAGs were quantified using the targeted LC-MS/MS method TAG 1 and a concentration curve (Section 2.4.2.3). A students t test (two-tailed, unequal variance) used to determine if concentration in NPHSII samples differed significantly from concentration in fresh samples (n = 10). None of the TAG species measured were up- or downregulated in NPHSII plasma compared to control. Several polyunsaturated species such as TAG(52:2), TAG(54:3) and TAG(54:4) trended towards being lower in NPHSII, however these did not reach significance (Figure 4.7).

4.3 Discussion

The NPHSII cohort kindly donated 99 genotyped plasma samples from participants homozygous for *APOE* ε2*, APOE* ε3 (to be used as control) and *APOE* ε4. I plan to analyse the global plasma lipidome of APOE homozygotes, as this is a novel investigation of a common genetic risk factor for LOAD (Corder et al., 1994, Corder et al., 1993). Before analysis, it was important to determine if lipids in NPHSII samples had altered during 20 years storage at – 70 °C. I compared 10 randomly chosen samples from the NPHSII cohort with 10 freshly drawn plasma samples taken from healthy volunteers. First, I found that TICs do not differ either visually or statistically between NPHSII and fresh plasma (Figure 4.1, Figure 4.2).

While most endogenous lipids are present at similar levels in NPHSII and fresh plasma, GPL and oxPL data suggests one of two scenarios (Figure 4.3 – 4.5). Firstly, oxidation of some polyunsaturated lipids may have taken place during storage, which could hide differences in oxidised lipids in NPHSII plasma. Secondly, the demographics of the participants is different, in that the fresh samples originate from mixed gender subjects, aged 20 to 40, whilst NPHSII samples originate from males aged 40-60. Age is associated with markers of lipid peroxidation in blood, therefore plasma from an older demographic may be expected to contain fewer polyunsaturates and more oxidised species (Sanderson et al., 1995). Also, peaks in the region of 10 – 17 minutes which are higher in NPHSII plasma samples are not uniformly elevated in all NPHSII samples (Figures 4.1 and 4.2). Thus, whilst lipids which increased in intensity in

NPHSII plasma could originate solely from storage, participant demographics could also be responsible. The endogenous lipid panel was used to identify which lipid classes were increased in NPHSII plasma. 3 of the 17 endogenous species (18 % of total) detected were significantly changed between the groups (Figure 4.3, Figure 4.4), which was a higher proportion than previously reported (Zivkovic et al., 2009). However, that study was an investigation of the same plasma over multiple timepoints, whilst in this chapter the fresh and NPHSII plasma come from different donor pools. The higher proportion of changed lipids between groups probably reflects differences in the plasma donors, however, the effect of gender and age on the global lipidomic plasma profile is unknown in this instance.

My data indicate that whilst some oxidation of polyunsaturated species occurred, long-term storage of plasma does not significantly affect abundance of the majority of CE and TAG species (Figure 4.6, Figure 4.7). This is in accordance with literature reporting no change in total cholesterol or TAGs (Nanjee and Miller, 1990). It was reassuring to determine that CEs and TAGs are not altered between the fresh and NPHSII plasma, especially considering that the fresh samples were not taken from a participant pool of the same age and gender as the NPHSII samples. Both age and gender were previously shown to affect both total cholesterol and total triglycerides in an investigation of 2,987 Danish citizens (Heitmann, 1992). Therefore, trends towards significance in some TAGs may be due to differences in participant demographics. Quantification of CE and TAG species in the NPHSII plasma revealed a similar range of concentrations to previous studies, providing confidence in our method of quantification (Table 4.3, Table 4.4) (Quehenberger et al., 2010). CE(18:0) was the least abundant and CE(18:2) the most abundant CE species in both datasets (Table 4.3). CEs ranged in concentration in NPHSII samples from 33 – 4266 µM, compared to a range from 59 – 1820 µM. CE(20:4) was significantly higher in NPHSII samples and could be easily oxidised due to its polyunsaturated nature. However, the wider range of quantified CEs in fresh samples could, as previously discussed, represent more diversity in the participants.

Cohort plasma is often used as an experimental material, however, there have been relatively few studies investigating the long-term storage of plasma lipids. Also, many studies which use long-term stored plasma have not compared cohort plasma with fresh. For example, in 2017, four plasma lipids were found to be an accurate predictor of early stage lung carcinoma, with

Table 4.2: Mean cholesterol and cholesterol esters concentrations (µM) in fresh and NPHSII plasma are similar to those published in Quehenberger et al., 2010

	Mean fresh (µM)	Mean NPHSII (µM)	Mean Quehenberger et al., 2010 (µM)
CE(14:0)	91	101	80
CE(16:0)	519	533	190
CE(16:1)	273	360	111
CE(18:0)	35	33	59
CE(18:1)	881	992	533
CE(18:2)	4266	4047	1820
CE(20:4)	761	468	237

Table 4.3: Triglyceride concentrations (µM) in fresh and NPHSII plasma are similar to those published in Quehenberger et al., 2010

	Mean fresh (µM)	Mean NPHSII (µM)	Mean Quehenberger et al., 2010 (µM)
TAG(50:0)	18	12	11
TAG(50:1)	42	39	64
TAG(50:2)	65	82	80
TAG(50:3)	34	44	57
TAG(52:2)	209	113	140
TAG(52:3)	207	137	215
TAG(52:4)	83	53	91
TAG(54:3)	52	36	69
TAG(54:4)	54	37	69
TAG(54:5)	36	26	54

Tables 4.2 and 4.3: Cholesterol, cholesterol esters (CE) and triglycerides (TAG) measurements fall in the same range as measurements by Quehenberger et al., 2010. Table 4.2: CEs measured by targeted assay using LC-MS/MS and quantified against a curve of known concentrations (n = 10, 10 and 3 for fresh, NPHSII and Quehenberger respectively). **Table 4.3:** TAGs measured by targeted assay using LC-MS and quantified against a curve of known concentrations (n = 10, 10 and 3 for fresh, NPHSII and Quehenberger respectively).

80.08 % accuracy, 78.7 % sensitivity and 69.4 % specificity (Yu et al., 2017). Plasma samples were collected between 2004 and 2010 and stored at – 80 ° C, making them 7 – 13 years old at time of analysis. No comparison with fresh plasma was presented. The four lipids which gave the best prediction of early stage lung carcinoma were LPE(18:1), PE(40:4e), CE(18:2) and SM(22:0). My data demonstrates that long chain polyunsaturates such as PE(40:4e) decrease during storage. I suggest that it would therefore be important in this case to compare the mean time that control and cancer samples spent in storage to determine if this differed between the two groups. In summary, many research centres have long-term stored plasma, which may contain important biological insights. Before analysis of any long-term stored sample, I would recommend an investigation of storage conditions and a quality control test.

4.4 Conclusions

In conclusion, here, I conducted a lipidomic comparison between fresh and stored NPHSII plasma, using the global method and also using a series of targeted assays. My analysis revealed selected alterations in lipid levels. However, as (i) control and risk-SNP samples from NPHSII have been in storage for approximately the same amount of time, (ii) age and gender differences may account for the small increase in oxidised lipids and (iii) most lipid classes analysed are not are not significantly different, I conclude that NPHSII samples are not too degraded for lipidomic analysis.

Chapter 5: Global lipidomic analysis of *APOE* homozygote plasma reveals a dysregulated sphingolipidome in *APOE* 22

5.1 Introduction

As discussed in Chapter 1, *APOE* alleles are associated with changes in risk of LOAD and the apoE protein plays a key role in lipid transport and metabolism. Previous investigations of the lipidomics of *APOE* alleles have measured total cholesterol and TGs rather than individual lipid molecular species levels. These reports have found that plasma cholesterol is lower when at least one ε2 allele is present and higher with one or two ε4 alleles (Sing and Davignon, 1985). Furthermore, total TGs are higher in plasma of *APOE* ε2 and ε4 carriers when compared to *APOE* 33 (Dallongeville et al., 1992).

However, there are large numbers of individual molecular species in plasma, including CEs and TAGs (Quehenberger et al., 2010). Therefore, measures of total cholesterol and TAGs do not provide full information on the many molecular species present in plasma. Advances in LC/MS now allow all lipids within a sample to be profiled in a targeted or untargeted manner, facilitating the detection of lipidomic changes occurring across genotypes or during disease (Oresic et al., 2008). Indeed, many lipid species have now been identified and targeted lipidomic profiling of plasma using LC/MS/MS quantified over 500 quantifiable species, which fell into six LIPID MAPS categories (fatty acyls (FAs), glycerolipids (GLs), glycerophospholipids (GPs), prenol lipids (PRs), sphingolipids (SPs) and sterol lipids (SLs)) (Quehenberger et al., 2010). Lipoproteins are lipid-protein complexes which regulate fat distribution between the intestines, various tissues and the liver, and are composed of phospholipids, cholesterol, CEs, TGs and SPs (Skipski et al., 1967, Hidaka et al., 2007). Ultracentrifugation only separates lipoproteins from plasma after 2 hours at 172,000 g, whilst NPHSII samples were centrifuged at 724 g for a total of 20 mins (Wilcox et al., 1971). Therefore, lipoproteins will be present in the NPHSII plasma. Circulating lipids can act as biological signalling mediators, for example, leukotriene B4, platelet activating factor (PAF) and steroid hormones (Ford-Hutchinson et al., 1980, Jagels and Hugli, 1992, Ghayee and Auchus, 2007). As lipids play roles in homeostasis and are altered in various disorders, lipidomic profiling could aid disease diagnosis. For

example, LC/MS of plasma or serum can separate LOAD and lung cancer patients from healthy controls (Proitsi et al., 2015, Yu et al., 2017).

Here, I analysed the global lipidome of homozygotes for the 3 common *APOE* alleles by LC/MS, in an attempt to identify lipids which alter risk of LOAD. Plasma samples from *APOE* ε2, ε3 and ε4 homozygotes were provided by the NPHSII cohort (Miller et al., 1995), and chosen as discussed previously (Section 2.2.2). *APOE33* plasma was used as control throughout this chapter as this is the most common allele.

5.1.1 Aims and hypotheses

To my knowledge, there has been no untargeted LC-MS analysis of human plasma from participants homozygous for all three *APOE* alleles. Therefore, the effect of *APOE* allele on lipid categories and individual species in the human is yet to be elucidated.

My aims were as follows:

- To profile the global lipidome of *APOE* 22, control and *APOE* 44 participants.
- To investigate which lipid species and categories differ the most between *APOE* alleles.

The null hypothesis is the presence of *APOE* ε2 or *APOE* ε4 will not affect levels of either lipid categories or individual lipid species in human plasma.

5.2 Results

5.2.1 Global LC-MS methods suggest that over 10 % of lipid species decrease in *APOE* 22 plasma compared to *APOE* 33 controls.

5.2.1.1 Levels of SPs, unknown species and GLs are lower in APOE 22 plasma than control

I analysed the lipidome of *APOE* 22 and control plasma (n = 22) using untargeted high-resolution LC/MS (Section 2.4.1), and the XCMS-LipidFinder workflow (Section 2.5.2). This is a semi-quantitative method, thus fold change (FC) for all lipids identified was calculated as signal intensity (cps) in *APOE* 22 divided by signal intensity in control, using means for each genotype. *m/z* values were compared to the LIPID MAPS curated database. If a match was found then lipid category was assigned, whereas if multiple matches were found then the lipid was designated as the category with the most *m/z* matches. Lipids were allocated identifiers made up of *m/z*, RT and lipid category. In some cases, putative identifications (IDs) were made, based on accurate mass and match to an in-house built RT repository. This database contains lipids and their RTs which have previously been identified via the untargeted LC-MS/MS method (Section 2.4.1). It is important to note that IDs in this Chapter were assigned only on accurate *m/z* and RT and as such cannot be considered validated using this approach.

Some lipid signals were removed from the dataset during analysis as they were present in less than 66.6 % of all samples, however, none of these were present in only one genotype. A total of 1,591 lipids were detected in *APOE* 22 and control plasma, and all of these were present in plasma from both genotypes. Of these, 33 lipids were assigned as fatty acyls, 91 as GLs, 281 as GPs, 6 as PRs, 133 as SPs and 22 as sterol lipids (Table 5.1). The remaining 1,025 lipids were designated as unknowns, since they are absent from the LIPID MAPS database. 197 of the 1,591 lipids detected were significantly altered in *APOE* 22 when compared using a students two-tailed t test, with most of these being decreased. A Benjamini-Hochberg (BH) correction was used to correct for multiple tests (Section 2.5.7). Briefly, lipids were ordered by rank and rank was divided by the total number of lipids then multiplied by the chosen false discovery

Lipids from 6 LIPID MAPS categories were found in APOE 22 and control plasma

	Total	% total*	Significant	Sig. after BHC†	% of cat. sig.‡
All lipids	1591		197	86	
Fatty acyls	33	2.1	1	0	3.0
Glycerolipids	91	5.7	0	0	0.0
Glycerophospholipids	281	17.7	15	3	5.3
Prenol lipids	6	0.4	0	0	0.0
Sphingolipids	133	8.4	34	15	11.2
Sterol lipids	22	1.4	1	0	0
Unknown‡	1025	64.4	145	68	6.6

Table 5.1: Lipids from 6 LIPID MAPS categories were found in APOE 22 and control plasma. *Number of lipids in each class as a percentage of the total number. †Number of lipids significantly changed ($p < 0.05$, two-tailed students t test) between APOE 22 and control as a percentage of all lipids in that category. ‡ Percentage of lipids significant after BH correction. N = 22/39 for APOE 22/control respectively.

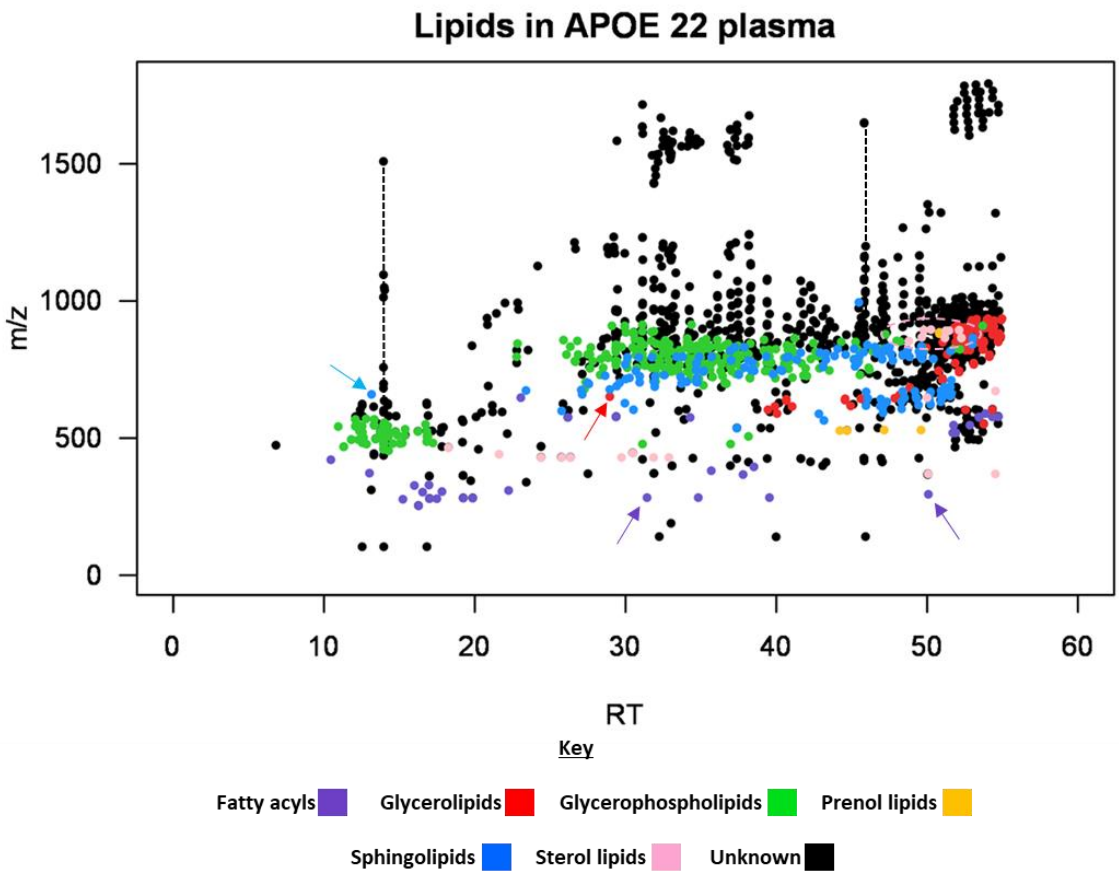

Figure 5.1: Plasma lipids in APOE 22 and control participants, separated by LC/MS, cluster according to lipid category. A scatter plot of lipids in APOE 22 and control plasma, separated by RT (x axis) and m/z (y axis). Each point represents one lipid and is coloured according to lipid category. Lipids within the same category behave in a similar manner when separated by LC/MS. For example, glycerolipids (red oval) all fall between RT 40 – 55 and m/z 500 – 100. Arrows indicate some outliers, i.e. lipids which did not fall within the expected *m/z* and RT windows, and are also coloured according to lipid category. 'Stacks' in the data, made up of adducts, are presented by black lines. Plot made in RStudio.

rate (FDR). A FDR value of 0.1 was chosen as a higher FDR may cause false negatives to occur and 0.05 is too low an FDR for most experiments. After the BH correction, 86 lipids were still significant ($P < 0.05$), of which 3 were GPs, 15 were SPs and the remainder were unknown.

All lipids in the dataset are visualised in a scatter plot, separated by *m/z* and RT and coloured by lipid category (Figure 5.1). Lipids putatively identified as being from the same category tend to cluster together along both axes. Most fatty acyls eluted between 10-23 min and with *m/z* 253-490. Some additional fatty acyls which eluted at RT 50-55 are most likely in source fragments of larger lipids, for example GPs, which eluted concurrently. GLs eluted between 40-55 min and *m/z* 551-935. GPs eluted between 22-55 min and *m/z* 678-913, as well as between 10-18 min and *m/z* 454-570. Those eluting earlier were smaller *m/z* and predominantly lysoPLs. There were few PRs, and these eluted between 45 – 50 min and *m/z* 527-885. SPs eluted between 22 – 52 min and *m/z* 536-994. Sterol lipids eluted from the LC column in two groups, the first between 19-34 min and *m/z* 369-465 and the second between 48-53 min and *m/z* 853-895. Lastly, over 50 % of lipids were not present in the LIPID MAPS dataset, and so were classified as unknowns. Unknown species are present throughout the LC separation and across a wide *m/z* range.

Volcano plots visualise lipids by log2(FC) and -log10(p value). Each point represents a lipid and is coloured according to the assigned category (Figure 5.2 A). All lipids below zero on the x-axis are decreased in *APOE* 22 plasma compared to control and conversely, all lipids above zero are increased in *APOE* 22. Most lipids of all categories fall below zero because they are reduced in abundance in *APOE* 22. Significance was calculated using a student's two-tailed t test and lipids with the most significance belong to the unknown, GP and SP categories. Unknown lipids appear most frequently above the 1.3 y-axis mark (equivalent to $p < 0.05$), furthermore the largest FC are within the unknown category (Figure 5.2 B).

Thirty-four putatively identified SPs (25.5 % of total number of SPs) are significantly lower in the *APOE* 22 group when testing using a students t test (Table 5.2), the largest percentage changes for any lipid category. After the BH procedure, 15 SLs from four subclasses maintain significance. Fifteen GPs are significantly reduced in *APOE* 22, with 8 of these being PCs which

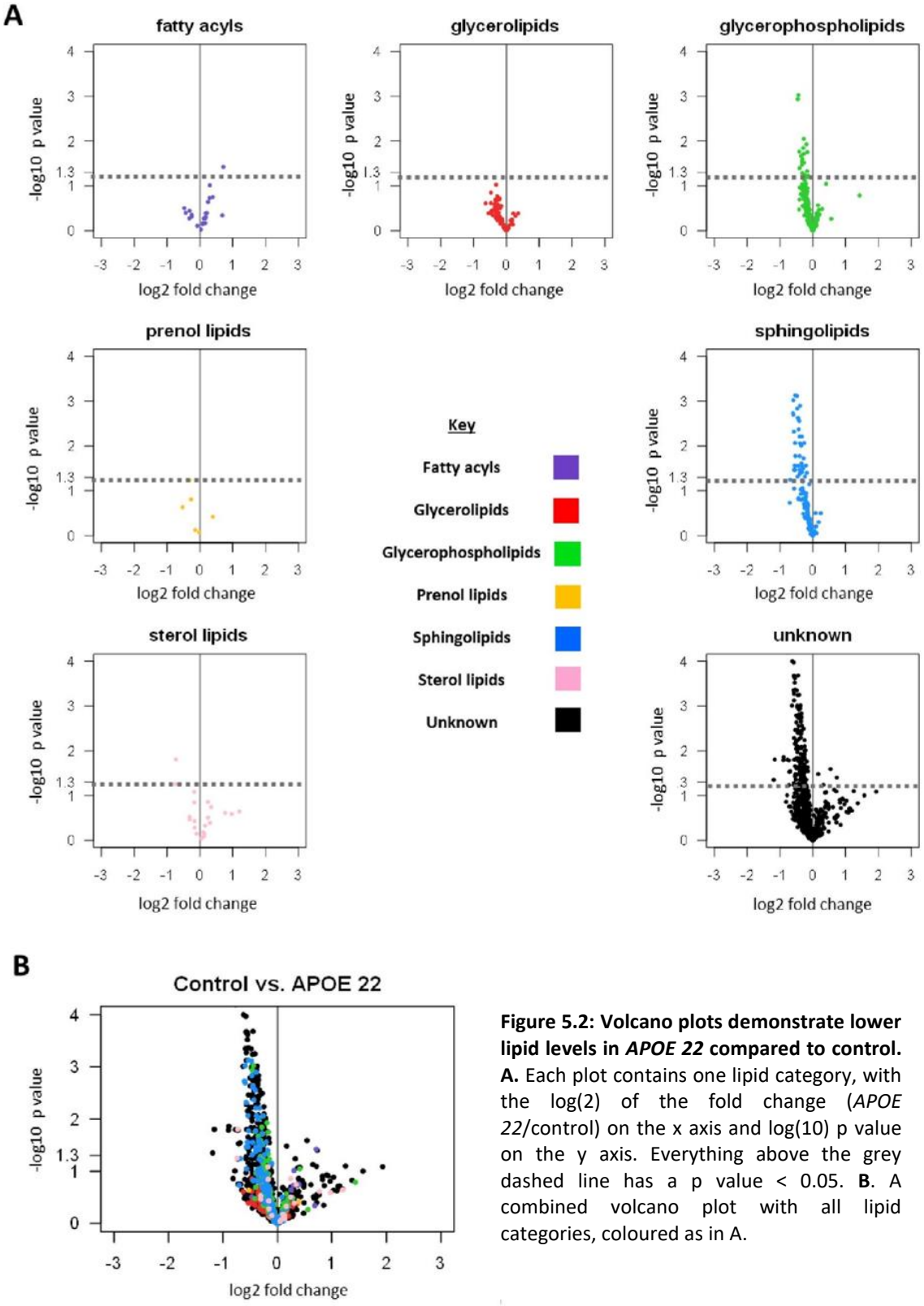

Figure 5.2: Volcano plots demonstrate lower lipid levels in *APOE 22* compared to control. A. Each plot contains one lipid category, with the log(2) of the fold change (*APOE 22*/control) on the x axis and log(10) p value on the y axis. Everything above the grey dashed line has a p value < 0.05. **B**. A combined volcano plot with all lipid categories, coloured as in A.

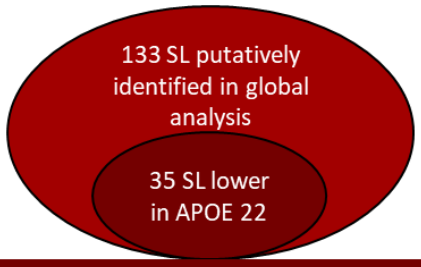

Sphingolipid species from four subclasses were lower in APOE 22 plasma compared to control					
Subclass*	**Number significantly different**	**Putative ID**	**Fold change**	**P value (two-tailed t test)**	**Sig. after BH procedure**
Ceramide phosphoethanol-amines	1	PE-Cer(43:1)	0.67	4.81E-03	Yes
Ceramides	1	CER(40:7)	0.82	1.89E-02	No
Monohexosylceramides	8	hexCER(42:1)	0.66	1.12E-03	Yes
		hexCER(42:1)	0.66	1.32E-03	Yes
		hexCER(40:1)	0.68	7.09E-03	No
		hexCER(40:1)	0.67	8.15E-03	No
		hexCER(42:2)	0.73	1.14E-02	No
		hexCER(42:2)	0.73	1.39E-02	No
		hexCER(41:1)	0.76	2.02E-02	No
		hexCER(41:1)	0.76	3.60E-02	No
Sphingomyelins	22	SMpc(36:2)	0.76	5.62E-04	Yes
		SMpc(41:1)	0.69	6.14E-04	Yes
		SMpc(40:0)	0.72	1.32E-03	Yes
		SMpc(42:1)	0.73	1.44E-03	Yes
		SMpc(42:2)	0.74	1.69E-03	Yes
		SMpc(38:1)	0.75	2.72E-03	Yes
		SMpc(40:1)	0.72	2.94E-03	Yes
		SMpc(40:1)	0.74	3.42E-03	Yes
		SMpc(40:2)	0.69	3.98E-03	Yes
		SMpc(36:1)	0.79	4.96E-03	Yes
		SMpc(41:1)	0.77	5.73E-03	No
		SMpc(34:2)	0.83	6.61E-03	No
		SMpc(34:0)	0.76	7.60E-03	No
		SMpc(35:1)	0.79	8.72E-03	No
		SMpc(42:2)	0.79	8.72E-03	No
		SMpc(42:3)	0.78	1.07E-02	No
		SMpc(38:0)	0.69	1.57E-02	No
		SMpc(34:0)	0.82	1.68E-02	No
		SMpc(36:0)	0.69	1.90E-02	No
		SMpc(39:1)	0.80	1.90E-02	No
		SMpc(34:1)	0.87	4.48E-02	No
		SMpc(34:1)	0.88	1.11E-01	No
Assigned to category only	2	785.6532/45.16/sphingolipids	0.66	6.70E-04	Yes
		757.622/37.89/sphingolipids	0.76	4.29E-03	Yes

Table 5.2: Putative identification suggests circulating sphingolipids are downregulated in APOE 22. *As determined by the LIPID MAPS lipid classification system (Fahy, 2005, Fahy, 2009). Lipids putatively identified using accurate mass to four decimal places and the LIPID MAPS curated database. Last column denotes which lipids are still significantly different after the Benjamini-Hochberg procedure to correct for multiple comparisons, which takes into account a chosen FDR (in this case 0.1).

tended overall to be unsaturated. These included lipids putatively identified as PC(34:1p)/(34:2e), PC(34:2), PC(34:1), PC(34:0p)/(34:1e), PC(36:3), PC(36:4), PC(32:2) and PC(34:3). Two highly unsaturated PE species are also reduced in *APOE* 22, as well as 2 PIs and 3 PSs. PC(36:1p), PC(34:2e), PC(34:0p) and PC(34:1e) are ether phospholipids, which are split into two subclasses, ethers (e) and plasmalogens (p). PC(34:1p)/(34:2e) has been identified as such because plasmalogens and ethers cannot be distinguished by this method and the *m/z* values for these two lipids match exactly. The two PEs which are significantly reduced, PE(40:8) and PE(36:3p)/(36:4e), are also either polyunsaturated or ether lipids. Only three GPs, PC(34:1p)/(34:2e), PE(40:8) and PI(38:4), remained significant after the BH correction.

PS(36:1), PS(38:1) and PS(40:1) are also significantly reduced. GPs with early RTs and lower *m/z* values were postulated to be lysoPLs, and *m/z* values matched both lysoPL *m/z* entries in the LIPID MAPS curated database and RT values in the in-house built database. Thirty-one lipids were putatively identified as lysoPCs and 15 as lysoPEs, and levels are not differentially regulated by *APOE* allele. Overall, these data suggest SPs and GPs (but not lysoPL) are downregulated in *APOE* 22.

One sterol lipid (4.5 % of total) is reduced in *APOE* 22, although it was no longer significant after BH correction. Finally, no GLs or PRs differed between alleles. As total cholesterol and TAGs are lower in *APOE* 22 when measured using enzymatic methods, it was unexpected that sterol lipids and GLs are not reduced in this untargeted analysis (Table 1.1). This may result from the semi-quantitative nature of the global analysis, or be because species are being analysed separately, whilst total enzymatic measures includes all TAG or sterol species. Thus, to quantify individual GLs and PRs, ands inform on chain length and saturation, I will analyse TAGs, cholesterol and CEs using targeted methods.

Several unknowns are also significantly different using a t test, specifically 145 (14.2 % of total), of which 142 are significantly decreased in *APOE* 22 while 3 are significantly increased. After BH correction, 67 unknowns are significantly decreased in *APOE* 22 compared to control, and 1 is increased.

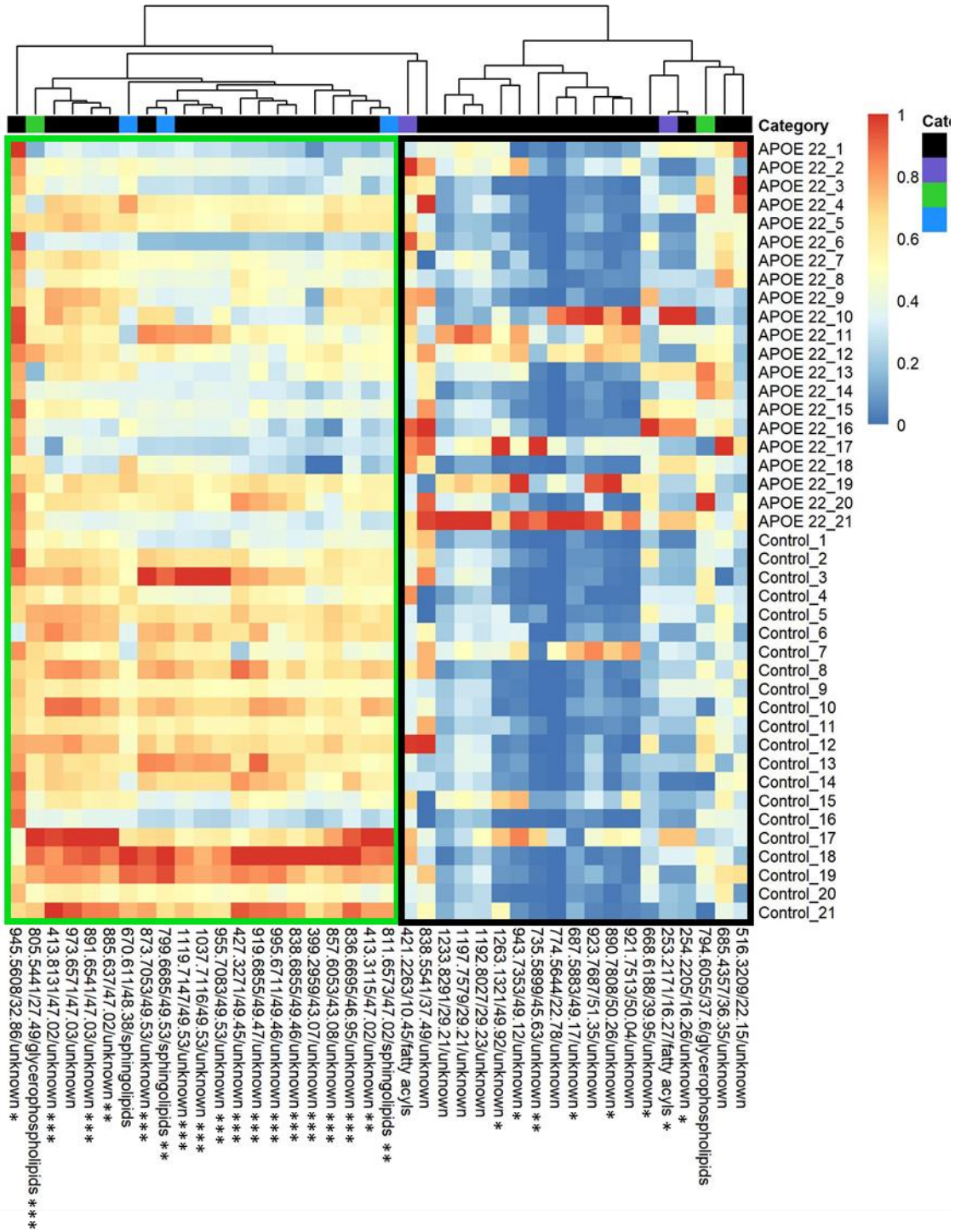

Figure 5.3: 30 of 40 lipids chosen by effect size were putatively identified as unknowns. Lipids with the highest effect size in the global lipidomics comparison of *APOE 22* and control plasma were visualised in a heatmap. The putative lipid identifier is on the x axis and sample genotype is along the y axis. Species coloured according to a normalised scale from a score of 1 and the highest sample intensity (red), to 0 and the lowest sample intensity (blue). Lipids which increased in control samples are clustered together (green box), as are those which decreased in control (black box). P value calculated using a students t test (two-tailed, unequal variance). * p value < 0.05. ** p value < 0.01. *** p value < 0.001

5.2.1.2 Lipid profiles can be used to differentiate APOE 22 and control samples with 80 % sensitivity

Effect size for lipids was calculated and a panel of 40 lipids was chosen, the 20 most upregulated in *APOE* 22 and the 20 most downregulated in *APOE* 22. 33 of the high effect size lipids are unknowns, 3 are SPs, 2 are fatty acyls and 2 are GPs. These species were used to produce a heatmap in RStudio (Figure 5.3). Lipids cluster into two groups, which are made up of those which decreased in *APOE* 22 (grey box) and those which increased (black box). Many lipids were significant using a two-tailed t test. Lipids reduced in *APOE* 22 are more significantly altered than lipids increased in *APOE* 22. There are 5 clusters of lipids which contain putatively identified lipids and unknowns.

PCA and PLS-DA are used to simplify complicated multi-level datasets (Pearson, 1901, Worley and Powers, 2013). Here, PCA and PLS-DA were used to determine whether *APOE* alleles can be separated using lipid abundance in the 40-lipid panel (Figure 5.4A). PCA (Figure 5.4B) and PLS-DA (Figure 5.4C) were produced in SIMCA using this lipid panel. The PCA scores plot (Figure 5.4B left panel) demonstrates that alleles are partially separated, and this is reflected in the loadings plot (Figure 5.4B right panel), which contains three clusters of lipids. The left cluster is lower in *APOE* 22 and right clusters are higher in *APOE* 22. Loadings plots for both PCA and PLS-DA models demonstrate the contribution of each lipid to variation, with a higher PC score on the loadings plot indicating that an individual lipid was more different in *APOE* 22. Positively correlated lipids are grouped, whereas highly negatively correlated lipids sit diagonally opposite. In the supervised PLS-DA method, APOE allele was the group ID inputted. The PLS-DA, which is optimised to separate alleles better, demonstrates that a supervised algorithm can separate *APOE* alleles based on the 40-lipid panel (Figure 5.4 C left panel). Lipids which are higher in *APOE* 22 are clustered on the left of the plot, and lipids which were lower in *APOE* 22 are on the right. The same 40 lipids as chosen for heatmaps, PCA and PLS-DA were used for ROC analysis to determine if an algorithm could correctly assign individual samples to genotype (Figure 5.5). ROC analysis can separate *APOE* 22 from control with 80 % accuracy.

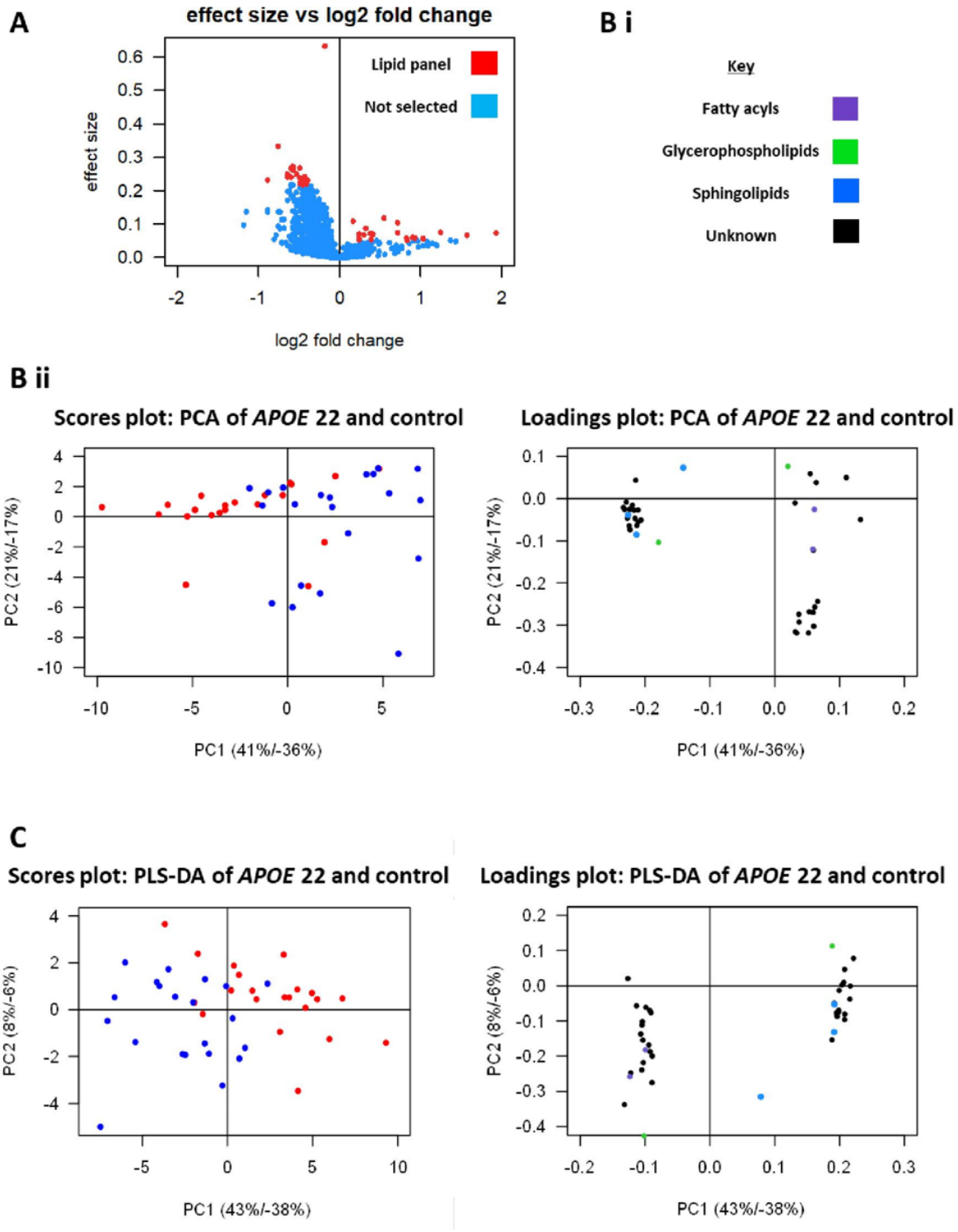

Figure 5.4: PCA and PLS-DA of the 40 lipids with the highest effect size in APOE 22 and control plasma. A. The 40 lipid panel (red) represented by volcano plot. **B** After a PCA, the variation between samples was represented as PC1 against PC2 in the scores plot on the left, while the loadings plot on the right visualises how much variation each individual species conferred to the dataset. **C**. Scores and loadings plots after a PLS-DA (a supervised algorithm). Models produced using SIMCA.

A

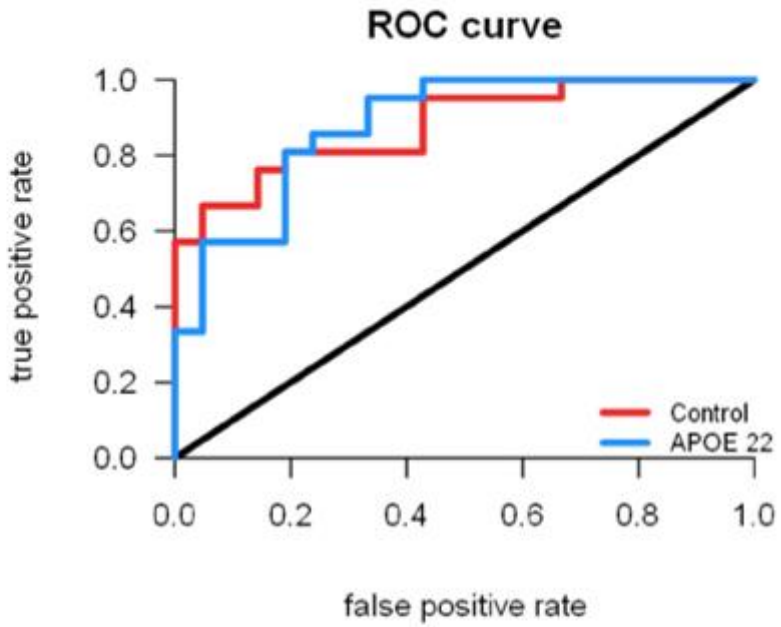

B

Misclassification table: *APOE22* vs. control

	Members	Correct	*APOE22*	Control
APOE22	21	80.95%	17	4
Control	21	80.95%	4	17
Total	42	80.95%	21	21
Fisher's prob.	7.00E-05			

Figure 5.5: A ROC analysis demonstrates that a 40 lipid panel can separate *APOE 22* and control samples with 80 % accuracy. A. A ROC curve comparing whether samples could be correctly assigned to a genotype using the 40 lipid panel previously mentioned. **B**. A misclassification table for the above ROC analysis.

5.2.2 High resolution LC/MS analysis of the global lipidome revealed few differences between *APOE* 44 and control plasma

5.2.2.1 Lipid profile of APOE 44 plasma is similar to that of control

Using the same untargeted LC/MS approach as used to analyse the *APOE* 22 dataset, and the XCMS-LipidFinder workflow (Section 2.4.1 and Section 2.5.2), I compared the lipidome of *APOE* 44 and control plasma (n = 39). I found a total of 2,527 lipids in the *APOE* 44 and control datasets (Table 5.3). Lipids eluted from the LC column as before, grouped with others of the same category (Figure 5.6). None of the lipids removed from the dataset were present in only one genotype. Fold change (FC) was calculated as signal intensity (cps) in *APOE* 44 divided by signal intensity in control. Using the LIPID MAPS curated database and our in-house built database, 39 lipids were putatively assigned to as fatty acyls, 130 as GLs, 364 as GPs, 9 as PRs, 173 as SPs, 25 as sterol lipids and 1,787 as unknown (Table 5.3). More lipids are assigned to each category than in the previous dataset, but this is proportional to the larger number of lipids found.

Compared with the *APOE* 22 dataset, far fewer significantly different lipids were detected. Only 10 lipids are significantly decreased in *APOE* 44 plasma versus control (Table 5.2), with 2 being GPs (0.6 % of total GPs) and 8 being unknowns (0.5 % of total unknowns). None were significantly increased. After BH correction, none of these lipids maintained significance.

Volcano plots demonstrate the small fold changes and sparsity of significantly different lipids in all categories in the *APOE* 44 and control comparison (Figure 5.7A). The most significant species are unknowns and GPs, similarly to the APOE 22 dataset (Figure 5.7B).

5.2.2.3 A selection of significantly different lipids can be used to separate APOE 44 and control samples with 100 % accuracy

A 40-lipid panel was chosen, as described previously (Section 6.1.2.1). These lipids are represented in a heatmap (Figure 5.8). 30 of these were unknowns, 5 were GPs, 1 was a GL,

Lipids from 6 LIPID MAPS categories were found in APOE 44 and control plasma

	Total	% of total*	Significant	Sig. after BHC†	% of cat. sig.‡
All lipids	2527		10	0	
Fatty acyls	39	1.5	0	0	0.0
Glycerolipids	130	5.1	0	0	0.0
Glycerophospholipids	364	14.4	2	0	0.5
Prenol lipids	9	0.4	0	0	0.0
Sphingolipids	173	6.8	0	0	0.0
Sterol lipids	25	1.0	0	0	0.0
Unknown‡	1787	70.7	8	0	0.4

Table 5.3: Lipids from 6 LIPID MAPS categories were found in *APOE 44* and control plasma. ***Number of lipids in each class as a percentage of the total number. **†Number of lipids significantly changed ($p < 0.05$, students two-tailed t test) between APOE 44 and control as a percentage of all lipids in that category. ‡ Percentage of category significant after BH correction. N = 39.

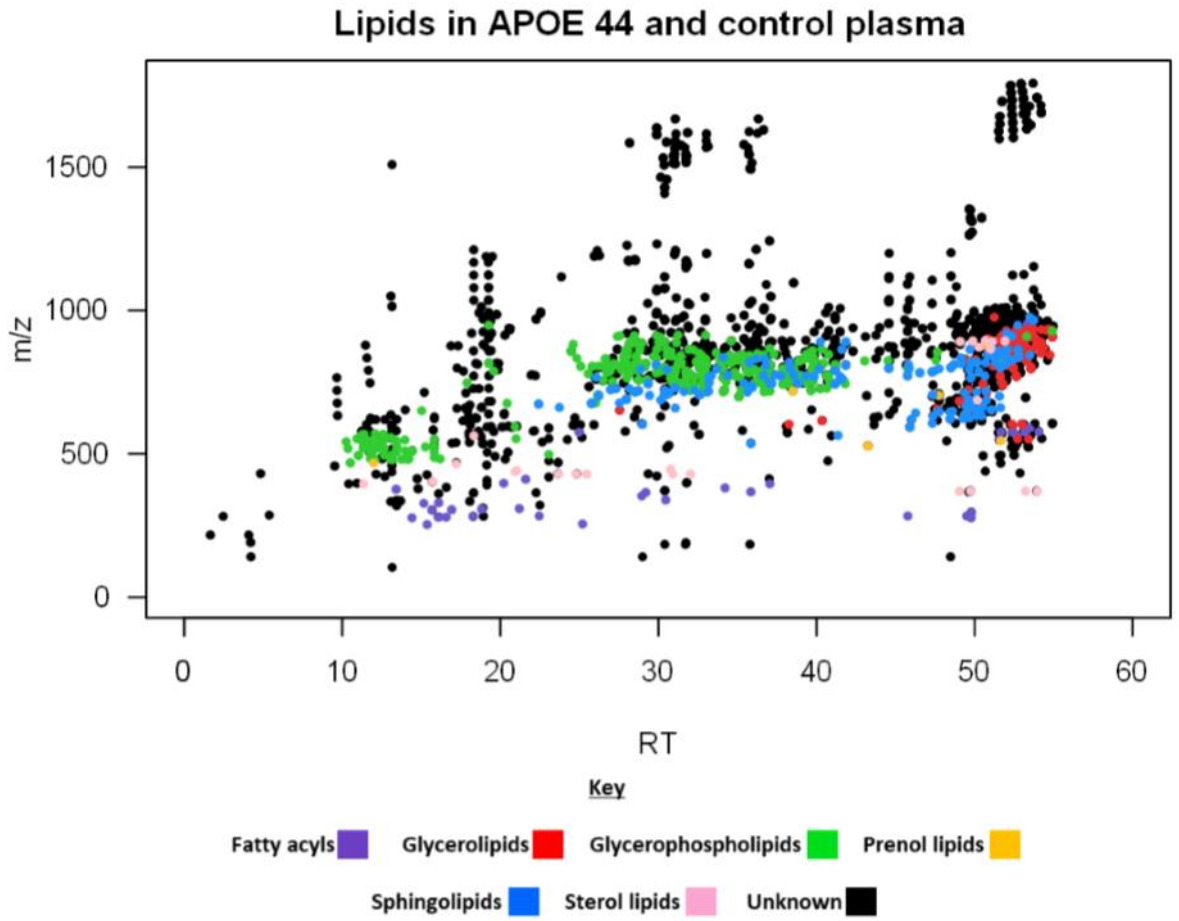

Figure 5.6: Plasma lipids in APOE 44 and control participants, separated by LC/MS, cluster according to lipid category. Lipids separated by RT (x axis) and m/z (y axis). Each point represents one lipid and is coloured according to lipid category. Lipids within the same category elute in groups when separated by LC/MS. Arrows indicate some outliers.

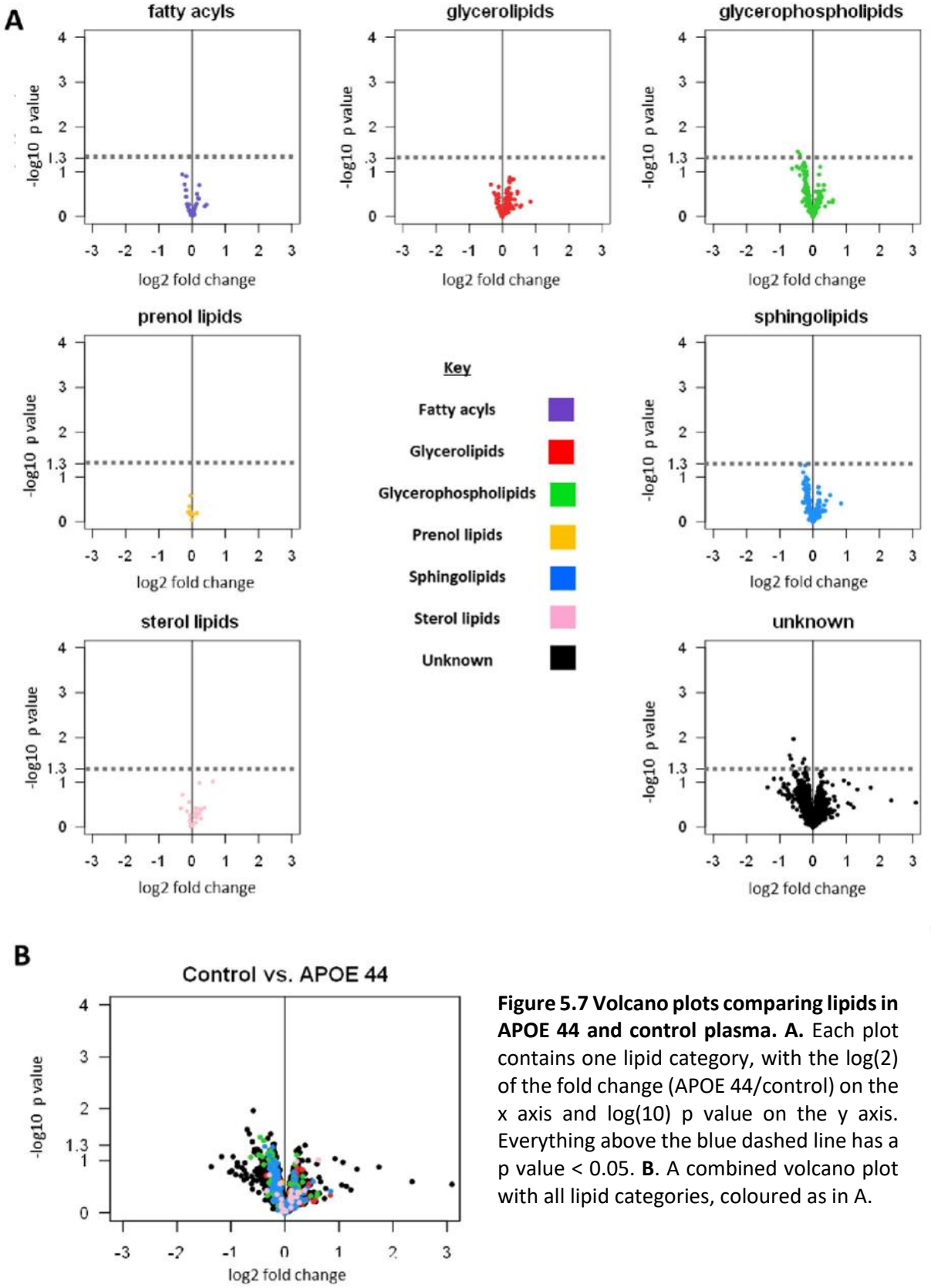

Figure 5.7 Volcano plots comparing lipids in APOE 44 and control plasma. A. Each plot contains one lipid category, with the log(2) of the fold change (APOE 44/control) on the x axis and log(10) p value on the y axis. Everything above the blue dashed line has a p value < 0.05. **B**. A combined volcano plot with all lipid categories, coloured as in A.

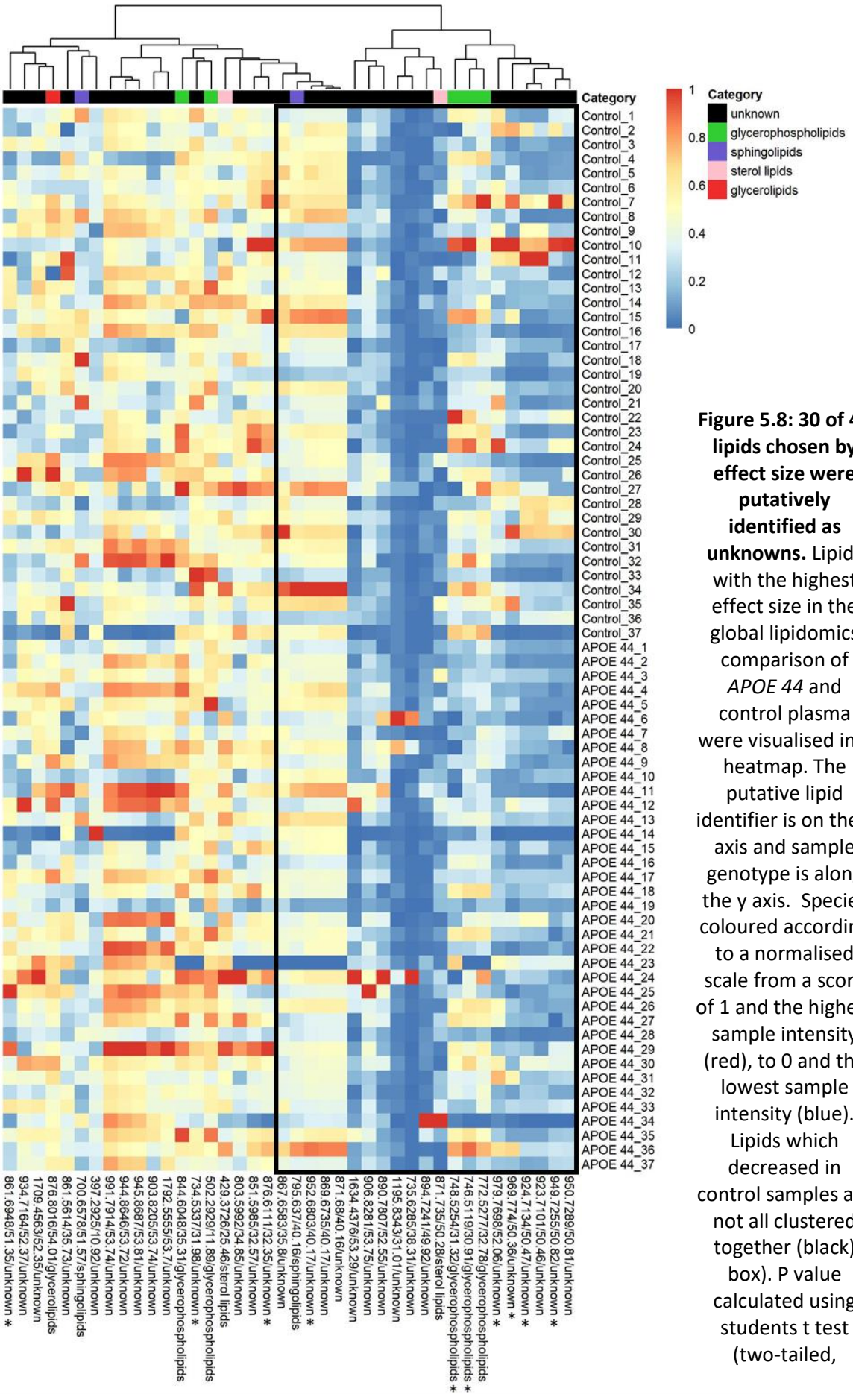

Figure 5.8: 30 of 40 lipids chosen by effect size were putatively identified as unknowns. Lipids with the highest effect size in the global lipidomics comparison of *APOE 44* and control plasma were visualised in a heatmap. The putative lipid identifier is on the x axis and sample genotype is along the y axis. Species coloured according to a normalised scale from a score of 1 and the highest sample intensity (red), to 0 and the lowest sample intensity (blue). Lipids which decreased in control samples are not all clustered together (black) box). P value calculated using students t test (two-tailed,

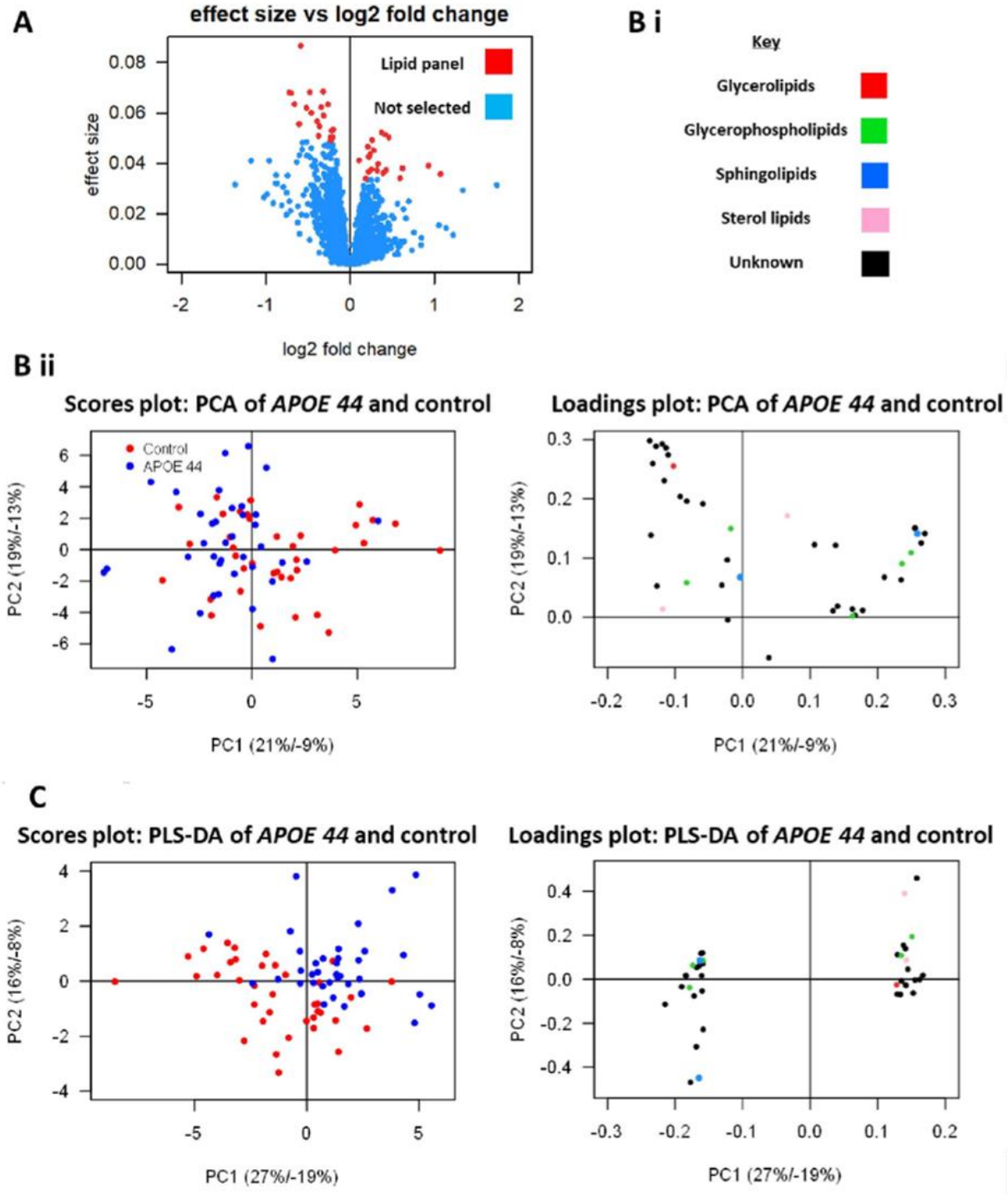

Figure 5.9: PCA and PLS-DA of the 40 lipids with the highest effect size in APOE 44 and control plasma. A. The 40 lipid panel (red) represented by volcano plot. **B** After a PCA, the variation between samples was represented as PC1 against PC2 in the scores plot on the left, while the loadings plot on the right visualises how much variation each individual species conferred to the dataset. **C**. Scores and loadings plots after a PLS-DA (a supervised algorithm). Models produced using SIMCA.

2 were sterol lipids and 2 were SPs. Lipids cluster in two groups, identified lipids are spread in both groups with unknowns rather than clustered with others from the same category. Also, lipids which differ significantly are not clustered together, suggesting that they are produced by more than one pathway. Heterogeneity within alleles is larger than between alleles, i.e. there is no visible allele difference but samples with each allele vary.

PCA, PLS-DA and ROC analysis were performed as before (Section 6.1.2.1), using the 40-lipid panel as described (Figure 5.9A). PCA of the panel (Figure 5.9B left panel), produced in the same manner as previously, partially separates alleles and the PCA loadings plot demonstrates two clusters of lipids (Figure 5.9B right panel). PLS-DA improves separation of the alleles (Figure 5.9C left panel). The PLS-DA loadings plot contains two clusters of lipids (Figure 5.9C right panel), which are well separated and represent lipids either reduced (left cluster) or increased in *APOE* 44 (right cluster). ROC analysis of the 40-lipid panel can separate lipids into either *APOE* 44 or control groups with 86 % sensitivity (Figure 5.10).

None of the lipids which differed significantly in *APOE* 44 versus control were assigned a species ID as none of the RTs fell within assigned windows on the RT database (Table 5.2), however, two lipids were designated as GPs by *m/z*. The two GPs found matched several LIPID MAPS database entries. The closest database match for 748.5254/31.32/glycerophospholipids was PG(34:0) and as expected RT for PG(34:0) is similar to that seen, I have putatively identified this lipid as PG(34:0). The closest *m/z* match for 746.5119/30.91/glycerophospholipids was 746.5098, which matched the mass of the lipids LBPA(16:1(9Z)/18:1(9Z)) and PG(34:2). Whilst LBPA has been widely described in endosomes, it was not found in exosomes using MS and is unlikely to be present in plasma (Wubbolts et al., 2003). Therefore, this lipid was putatively identified as PG(34:2).

A

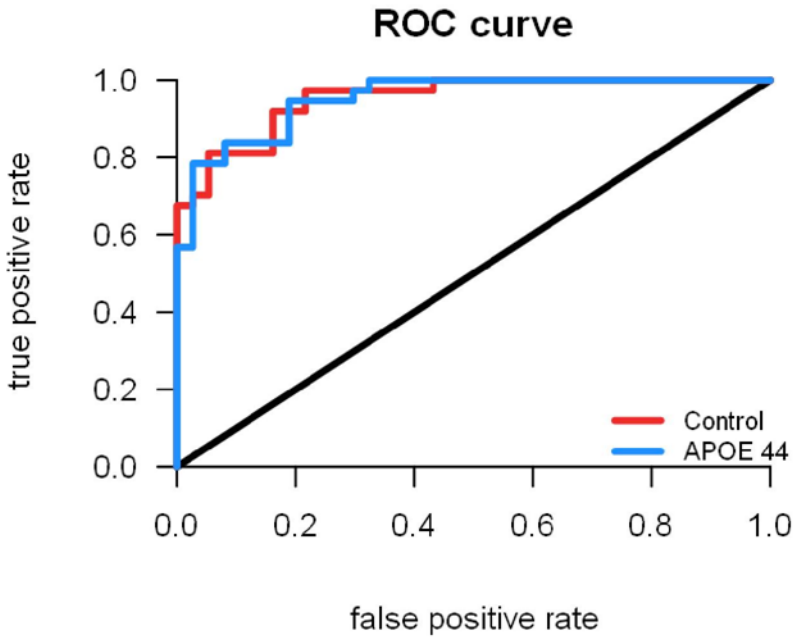

B

	Members	Correct	Control	*APOE44*
Control	37	78.38%	29	8
APOE44	37	94.59%	2	35
Total	74	86.49%	31	43
Fisher's prob.	3.9e-011			

Figure 5.10: A ROC curve demonstrates that a 40-lipid panel can separate *APOE 44* and control samples with 86 % accuracy. A. A ROC curve comparing whether samples could be correctly assigned to a genotype using the 40-lipid panel previously mentioned. **B.** A misclassification table for the above analysis.

5.2.2.2 A retention time shift when comparing APOE 22 and APOE 44 datasets was due to batch processing

I expected that many lipids measured in *APOE* 22 would also be found in *APOE* 44, especially as in both datasets, the same lipids are measured in risk and control samples. However, only 1,591 lipids are found in the *APOE* 22 dataset, and 2,527 in the *APOE* 44 dataset. I compared species names assigned across the *APOE* 22/control and *APOE* 44/control datasets to determine how many lipids were identified in both datasets. Only 104 identical species IDs were present in both datasets. To account for differences in measured RT and *m/z* between the two datasets, I truncated the *m/z* value to 2 decimal places and the RT value to mins and combined these two values with the category to give another ID for each lipid (trunc-ID). For example 399.2959/43.07/unknown became 399.29/43/unknown. A comparison of both datasets using trunc-ID revealed 255 matches between the *APOE* 22 and 44 datasets. This was a much lower number of matches than expected. Measurement of *m/z* using the Orbitrap Elite is very accurate and mass accuracy is checked in every sample using lipid standards, so RT is the factor which is more likely to have changed. To determine if a RT shift between *APOE* 22 and 44 datasets prevented comparison using trunc-ID, I compared 25 species between the two. Firstly, I searched by accurate mass. Then I excluded any species with more than one ion with the same mass, to ensure I was comparing the same species rather than isomers. This left 16 lipids (Table 5.4), for each I recorded RT in both datasets, then calculated the RT difference. RT difference ranged from 0.8 min to 1.69 min, i.e. there was an 'RT shift' towards later RTs in the *APOE* 44 dataset. Smaller RT differences occurred earlier on in the analysis and later lipids have a larger RT difference. Differences of almost 1 min in retention time, such as those seen in the *APOE* 22 and *APOE* 44 datasets, are enough to prevent matching by trunc-ID.

Several factors within the MS method could cause an RT shift between datasets. For example, the two datasets were analysed several months apart, using different HPLC columns and different batches of mobile phase. Also, a column pocket, as used in the global method, does not regulate temperature as effectively as a column oven and therefore, environmental temperature changes could cause a RT shift. To conclude, earlier RTs in the *APOE* 44 dataset

RT comparison for lipids found in APOE 22 and APOE 44 datasets

Lipid	Mode	RT *APOE 22* dataset (min)	RT *APOE 44* dataset (min)	RT difference (min)
Arachidonic acid	-	16.54	15.68	0.86
cis-9-palmitoleic acid	-	16.27	15.36	0.91
Coenzyme-Q10	+	50.81	50.69	0.12
hexCER(34:2)	+	30.01	28.53	1.48
hexCER(40:1)	-	47.72	46.54	1.18
LPC(14:0)	+	11.3	10.5	0.8
LPC(16:0)	-	13.99	13.07	0.92
LPE(18:2)	+	12.82	12.06	0.76
PA(36:2)	+	38.25	37.05	1.2
PI(38:4)	-	30.02	28.32	1.7
PI(40:6)	-	29.09	27.4	1.69
PS(36:0)	-	32.14	30.5	1.64
SMpe(44:3)	+	36.94	35.73	1.21
TG(36:0)	+	48.16	47.63	0.53
γ-linolenic acid	-	15.23	14.4	0.83

Table 5.4: Lipid retention times in *APOE 22* and *APOE 44* datasets. Retention times (RT) were taken from both datasets, where only one ion of the correct mass was present in either positive and negative mode. Mode column demonstrates which mode lipids were measured in. RT difference = RT in *APOE 22* dataset minus RT *in APOE 44* dataset.

Intensity comparison of lipids found in APOE 22 and APOE 44 datasets

Lipid	Mode	Intensity *APOE 22* dataset (cps)	Intensity *APOE 44* dataset (cps)	FC†
Arachidonic acid	-	5.73E+06	8.38E+06	0.68***
cis-9-palmitoleic acid	-	6.83E+06	6.02E+06	1.13
Coenzyme-Q10	+	4.07E+06	5.89E+06	0.69***
hexCER(34:2)	+	2.40E+06	2.20E+06	1.09
hexCER(40:1)	-	4.09E+06	2.96E+06	1.39**
LPC(14:0)	+	7.64E+06	6.52E+06	1.17
LPC(16:0)	-	1.71E+07	2.17E+07	0.79**
LPE(18:2)	+	4.91E+06	4.68E+06	1.05
PA(36:2)	+	2.45E+06	2.29E+06	1.07
PI(38:4)	-	2.13E+07	3.59E+07	0.59***
PI(40:6)	-	1.71E+06	2.30E+06	0.74**
PS(36:0)	-	5.08E+06	5.39E+06	0.94
SMpe(44:3)	+	2.70E+06	3.99E+06	0.68***
TG(36:0)	+	4.21E+06	3.91E+06	1.08
γ-linolenic acid	-	3.93E+06	3.65E+06	1.08

Table 5.5: Intensity of endogenous lipids in each dataset. † FC calculated as mean intensity in *APOE 22* dataset divided by mean intensity in *APOE 44* dataset. Mean intensity for each lipid across the whole dataset was calculated for both datasets, where only one ion of the correct mass was present in a particular mode. Intensity measured in counts per second (cps). * p value < 0.05. ** p value < 0.01. *** p value < 0.001.

are preventing a thorough comparison of the *APOE* 22 and 44 datasets, and lipids which elute later in the analysis are disproportionally affected.

To determine why fewer lipids were detected in the *APOE* 22 dataset, I compared the mean intensity value for the 16 species used for the RT comparison in both *APOE* 22 and 44 datasets (Table 5.5). To statistically compare the two datasets, I performed a students t test (two-tailed, unequal variance) for each lipid by comparing the lipid intensity (cps) between all samples in either dataset. Out of the 16 species tested, 6 were present at significantly lower intensity in the *APOE* 22 dataset, whilst 1 was significantly increased. The *APOE* 22 dataset does have lower levels of some lipids, which could have caused lower abundance lipids to be removed during data analysis either during background removal or at the low abundance cut off. I manually checked Lipidfinder output files, which revealed that no lipids were removed during the low abundance cut off in the *APOE* 22 dataset. Thus, sensitivity of the MS must have been lower during the analysis of the *APOE* 22 dataset, possibly due to contamination within the MS.

To investigate this, I compared TICs of 5 control samples analysed in both datasets. In negative mode, *APOE* 22 and *APOE* 44 TICs are similar (Table 5.6). However, in positive mode, TICs are significantly lower in *APOE* 22. A loss of some species due to low sensitivity in positive mode could explain both why fewer species were recorded in the *APOE* 22 dataset, and why only some species were present at lower abundance when comparing the datasets.

5.3 Discussion

5.3.1 A comparison of *APOE* 22 and control plasma demonstrates a possible downregulation of SPs, GLs and PRs in APOE 22 plasma

LC/MS and Lipidfinder analysis putatively identified a significant downregulation of 197 lipids in APOE 22 homozygote plasma ($P < 0.05$), 86 of which maintained significance after BH correction (Table 5.1). These lipids included SPs, GLs and PRs (Table 5.2, Figure 5.3). Comparatively, just 10, mostly unknown, lipids differ in APOE 44 plasma, and none maintain

A

A comparison of TICs of control samples in negative mode in *APOE* 22 and 44 datasets

Sample	Mode	TIC 22	TIC 44
Control 1	NEG	3.55E+07	2.90E+07
Control 2	NEG	2.65E+07	2.98E+07
Control 3	NEG	3.10E+07	2.88E+07
Control 4	NEG	2.85E+07	3.34E+07
Control 5	NEG	2.65E+07	2.59E+07
Mean		2.96E+07	2.94E+07
		P value	9.18E-01

B

A comparison of TICs of control samples in positive mode in *APOE* 22 and 44 datasets

Sample	Mode	TIC 22	TIC 44
Control 1	POS	5.02E+08	6.51E+08
Control 2	POS	5.14E+08	6.89E+08
Control 3	POS	4.90E+08	7.42E+08
Control 4	POS	6.27E+08	8.33E+08
Control 5	POS	5.51E+08	8.08E+08
Mean		5.36E+08	7.44E+08
		P value	1.19E-03

Table 5.6 A & B. Tables compare intensity of the same 5 control samples in the *APOE 22* and *APOE 44* datasets. TIC = total ion count, which is the sum of all the ions measured in an analysis. NEG = negative mode analysis on the Orbitrap Elite. POS = positive mode analysis on the Orbitrap Elite. P value calculated using a students two-tailed t test, assuming unequal variance.

significance after BH correction (Table 5.2). The APOE 44 dataset contains a larger number of lipids, and possible grounds for this were discussed (Section 5.2.2.2). To determine if MS sensitivity was lower in one analysis, I compared TICs and intensities of some endogenous species, and this analysis revealed lower sensitivity in the positive mode MS analysis of the APOE 22 dataset (Table 5.5, Table 5.6A & B). Multivariate analysis can separate both 22 and 44 plasma samples from control (Figure 5.4, Figure 5.5, Figure 5.9, Figure 5.10).

5.3.1.1 Global lipidomic analysis putatively identified a reduction in SPs, unknown lipids and GPs in APOE 22 plasma

Herein, a global untargeted analysis of the plasma lipidome from *APOE* 22 and control participants demonstrated 1,591 lipids, several of which were significantly lower in *APOE* 22 plasma than in control (n = 21) (Table 5.1). Current estimates of the total number of lipids in plasma vary widely, and the true number is still not clear. For example, a recent investigation of biomarkers of type 2 diabetes mellitus using global lipidomic methods claimed to have measured 11,077 circulating lipids (Zhong et al., 2017). In contrast, other untargeted LC/MS approaches have found 390, 277 and 3,579 plasma lipids, respectively (Yu et al., 2017, Suvitaival et al., 2018, Cai et al., 2014). I suggest the variation in these estimates of total circulating lipids can be explained by the methodology. For example, Yu et al., who described 390 species, did not separate lipids before analysis using LC, instead all lipids entered the MS in a single injection. This can cause massive underestimation for two reasons. First, the mass detector of the mass spectrometer can be flooded by higher abundance lipids, preventing lower abundance species from being measured (ion suppression). Second, this method does not allow the resolution of isobaric lipids with the same *m/z* but different fatty acyl chain lengths. Suvitaival et al., reported 277 lipids using LC/MS, however, there are several reasons why the number of lipids recorded is smaller than other studies. The single stage chloroform:methanol extraction used in that study could be expected to recover fewer lipids than the modified double extraction used in my work. Also, only 10 µL of serum was extracted, meaning low abundance lipids would not be measurable, and finally, targeted methods did not analysis unknown lipids (which made up half of my datasets). In another study, 3,579 lipids were detected in plasma, following a double stage extraction and LC/MS (Cai et al.,

2014). However, in that study, no adduct, isotope or background removal steps were detailed in the methods, meaning that many lipids measured could be isotopes, adducts or background ions. I postulate that treatment of this data with the XCMS-Lipidfinder workflow would result in fewer lipids as the isotope, adduct and background ions will be removed. This would significantly clean up the dataset. Lastly, a recent LC/MS/MS study of plasma demonstrated 11,077 lipids (Zhong et al., 2017), but as in Cai et al., 2014, no post-acquisition data removal or minimum intensity thresholds were described. Thus, this is likely a significant overestimation since isotopes, adducts and background ions will not have been removed. The LipidFinder approach is designed to minimise false identification of lipids through extensive data clean up, however, there are also caveats using this approach. First, a minimum intensity threshold in the XCMS-Lipidfinder flow, adopted to remove low intensity species with high coefficient of variation, may remove some low abundance species from the *APOE* datasets. To conclude, the vastly differing numbers of lipids found in published studies of the global plasma lipidome are likely to be explained by differences in methodology and post-acquisition data treatment. The data presented in this chapter, combined with the literature evidence, suggest that human plasma contains several thousand circulating lipids, although current estimates may still be inherently inaccurate due to methodological limitations outlined above. How APOE alleles regulate circulating lipids is unknown, and this is the first LC/MS analysis comparing *APOE* homozygote plasma. *APOE* acts as a stabilising protein for lipoprotein particles, as well as interacting with lipids and receptors such as the *APOE* receptor and LDLR. The various *APOE* protein isoforms differ in quaternary structure, which affects receptor and lipid binding ability (Section 1.2.1). Briefly, the apoE 2 protein has lower binding affinity for the LDLR, preventing the efficient internalisation of low-density lipoproteins (LDLs) (Weisgraber et al., 1982). This reduces the entry of lipids into the cell through the LDLR, and, intuitively, would increase circulating lipids. TAGs are increased in the plasma of humans and mice who carry *APOE 2*, due to the reduction in lipolysis of lipoproteins through the LDLR (Dallongeville et al., 1992, Huang et al., 1998). However, in NPHSII samples, several lipid categories (SPs, GLs, unknown) are lower in the presence of *APOE* 2. This is the first demonstration of downregulation of these lipids in *APOE* 22 plasma.

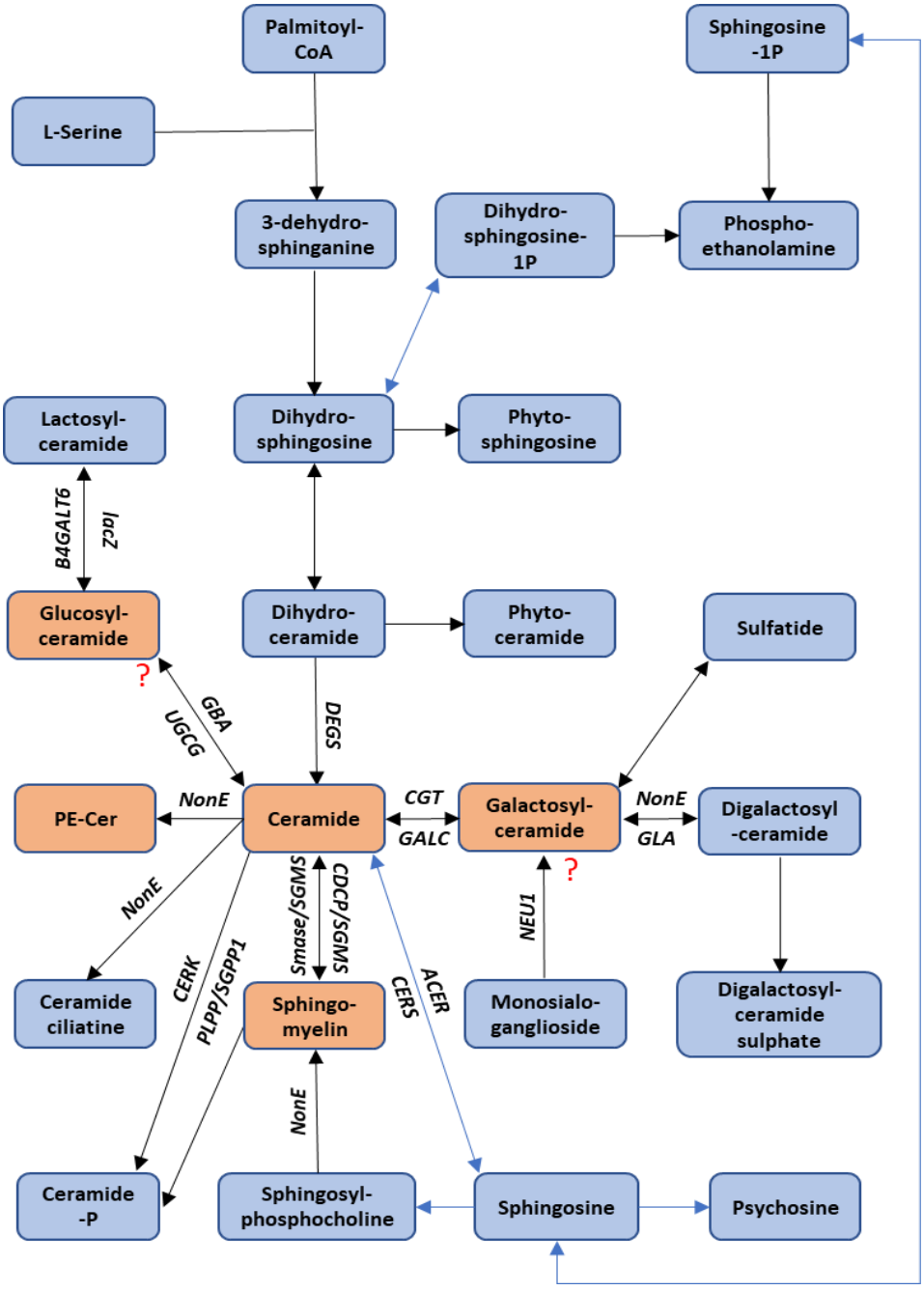

Figure 5.11: Ceramide and ceramide metabolites are reduced in *APOE 22* plasma compared to control. Figure adapted from KEGG pathway 'Sphingolipid metabolism' (Kanehisa and Goto, 2000, Kanehisa et al., 2016, Kanehisa et al., 2017). Arrows indicate a possible metabolic conversion of one species to another. This may be reversible (double arrow) or irreversible (single arrow). Species in orange were identified as being downregulated in APOE 22, whilst blue species were not significantly altered between *APOE* alleles. ? = glucosyl ceramides and galactosylceramides cannot be differentiated using global analysis. Enzymes are noted where lipids downregulated in *APOE* 22 are either products or substrates. B4GALT6 = beta-1,4-galactosyltransferase 6, lacZ = beta-galactosidase, UGCG = ceramide glucosyltransferase, GBA = glycosylceramide, DEGS = sphingolipid 4-desaturase/C4-monooxygenase, NonE = non-enzymatic, CGT = ceramide galactosyltransferase, GALC = galactosylceramide, GLA = alpha-galactosidase, SMase = sphingomyelin phosphodiesterase, SGMS = sphingomyelin synthase, CDCP = ceramide cholinephosphotransferase, NEU1 = sialidase-1, CERK = ceramide kinase, PLPP = phosphatidate phosphatase, SGPP1 = sphingosine-1-phosphate 1, CERS = ceramide synthase, ACER = alkaline ceramidase.

5.3.1.2 LC/MS putatively identifies downregulation of some SPs and GPs in APOE 22 plasma

Global lipidomic analysis by LC/MS, followed by putative identification of lipids, suggested that the plasma sphingolipidome is downregulated in *APOE* 22 compared to control (Figure 5.3), implying an association between *APOE* allele and SP production, metabolism or trafficking. SL metabolism is well defined (Figure 5.11) with all SLs containing a sphingoid base, sphingosine, which may be acylated with fatty acids to form ceramide. Other SLs, for example SM, glucosylceramide (GlcCer) and galactosylceramides (GalCer) are produced by the replacement of hydrogen atoms on ceramide with head groups. Sphingosine is phosphorylated by sphingosine kinase to form sphingosine-1-phosphate. Sphingomyelins have a wide range of biological roles, including the maintenance of cell membrane dynamics (Lahiri and Futerman, 2007, Silva et al., 2007). It is worth noting that all species altered are either ceramides or can be produced from ceramide metabolism (Figure 5.11).

Circulating SLs originate from many sources, with targeted LC/MS of plasma demonstrating a total of 204 molecular species of these lipids (Quehenberger et al., 2010). For example, studies of abetalipoproteinemia patients and microsomal triglyceride transfer protein (MTP) KO mice suggest that MTP facilitates sphingomyelin and ceramide transport from hepatocytes into the blood by attaching these lipids to apoB-containing lipoproteins, which are then secreted (Iqbal et al., 2015). Sphingomyelin makes up about 10 % of the total lipid content of microparticles, which are derived from platelets and other blood cells (Hu et al., 2016). Cell-derived sphingomyelin can be exported through ABCA1, ABCA7 or ABCG1 (Quazi and Molday, 2013, Wang et al., 2003, Kobayashi et al., 2006). Furthermore, in cell culture, the presence of apoA-1 induces sphingomyelin release (Schifferer et al., 2007). Sphingosine-1-phosphate is released from cells including platelets, erythrocytes, leukocytes and vascular endothelial cells (Yatomi et al., 2001, Hänel et al., 2007, Książek et al., 2015). The origin of glycosphingolipids like glucosylceramides and galactosylceramides in plasma is unknown (Iqbal et al., 2017).

SP decreases in *APOE* 22 allele plasma could be related to the role of apoE as a lipid transporter, apoE 2 binds to the LDLR with less than 2 % efficiency of the other alleles (Corder et al., 1994). Circulating SM and ceramide associate with VLDL, sphingosine-1-phosphate associates with HDL and ceramides and dehydrosphingosines with LDL (Ng et al., 2015,

Hammad et al., 2010). Lipids carried on lipoproteins which associate with the LDLR, i.e, SM, ceramide and dehydrosphingosines, would intuitively be upregulated in *APOE* 22 homozygotes as *APOE 2* could reduce trafficking of these lipids into cells via the LDLR. However, this would be expected to raise SP level, in contrast with my findings. It has been suggested that the total amount of SP modulating enzymes is changed in LOAD, for example, sphingomyelinase and acid ceramidase (AC) expression are upregulated in brain samples from LOAD patients (He et al., 2010). I postulate that these enzymes could be downregulated in the protective *APOE* 2 allele. To investigate this further, SP findings are being validated using targeted methods, and if confirmed, in a second plasma cohort. After this, cell culture or animal models could be used to evaluate the effect of *APOE* allele on the production of both SP and SP modulating enzymes.

Plasma SP measurements are of interest as lipidomics has implicated SPs as circulating biomarkers of LOAD. Specifically, increased serum sphingomyelins and ceramides C16:0, C18:0, C22:0, C24:0, C24:1, stearoyl and sulfatide were associated with an increased risk of healthy participants developing cognitive impairment over nine years (Mielke et al., 2010). However, the same study found that these lipids were significantly decreased in participants with baseline cognitive impairment, together suggesting that SLs are increased in plasma before disease but lower or are downregulated once disease has begun. SLs could therefore be a useful biomarker of AD disease staging. In line with this, higher levels of ceramide C16:0, C18:0, C20:0, C22:0, C24:0 and the monohexosylceramides C16:0, C20:0 and C24:0 were associated with impending cognitive impairment in one study (Mielke et al., 2013). Contrastingly, plasma ceramides C16:0, C18:1, C20:0 and monohexosylceramides C18:1 and C24:1 were increased in patients with AD and Dementia with Lewy bodies (Savica et al., 2016), which is in direct opposition to the previously stated study suggesting that SLs decrease once disease has started. However, most studies on brain and plasma are in accordance that SPs are increased in LOAD. This is consistent with my findings that the *APOE* 22 participants, who are at a lower risk of developing AD, also had lower plasma ceramide and monohexosylceramide. One ceramide species and 8 monohexoceramides are significantly lower in *APOE 22* plasma, and two of these monohexoceramides maintain significance after the BH procedure. To conclude, *APOE* 22 plasma displays a SP profile which would be considered by the above studies as low risk of developing LOAD in the future. Lower

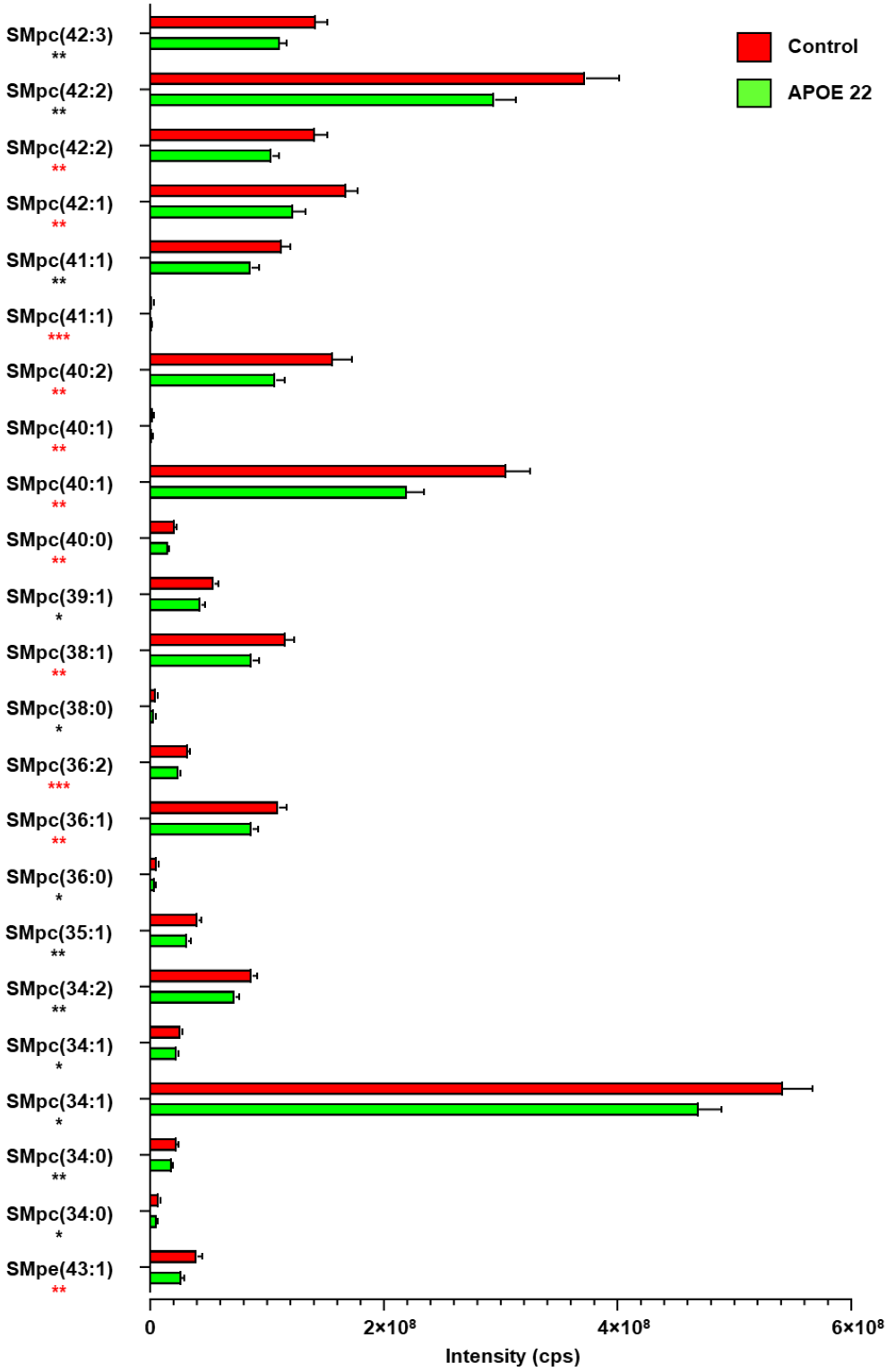

Figure 5.12: Sphingomyelins which are significantly reduced in *APOE 22* plasma. Significance using students two-tailed t test (unequal variance) is designated by asterisks, which are coloured red if the lipid maintained significance after BH correction. * = $p < 0.05$, ** = $p < 0.01$, *** = $p < 0.001$. Error bars represent SEM.

ceramides in *APOE* 22 could be protective against neurodegeneration if SPs are indeed implicated in neurodegeneration (Han et al., 2002a, Cutler et al., 2004, He et al., 2010). Many of the species which are significantly lower in *APOE* 22 plasma have recognised biological functions or are metabolites of each other, and this is discussed below. 22 sphingomyelin (SM) species were significantly reduced in *APOE* 22 (Figure 5.12). As ceramides were not increased, this is unlikely to be explained by upregulated conversion of sphingomyelin into ceramide.

A lipid putatively identified as ceramide phosphoethanolamine (43:1) (PE-Cer(43:1)) is significantly lower in *APOE* 22 compared to control and maintained significance after BH correction (Figure 5.12). PE-Cer is produced from ceramide, catalysed by ceramide phosphoethanolamine synthase (SMSr) in two steps, (i) addition of the PE headgroup to ceramide and (ii) elongation of the fatty acid chains by methylation (Malgat et al., 1986). Thus, lower PE-Cer in *APOE* 22 could be a result of a reduced pool of circulating total ceramide. However, only one ceramide species is lower in *APOE* 22 plasma, which was not significant after BH correction and has a different putatively identified chain length. This indicates that lower PE-Cer is not caused by a lower pool of ceramide, and as PE-Cer is produced non-enzymatically, this reduction in PE-Cer cannot be caused by an alteration in enzyme levels.

CER(40:7) was putatively identified as reduced in *APOE* 22 plasma, although this did not maintain significance after BH correction (Figure 5.12). Ceramides are biologically active species, for example, ceramides act as activators of autophagy (Okazaki et al., 1998), maintain homeostasis via regulation of cell membrane fluidity (Pinto et al., 2013) and in membranes, form gel domains with one to three palmitoyl-sphingomyelin species, around which liquid-ordered phase domains called lipid rafts then form (Silva et al., 2007). Lipid rafts may play a role in stabilising signalling molecules in the same region. Lipid rafts may be important in LOAD pathology as APP processing on lipid rafts is more amyloidogenic than in non-ordered membrane regions (Ehehalt et al., 2003). Therefore, if circulating ceramide is representative of brain ceramide content and ceramide induces lipid rafts to form on cell membranes, higher ceramides in plasma could indicate amyloid pathology is more likely to form.

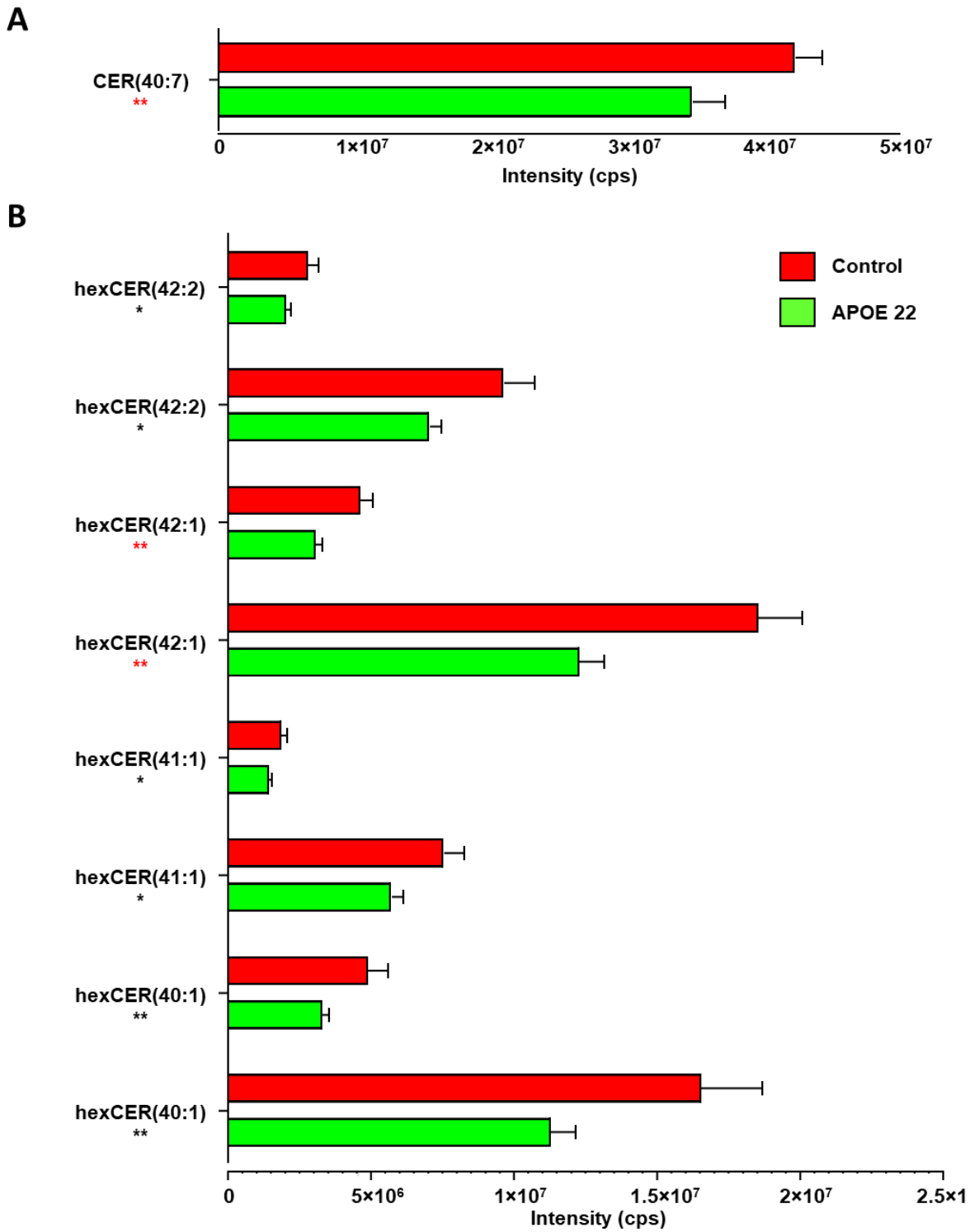

Figure 5.13: Ceramide and hexylceramides which are significantly reduced in *APOE 22* plasma. A Ceramide which is significantly reduced in *APOE* 22 plasma. **B.** Hexylceramides which are significantly reduced in *APOE* 22 plasma. Significance using students two-tailed t test (unequal variance) is designated by asterisks, which are coloured red if the lipid maintained significance after BH correction. * = $p < 0.05$, ** = $p < 0.01$, *** = $p < 0.001$. Error bars represent SEM.

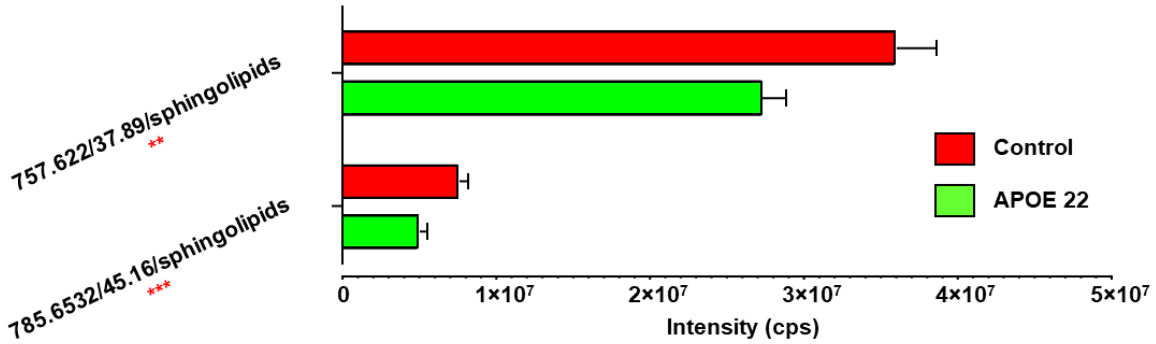

Figure 5.14: Sphingolipids with multiple putative identifications, which are significantly reduced in *APOE 22* plasma. Significance using students two-tailed t test (unequal variance) is designated by asterisks, which are coloured red if the lipid maintained significance after BH correction. * = $p < 0.05$, ** = $p < 0.01$, *** = $p < 0.001$. Error bars represent SEM.

Two of the putatively identified hexylceramides species remained significant after BH correction, and function of these lipids is currently unknown (Figure 5.13). Lastly, two species which matched multiple SP entries in LIPID MAPS retained significance after BH correction and I aim to identify these in targeted SP analyses (Figure 5.14).

SP dysregulation is biologically relevant since these lipids can be potent bioactive mediators which can influence a variety of processes such as cell growth, differentiation and proliferation, apoptosis or necrosis (Lahiri and Futerman, 2007). Approximately 10 % of brain lipids are SPs, which are a major constituent of the myelin sheath, and SP metabolism is important in maintaining brain function. Changes in SP content within the brain have been documented in LOAD, for example, in areas of neurodegeneration there are reductions in sulfatide, sphingomyelin and sphingosine-1-phosphate, and increased ceramides and sphingosine (Han et al., 2002b, He et al., 2010). It is unknown if these alterations in LOAD brain would be reflected in plasma. Changes in enzyme activity could be expected to occur throughout the body, however much of the variation in SP content in LOAD is brain region-specific, which indicates that global alterations in enzyme activity are not to blame. Therefore, unless the BBB is compromised, plasma SPs most likely do not reflect variation in SPs in the brain.

It is not known if higher ceramides in the brain in LOAD are a causal factor in cognitive deficit or a by-product of another pathological process, such as the activation of autophagy pathways by ceramide. Possible breakdown of the BBB early on in LOAD provides direct passage for lipids from the CNS to the peripheral circulation (Sweeney et al., 2018). However, it is not possible in most cases to distinguish from which tissue a particular lipid has originated, with the exception of lipids which are only produced in specific locations. Thus, future plasma biomarkers of CNS disease could be directly sourced from the brain or be lipids which are sourced in the periphery and are representative of changes within the brain. This work is the first such analysis of *APOE* plasma and as such, no direct comparison can be made between LOAD samples and low-risk *APOE* homozygotes. However, SP changes in *APOE* 22 plasma are opposed to alterations seen in LOAD brain and as such, may be indicative of a low-LOAD-risk environment. Targeted analysis of SL species in APOE alleles by LC/MS/MS is required to

validate SLs in APOE 22, due to the biological relevance of SLs and putative nature of lipid identifications provided by the global analysis.

Most lipids found in the *APOE* 22 dataset do not match an *m/z* in the LIPID MAPS database, and so were designated as unknowns. Fourteen percent of these are significantly decreased in *APOE* 22 plasma compared to control after BH correction. Although some unknowns may be artefacts of the extraction or data analysis, these data suggest that over half of lipid species present in plasma have yet to be identified. Characterisation of unknown lipids by LC/MS/MS could determine structure and identify biologically relevant species.

Some GPs were reduced in *APOE* 22 plasma versus controls. GPs putatively identified as reduced in *APOE* 22 tended to be plasmalogens or ethers, which were high in polyunsaturated fatty acids and represented all four GP head groups. Plasmalogens are synthesised in the liver and travel to tissues in lipoproteins in the circulation (Vance, 1990), where they are distributed through tissues. Three GPs, PC(34:1p)/(34:2e), PE(40:8), PI(38:4), maintained significance after BH correction, a PC, a PE, a PI and a PS. It should be noted that some PC and PE species are isobaric and identifications have been assigned based on *m/z* and RT. The RT shift seen between the two datasets could therefore affect identifications, which will have to be confirmed using LC/MS/MS.

PLs are produced by the Kennedy pathway and modified by the Land's cycle, but there is no known link between *APOE* alleles and dysfunction in either of these pathways. Land's cycle disruptions have, however, been described in the brain of 2 murine AD models (Granger et al., 2018). Absolute amounts of lyso-PCs, lyso-PAF and PAF were lowered in mice with cognitive deficits, regardless of age, and an age-dependant accumulation of PAF took place in brain tissue. Determination of plasma PL species by LC-MS/MS would allow the definitive identification of lipids and a network analysis to take place to determine if Land's cycle enzyme activity is affected by *APOE* allele status.

Palmitoleic acid was significantly elevated between *APOE* 22 and controls in the NPHSII dataset (Quehenberger et al., 2010, Abdelmagid et al., 2015). This lipid makes up a large proportion of the fatty acids present in PLs in the brain, liver, and other tissues (Abbott et al.,

2012) and can come from dietary sources or be synthesised from the elongation of malonyl-CoA, a citrate derivative. Recent work suggests palmitoleic acid reduces inflammatory markers in patients with ulcerative colitis, which is an inflammatory bowel disorder (Bueno-Hernández et al., 2017). Inflammatory markers are increased in Alzheimer's disease. If peripheral inflammation has a causative effect in LOAD, reduction of inflammatory markers via cis-9-palmitoleic acid could be beneficial. However, any benefit may be outweighed by liver pathology as cis-9-palmitoleic acid stimulates fatty acid accumulation and liver steatosis (Cao et al., 2008, Guo et al., 2012).

Lower levels of some lipids, including TGs (which fall into the GL category) and cholesterol (sterol lipids) are associated with a lower risk of developing CVD and *APOE* 22 homozygotes have a reduced risk of developing CVD (Hokanson and Austin, 1996, Luc et al., 1994). A meta-analysis of 45 investigations observed that *APOE* 22 homozygotes have lower plasma cholesterol but higher TGs (Dallongeville et al., 1992). Also, measurements taken at time of blood collection suggest that total cholesterol is significantly reduced in NPHSII *APOE* 22 samples. Therefore, it was unexpected that in the NPHSII data only a single sterol lipid, and no glycerolipids, were significantly different in *APOE* 22. However, this result may be an artefact of the small sample size. To investigate this further, I will extract plasma lipids from *APOE* 22, control and *APOE* 44 and quantify cholesterol, CEs and TGs using targeted LC/MS/MS.

5.3.1.3 APOE 22 samples can be separated from control using PLS-DA and a ROC analysis

Alleles were separated by PCA and PLS-DA, as well as the ROC analysis, indicating again that lipids can be used as biomarkers to separate patient samples. This is in agreement with several other studies which used lipid panels to distinguish between disease and control samples, or determine disease progression (Björkqvist et al., 2012, Chatterjee et al., 2016, Liu et al., 2016, Floegel et al., 2018, Mielke et al., 2010, Suvitaival et al., 2018) . In the future, lipid panels could be used either for diagnosis or patient stratification.

Most lipids with the highest effect size were unknowns. Some of these clustered with putatively identified lipids (Figure 5.6), suggesting that they may belong to the same lipid category. The heatmap visually demonstrates which lipids have the highest effect size (blue box). These unknowns and SPs deserve further research as they may be of biological importance. Both univariate and multivariate analyses identify unknown lipids and SPLs as the categories which differ the most between alleles.

5.3.2 Global lipidomic analysis of *APOE* 44 plasma revealed similarities with control

Traditionally, *APOE* 44 is associated with higher cholesterol and TGs, however my global analysis did not confirm this pattern in these samples (Sing and Davignon, 1985, Dallongeville et al., 1992). To investigate this further, CEs and TGs will be quantified via a targeted LC/MS/MS analysis. Global analysis revealed very few changes in lipid levels when comparing *APOE* 44 plasma to control. PG(32:4) was putatively identified in both *APOE 44* and control plasma. PGs could be present in plasma due to platelet contamination or the presence of platelet-derived microparticles, as both of these contain minimal amounts of PG (Hu et al., 2016).

The heatmap of the 40-lipid panel reveals that many of the lipids with the highest effect size are unknown. These data suggest that over 50 % of the lipidome is yet to be described, and that some of these lipid levels are regulated by *APOE* isoform. *APOE* 44 and control samples could be separated by PCA, PLS-DA and ROC analysis, demonstrating that lipids can be used as biomarkers to stratify samples with multivariate methods. Stratification is possible, and effective, even when few or no significant differences between groups are present. Also, all species which differed significantly in ANOVA were selected for the heatmap. Therefore, both t tests and multivariate analysis identified the same lipids as conferring the largest difference between alleles.

The *APOE* 22 and *APOE* 44 datasets were analysed several months apart, and it is likely that the larger number of lipids found in the *APOE* 44 dataset was caused by increased sensitivity of the instrument during analysis of my samples. This could be a result of there being lower

background noise due to a reduction in contaminants either in the MS system or in the solvents and is discussed later (Section 6.3.2.2).

Differences in RTs and MS sensitivity in the 2 datasets prevented batches from being combined into one analysis and there was no direct comparison between *APOE* 22 and *APOE* 44 homozygotes. Both groups were compared only to control samples and PCA and PLS-DA of all alleles was not possible. This prevented unknown lipids from being compared based on mass and RT. Both alleles demonstrated interesting results when compared to their respective controls, however, any further analysis of *APOE* alleles would need to be performed as one experiment to prevent batch effects (Section 6.2.2.2).

5.4 Conclusions

SPs, GPs and unknown lipids are lower in *APOE* 22 plasma and some maintained significance after BH correction. This suggests specific changes to SP and GP content of plasma, dependent on *APOE* allele and possibly due to the role of apoE in lipid transport. However, these are only putative identifications and it is essential to carefully validate identifications by MS/MS. Given the changes I observed for both SL and GPs in the *APOE* group, I would also like to carry out targeted analysis of those lipids to validate my global lipidomics findings, but this is beyond the scope of my current project. Many of the lipids which were the most significant, had the highest FC or largest effect size were unknowns, stressing the importance of further profiling of the lipidome. Identification of some species, which appeared to derive from several categories, could reveal novel bioactive lipids.

Chapter 6: Quantitative analysis of cholesterol, cholesterol esters and triglycerides in *APOE* homozygote plasma reveals lower lipid levels in *APOE 22* and *APOE 44*

6.1 Introduction

Circulating levels of total triglycerides (TAGs) and total cholesterol are currently used as risk assessment measures for CVD alongside blood pressure, and several studies have suggested that these may also be altered in LOAD (Ramdane and Daoudi-Gueddah, 2011, Presećki et al., 2011, Nägga et al., 2018). Also, LC-MS/MS analysis of plasma suggests that individual CE species may be altered in LOAD (Proitsi et al., 2015).

The principal genetic component for LOAD is *APOE*, with the ε4 allele raising risk and the ε2 allele lowering it (Corder et al., 1993, Corder et al., 1994). The *APOE* gene product, apoE, is a lipid transport protein which plays an important role in lipid metabolism and the presence of *APOE* ε2, ε3 or ε4 has also been found to be associated with altered circulating total cholesterol and TAGs (Sing and Davignon, 1985, Dallongeville et al., 1992, Maxwell et al., 2013). To elucidate the relationship between *APOE* and individual CE and TAG species, I quantified free cholesterol and CEs in the NPHSII samples using LC-MS/MS, comparing *APOE 22* and 44 against control (*APOE* 33) samples. I also measured TAGs in plasma using a Q1 method.

When NPHSII samples were collected, total cholesterol and TAGs were quantified, and total cholesterol and TAGs for the subset of NPHSII analysed in this chapter are in Table 6.1 (Cooper et al., 2005). The methods used measure only total cholesterol and TAGs and do not give any information on individual molecular species. My results from Chapter 5, together with the total cholesterol and TAG measurements at time of collection, suggest that cholesterol and CEs are significantly reduced in *APOE 22* compared to control (Table 6.1). These data may have biological significance as individual CE species have been associated with LOAD (Proitsi et al., 2015). Thus, a targeted LC-MS/MS analysis of cholesterol, CEs and TAGs will be

Genotype	n	Total cholesterol mmol (mean ± SD)	Total triglycerides mmol (mean ± SD)
Control	39	6.02 ± 0.96	1.91 ± 1.17
APOE 22	21	5.08 ± 0.99***	2.15 ± 0.99
APOE 44	37	5.69 ± 0.85	2.08 ± 1.39

Table 6.1. Total cholesterol and triglyceride measurements taken from NPHSII samples at time of collection and made using enzymatic methods. Measurements taken from work by Cooper et al., 2005.

undertaken, and then compared with my data from the global analysis. The LC-MS/MS methods used in this Chapter (Section 2.1.3.3 and Section 2.1.3.5) allow the quantification of 48 molecular species (cholesterol, 11 CEs and 36 TAGs). Methods were developed from those used to analyse the data in Chapter 4 (Section 2.1.3.2 and Section 2.1.3.4). Methods used in Chapter 4 were optimised, including the addition of heat at the electrospray source, and more lipids were monitored.

6.1.1 Aims and hypothesis

The effect of *APOE* allele on circulating cholesterol and individual CEs and TAGs is unknown.

Therefore, my aims were as follows:

- To measure 48 circulating cholesterol, CE and TAG species in plasma from homozygotes for *APOE* ε22, ε33 (control) and ε44 using in-house-made LC-MS/MS methods.
- To determine if *APOE* allele is associated with patterns in CE and TAG chain length or saturation.

The null hypothesis states that *APOE 22* and *APOE 44* will not be associated with an increase or decrease in cholesterol or any individual CE or TAG species.

6.2 Results

6.2.1 Cholesterol and cholesterol esters were lower in *APOE 22* and APO4 44 plasma compared to control

APOE 22 (n = 22), *APOE* 33 (n = 39) and *APOE 44* (n = 39) samples from the NPHSII cohort, chosen as described earlier (Section 2.2.2), were spiked with CE and TAG internal standards (Section 2.1.5.3) and extracted (Section 2.3.1). Amounts of cholesterol, and individual CE and TAG species were quantified in the lipid extracts using a targeted LC-MS/MS method (Section

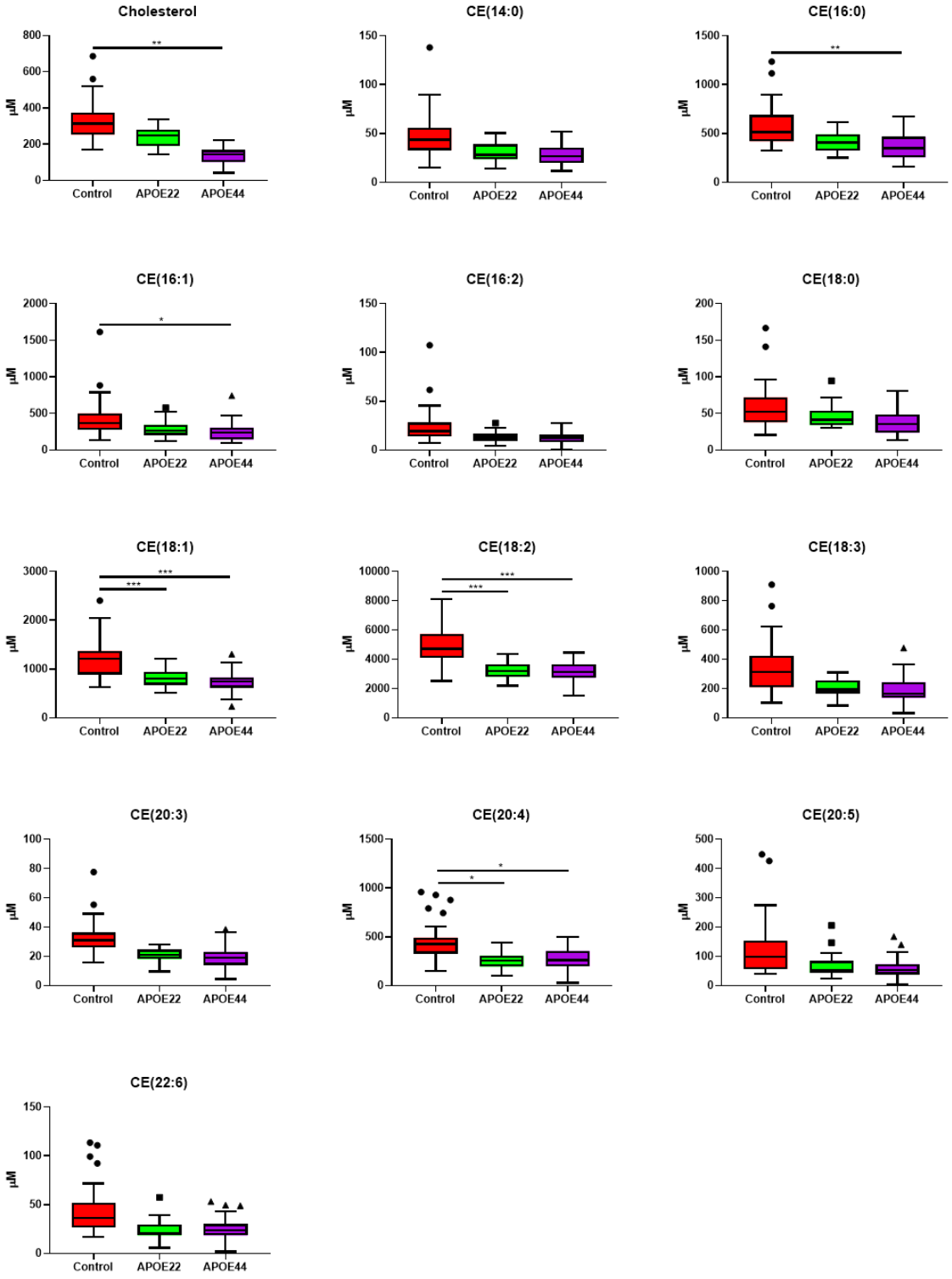

Figure 6.1: Tukey boxplots of quantified cholesterol and cholesterol esters in plasma from control, APOE 22 and APOE 44 participants. Species were quantified using LC/MS (Materials and methods 2.5.2.2). P values calculated using a two-way ANOVA with Tukey correction for multiple comparisons (n = 22, 39 and 39 for *APOE 22,* control and *APOE 44*, respectively). Lower fence of boxplots represent the data point which is the lowest value greater than the 25th percentile minus 1.5 times the IQR. The upper fence represents the data point which is the greatest value lower than the 75th percentile pus 1.5 times the IQR.

2.4.2.2). Cholesterol and 10 CEs are significantly decreased in *APOE 22* compared to control (Figure 6.1), mirroring the results from the enzymatic analysis (Table 6.1) (Cooper et al., 2005). All of these species, as well as CE(18:0), were significantly lower in *APOE 44* compared to control. None of the species quantified reached significance when comparing *APOE 22* and *APOE 44*. Control samples had a larger range than either *APOE 22* or *APOE 44*, demonstrating that levels of cholesterol and CEs varied more between individuals in the control group than in either *APOE 22* or 44. Most species were present at lowest abundance in *APOE 44*, followed by *APOE 22* and were at highest abundance in control samples.

6.2.2 Most TAGs are unaltered between *APOE* alleles

Lipid extracts were prepared as for the cholesterol and CE analysis, then 36 individual TAG species were quantified using targeted LC-MS/MS (Section 2.4.2.4). Most of the TAGs measured were not significantly altered between alleles. These unaltered TAGs are TAG(44:0), TAG(46:0), TAG(48:1), TAG(48:2), TAG(50:2), TAG(52:2), TAG(52:3), TAG(52:4), TAG(52:5), TAG(54:1), TAG(54:2), TAG(54:3), TAG(54:4), TAG(54:5), TAG(54:6), TAG(56:2), TAG(56:3), TAG(56:4), TAG(56:5) and TAG(56:6). Four of the triglycerides quantified (TAG(48:0), TAG(50:0), TAG(50:1), TAG(52:1)) are significantly increased in *APOE 22* compared to control and *APOE 44*. Two TAGs (TAG(50:3) and TAG(50:4)) are significantly lower in *APOE 44* than control (Figure 6.2). None of the TAGs measured achieved significance when comparing *APOE 22* with 44 plasma samples. Several TAG species (TAG(32:0), TAG(34:0), TAG(36:0), TAG(38:0), TAG(40:0), TAG(42:0), TAG(52:0), TAG(54:0), TAG(56:0), TAG(56:1)) did not have enough data points to produce boxplots or do statistical analysis. TAG(34:0) and TAG(38:0) are present in order of abundance: *APOE 22* < *APOE 44* < control. TAG(36:0), TAG(40:0) and TAG(42:0) are present in order of abundance: *APOE 22* < control < *APOE 44*. TAG(52:0), TAG(54:0), and TAG(56:1) are present at abundance: control < *APOE 22* < *APOE 44*. TAG(32:0) was found only in some control and *APOE 44* samples and TAG(56:0) was found only in one control sample. To conclude, a few TAG species did differ between control and either *APOE 22* or *APOE 44* but most TAGs were unaltered between alleles.

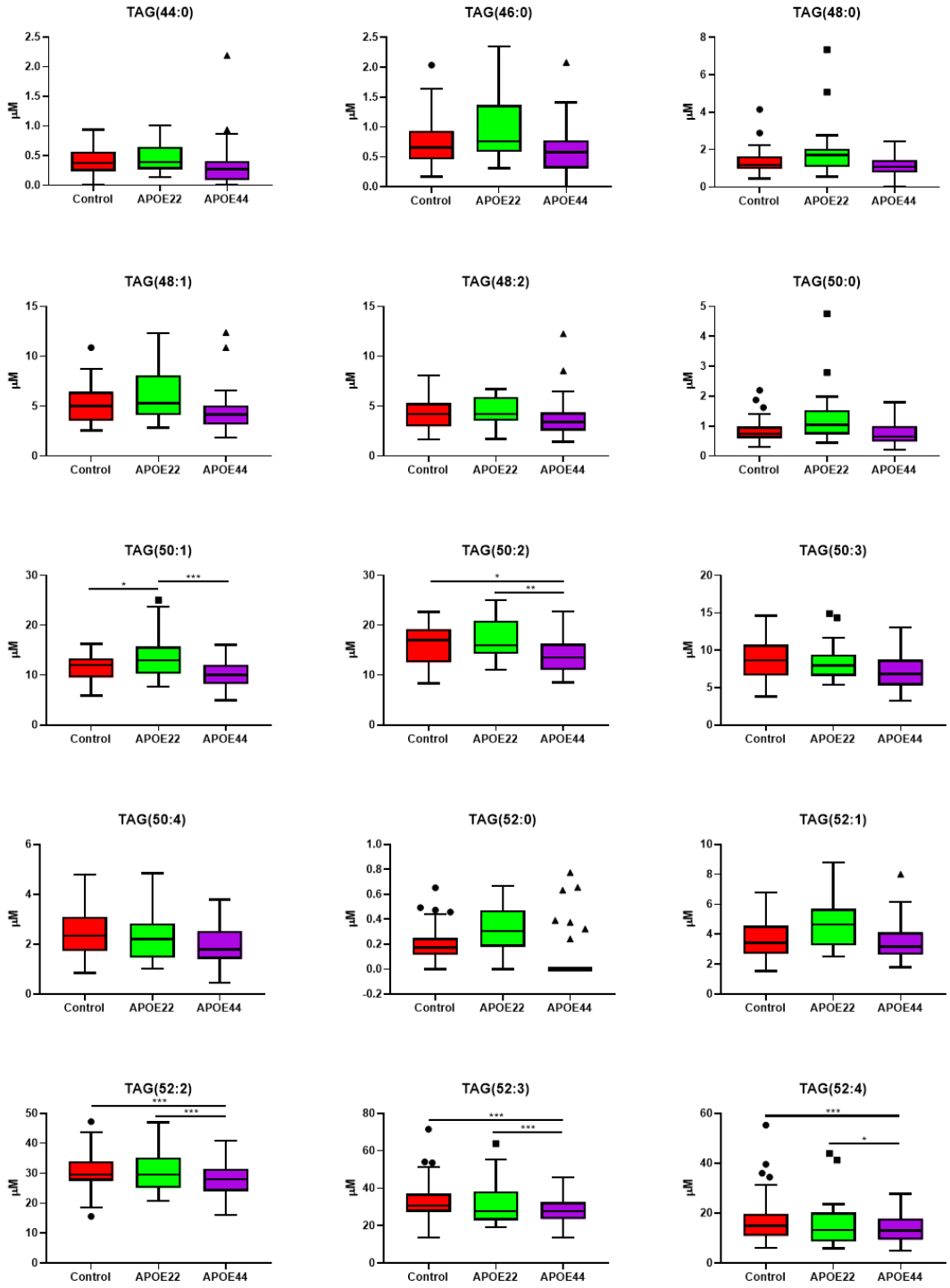

Figure 6.2: Tukey boxplots of quantified triglycerides in plasma from control, APOE 22 and APOE 44 participants. Species were quantified using LC/MS (Materials and methods 2.5.2.4). P values calculated using a two-way ANOVA with Tukey correction for multiple comparisons (n = 22, 39 and 39 for *APOE 22,* control and *APOE 44*, respectively). Lower fence of boxplots represent the data point which is the lowest value greater than the 25th percentile minus 1.5 times the IQR. The upper fence represents the data point which is the greatest value lower than the 75th percentile pus 1.5 times the IQR.

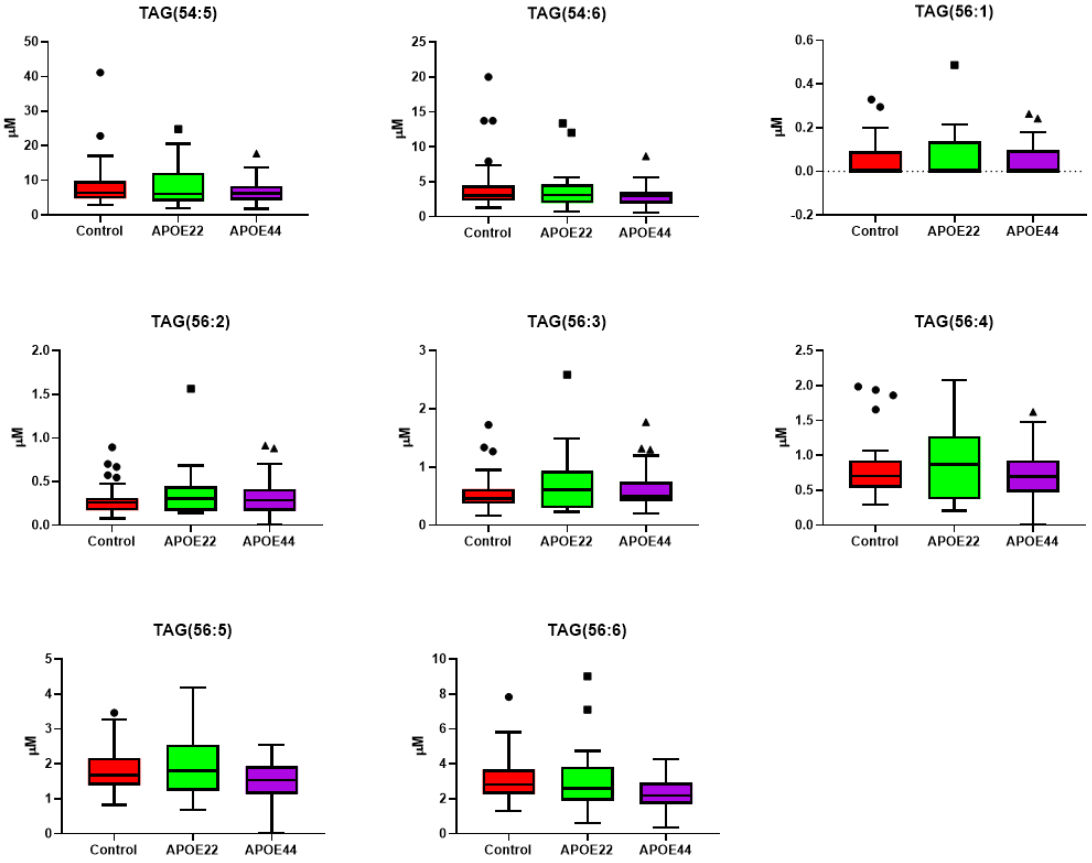

Figure 6.2 cont.: Tukey boxplots of quantified triglycerides in plasma from control, APOE 22 and APOE 44 participants. Species were quantified using LC/MS (Materials and methods 2.5.2.4).). P values calculated using a two-way ANOVA with Tukey correction for multiple comparisons (n = 22, 39 and 39 for *APOE 22,* control and *APOE 44*, respectively). Lower fence of boxplots represent the data point which is the lowest value greater than the 25th percentile minus 1.5 times the IQR. The upper fence represents the data point which is the greatest value lower than the 75th percentile pus 1.5 times the IQR.

6.2.3 TAG species cluster according to saturation

CE and TAG data was normalised to log^{10} and heatmaps of CE and TAG data were made in RStudio. The heatmap of the CE data demonstrates that cholesterol and CEs are higher in control plasma, however lipids do not cluster according to saturation or chain length (Figure 6.3A). The most and least abundant species do not change between genotypes, and the pattern of abundance is similar to control (Figure 6.3B). However, *APOE 22* contains more CE(16:1) is than CE(20:4). Also, *APOE 44* contains more CE(18:3) than cholesterol. TAGs are clustered along the x axis according to saturation, as most polyunsaturated TAGs are clustered, whilst all saturated TAGs cluster with a few polyunsaturates (Figure 6.4A). It is worth noting that the range of the TAGs data was smaller than CEs, and therefore the heatmap scale is smaller.

6.2.4 Global and targeted methods of lipid profiling provide similar fold changes for some individual lipids

Fold change (FC) for lipids measured in both global and targeted analyses was compared to determine if the global and targeted methods gave similar results. For simplicity, I compared FC values for *APOE 22* and control samples only. In the global data FC is calculated as signal intensity in *APOE 22* divided by signal intensity in control samples. In the targeted data, FC is calculated as amount of lipid in *APOE 22* divided by amount in control. Several CE and TAG species were measured in both global and targeted analyses, these species were used for this comparison. Global and targeted methods demonstrated the same trends for two of the three CE species measured in both analyses, i.e. lipids were either increased in *APOE 22* in both analyses or decreased in *APOE 22* in both analyses. However, CE(16:0) had a FC of 2.29 in global analysis and just 0.72 in the targeted analysis. Patterns of lipid abundance were similar, for example, in both analyses CEs were measured in order of abundance CE(18:0) > CE(18:2) > CE(20:4). Whilst CE(18:0) is the most abundant sterol measured using targeted methods, it was not found in global analysis during optimisation or analysis of NPHSII samples (Chapter 5). The reason for this discrepancy is unknown. Most TAGs are unchanged when using global

A

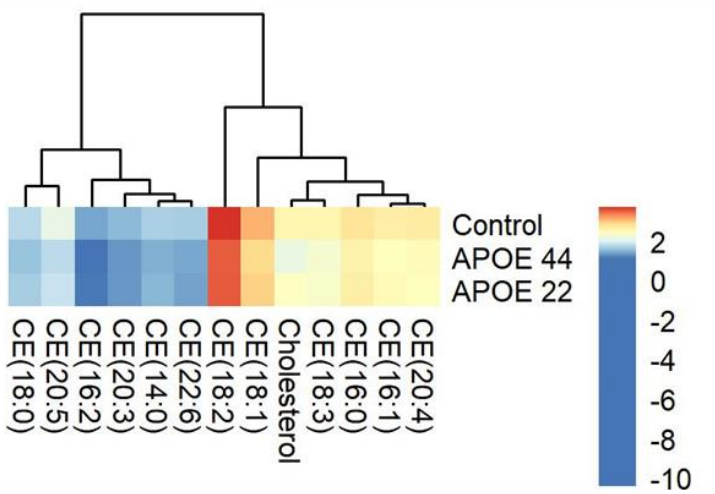

B

	Control	*APOE22*	*APOE44*
Most abundant	CE(18:2)	CE(18:2)	CE(18:2)
	CE(18:1)	CE(18:1)	CE(18:1)
	CE(16:0)	CE(16:0)	CE(16:0)
	CE(20:4)	CE(16:1)	CE(20:4)
	CE(16:1)	CE(20:4)	CE(16:1)
	Cholesterol	Cholesterol	CE(18:3)
	CE(18:3)	CE(18:3)	Cholesterol
	CE(20:5)	CE(20:5)	CE(20:5)
	CE(18:0)	CE(18:0)	CE(18:0)
	CE(14:0)	CE(14:0)	CE(14:0)
	CE(22:6)	CE(22:6)	CE(22:6)
	CE(20:3)	CE(20:3)	CE(20:3)
Least abundant	CE(16:2)	CE(16:2)	CE(16:2)

Figure 6.3: Quantified free cholesterol and CEs from control, APOE 22 and APOE 44 participants. A. Cholesterol and CEs across the three alleles were quantified using LC/MS/MS and absolute amount normalised by $\log^{10}$ Cholesterol and CEs across the three alleles. **B.** Cholesterol and CE species in order of abundance, from most to least abundant.

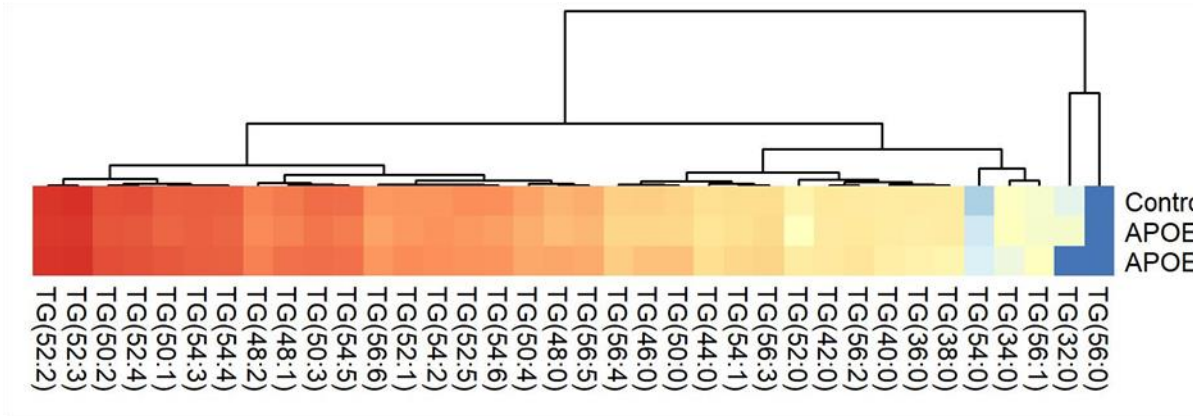

Figure 6.4: Heatmaps representing quantified TAGs in plasma from control, *APOE 22* and *APOE 44* participants. Species were quantified using LC/MS/MS and absolute amount normalised by $\log^{10}$. TAGs across the three alleles. Polyusaturated species cluster on the left (green box), and saturated TAGs cluster with some polyunsaturates on the right (grey box). n = 22, 39 and 39 for *APOE 22,* control and *APOE 44*, respectively.

B

	Control	APOE22	APOE44
Most abundant	TAG(52:3)	TAG(52:3)	TAG(52:3)
	TAG(52:2)	TAG(52:2)	TAG(52:2)
	TAG(52:4)	TAG(50:2)	TAG(50:2)
	TAG(50:2)	TAG(52:4)	TAG(52:4)
	TAG(54:3)	TAG(50:1)	TAG(54:3)
	TAG(54:4)	TAG(54:3)	TAG(50:1)
	TAG(50:1)	TAG(54:4)	TAG(54:4)
	TAG(54:5)	TAG(54:5)	TAG(54:5)
	TAG(50:3)	TAG(50:3)	TAG(50:3)
	TAG(48:1)	TAG(48:1)	TAG(48:1)
	TAG(48:2)	TAG(48:2)	TAG(48:2)
	TAG(54:6)	TAG(52:1)	TAG(54:2)
	TAG(52:5)	TAG(54:6)	TAG(52:1)
	TAG(52:1)	TAG(54:2)	TAG(54:6)
	TAG(54:2)	TAG(52:5)	TAG(52:5)
	TAG(56:6)	TAG(56:6)	TAG(56:6)
	TAG(50:4)	TAG(48:0)	TAG(50:4)
	TAG(56:5)	TAG(50:4)	TAG(56:5)
	TAG(48:0)	TAG(56:5)	TAG(48:0)
	TAG(46:0)	TAG(50:0)	TAG(56:4)
	TAG(56:4)	TAG(46:0)	TAG(46:0)
	TAG(50:0)	TAG(56:4)	TAG(36:0)
	TAG(36:0)	TAG(56:3)	TAG(50:0)
	TAG(34:0)	TAG(54:1)	TAG(56:3)
	TAG(32:0)	TAG(44:0)	TAG(44:0)
	TAG(38:0)	TAG(36:0)	TAG(38:0)
	TAG(56:3)	TAG(56:2)	TAG(34:0)
	TAG(44:0)	TAG(42:0)	TAG(54:1)
	TAG(54:1)	TAG(38:0)	TAG(32:0)
	TAG(42:0)	TAG(40:0)	TAG(52:0)
	TAG(40:0)	TAG(52:0)	TAG(42:0)
	TAG(56:2)	TAG(34:0)	TAG(40:0)
	TAG(52:0)	TAG(56:1)	TAG(56:2)
	TAG(56:1)	TAG(54:0)	TAG(56:1)
	TAG(54:0)		TAG(54:0)
Least abundant	TAG(56:0)		

Figure 6.4. continued: Heatmaps representing quantified cholesterol, CEs and TAGs in plasma from control, *APOE 22* and *APOE 44* participants. Species were quantified using LC/MS/MS and absolute amount normalised to a scale of -1 to 1. **B.** TAGs in order of abundance in control, *APOE 22* and *APOE 44* plasma.

or targeted methods. TAGs in global and targeted analyses could not be compared by order of abundance as several species were identified more than once in the global analysis, probably due to the presence of positional isomers.

6.3 Discussion

6.3.1 Cholesterol and CEs are lower in *APOE 22* and *APOE 44* compared to control

Lower cholesterol and CEs in *APOE 22* were suggested by the enzymatic total cholesterol measurement taken at time of sample collection (Table 6.1), however LC-MS/MS analysis in this Chapter revealed that cholesterol and CEs are decreased in both *APOE 22* and 44 plasma compared to control. This is not in accordance with the literature on total cholesterol, which tends to associate *APOE 22* with decreased circulating cholesterol, whilst ε4 is associated with increased cholesterol (Dallongeville et al., 1992, Sing and Davignon, 1985, Boulenouar et al., 2013). I considered the fasting, or non-fasting state of the participants in the NPHSII cohort, and other studies mentioned previously. NPHSII plasma was drawn from non-fasting participants, whilst other studies used fasted plasma or did not state whether participants had fasted (Miller et al., 1996, Sing and Davignon, 1985, Boulenouar et al., 2013, Dallongeville et al., 1992). *APOE* allele may affect how quickly dietary fats are cleared from circulation, however, studies disagree as to if the presence of *APOE ε2* slows postprandial lipid metabolism, or if *APOE ε4* is associated with faster metabolism (Weintraub et al., 1987, Bergeron and Havel, 1996). Slower postprandial lipid clearance could cause higher lipids in non-fasting *APOE 22* plasma; however this offers no explanation for why cholesterol and CEs are not increased in *APOE 44*.

The reason for this disparity between the literature and my data may be the levels of total cholesterol in the control samples. A normal cholesterol level is considered to be below 5 mmol. Also, a study of another set of NPHSII plasma samples found that there was an average cholesterol of 5.69 mmol/L in males with no current or future CVD and 6.05 mmol/L in males who went on to have CVD (Cooper et al., 2005). In the subset of the NPHSII samples I analysed, average total (enzymatic) cholesterol was 6.02 mmol/L , which is higher than considered

normal and much closer to the CVD group than the control group in Cooper et al., 2005. The randomly chosen control samples have high total cholesterol, which is likely why cholesterol and CEs measured by LC-MS/MS in NPHSII samples are not higher in *APOE 44* than control. The small sample size may have contributed, as cholesterol levels in the control group do not accurately represent the wider *APOE* 33 population.

In the CNS, cholesterol is produced solely by *de novo* synthesis and lipoproteins carrying cholesterol are blocked from exchange with the periphery by the blood brain barrier (Ballabh et al., 2004). However, cholesterol can be transported out of the CNS as 24S-hydroxycholesterol, and this makes up a significant proportion of circulating 24-hydroxycholesterol (Lütjohann et al., 1996, Björkhem et al., 1998). In fact, plasma 24S-hydroxycholesterol is increased in LOAD (Zuliani et al., 2011). I would like to compare levels of this lipid across *APOE* alleles in the NPHSII data.

To summarise, studying NPHSII plasma using targeted LC-MS/MS methods demonstrates that *APOE 22* plasma is associated with lower CEs but *APOE 44* plasma is not associated with high CEs. This disparity between my data and the literature may be due to the high total cholesterol nature of the NPHSII samples.

6.3.2 TAGs are not altered between *APOE* alleles

Most TAGs (22 out of 27 in total) are unchanged between *APOE* alleles in NPHSII data. This was not unexpected as enzymatic total TAG measures made at time of collection for this particular set of samples did not demonstrate any differences (Figure 6.1). However, this is not in agreement with the literature, for example, a meta-analysis which re-analysed data from 38 studies suggested that all *APOE* allele combinations tested (*22, 23, 34, 44*) have higher total TAG than control (Dallongeville et al., 1992). As discussed above (Section 6.3.1), *APOE* allele could alter the speed of postprandial lipid metabolism, however, neither *APOE 22 n*or *APOE 44* affect speed of clearance of postprandial TAGs (Weintraub et al., 1987, Brown and Roberts, 1991, Boerwinkle et al., 1994, Bergeron and Havel, 1996). Therefore, I postulate that,

as with cholesterol and CEs, the smaller sample size of the subset of NPHSII samples analysed may explain why TAGs are not increased in *APOE 44*.

Heatmaps demonstrate TAG clustering according to carbon chain saturation (Figure 6.3). Clustering of TAGs according to saturation could reflect the hydrolysis and re-esterification of dietary lipids. Some dietary fats are hydrolysed by luminal and gastric lipases to form DAGs (Hamosh and Scow, 1973, Schønheyder and Volqvartz, 1946). In the intestinal lumen, pancreatic lipase completes hydrolysis of TAGs and DAGs into MAGs, which are actively or passively transported into enterocytes (Mansbach and Gorelick, 2007). Here, fatty acyls, sourced from digested TAGs and other lipids, are esterified back into TAGs (Mattson and Volpenhein, 1964). Saturated and polyunsaturated species come from different dietary sources, for example, polyunsaturated fatty acids are present at highest quantities in food like meat, fish and dairy (Meyer et al., 2003). Therefore, TAG clustering could reflect meal content and the subsequent esterification of fatty acyls into TAGs in the enterocytes, as high fat meals might be expected to produce clusters of more saturated lipids. TAG species found in only some samples are low (< μM) abundance species and may have been present below the level of detection of the mass spectrometer in some samples.

6.3.4 Global and targeted methods of lipid profiling give similar trends

It was important to consider whether trends in the global dataset reflected results in the targeted analysis. Cholesterol, two CEs and some TAGs have a similar FC using both global and targeted methods (Table 6.2, Table 6.3). However, CE(16:0) and 8 of the 24 TAGs measured were incorrectly labelled as increased or decreasing. All lipids which were incorrectly labelled had relatively small fold changes when measured by LC-MS/MS (range 1.00 – 1.29) and only one was significantly higher in *APOE 22* plasma compared to control ($p < 0.05$). Whilst it was not possible to directly compare between all species, CEs were present at the same order of abundance in both analyses. Together, this indicates that the global method used within provides similar results to the targeted methods, but that some trends may have missed, and biologically relevant results, like the SP and GPL decreases in *APOE 22* homozygote plasma should be validated using LC-MS/MS.

A comparison of trends in cholesterol esters in targeted and global assays and between APOE 22 and control plasma

Species	FC* global	FC targeted
CE(16:0)	2.29	0.72**
CE(18:2)	0.60	0.65***
CE(20:4)	0.45	0.56***

Table 6.2: A comparison of trends in cholesterol esters in targeted and global assays and between APOE 22 and control plasma. CE species were quantified in Chapter 5 and oxPL species measured using a targeted assay in Chapter 4. n = 22, 39 and 39 for *APOE 22, control AND APOE 44*, respectively. The CE species not mentioned here were not reproducibly measurable in the global analysis. *FC = fold change calculated as APOE 22/control. †Ratio global:targeted calculated as FC global / FC targeted. ‡FC calculated as NPHSII/fresh. Ratio global:targeted calculated as global FC / targeted FC.

A comparison of trends in APOE 22 and control plasma using global and targeted methods

Species†	FC‡ global	FC targeted
TAG(36:0)	0.81	0.62
TAG(38:0)	0.97	0.59
TAG(40:0)	0.73	0.88
TAG(42:0)	0.72	1.01
TAG(44:0)	0.83	1.14
TAG(46:0)	1.03	1.36
TAG(48:1)	0.97	1.21
TAG(48:2)	0.89	1.06
TAG(50:1)	0.98	1.20*
TAG(50:2)	0.91	1.08
TAG(50:3)	0.88	0.97
TAG(50:4)	0.94	0.92
TAG(52:2)	0.90	1.02
TAG(52:3)	0.80	0.98
TAG(52:4)	0.81	0.91
TAG(52:5)	0.78	0.93
TAG(54:3)	0.89	1.00
TAG(54:4)	0.80	0.98
TAG(54:5)	0.72	0.95
TAG(54:6)	0.74	0.90
TAG(56:3)	0.88	1.29
TAG(56:4)	1.21	1.08
TAG(56:5)	0.90	1.10
TAG(56:6)	0.94	1.03

Table 6.3: A comparison of trends in APOE 22 and control plasma using global and targeted methods. The TAG species not mentioned here were not measurable in the global analysis. † Identifications from global analysis are putative and based on accurate m/z and RT, whilst targeted

identifications are confirmed by LC/MS/MS. ‡ FC = fold change calculated as APOE 22/control. * = p value < 0.05.

6.3.4 Conclusions

In conclusion, LC-MS/MS of NPHSII samples suggests the *APOE* alleles are associated with altered circulating cholesterol and CEs, but not TAGs. Cholesterol and CEs were reduced in both *APOE 22* and 44 in this subset of NPHSII data, but my data, combined with the literature, suggests control samples contain higher cholesterol and CEs than would be expected. Also, previous studies suggest that TAGs are higher in *APOE 44*. The lack of uniformity between the subset of NPHSII samples studied and published work is probably due to the unexpectedly high total cholesterol in low CVD-risk NPHSII samples. However, the data contained within this chapter has not furthered knowledge of how *APOE* allele affects LOAD risk.

Chapter 7: ApoE deficiency causes memory deficits and is associated with higher cortical oxPLs

7.1 12/15-lipoxygenase has been implicated in neurodegeneration

As discussed previously, the lipid-modulating enzyme 12/15-LOX has been implicated in LOAD (Section 1.3). Briefly, cell culture experiments suggest that pharmacological inhibition of 12/15-LOX in human cell lines reduces Aβ production and prevents apoptosis (Li et al., 1997, Succol and Pratico, 2007). Mouse models of AD demonstrate that reducing 12/15-LOX, either genetically or through a drug, reverses cognitive impairment and reduces amyloid and tau pathology (Yang et al., 2010, Chu et al., 2015, Di Meco et al., 2017). Lastly, 12/15-LOX and its enzyme products 12- and 15-HETE are increased in the brain of LOAD patients (Praticò et al., 2004, Yao et al., 2005).

Genetic deletion of *ApoE* is associated with neurodegeneration and working memory loss in male mice (Gordon et al., 1995, Masliah et al., 1995). To determine whether the absence of 12/15-LOX prevents this neurodegeneration, I compared four strains of knock out mice (WT, *ApoE* $^{-/-}$, *Alox12/15* $^{-/-}$, *ApoE* $^{-/-}$*/Alox12/15* $^{-/-}$ double knockouts) in two behavioural tests, then dissected brains into four regions and extracted lipids for analysis. Previous research, reviewed in Section 1.2.3, focused on male or female mice only, therefore I compared both male and female mice, to determine if gender modulates response to genetic deletion of either ApoE or 12/15-LOX.

Both behavioural tests rely on the natural inclination of a rodent to explore a novel object over a familiar one, as exploration gives a dopaminergic reward (Burke et al., 2010, Baxter, 2010, Bevins et al., 2002). The ability to recognise novel objects is called recognition memory and this form of memory is controlled primarily by the perirhinal cortex (Brown and Aggleton, 2001). There is no described deficit in recognition memory in *ApoE* $^{-/-}$ mice (Gordon et al., 1995, Masliah et al., 1995). To determine if this is the case in my mouse models, I used the "novel object test" to investigate recognition memory in *ApoE* $^{-/-}$, *Alox12/15* $^{-/-}$, and *ApoE* $^{-/-}$*/Alox12/15* $^{-/-}$ double knock-out mice (Antunes and Biala, 2012).

Recollection memory involves the hippocampus, as well as perirhinal cortex and medial prefrontal cortex (Barker and Warburton, 2015). Recollection memory is a slower form of memory which includes information about past events such as previous object placement (Brown and Aggleton, 2001). A deficit in recollection memory has been described in *ApoE* $^{-/-}$ mice, measured using the Morris Water Maze (MWM). Here, as an alternative approach I used the "object-in-place test" to determine if *ApoE*$^{-/-}$ mice demonstrate intact recollection memory (Gordon et al., 1995, Masliah et al., 1995, Lesburgueres et al., 2017).

7.1.2 Aims and hypotheses

After reading the literature, there are three unanswered questions I wanted to address. First, the effect of knockout of 12/15-LOX on recollection memory has not been studied. Second, whether the knockout of 12/15-LOX could rescue the recollection memory of *ApoE*$^{-/-}$ mice. The third question is whether free or esterified 12/15-LOX products are associated with performance in either the 'novel object' or 'object-in-place' tests.

My aims were as follows:

- To determine if deletion of 12/15-LOX can rescue cognitive deficit associated with ApoE$^{-/-}$
- To investigate the effect of gender on cognitive deficit and cognitive rescue in these strains
- To study the effect of *ApoE* $^{-/-}$, *Alox12/15* $^{-/-}$ and *ApoE* $^{-/-}$/*Alox12/15* $^{-/-}$ double knock out on brain content of oxPLs and eicosanoids using LC/MS-MS

My null hypotheses state that (i) 12/15-LOX deletion will not rescue cognitive deficit in an *ApoE* $^{-/-}$ mouse, and (ii) performance in memory tests will not be associated with levels of 12/15-LOX products.

7.2 Results

7.2.1 Behavioural tests identify a deficit in recollection memory in ApoE $^{-/-}$ mice

7.2.1.1 Genetic deletion of ApoE and 12/15-LOX does not affect performance in the novel object task

Mice were tested in the "novel object test" (Section 2.6.2), which measures ability to recognise a new object, versus those which have been seen before. Prior to testing, mice were acclimatised to an arena over the course of four days (Figure 7.1A). Mice were then tested over the next two days. Half the mice were tested first in the "novel object test", and the other half in the "object-in-place test" (Section 7.2.1.2). In the "novel object test", an animal is first acclimatised to an arena, and two objects, for two sets of 10 minutes. In the third, 'testing', phase, one of the objects has been replaced with a novel one, and the mouse is recorded for 10 minutes as it interacts with the objects (Figure 7.1B). Discrimination ratio was calculated as the time spent interacting with the novel object, as a percentage of total time interacting with objects. A discrimination ratio above 0.5 indicates that a mouse has spent more time with the novel object than the familiar one and is demonstrating recognition memory.

A two-way ANOVA did not find any statistical difference between wildtype and *ApoE*$^{-/-}$, *Alox12/15* $^{-/-}$, or *ApoE* $^{-/-}$/*Alox12/15* $^{-/-}$ double knock out animals in the novel object task, in that discrimination ratios were similar for all groups (Figure 7.2A). I chose to test both male and female mice, as gender in C57BL/6 (wildtype) mice can affect anxiety and exploratory behaviour, and previous explorations of *ApoE* knock out have used one gender only, or have not disclosed sex (An et al., 2011, Gordon et al., 1995, Masliah et al., 1995). Gender did not affect performance in the novel object class (Figure 7.2B).

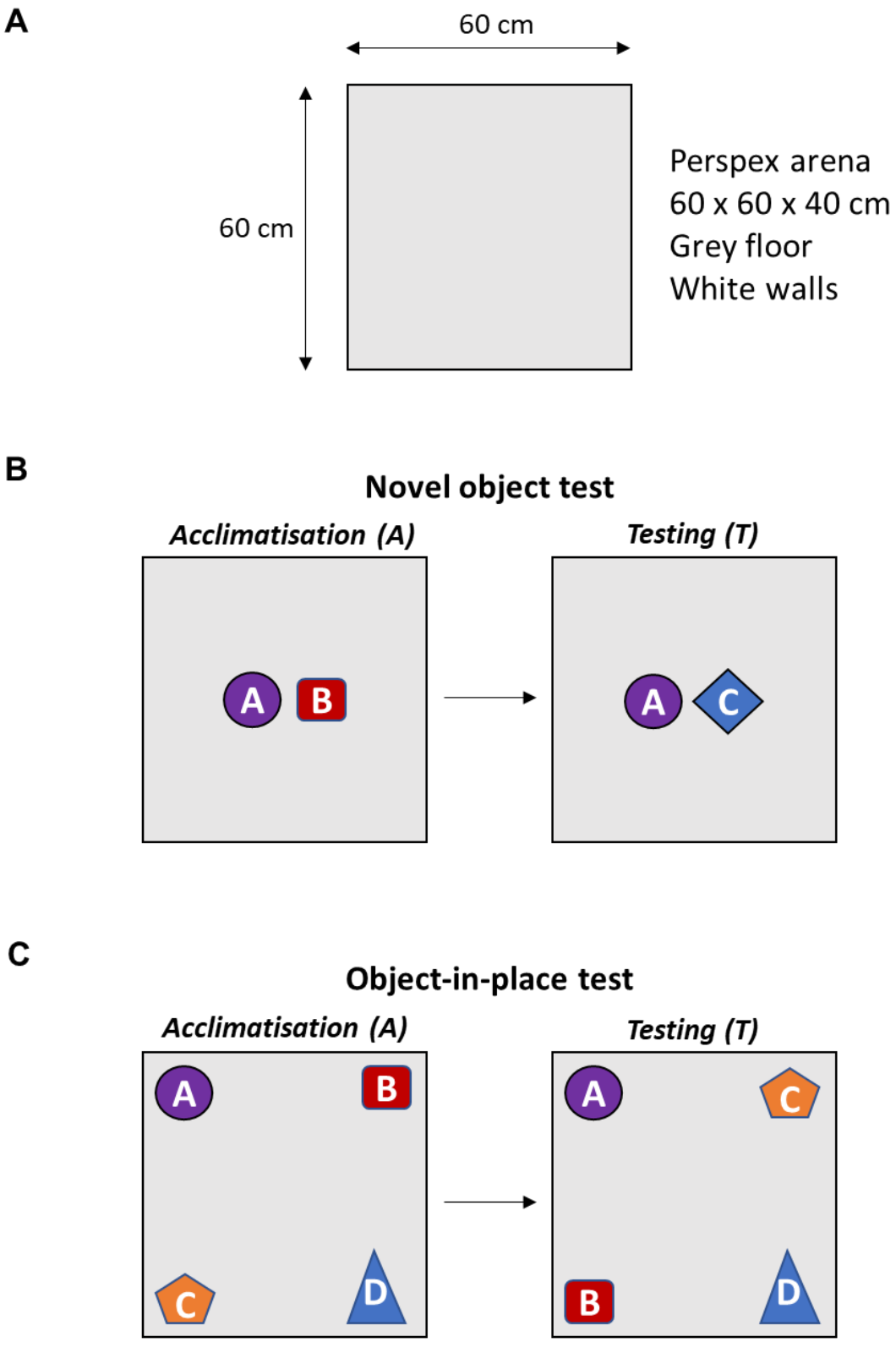

Figure 7.1: Arena arrangement during acclimatisation and behavioural testing of knock out mice using the novel object and object-in-place test. Control, *Apoe* $^{-/-}$, *Alox12/15* $^{-/-}$ and *ApoE*$^{-/-}$*/Alox12/15*$^{-/-}$ double knock out mice will be compared using the arena set up detailed above. **A.** Arena dimensions. **B.** Arena staging during acclimatisation and testing phases of the "novel object test". **C.** Arena staging during acclimatisation and testing phases of the "object-in-place test".

7.2.1.2 ApoE deficiency causes a deficit in recollection memory as measured by the object-in-place task

Mice were next tested in the "object-in-place test" (Section 2.6.3), which determines if mice spend more time with an object which has moved than one which has not, and therefore have recognised the movement. In the two 10 minute 'acclimatisation' periods, mice explore four objects in the corners of the arena (Figure 7.1C). In the videoed 'testing' phase, two objects are swopped diagonally. Discrimination ratio is calculated as the time spent interacting with the object which has moved position within the arena, as a percentage of total time interacting. A discrimination ratio above 0.5 indicates that a mouse has spent more time with the object which moved than the object which did not move and therefore is demonstrating recollection memory. A two-way ANOVA suggests that *ApoE* $^{-/-}$ mice perform statistically worse than wildtype, *Alox12/15* $^{-/-}$ and *ApoE* $^{-/-}$/*Alox12/15* $^{-/-}$ double knock out mice in the "object-in-place test" (Figure 7.3A). The *ApoE* $^{-/-}$/*Alox12/15* $^{-/-}$ double knock out mouse trends to a lower discrimination ratio than wildtype, but this is not statistically significant. It must be noted that there is a large amount of variability within the *ApoE* $^{-/-}$/*Alox12/15* $^{-/-}$ double knock out group. Males and females were compared using a two-way ANOVA and both with all genotypes together and genotypes separated (Figure 7.3B left and right panel). Whilst there is no statistical significance between the two genders, male *ApoE* $^{-/-}$ and *Alox12/15* $^{-/-}$ mice trend towards performing worse in the "object-in-place test" (Figure 7.3B right panel).

7.2.2 LC/MS-MS analysis of oxPLs, HETEs and HDOHEs suggests that these species are produced by non-enzymatic methods

7.2.2.1 LC/MS-MS analysis of oxPLs identifies two species increased in ApoE $^{-/-}$ *cortex*

Brains from mice tested previously were dissected into four regions: cerebellum, hippocampus, frontal cortex and cortex (Section 2.6.4.1). Lipids were extracted from brain regions and resuspended into methanol (Section 2.3.2). Human and murine 12/15-LOX enzymes yield a mixture of products from two substrates (Brash, 1999). The first

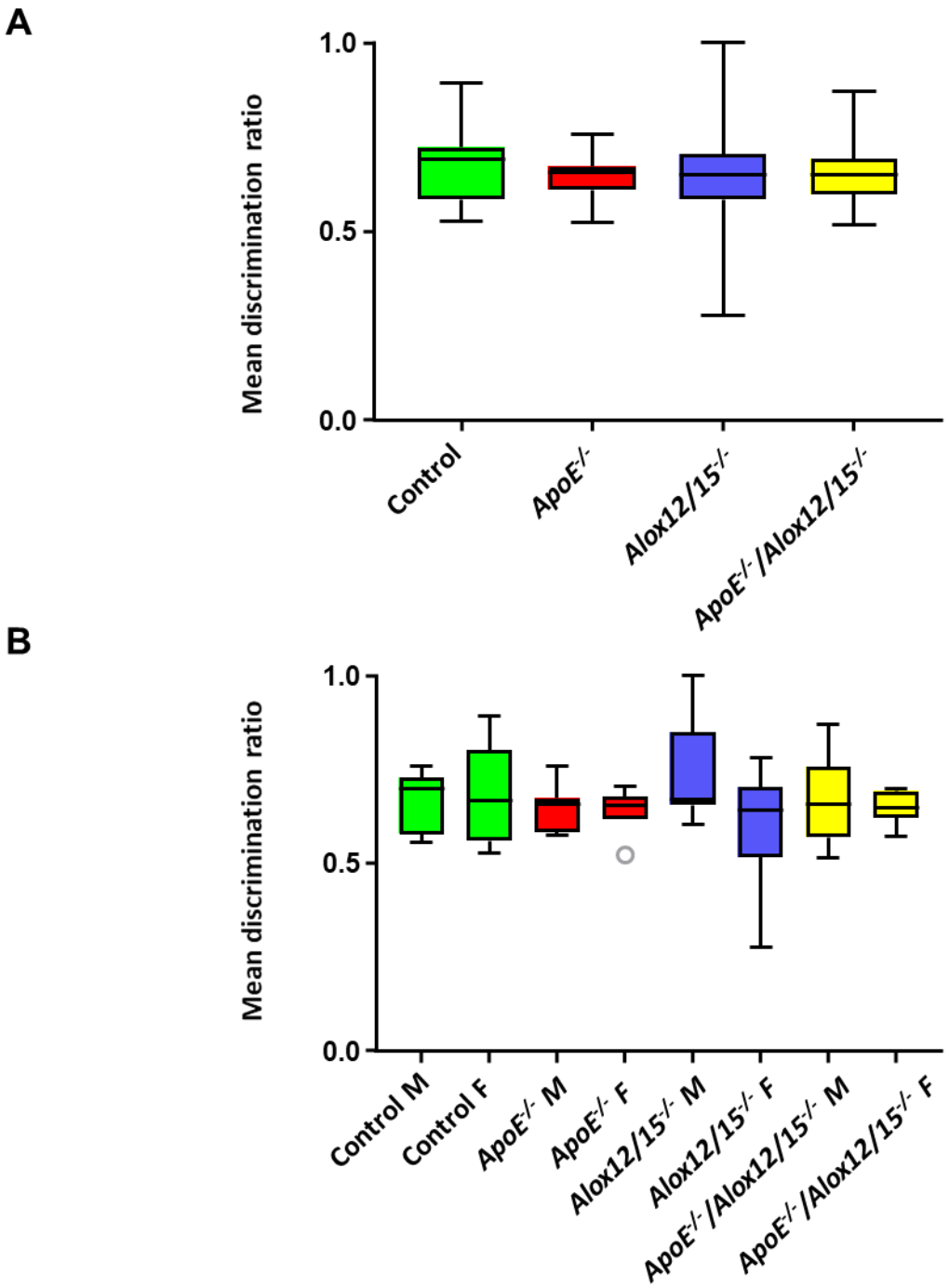

Figure 7.2: Discrimination ratios in the "novel object test" for control, *ApoE$^{-/-}$*, *Alox12/15$^{-/-}$* and *ApoE$^{-/-}$/Alox12/15$^{-/-}$* double knock out mice. A. Results according to genotype, with Tukey boxplots plotted with mean and SD (n = 20). **B.** Results according to genotype and gender (n = 10). Tested statistically using a two-way ANOVA. Lower fence of boxplots represent the data point which is the lowest value greater than the 25th percentile minus 1.5 times the IQR. The upper fence represents the data point which is the greatest value lower than the 75th percentile pus 1.5 times the IQR. * = $p < 0.05$, ** = $p < 0.01$, *** = $p < 0.001$.

substrate is arachidonic acid (AA, m/z 319.2) Human and murine 12-LOX produce only 12-HETE (Brash, 1999). 15-LOX in humans generates mainly 15-HETE, and in mice predominantly 12-HETE, and some 15-HETE (Chen et al., 1994). The second substrate I will be considering is docosahexaenoic acid (DHA, m/z 343.2). DHA has a similar carbon chain arrangement to AA, as both are polyunsaturated, with carbon chains of 20 or more. Human 12-LOX can produce select HDOHEs when incubated with DHA (Aveldaño and Sprecher, 1983). 12/15-LOX products such as 12-HETE and 11-HDOHE were quantified, as well as other HETEs and HDOHEs and some esterified LOX products esterified to GPs (Carrié et al., 2000). A panel of oxPLs containing 12/15-LOX products was identified from the literature, and of these, 5 were found in preliminary analysis of brain samples using LC/MS-MS (Bascoul-Colombo et al., 2016). These 5 oxPLs were analysed using a targeted LC/MS-MS method (Section 2.4.3). Nomenclature describes oxPLs with first their parent mass, and then the mass of the daughter ion. 319.2 is an oxidised HETE fragment, and 343.2 an oxidised HDOHE fragment. Data was normalised to the standard, then means for each genotype were compared using a two-way ANOVA (Section 2.4.3). There is no downregulation of oxPLs in *Alox12/15* $^{-/-}$ compared to WT. In the cerebellum and hippocampus, none of the five oxPL species monitored differ between genotypes (Figure 7.4, Figure 7.5). In the frontal cortex, 782.2/319.2 and 810.7/319.2 are significantly higher in *ApoE*$^{-/-}$ than *Alox12/15* $^{-/-}$ (Figure 7.6). In the cortex, 782.2/319.2 is significantly higher in *ApoE*$^{-/-}$ than wildtype or *Alox12/15* $^{-/-}$ (Figure 7.7). Also, 810.7/319.2 and 834.7/343.2 are significantly higher in *ApoE*$^{-/-}$ than *Alox12/15*. Some oxPL masses could be several GPs, or a mix of thereof. Others have been putatively identified but these identifications must be validated. Possible identifications for 782.2/319.2 are PC(O-20:4_11:0) or PE(O-20:4_14:0). 788.6/343.3 may be PA(O-22:6_20:2). 808.7/319.2 is a possible oxPLs as it elutes with oxPLs, has a similar parent mass, and contains the oxidised HETE fragment. 810.7/319.2 could be PC(O-20:4_17:0), PE(O-20:4_20:0) or PS(20:4_13:1). 834.7/343.2 could be PC(O-22:6_13:0) or PE(O-22:6_20:0).To summarise, some oxPLs in the frontal cortex and cortex are significantly higher in *ApoE*$^{-/-}$ mice. Further LC/MS-MS analysis is needed to confirm the identities of these three oxPLs.

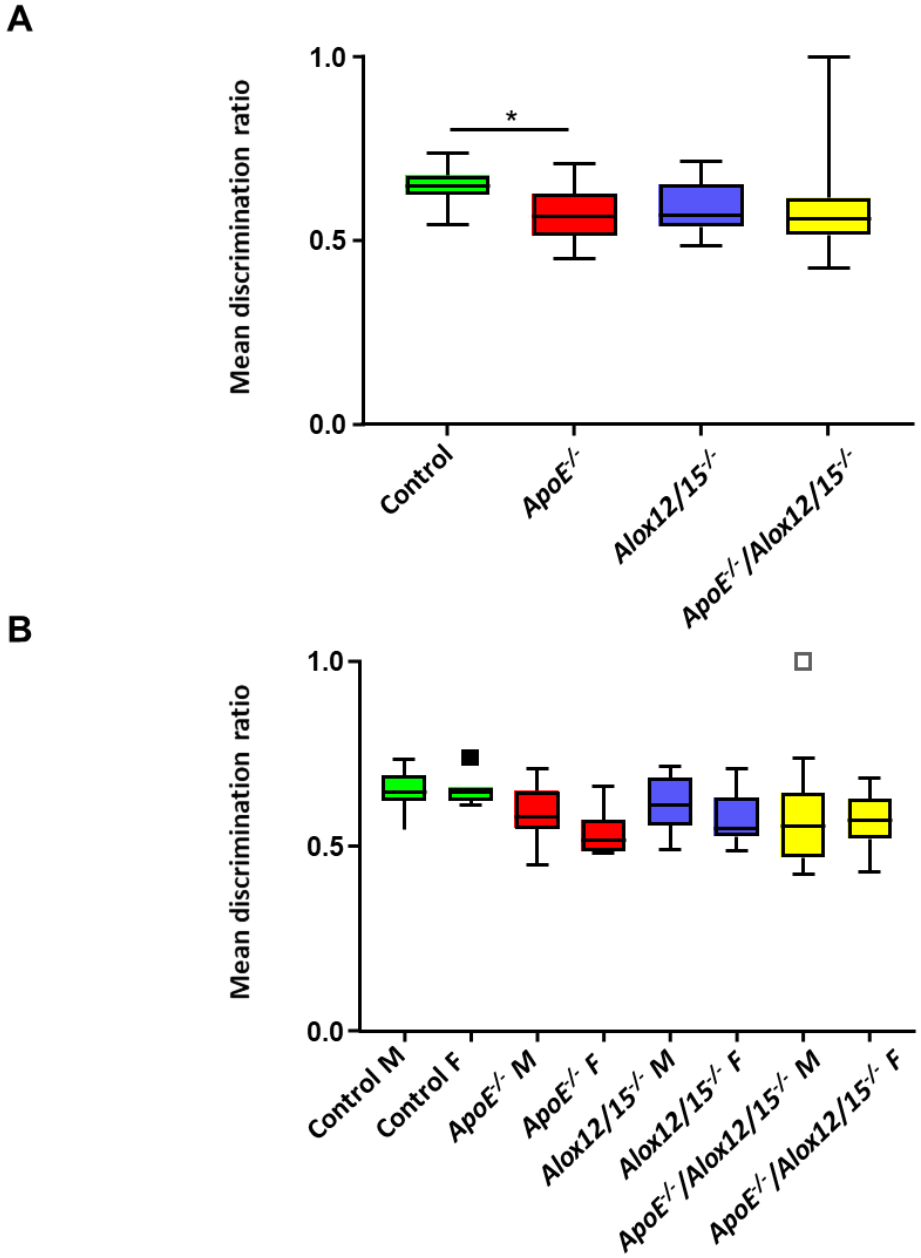

Figure 7.3: Discrimination ratios in the "object-in-place test" for control, *ApoE*$^{-/-}$, *Alox12/15*$^{-/-}$ and *ApoE*$^{-/-}$*/Alox12/15*$^{-/-}$ double knock out mice. A. Results according to genotype, with Tukey boxplots plotted with mean and SD (n = 20). **B.** Results according to genotype and gender (n = 10). Tested statistically using a two-way ANOVA. Lower fence of boxplots represent the data point which is the lowest value greater than the 25th percentile minus 1.5 times the IQR. The upper fence represents the data point which is the greatest value lower than the 75th percentile pus 1.5 times the IQR. * = $p < 0.05$, ** = $p < 0.01$, *** = $p < 0.001$.

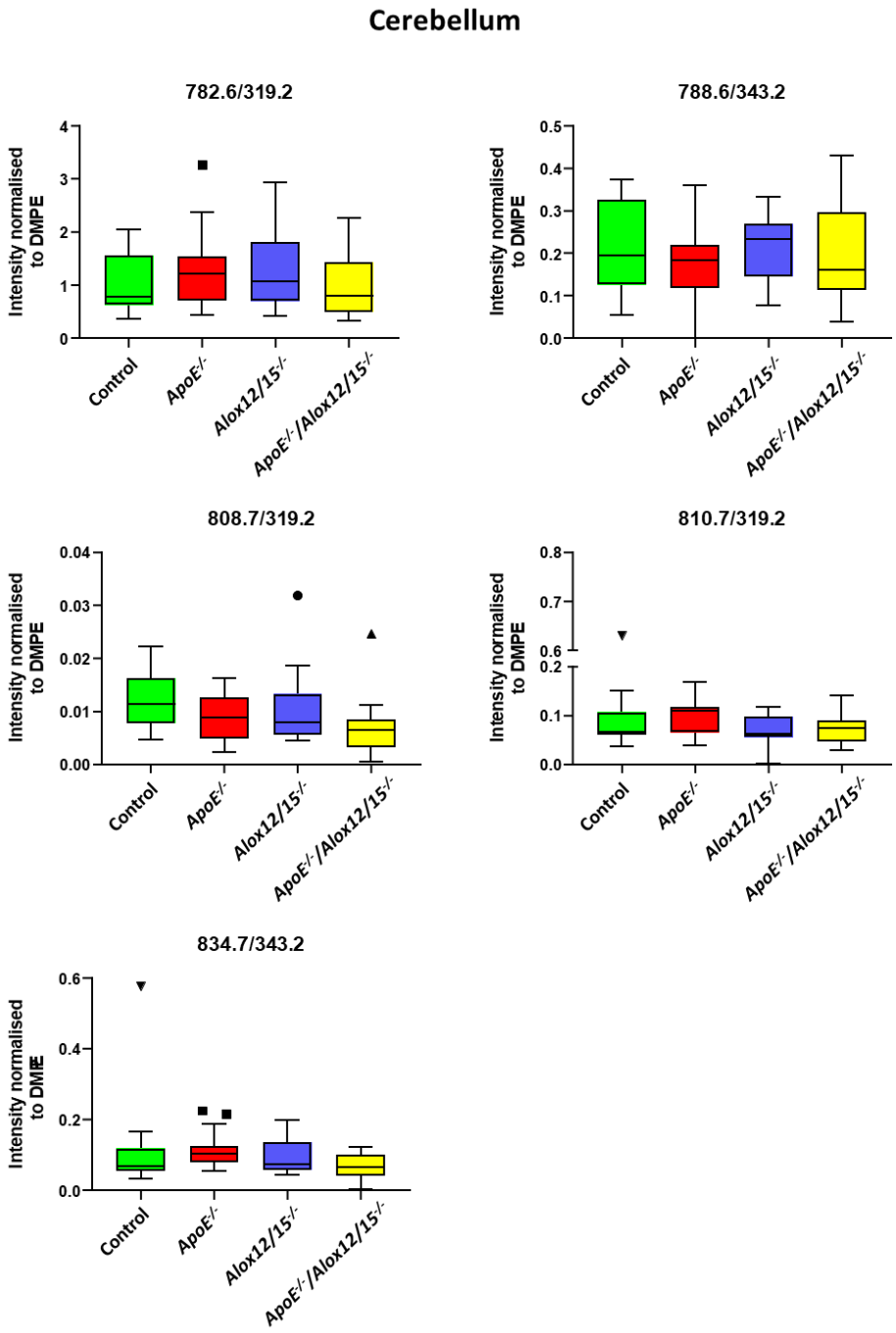

Figure 7.4: Select oxPLs in the cerebellum in control, *ApoE*$^{-/-}$, *Alox12/15*$^{-/-}$ and *ApoE*$^{-/-}$*/Alox12/15*$^{-/-}$ double knock out mice. OxPLs were normalised to DMPE and visualised in Tukey boxplots (n = 8). Data was tested statistically using a two-way ANOVA. Some oxPL masses could be several GPs, or a mix of thereof. Others have been putatively identified but these identifications must be validated. Possible identifications for 782.2/319.2 are PC(O-20:4_11:0) or PE(O-20:4_14:0). 788.6/343.3 may be PA(O-22:6_20:2). 808.7/319.2 is a possible oxPLs as it elutes with oxPLs, has a similar parent mass, and contains the oxidised HETE fragment. 810.7/319.2 could be PC(O-20:4_17:0), PE(O-20:4_20:0) or PS(20:4_13:1). 834.7/343.2 could be PC(O-22:6_13:0) or PE(O-22:6_20:0). Lower fence of boxplots represent the data point which is the lowest value greater than the 25th percentile minus 1.5 times the IQR. The upper fence represents the data point which is the greatest value lower than the 75th percentile pus 1.5 times the IQR. * = $p < 0.05$, ** = $p < 0.01$, *** = $p < 0.001$.

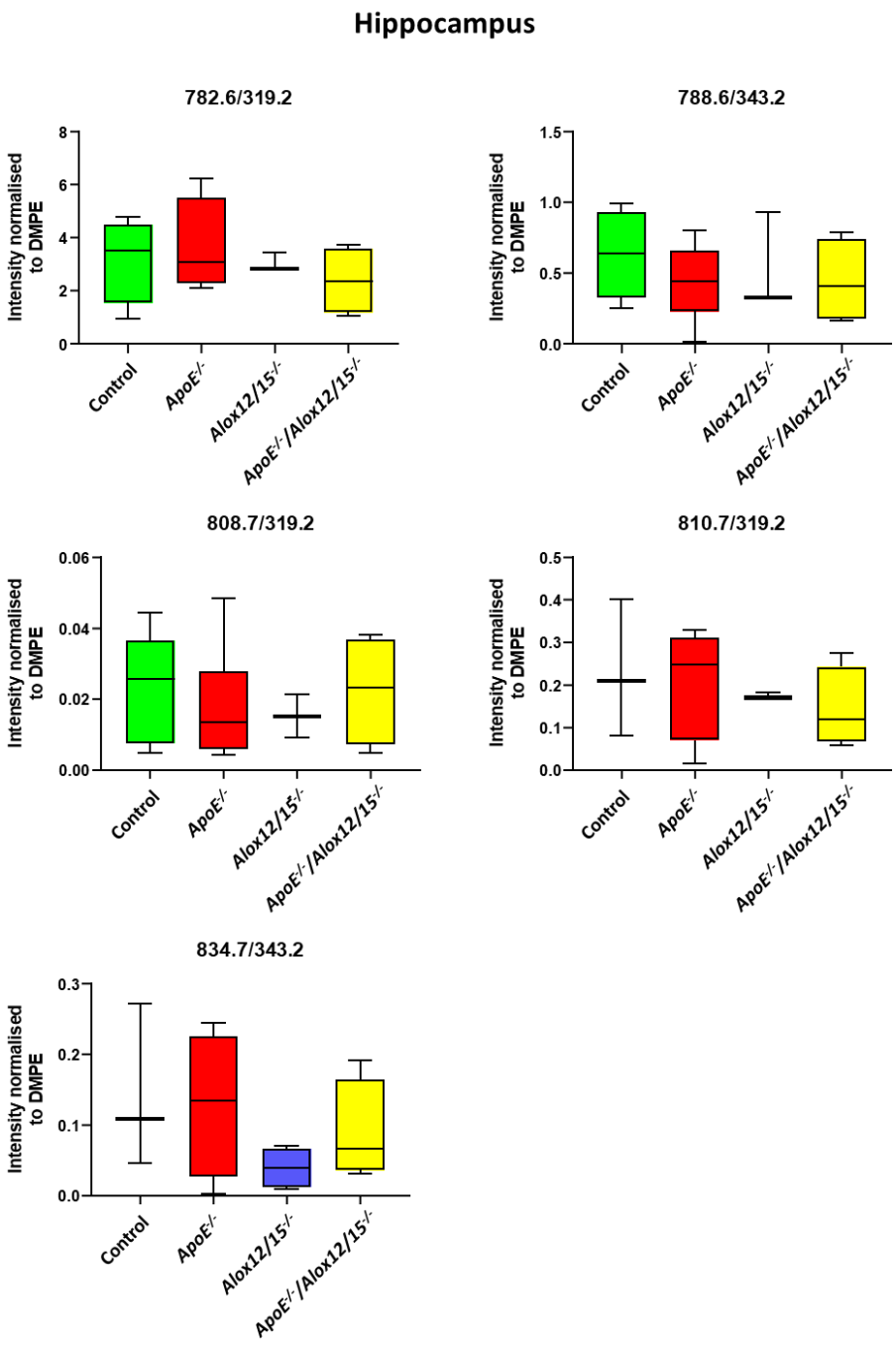

Figure 7.5: Select oxPLs in the hippocampus in control, *ApoE*$^{-/-}$, *Alox12/15*$^{-/-}$ and *ApoE*$^{-/-}$*/Alox12/15*$^{-/-}$ double knock out mice. OxPLs were normalised to DMPE and visualised in Tukey boxplots (n = 8). Some oxPL masses could be several GPs, or a mix of thereof. Others have been putatively identified but these identifications must be validated. Possible identifications for 782.2/319.2 are PC(O-20:4_11:0) or PE(O-20:4_14:0). 788.6/343.3 may be PA(O-22:6_20:2). 808.7/319.2 is a possible oxPLs as it elutes with oxPLs, has a similar parent mass, and contains the oxidised HETE fragment. 810.7/319.2 could be PC(O-20:4_17:0), PE(O-20:4_20:0) or PS(20:4_13:1). 834.7/343.2 could be PC(O-22:6_13:0) or PE(O-22:6_20:0).Data was tested statistically using a two-way ANOVA. Lower fence of boxplots represent the data point which is the lowest value greater than the 25th percentile minus 1.5 times the IQR. The upper fence represents the data point which is the greatest value lower than the 75th percentile pus 1.5 times the IQR. * = $p < 0.05$, ** = $p < 0.01$, *** = $p < 0.001$.

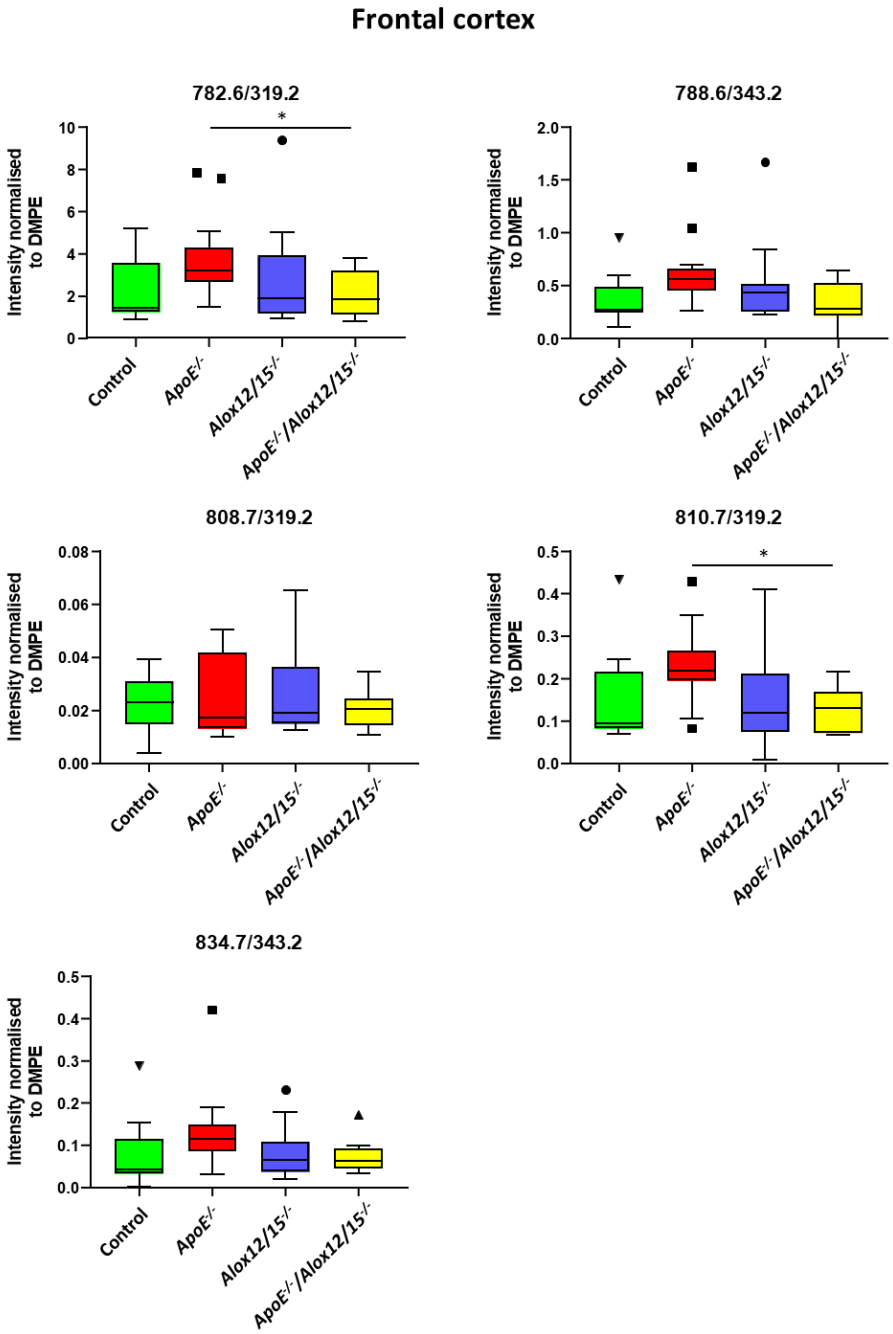

Figure 7.6: Select oxPLs in the frontal cortex in control, *ApoE*$^{-/-}$, *Alox12/15*$^{-/-}$ and *ApoE*$^{-/-}$*/Alox12/15*$^{-/-}$ double knock out mice. OxPLs were normalised to DMPE and visualised in Tukey boxplots (n = 8). Data was tested statistically using a two-way ANOVA. Some oxPL masses could be several GPs, or a mix of thereof. Others have been putatively identified but these identifications must be validated. Possible identifications for 782.2/319.2 are PC(O-20:4_11:0) or PE(O-20:4_14:0). 788.6/343.3 may be PA(O-22:6_20:2). 808.7/319.2 is a possible oxPLs as it elutes with oxPLs, has a similar parent mass, and contains the oxidised HETE fragment. 810.7/319.2 could be PC(O-20:4_17:0), PE(O-20:4_20:0) or PS(20:4_13:1). 834.7/343.2 could be PC(O-22:6_13:0) or PE(O-22:6_20:0).Lower fence of boxplots represent the data point which is the lowest value greater than the 25th percentile minus 1.5 times the IQR. The upper fence represents the data point which is the greatest value lower than the 75th percentile pus 1.5 times the IQR. * = $p < 0.05$, ** = $p < 0.01$, *** = $p < 0.001$.

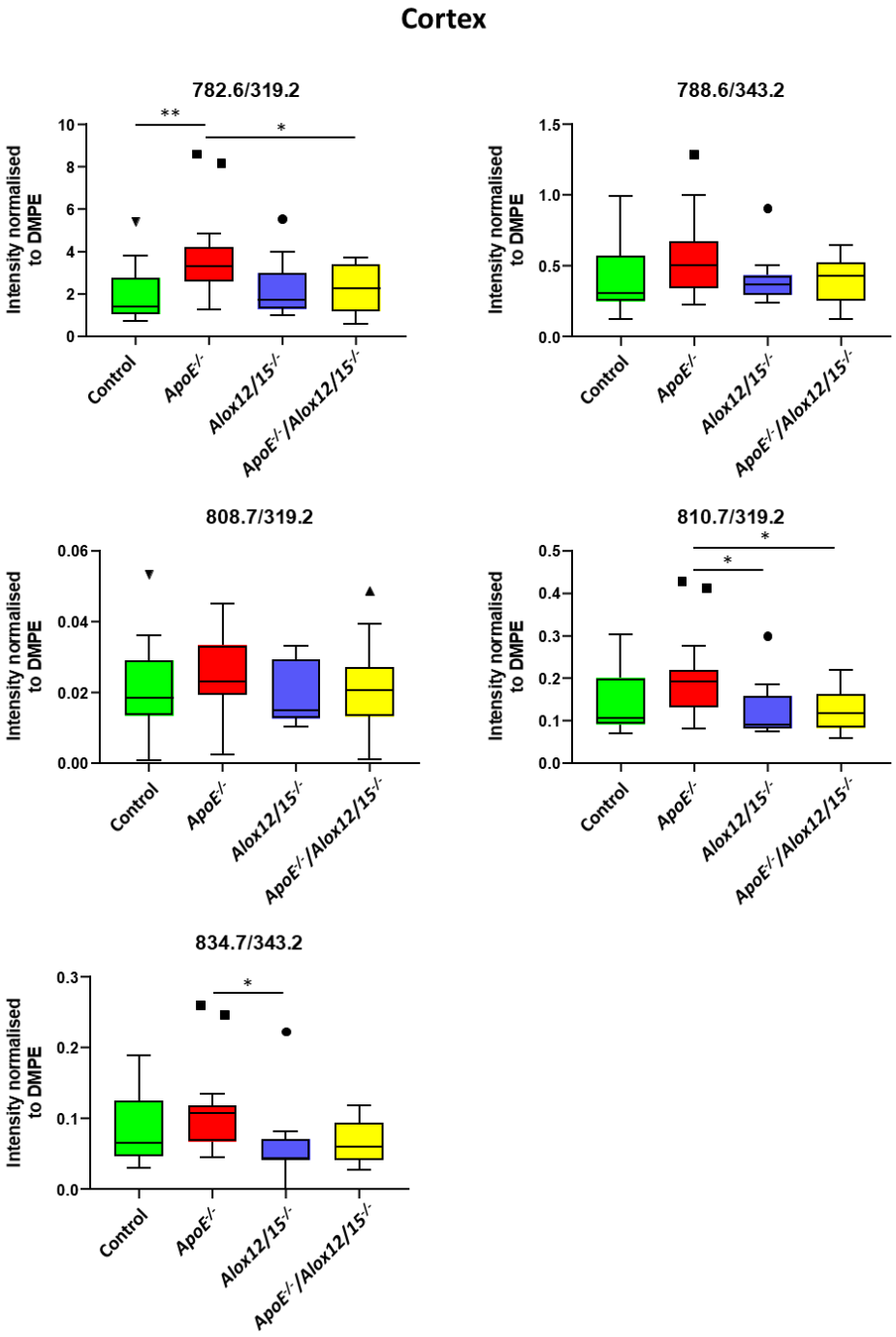

Figure 7.7: Select oxPLs in the cerebellum in control, *ApoE$^{-/-}$*, *Alox12/15$^{-/-}$* and *ApoE$^{-/-}$/Alox12/15$^{-/-}$* double knock out mice. OxPLs were normalised to DMPE and visualised in Tukey boxplots (n = 8). Data was tested statistically using a two-way ANOVA. Some oxPL masses could be several GPs, or a mix of thereof. Others have been putatively identified but these identifications must be validated. Possible identifications for 782.2/319.2 are PC(O-20:4_11:0) or PE(O-20:4_14:0). 788.6/343.3 may be PA(O-22:6_20:2). 808.7/319.2 is a possible oxPLs as it elutes with oxPLs, has a similar parent mass, and contains the oxidised HETE fragment. 810.7/319.2 could be PC(O-20:4_17:0), PE(O-20:4_20:0) or PS(20:4_13:1). 834.7/343.2 could be PC(O-22:6_13:0) or PE(O-22:6_20:0).Lower fence of boxplots represent the data point which is the lowest value greater than the 25th percentile minus 1.5 times the IQR. The upper fence represents the data point which is the greatest value lower than the 75th percentile pus 1.5 times the IQR. * = $p < 0.05$, ** = $p < 0.01$, *** = $p < 0.001$.

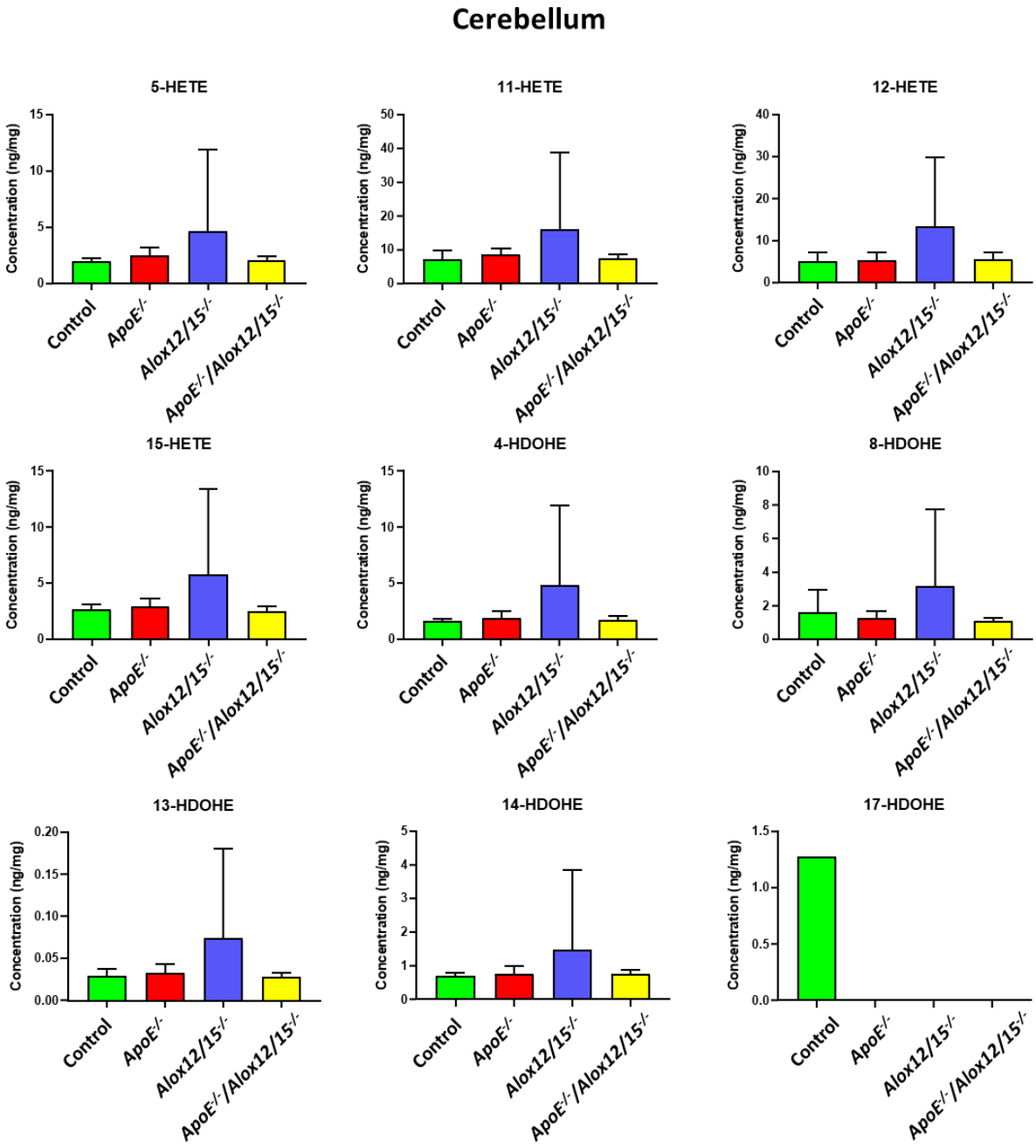

Figure 7.8: HETEs and HDOHEs in cerebellum in control, *ApoE*$^{-/-}$, *Alox12/15*$^{-/-}$ and *ApoE*$^{-/-}$*/Alox12/15*$^{-/-}$ double knock out mice. HETEs and HDOHEs were quantified using an internal standard and curve of known concentrations, and visualised in histograms, where error bars represent standard deviation (n = 3/4). Data was tested statistically using a two-way ANOVA. * = $p < 0.05$, ** = $p < 0.01$, *** = $p < 0.001$.

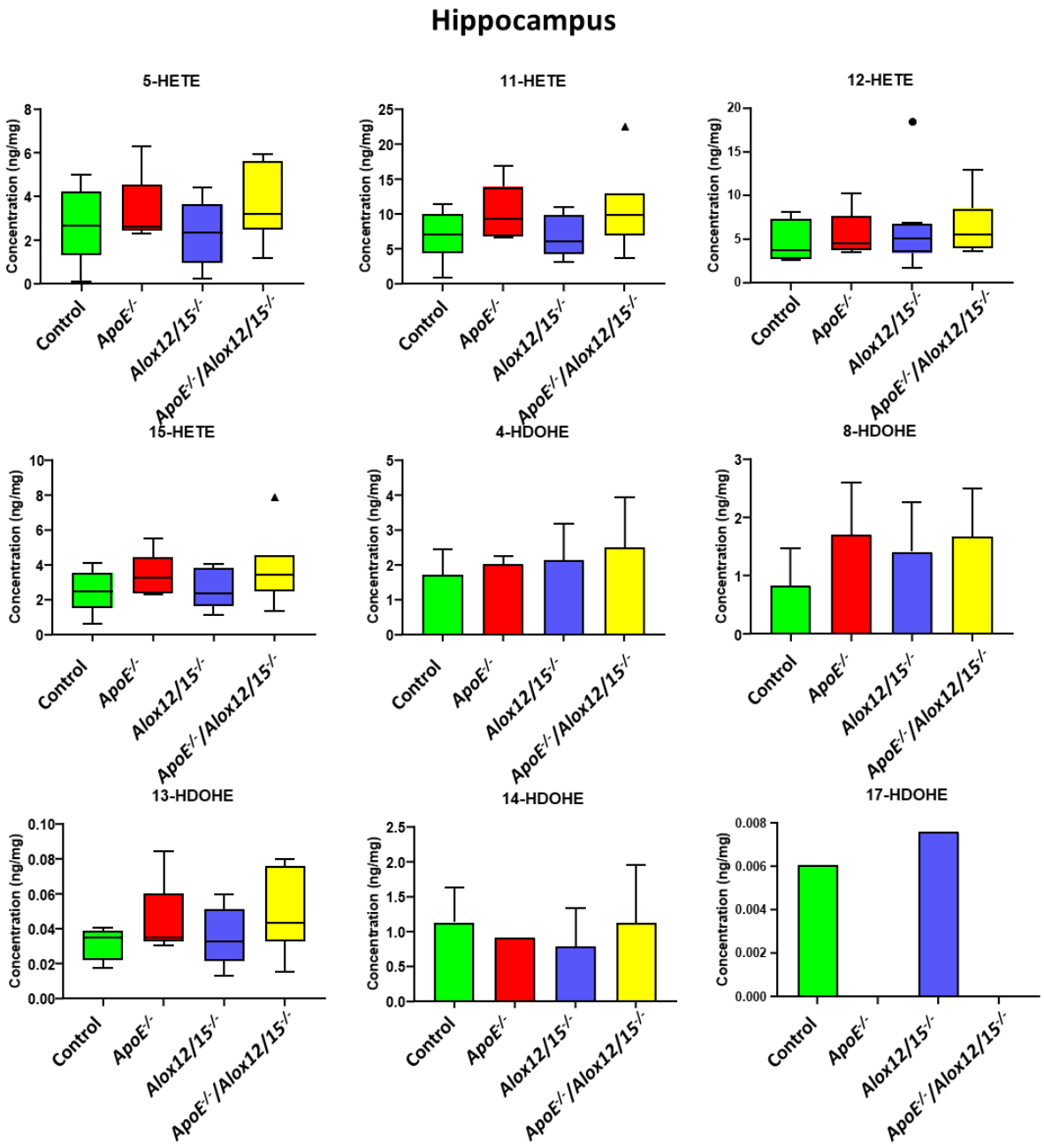

Figure 7.9: HETEs and HDOHEs in hippocampus in control, *ApoE*$^{-/-}$, *Alox12/15*$^{-/-}$ and *ApoE*$^{-/-}$*/Alox12/15*$^{-/-}$ double knock out mice. HETEs and HDOHEs were quantified using an internal standard and curve of known concentrations, and visualised in histograms, where error bars represent standard deviation (n = 3/4). Data was tested statistically using a two-way ANOVA. Lower fence of boxplots represent the data point which is the lowest value greater than the 25th percentile minus 1.5 times the IQR. The upper fence represents the data point which is the greatest value lower than the 75th percentile pus 1.5 times the IQR. * = $p < 0.05$, ** = $p < 0.01$, *** = $p < 0.001$.

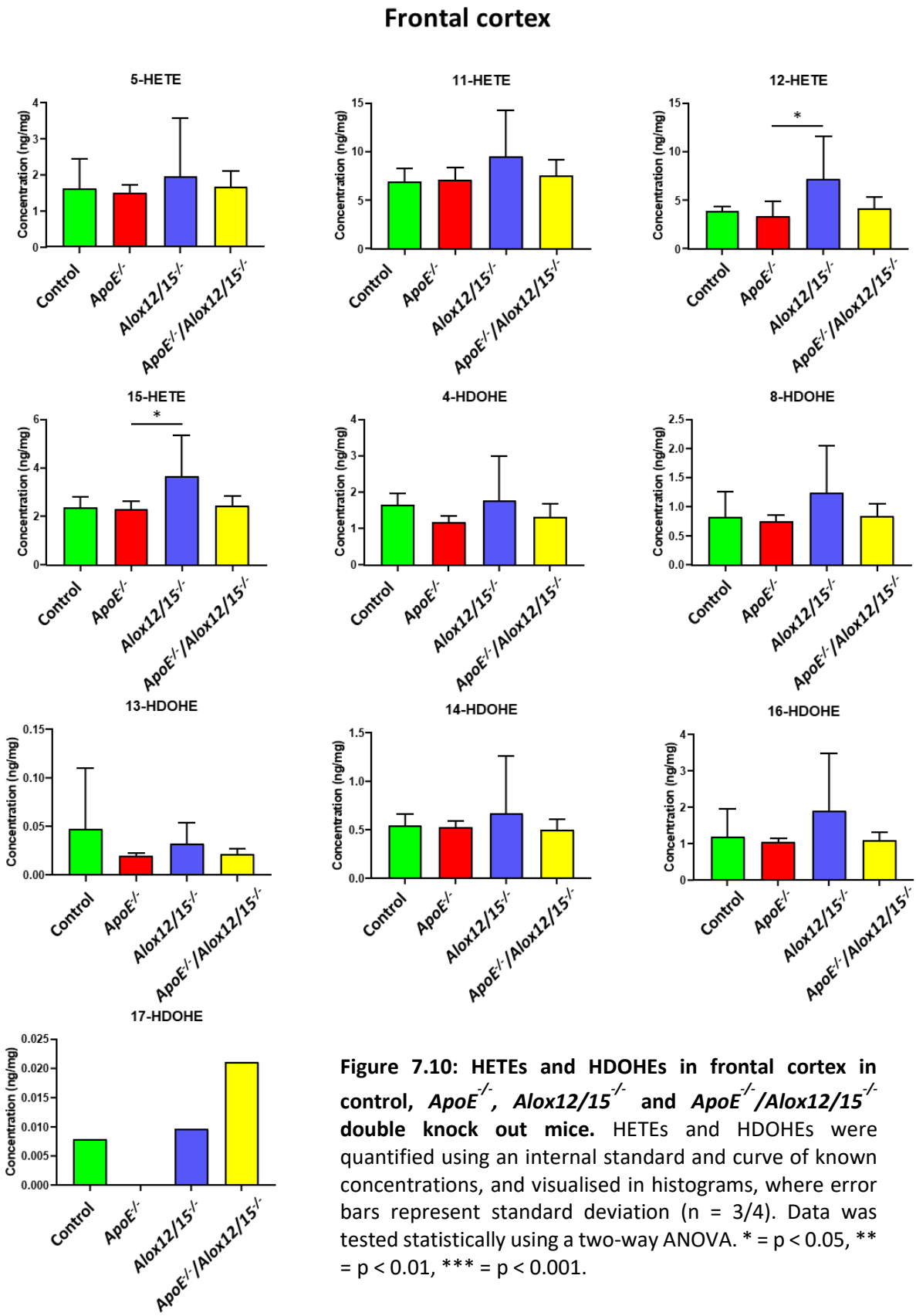

Figure 7.10: HETEs and HDOHEs in frontal cortex in control, *ApoE*$^{-/-}$, *Alox12/15*$^{-/-}$ and *ApoE*$^{-/-}$*/Alox12/15*$^{-/-}$ double knock out mice. HETEs and HDOHEs were quantified using an internal standard and curve of known concentrations, and visualised in histograms, where error bars represent standard deviation (n = 3/4). Data was tested statistically using a two-way ANOVA. * = $p < 0.05$, ** = $p < 0.01$, *** = $p < 0.001$.

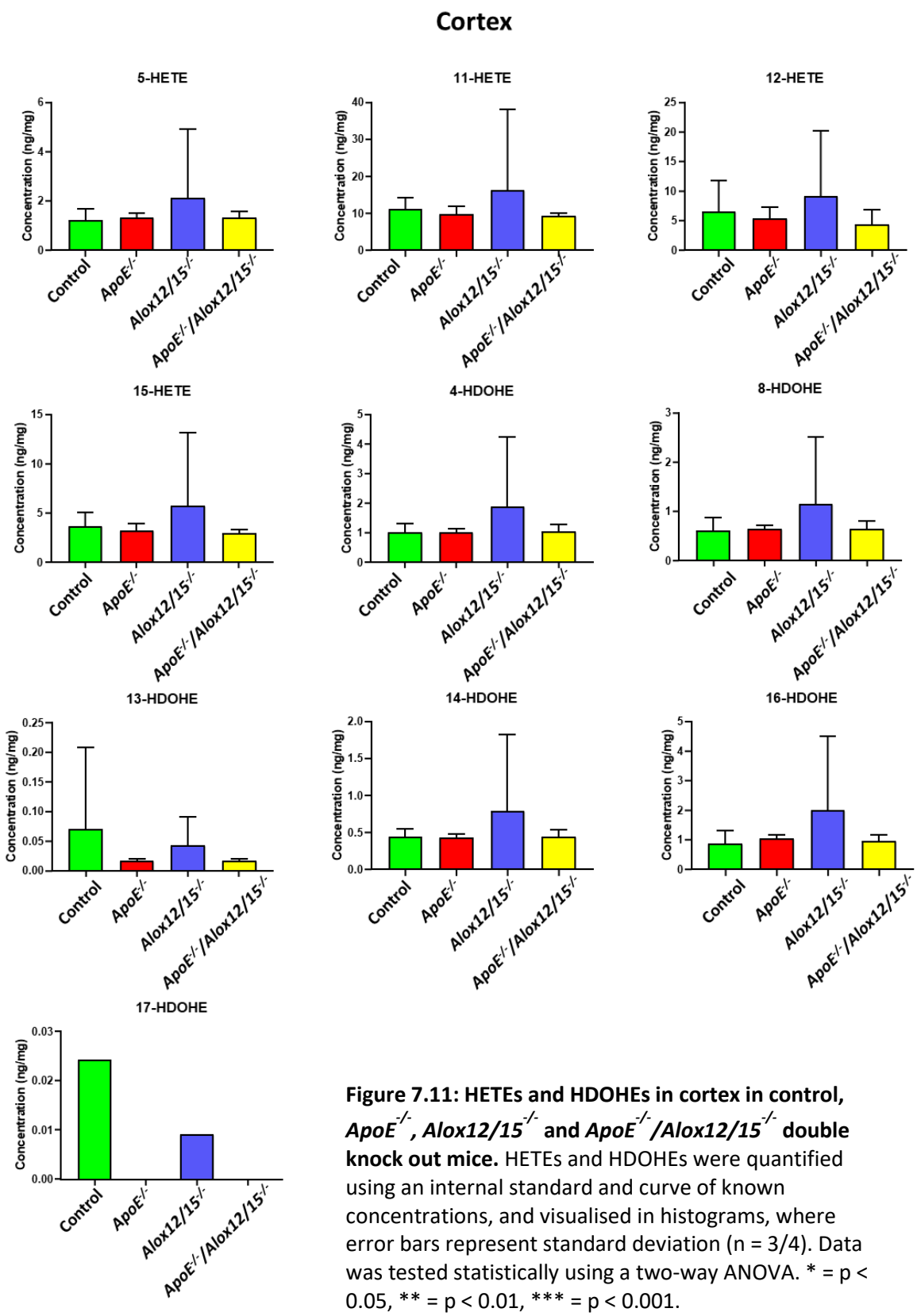

Figure 7.11: HETEs and HDOHEs in cortex in control, *ApoE*$^{-/-}$, *Alox12/15*$^{-/-}$ and *ApoE*$^{-/-}$*/Alox12/15*$^{-/-}$ double knock out mice. HETEs and HDOHEs were quantified using an internal standard and curve of known concentrations, and visualised in histograms, where error bars represent standard deviation (n = 3/4). Data was tested statistically using a two-way ANOVA. * = $p < 0.05$, ** = $p < 0.01$, *** = $p < 0.001$.

7.2.2.2 HETE and HDOHE content in the brain is not produced by 12/15-LOX

Eicosanoids in the same brain regions as above were quantified using LC/MS-MS and a standard curve (Section 2.4.4). Average values for each genotype were compared using a two-way ANOVA. Total eicosanoid content was calculated as ng per mg brain tissue. In all regions, HETEs and HDOHEs do not significantly differ between WT or *ApoE*$^{-/-}$, *Alox12/15* $^{-/-}$ and *Apoe* $^{-/-}$/*Alox12/15* $^{-/-}$ double knock out mice (Figure 7.8, Figure 7.9, Figure 7.10, Figure 7.11). In frontal cortex, 12-HETE and 15-HETE are significantly higher in *Alox12/15*$^{-/-}$ than ApoE$^{-/-}$ (Figure 7.10). Taken together, these data indicate that there is no net downregulation of the LOX products measured (oxPLs, HETEs and HDOHEs) in *Alox12/15* $^{-/-}$, and therefore these species are produced by another source.

7.3 Discussion

7.3.1 Genetic deletion of *ApoE* causes an impairment in recollection memory

N numbers decreased throughout the chapter as several mice were excluded from testing or lipid analysis due to illness. Rather than a side effect of testing, these stroke-like episodes were more likely due to the high risk of cardiovascular disease in *ApoE*$^{-/-}$ mice (Lo Sasso et al., 2016).

ApoE$^{-/-}$ mice have select hippocampal and cortical neurodegeneration but don't demonstrate any deficit in recognition memory (Gordon et al., 1995, Masliah et al., 1995). My data also demonstrates that *ApoE*$^{-/-}$ mice are not impaired when examined by the "novel object test" (Figure 7.2). The "novel object test" is a investigation of recognition memory, the ability to perceive a new object. The results of the "novel object test" indicate that (i) ApoE deficiency does not cause a deficit in recognition memory, (ii) 12/15-LOX deficiency does not cause a deficit in recognition memory, and (iii) gender does not affect recognition memory. Other research has previously suggested that a deficiency in ApoE does not cause an impairment in recognition memory (Gordon et al., 1995, Masliah et al., 1995). However, to my knowledge this is the first time that 12/15-LOX deficiency has been studied using the "novel object test".

Data from the "object-in-place test" demonstrates that ApoE supports spatial memory, in accordance with my first hypothesis, as *ApoE*$^{-/-}$ mice perform significantly worse than control (Figure 7.3). This is in line with other research, which has demonstrated deficits in recollection memory in *ApoE*$^{-/-}$ through the MWM (Gordon et al., 1995, Oitzl et al., 1997). Memory impairment is associated with a loss in synapse density in *ApoE* $^{-/-}$ hippocampus and neocortex (Masliah et al., 1995). This could be explained by a possible role for ApoE in long-term potentiation (LTP), the process through which synapses are strengthened through activity. LTP in the hippocampus has been implicated in recollection memory (Bliss and Lomo, 1973, Izquierdo et al., 2008). LTP is reduced in the hippocampus of *ApoE* $^{-/-}$ mice, and a decrease in LTP could cause the reduction in synapse density in the hippocampus and cortex of the *ApoE*$^{-/-}$ mice described in other research (Veinbergs et al., 1998, Masliah et al., 1995).

Data from the "object-in-place test" suggests that 12/15-LOX deletion could prevent neurodegeneration caused by *ApoE* $^{-/-}$, as the *ApoE*$^{-/-}$*/Alox12/15*$^{-/-}$ double knock out does not demonstrate an impairment in the "object-in-place test" (Figure 7.3). However, one *ApoE*$^{-/-}$*/Alox12/15*$^{-/-}$ double knock out female has a much higher discrimination ratio than all the other animals. Mean discrimination ratio for *ApoE*$^{-/-}$*/Alox12/15*$^{-/-}$ double knock out mice is similar to that of *ApoE*$^{-/-}$ mice, and the range of the *ApoE*$^{-/-}$*/Alox12/15*$^{-/-}$ double knock out data is large. Therefore, I want to repeat this experiment before drawing any concrete conclusions. Gender does not appear to influence performance in the "object-in-place test".

Nonetheless, I will the discuss the implications herein. Previous research has demonstrated that 12/15-LOX could be implicated in Alzheimer's disease. Studies have suggested 12/15-LOX deficiency prevents neurodegeneration in Alzheimer's disease mouse models (Yang et al., 2010, Di Meco et al., 2017). Also, 12/15-LOX, 12-HETE and 15-HETE are upregulated in post-mortem LOAD brain samples (Praticò et al., 2004, Yao et al., 2005). 12/15-LOX may be interacting with a neuropathology like amyloid or tau pathology (Sections 1.1.1-1.1.2). Pharmacological or genetic blockade of 12/15-LOX reduces or prevents both amyloid and tau pathology in two genetic models of Alzheimer's disease (Yang et al., 2010, Di Meco et al., 2017). However, neither amyloid or tau pathology is present in the *ApoE*$^{-/-}$ mouse, suggesting

a role for 12/15-LOX in neurodegeneration, which is separate to the amyloid and tau pathways.

Modelling oxidative stress in neural and oligodendrocyte cell culture implicates 12/15-LOX as an intermediary in cell death (Wang et al., 2004, Pallast et al., 2009). Also, indicators of both lipid peroxidation and protein oxidation are lower in brain samples from the *ApoE*$^{-/-}$ /*Alox12/15*$^{-/-}$ mouse when compared to *ApoE*$^{-/-}$ (Chinnici et al., 2005). Together, these studies suggest that 12/15-LOX deficiency may be protective against oxidative stress-mediated cell death. The improved performance of *Alox12/15*$^{-/-}$mice in the "object-in-place test" could be caused by a reduction in oxidation stress within the brain, although further work would be needed to test this assumption (Figure 7.3).

7.3.2 LC/MS-MS analysis of LOX products indicates that 12/15-LOX is not the source of oxPLs, HETEs and HDOHEs

12-HETE, 15-HETE, 11-HDOHE and 14-HDOHE and oxPLs are not downregulated in *Alox12/15* $^{-/-}$ animals, suggesting these species are not being produced by 12/15-LOX in the mouse brain, and must originate from other sources. 12- AND 15-HPETE, the reactive intermediaries in producing 12- and 15-HETE, can be made by cyclooxygenase (COX) enzymes (Adesuyi et al., 1985). Thus, the presence of possible 12/15-LOX products in the *12/15-LOX*$^{-/-}$ mouse and other strains could due to cyclooxygenase activity. It cannot be discounted that some autoxidation of the samples occurred during extraction, however, this would not account for differences between genotypes.

HETEs and HDOHEs did not differ in *ApoE*$^{-/-}$ animals compared to other groups. However, three oxPLs, containing either AA or DHA, were higher in *ApoE*$^{-/-}$ frontal cortex and cortex (Figures 7.6 and 7.7). Although specific functions for 782.6/319.2, 810.2/319.2 and 834.2/343.2 are not known, oxPLs are biologically active species, and phospholipid oxidation could play a role in membrane permeability (Bochkov et al., 2017, Manni et al., 2018).

7.3.3 Conclusions

Deficiency in ApoE leads to an impairment in murine recollection memory, however (i) this impairment is not prevented by ablation of 12/15-LOX and (ii) this impairment does not correlate with levels of HETEs or HDOHEs. HETEs, HDOHEs and oxPLs in the brain do not appear to originate from 12/15-LOX. Three oxPLs are increased in cortex in *ApoE*$^{-/-}$ and correlate with recollection memory. The carbon chain arrangement of these species must be established.

Chapter 8 – Discussion

In this thesis, I used LC-MS and LC-MS/MS to investigate the human plasma lipidome of *APOE* homozygotes, as well as performing targeted analyses of brain samples from *ApoE*$^{-/-}$ mice. Below, I summarise my key findings, and discuss how they relate to the literature.

8.1 The LC-MS and LC-MS/MS methods used within are reliable and reproducible

A variety of lipid extraction techniques are used within the literature. Some choose to extract lipids according to category, for example, over 500 lipids were described using LC/MS-MS after targeted extractions for each lipid category (Quehenberger et al., 2010). Others suggest a single extraction, using chloroform/methanol or hexane/IPA (Bligh and Dyer, 1959, Hara and Radin, 1978). The LC-MS and LC-MS/MS techniques used within this work are relatively low throughput, analysing one sample in 30 minutes to 1 hour (Section 2.4). Therefore, I selected an extraction protocol to isolate as wide a range of lipids as possible, reducing both the number of extractions required and number of samples to be analysed using LC-MS. The lipid extraction used in this thesis was adapted from the work of Bligh and Dyer, and incorporated a hexane extraction to ensure the extraction of both polar and non-polar lipids (Section 2.3) (Bligh and Dyer, 1959). I tested extraction efficiency and coefficient of variation for global LC/MS data. The high extraction efficiency and low CV of the methods used in this thesis are comparable with published work in the field of lipidomics (Section 3.2.1) (Bligh and Dyer, 1959, McDonald et al., 2012, Alshehry et al., 2015, Maile et al., 2018, Surma et al., 2015, Li et al., 2013). A comparison of lipids in extractions of four different volumes of plasma suggested that a 50 uL extraction of plasma and 100 uL plasma extraction demonstrate the same number of endogenous lipids from a pre-chosen panel (Section 3.3.2). Also, peak area for some eicosanoids is higher when a lower volume of plasma has been extracted, suggesting either (i) extraction efficiency could be improved with a higher ratio of extraction solvent to plasma, or (ii) ion suppression is occurring during ESI at higher plasma concentrations. Reducing concentration of lipid within the injected sample could prevent matrix effects by lessening competition between analytes to be ionised and thus, may improve data quality (Taylor, 2005). Therefore, there are several benefits to reducing the volume of plasma extracted from

100 µL to 50 µL. Overall, the optimisation and validation steps taken in Chapter 3 imply that the LC-MS and LC-MS/MS methods used within are reliable and reproducible.

Comparison of long-term-stored NPHSII samples with freshly isolated plasma demonstrated few differences between the two (Sections 4.2.1-4.2.3), and some differences in lipid levels which are possibly caused by differences in age and gender in the two sample groups. Oxidation of some lipids map have taken place during storage, however, NPHSII plasma samples contained similar numbers of lipid ions as fresh samples ($P>0.05$), endogenous species could be found in both NPHSII and fresh plasma, and CE and TAGs did not differ between the two groups. Thus, I decided to analyse the global lipidome of NPHSII samples. This work has wider implications as it suggests that other long-term stored cohort plasma samples may be worthy of analysis. However, the n number was small and only a subset of lipids was compared. Therefore, I would want to compare all lipids in a larger number of samples, and complete targeted analysis of GPLs to confirm this finding.

8.2 SPs, GLs and unknown species are reduced in *APOE* 2 homozygote plasma

This thesis contains the first global lipidomic analysis of human *APOE ε2, ε3* and *ε4* homozygote plasma, filling a gap in the literature. I identified a possible downregulation of SPs in *APOE 22* plasma. SPs which differ are all ceramide precursors or products (Figure 5.11), suggesting that ceramide metabolism or transport may be dysregulated in *APOE 22*. SPs have numerous biological functions. For example, sphingolipids are an important constituent of lipid rafts, phase ordered regions which may facilitate signalling through surface proteins or receptors (de Almeida et al., 2003, Simons and Toomre, 2000). APP is preferentially cleaved to produce Aβ in lipid raft sections, therefore a low SP environment could theoretically reduce the amount of soluble Aβ and so reduce accumulation of amyloid plaques (Ehehalt et al., 2003). Also, circulating SPs are associated with both fasting glucose and fasting insulin levels, and most SPs which differ are positively correlated with both glucose and insulin (Lemaitre et al., 2018, Jensen et al., 2019). A downregulation of circulating sphingolipids could protect against LOAD by lowering risk of type II diabetes, which is a risk factor for development of dementia (Arvanitakis et al., 2004).

A number of GPLs are also reduced in *APOE 22* plasma (Table 5.1). GPLs can cross the BBB in the form of lyso-PCs bound to albumin, suggesting that (a) circulating GPLs could be integrated into the brain, and (b) plasma could provide a source for brain-derived GPL biomarkers (Broadwell and Sofroniew, 1993, Picq et al., 2010). GPLs are also dysregulated in LOAD animal models following alterations to the Land's cycle, and alterations are associated with cognitive deficit (Granger et al., 2018). I would like to identify the GPL species which are lower in *APOE 22* plasma by LC-MS/MS, to determine if any of these species have been linked with cognition by other research.

A study of *hAPOE* knock in mice demonstrated changes in plasma lipid profile in *APOE 22* and *APOE 44* mice when compared to *APOE 33* as control (Sharman et al., 2010). Total PE was reduced in 2-month-old murine *hAPOE 22* plasma. Also, total sphingomyelin and total ceramide are increased in the plasma of both 2-month-old and 4-month-old *hAPOE 22* mice. These data are at odds with the untargeted analysis of human plasma in Chapter 5, which found that SPs (including sphingomyelins and ceramides) are decreased in human *APOE 22* plasma (Table 5.2). I have identified two factors which could cause the disparity between these results. Firstly, Sharman et al., 2010 analysed samples from *hAPOE* knock in mice, whilst NPHSII samples are human plasma samples and the species effect is unknown. The *hAPOE* knock in mice were analysed at a young age, whilst NPHSII samples are sourced from participants of 40 to 60 years of age. Age has been associated with changes in plasma lipids and lipid-associated gene expression in humans (Ishikawa et al., 2014, Snieder et al., 1997). Secondly, Sharman et al. analysed human *APOE* alleles knocked into a mouse model. Whilst lipids are highly conserved between the two species, it is possible that differences between human and murine lipid metabolism caused this discrepancy in results .

Power calculations are calculations to decide on the smallest number of samples needed to measure a clinically relevant change, taking into account the standard deviation of the data (Jones et al., 2003). Completing power calculations during study design reduces the possibility of type I or type II errors. The lack of power calculations could cause errors of either type, for

example, the absence of significantly differences in lipid levels in *APOE 44* and control could be a type II error. Power calculations would have been difficult to implement in this study as it is hard to define a clinically relevant change for most plasma lipids, as the biological relevance of changes is currently unknown. Also, during study design, standard deviation of lipids across samples was unknown. In the future, I would implement a smaller pilot study to define these variables, followed by power calculations and analysis of the appropriate group size. I could not compare between the APOE 22 and APOE 44 global analysis datasets due to batch effects from extracting and analysing the datasets separately (Section 5.2.2.2). This included a RT shift, and analysis of endogenous species suggests that sensitivity may have been compromised in the APOE 22 positive mode analysis. In the future, I will avoid batch effects such as these by completing extraction and analysis of all samples as one dataset.

To summarise the results of the global analysis, *APOE 22* plasma from the NPHSII cohort demonstrates a reduction in SPs and GPLs, alongside a number of unknown species. SPs are linked to risk of LOAD through promotion of Aβ production and risk of type II diabetes and GPL metabolism is dysregulated in LOAD (Lemaitre et al., 2018, Jensen et al., 2019, Arvanitakis et al., 2004, Ehehalt et al., 2003, Granger et al., 2018). Therefore, I need to validate my finding of lower SPs and GPLs in human *APOE 22* plasma and determine if these lipids are increased or decreased in *APOE 22* homozygote human brain samples.

Total cholesterol and TAGs have been profiled in *APOE* homozygote and heterozygote plasma by several groups. A meta-analysis of 45 studies found that total cholesterol was lower in *APOE* ε2 carriers and higher in *APOE* ε4 carriers, whilst total TAGs are higher in all allele combinations compared to *APOE 33* (Dallongeville et al., 1992). In comparison, I combined untargeted and targeted analyses of cholesterol, CEs and TAGs to determine if individual species are altered between the alleles, providing another level of detail. However, the LC/MS-MS analysis of individual CEs and TAGs in *APOE* homozygote plasma did not reveal any allele-specific changes in chain length or saturation. This is not in accordance with the literature on total cholesterol, which tends to associate *APOE 22* with decreased circulating cholesterol, whilst the presence of *APOE* ε4 is associated with increased cholesterol (Dallongeville et al., 1992, Sing and Davignon, 1985, Boulenouar et al., 2013). As previously

discussed, NPHSII samples demonstrate high cholesterol and CEs in the *APOE33* group (Section 6.2.1 – 6.2.2), which is at odds with previous analyses of NPHSII data (Cooper et al., 2005). The subset of NPHSII samples analysed may not represent the population as a whole. I would like to increase n numbers to determine the expected patterns of lower cholesterol and CEs in *APOE 22* and higher cholesterol and CEs in *APOE 44* emerge.

Whilst analysis of cholesterol, CEs and TAGs in the subset of NPHSII data analysed did not reveal any alterations between alleles, these species have been implicated in the risk of developing LOAD. High circulating levels of cholesterol and TAG are associated with an increased risk of developing amyloid and tau pathology (Sections 1.5.1 and 1.1.5.2) (Bodovitz and Klein, 1996, Refolo et al., 2001, Burgess et al., 2006, Kurata et al., 2011, Matsuzaki et al., 2011, Nägga et al., 2018). Also, polymorphisms of the cholesterol ester transfer protein (CETP) gene modify AD disease risk carried by *APOE* ε4 by up to three-fold (Rodríguez et al., 2006). Cholesterol, CEs and TAGs are all lipids which could cross the BBB as lipoprotein constituents, and a cholesterol metabolite, 24-hydroxycholesterol, can also cross (Balazs et al., 2004, Candela et al., 2008, Dehouck et al., 1997, Panzenboeck et al., 2002, Lütjohann et al., 1996). Therefore, circulating levels of cholesterol, CEs and TAGs may be correlated with levels in the brain, and these species may exacerbate amyloid and tau pathology.

TAG alterations in LOAD have been linked to cognitive symptoms through the disruption of the BBB. Specifically, AD patients with BBB breakdown are significantly more likely to have elevated TAGs than those who do not (Bowman et al., 2012). In human astrocytic cell culture, high physiological levels of the products of TAG-rich lipoprotein (TAGRL) lipolysis caused lipid drop formation, activation of inflammatory gene pathways and release of inflammatory mediators (Lee et al., 2017), suggesting that high TAGs could cause BBB stress *in vivo*. These results were furthered by data in rat which suggested postprandial TAGRLs increased BBB permeability in a transient manner (Ng et al., 2016). Subsequently to completing the analysis in this Chapter, global LC/MS putatively identified 14 TAG species as being altered in plasma of LOAD, 10 lower and 4 higher (Di Gaudio et al., 2016). However, none of these species were measured in this work. I would include these species in any further analysis of *APOE* homozygote plasma. To conclude, there is extensive literature on cholesterol, CEs and TAGs both in *APOE* and LOAD, which suggests that these species could exacerbate pathology when

circulating at high levels. However, targeted analysis of NPHSII plasma by LC-MS/MS did not find any patterns in cholesterol, CEs and TAGs associated with either *APOE 22* or *APOE 44*. Results may have been confounded by a small sample size, as data is not in line with the literature.

8.2.1 Routes by which lipids cross the BBB and the implications of circulating lipids for the CNS

Throughout this work I discuss the implications of my work in the context of LOAD, however, it is important to consider how lipids in the circulation are related to those within the brain. The brain is separated from the circulation by the BBB, which is made up of endothelial cells, astrocytes and pericytes, surrounding each blood vessel in the brain (Figure 8.1) (Pardridge et al., 1975). Endothelial cells are joined by tight junctions, preventing molecules from passing between cells (Reese and Karnovsky, 1967, Brightman and Reese, 1969). Historically, the BBB has been considered a tight barrier which prevents cells and molecules from entering the CNS, and certainly detectable circulating biomarkers of LOAD could be present due to degeneration of the BBB as part of disease (Montagne et al., 2017). However, permeability of the BBB could be affected by a range of factors, like inflammatory mediators, or even the gut microbiota (Abbott, 2000, Braniste et al., 2014)

Experiments do suggest that some lipids and proteins can cross the CNS through a variety of methods (Table 8.1). Lipids may cross the BBB in both directions through passive diffusion, bound to serum proteins, using receptors or as constituents of peripheral immune cells such as bone marrow derived macrophages (BMDMs) or T cells (Picq et al., 2010, Balazs et al., 2004, Dehouck et al., 1997, Candela et al., 2008, Ouellet et al., 2009, Nguyen et al., 2014, Simard et al., 2006, Simard and Rivest, 2006, Engelhardt and Ransohoff, 2012, Panzenboeck et al., 2002, Lütjohann et al., 1996, Mitchell et al., 2011). Therefore, it is possible that circulating lipids could reflect the lipid environment within the CNS to a greater extent than previously considered. More work is needed in this area to elucidate exactly how many lipid species can cross the BBB.

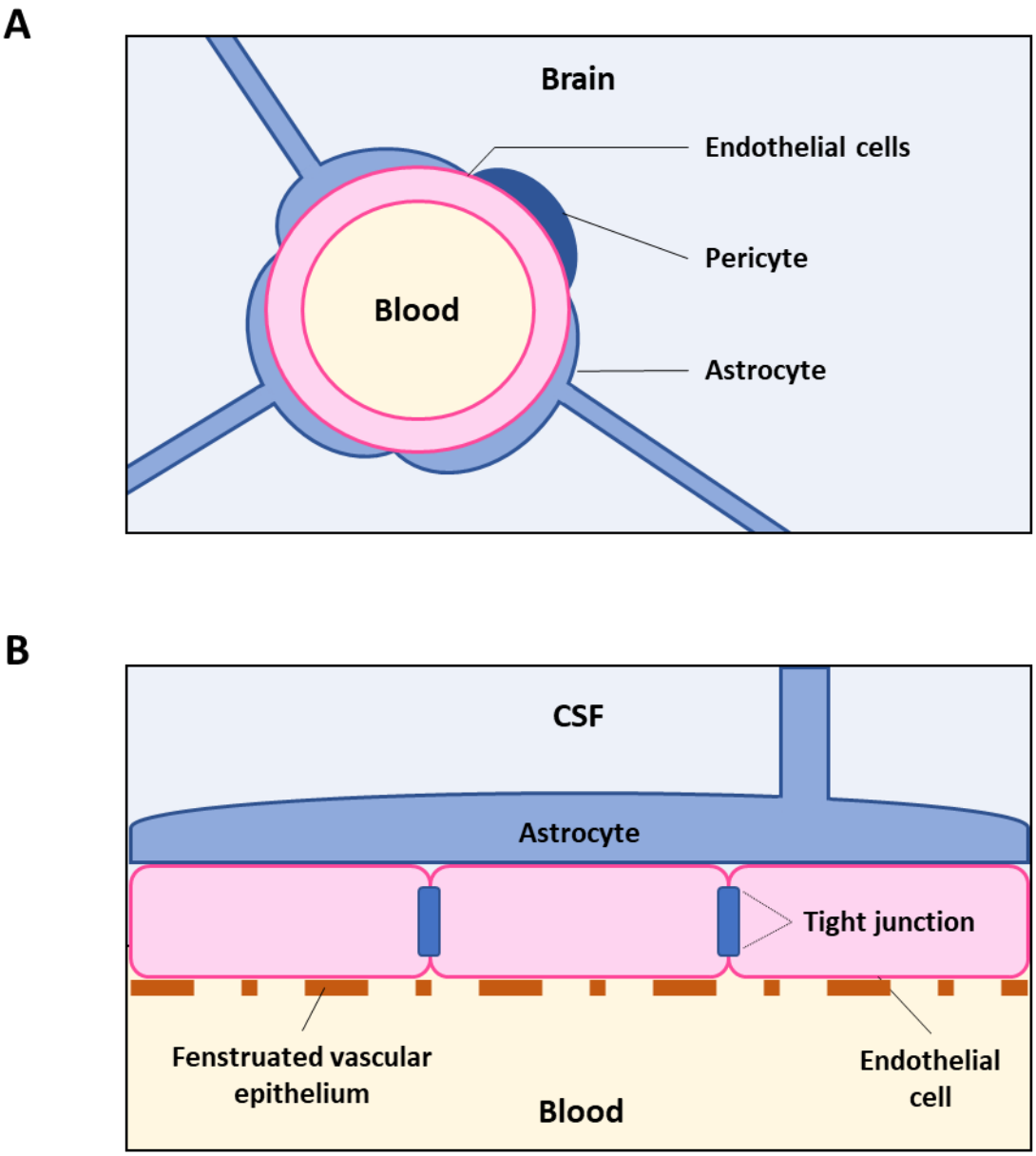

Figure 8.1: The BBB is a tight barrier between the circulating blood and the brain. A. Endothelial cells surround the blood vessels and micro vessels of the brain, after which astrocytic endfeet and pericytes encircle blood vessels. **B.** A small representative section of the BBB, demonstrating pericytes and astrocytes, tight junctions between endothelial cells, and the fenestrated epithelium of a capillary.

Mechanisms for lipid transport across the BBB

Study	Lipids	Mechanism	Direction
Reviewed in Picq et al., 2010	Fatty acyls and PCs	Bound to albumin, which can cross BBB due to hydrophobic nature	In
Balazs et al., 2004	HDL	Scavenger receptor class B, type I (SR-B1)	In
Dehouck et al., 1997, Candela et al., 2008	LDL	Transcytosis	In
Ouellet et al., 2009	DHA and eicosapentaenoic acid	Passive diffusion	In
Nguyen et al., 2014	LysoPC	Sodium-dependent lysophosphatidylcholine symporter 1	In
Simard et al., 2006, Simard and Rivest, 2006	Cellular lipids from bone marrow derived macrophages (BMDM)	BMDM cross BBB due to chemoattraction	In
Reviewed in Engelhard and Ransohoff, 2012	Cellular lipids from T cells	T cells interact with adhesion factors then G-protein coupled receptors	In
Panzenboeck et al., 2002	HDL, LDL, and 24-hydroxycholesterol	Apolipoprotein A1 ABCA1 SR-B1	Out
Lütjohann et al., 1996	24-hydroxycholesterol	?	Out
Mitchell et al., 2011	Fatty acyls	Bound to albumin through fatty acyl transport proteins 1-5	Out

Table 8.1: Studies which have suggested that lipids can travel across the BBB. Studies which have identified mechanisms for lipid transport in and out of the brain are summarised. The lipids which can cross the membrane, route through the BBB and direction of travel (into or out of the CNS) are listed. Where mechanism is listed as "?", mechanism of lipid movement was not investigated.

8.3 Recollection memory is not associated with levels of 12 LOX products in the brain

ApoE$^{-/-}$ mice, which demonstrate hippocampal neurodegeneration after 4 months of age, have no deficit in recognition memory at 7 months of age, as measured by the "novel object test" (Figure 7.2) (Gordon et al., 1995, Masliah et al., 1995). This is accordance with a recent study, where *ApoE*$^{-/-}$mice perform significantly worse than wildtype in the "novel object test" at 18-20 months of age (Fuentes et al., 2018). Therefore, my data together with other work suggests that ApoE deficiency does not impact the ability to recognise an object as new. Also, *Alox12/15*$^{-/-}$ and *ApoE*$^{-/-}$*/ALOX12/15*$^{-/-}$ double knock out mice do not have a deficit in recognition memory (Figure 7.2). To my knowledge, this is the first test of recognition memory in these strains.

The "object in place test" demonstrates a recollection memory deficit in the *ApoE*$^{-/-}$ mice at 7 months of age (Figure 7.3). My experimental data is in agreement with other studies of *ApoE*$^{-/-}$ mice using a different test of recollection memory, the Morris Water Maze (Gordon et al., 1995, Masliah et al., 1995). Memory impairment in *ApoE*$^{-/-}$ mice is probably due to the integral role of ApoE in lipid transport within the CNS (Figure 1.4). Lipids in the brain are produced in astrocytes alongside ApoE, and then exported by TREM2, therefore transport of lipids from astrocytes and microglia to neurons would be decreased in *ApoE*$^{-/-}$ mice (Nieweg et al., 2009, Pitas et al., 1987b). *ApoE*$^{-/-}$ is not fatal, therefore compensatory mechanisms of lipid transport must occur. *ApoE*$^{-/-}$ mice also suffer from a loss in hippocampal synapse density, measured by immunofluorescent probes for synaptophysin and microtubule associated protein 2 (MAP2), and a reduction in LTP in the hippocampus, which is necessary for recollection memory (Masliah et al., 1995, Veinbergs et al., 1998, Bliss and Lomo, 1973). To extend my analysis further, I would like to quantify synapse density using synaptophysin and MAP2 in the *ApoE*$^{-/-}$, *ALOX12/15*$^{-/-}$ and *ApoE*$^{-/-}$*/ALOX12/15*$^{-/-}$ double knock out mouse, to determine if this correlates with either behaviour or lipidomic analysis of brain regions.

12/15-LOX improves cognitive deficit in 3xTG mouse models (Di Meco et al., 2017, Praticò et al., 2004). 12/15-LOX has been implicated in both oxidative stress and amyloid processing (Praticò et al., 2004, Succol and Praticò, 2007). I tested wildtype mice against *ApoE*$^{-/-}$,

Alox12/15$^{-/-}$ and *ApoE*$^{-/-}$*/Alox12/15*$^{-/-}$ in the "object-in-place test" to determine if 12/15-LOX removal would prevent spatial recollection memory loss associated with ApoE deficiency (Gordon et al., 1995, Masliah et al., 1995). Indeed, the *Alox12/15*$^{-/-}$ and *ApoE*$^{-/-}$*/Alox12/15*$^{-/-}$ mice were not impaired in the object-in-place test", whilst the *ApoE*$^{-/-}$ mouse was (Figure 7.3). However, I do not believe that this data suggests a protective effect for 12/15-LOX ablation. The range of the *Alox12/15*$^{-/-}$ data was large, and most or all of the 'protective' effect was driven by one mouse with an extremely high discrimination ratio. Both *Alox12/15*$^{-/-}$ and *ApoE*$^{-/-}$*/Alox12/15*$^{-/-}$ mice trended towards performing worse in the task, although this did not reach significance.

Whilst 12/15-LOX deficiency may be protective under pathological circumstances, 12/15-LOX may support normal brain function (Di Meco et al., 2017, DeCostanzo et al., 2010, Normandin et al., 1996, Feinmark et al., 2003, Shalini et al., 2018, Dorman et al., 1992). However, there is no consensus as to how this may occur. Studies of hippocampal slices have indicated that 12/15-LOXs may be essential for either LTP or long-term depression (LTD) (DeCostanzo et al., 2010, Normandin et al., 1996, Feinmark et al., 2003). In the rat, 15-LOX is expressed throughout the brain and inhibition prevents LTP and causes errors in behavioural tasks (Shalini et al., 2018). In cell culture, 12-LOX metabolites inhibit neurotransmitter release from synapses (Dorman et al., 1992). My data also supports the concept that, under normal conditions, 12/15-LOX supports brain function. Further work is needed in this area to clarify the exact role of 12/15-LOX in LTP and LTD.

Two oxPLs are increased in the frontal cortex and *ApoE*$^{-/-}$ mouse (Figure 7.6, Figure 7.7), suggesting an association between PL oxidation in these regions and recollection memory. It is not possible to determine the structure of these species using the LC-MS/MS techniques used in this thesis, as PCs and PEs can share both Q1 and Q3 masses. However, these could be determined using LC-MS/MS. However, the range of behavioural data is too large to draw any conclusions between oxPLs and memory. LC-MS/MS analysis of select HETEs and HDOHEs in brain regions demonstrates a range of positional isomers, suggesting that these species are not produced by 12/15-LOX (Figure 7.8 – 7.11). However, several studies have suggested that 12/15-LOX is present in the brain and may support brain function (see above). I suggest that, as most positional isomers of both HETEs and HDOHEs are present, non-enzymatic oxidation

of the brain regions may have taken place during extraction, masking any changes in low abundance 12/15-LOX species. Oxidation of the brain samples during extraction could also impact oxPLs data, as trends in oxPLs could be harder to identify.

In neurodegenerative disorders such as LOAD, oxidative activity is upregulated, and lipid peroxidation takes place (Bradley-Whitman and Lovell, 2015). While this was beyond the scope of my current work, I would like to investigate this further to determine if oxPL increases are indicative of lipid peroxidation. The next step in this work would be to identify the oxPL species increased in *ApoE*$^{-/-}$ and test their biological activity. As previously discussed, I would also use synaptophysin and microtubule-associated protein 2 (MAP2) to assess pre- and post-synaptic density within brain regions, to determine if synapse density is correlated with lipid content of brain regions.

I completed only a rough dissection of the brain regions (Figure 2.2). Therefore, the 'frontal cortex' regions actually contain the cerebral cortex, anterior olfactory nucleus and ventral striatum, whilst 'cortex' regions included the cortex, thalamus, hypothalamus and midbrain. Therefore, dissection into complete brain regions would have yielded more data, and the method of dissection may have hidden changes in specific regions. oxPLs, HETE and HDOHE data suggests that, before repeating this experiment with all brain regions, I would have to adapt the method to reduce oxidation during extraction. Another drawback of this experiment would be a lack of power calculations, increasing the likelihood of a type I or type II error (Jones et al., 2003). Therefore, I would like do these calculations with the current data before repeating the experiment.

8.4 Conclusions

LC/MS, LC/MS-MS and LipidFinder provide a platform for reliable and reproducible lipid analysis. Methods of lipid extraction, MS analysis and data analysis should be optimised to the tissue of analysis and study design, and multiple comparisons adjustment performed if necessary. Herein, LC/MS putatively identified a downregulation of SPs and GPLs in *APOE 22* homozygote plasma. Further work is needed to validate these data and determine if

downregulation of these species occurs in *APOE 22* homozygote brain. Also, LC-MS/MS suggested that 12/15-LOX is not active in the brain under physiological conditions, although oxidation during extraction could be a confounding factor in the analysis. I detected two oxPL species which are associated with recognition memory loss in *ApoE*$^{-/-}$ mice, which require structural identification.

1978. The nomenclature of lipids (Recommendations 1976) IUPAC-IUB Commission on Biochemical Nomenclature. *Biochem J,* 171**,** 21-35.

ABBASSI-GHADI, N., JONES, E. A., GOMEZ-ROMERO, M., GOLF, O., KUMAR, S., HUANG, J., KUDO, H., GOLDIN, R. D., HANNA, G. B. & TAKATS, Z. 2016. A Comparison of DESI-MS and LC-MS for the Lipidomic Profiling of Human Cancer Tissue. *J Am Soc Mass Spectrom,* 27**,** 255-64.

ABBOTT, N. J. 2000. Inflammatory mediators and modulation of blood-brain barrier permeability. *Cell Mol Neurobiol,* 20**,** 131-47.

ABBOTT, S. K., ELSE, P. L., ATKINS, T. A. & HULBERT, A. J. 2012. Fatty acid composition of membrane bilayers: importance of diet polyunsaturated fat balance. *Biochim Biophys Acta,* 1818**,** 1309-17.

ABDELMAGID, S. A., CLARKE, S. E., NIELSEN, D. E., BADAWI, A., EL-SOHEMY, A., MUTCH, D. M. & MA, D. W. 2015. Comprehensive profiling of plasma fatty acid concentrations in young healthy Canadian adults. *PLoS One,* 10**,** e0116195.

ABDULLAH, L., EVANS, J. E., EMMERICH, T., CRYNEN, G., SHACKLETON, B., KEEGAN, A. P., LUIS, C., TAI, L., LADU, M. J., MULLAN, M., CRAWFORD, F. & BACHMEIER, C. 2017. APOE ε4 specific imbalance of arachidonic acid and docosahexaenoic acid in serum phospholipids identifies individuals with preclinical Mild Cognitive Impairment/Alzheimer's Disease. *Aging (Albany NY),* 9**,** 964-985.

ABE, S., EZAKI, O. & SUZUKI, M. 2017. Medium-Chain Triglycerides in Combination with Leucine and Vitamin D Benefit Cognition in Frail Elderly Adults: A Randomized Controlled Trial. *J Nutr Sci Vitaminol (Tokyo),* 63**,** 133-140.

ADESUYI, S. A., COCKRELL, C. S., GAMACHE, D. A. & ELLIS, E. F. 1985. Lipoxygenase metabolism of arachidonic acid in brain. *J Neurochem,* 45**,** 770-6.

AGUAYO-ORTIZ, R., STRAUB, J. E. & DOMINGUEZ, L. 2018. Influence of membrane lipid composition on the structure and activity of γ-secretase. *Phys Chem Chem Phys*.

ALONSO, A. C., GRUNDKE-IQBAL, I. & IQBAL, K. 1996. Alzheimer's disease hyperphosphorylated tau sequesters normal tau into tangles of filaments and disassembles microtubules. *Nat Med,* 2**,** 783-7.

ALSHEHRY, Z. H., BARLOW, C. K., WEIR, J. M., ZHOU, Y., MCCONVILLE, M. J. & MEIKLE, P. J. 2015. An Efficient Single Phase Method for the Extraction of Plasma Lipids. *Metabolites,* 5**,** 389-403.

ALZGENE. 2010. *ALZGENE - META-ANALYSIS OF ALL PUBLISHED AD ASSOCIATION STUDIES (CASE-CONTROL ONLY) APOE_E2/3/4* [Online]. Alzforum. Available: http://www.alzgene.org/meta.asp?geneID=83 [Accessed November 6 2017].

AL-SAAD, K. A., ZABROUSKOV, V., SIEMS, W. F., KNOWLES, N. R., HANNAN, R. M. & HILL, H. H. 2002. Matrix-assisted laser desorption/ionization time-of-flight mass spectrometry of lipids: ionization and prompt fragmentation patterns. *Rapid Communications in Mass Spectrometry,* 17**,** 87-96.

AN, X. L., ZOU, J. X., WU, R. Y., YANG, Y., TAI, F. D., ZENG, S. Y., JIA, R., ZHANG, X., LIU, E. Q. & BRODERS, H. 2011. Strain and sex differences in anxiety-like and social behaviors in C57BL/6J and BALB/cJ mice. *Exp Anim,* 60**,** 111-23.

ANAND, S., BARNES, J. M., YOUNG, S. A., GARCIA, D. M., TOLLEY, H. D., KAUWE, J. S. K. & GRAVES, S. W. 2017. Discovery and Confirmation of Diagnostic Serum Lipid Biomarkers for Alzheimer's Disease Using Direct Infusion Mass Spectrometry. *J Alzheimers Dis,* 59**,** 277-290.

ANDREADIS, A., BROWN, W. M. & KOSIK, K. S. 1992. Structure and novel exons of the human tau gene. *Biochemistry,* 31**,** 10626-33.

ANTUNES, M. & BIALA, G. 2012. The novel object recognition memory: neurobiology, test procedure, and its modifications. *Cogn Process,* 13**,** 93-110.

ARVANITAKIS, Z., WILSON, R. S., BIENIAS, J. L., EVANS, D. A. & BENNETT, D. A. 2004. Diabetes mellitus and risk of Alzheimer disease and decline in cognitive function. *Arch Neurol,* 61**,** 661-6.

ASUNI, A. A., BOUTAJANGOUT, A., QUARTERMAIN, D. & SIGURDSSON, E. M. 2007. Immunotherapy targeting pathological tau conformers in a tangle mouse model reduces brain pathology with associated functional improvements. *J Neurosci,* 27**,** 9115-29.

ATAGI, Y., LIU, C. C., PAINTER, M. M., CHEN, X. F., VERBEECK, C., ZHENG, H., LI, X., RADEMAKERS, R., KANG, S. S., XU, H., YOUNKIN, S., DAS, P., FRYER, J. D. & BU, G. 2015. Apolipoprotein E Is a Ligand for Triggering Receptor Expressed on Myeloid Cells 2 (TREM2). *J Biol Chem,* 290**,** 26043-50.

ATTIE, A. D., KASTELEIN, J. P. & HAYDEN, M. R. 2001. Pivotal role of ABCA1 in reverse cholesterol transport influencing HDL levels and susceptibility to atherosclerosis. *J Lipid Res,* 42**,** 1717-26.

AVELDAÑO, M. I. & SPRECHER, H. 1983. Synthesis of hydroxy fatty acids from 4, 7, 10, 13, 16, 19-[1-14C] docosahexaenoic acid by human platelets. *J Biol Chem,* 258**,** 9339-43.

AYCIRIEX, S., GERBER, H., OSUNA, G. M., CHAMI, M., STAHLBERG, H., SHEVCHENKO, A. & FRAERING, P. C. 2016. The lipidome associated with the γ-secretase complex is required for its integrity and activity. *Biochem J,* 473**,** 321-34.

BAILEY, C. C., DEVAUX, L. B. & FARZAN, M. 2015. The Triggering Receptor Expressed on Myeloid Cells 2 Binds Apolipoprotein E. *J Biol Chem,* 290**,** 26033-42.

BALAZS, Z., PANZENBOECK, U., HAMMER, A., SOVIC, A., QUEHENBERGER, O., MALLE, E. & SATTLER, W. 2004. Uptake and transport of high-density lipoprotein (HDL) and HDL-associated alpha-tocopherol by an in vitro blood-brain barrier model. *J Neurochem,* 89**,** 939-50.

BALLABH, P., BRAUN, A. & NEDERGAARD, M. 2004. The blood-brain barrier: an overview: structure, regulation, and clinical implications. *Neurobiol Dis,* 16**,** 1-13.

BALLARD, C., THOMAS, A., KHAN, Z., HANNEY, M., YU, L. M., MERRICK, C., FERREIRA, N., CREESE, B., BANNISTER, C., BURNS, A. & WALKER, Z. 2013. *Memantine for the Long Term Management of Neuropsychiatric Symptoms in Alzheimer's disease - MAIN-AD* [Online]. EU Clinical Trials Register: EU Clinical Trials Register. [Accessed 31st October 2018].

BANATI, R. B., GEHRMANN, J., CZECH, C., MÖNNING, U., JONES, L. L., KÖNIG, G., BEYREUTHER, K. & KREUTZBERG, G. W. 1993. Early and rapid de novo synthesis of Alzheimer beta A4-amyloid precursor protein (APP) in activated microglia. *Glia,* 9**,** 199-210.

BANATI, R. B., GEHRMANN, J., WIESSNER, C., HOSSMANN, K. A. & KREUTZBERG, G. W. 1995. Glial expression of the beta-amyloid precursor protein (APP) in global ischemia. *J Cereb Blood Flow Metab,* 15**,** 647-54.

BAO, F., WICKLUND, L., LACOR, P. N., KLEIN, W. L., NORDBERG, A. & MARUTLE, A. 2012. Different β-amyloid oligomer assemblies in Alzheimer brains correlate with age of disease onset and impaired cholinergic activity. *Neurobiol Aging,* 33**,** 825.e1-13.

BARBER, R. C. 2010. Biomarkers for early detection of Alzheimer disease. *J Am Osteopath Assoc,* 110**,** S10-5.

BARKER, G. R. & WARBURTON, E. C. 2015. Object-in-place associative recognition memory depends on glutamate receptor neurotransmission within two defined hippocampal-cortical circuits: a critical role for AMPA and NMDA receptors in the hippocampus, perirhinal, and prefrontal cortices. *Cereb Cortex,* 25**,** 472-81.

BARKER, W. W., LUIS, C. A., KASHUBA, A., LUIS, M., HARWOOD, D. G., LOEWENSTEIN, D., WATERS, C., JIMISON, P., SHEPHERD, E., SEVUSH, S., GRAFF-RADFORD, N., NEWLAND, D., TODD, M., MILLER, B., GOLD, M., HEILMAN, K., DOTY, L., GOODMAN, I., ROBINSON, B., PEARL, G., DICKSON, D. & DUARA, R. 2002. Relative frequencies of Alzheimer disease, Lewy body, vascular and frontotemporal dementia, and hippocampal sclerosis in the State of Florida Brain Bank. *Alzheimer Dis Assoc Disord,* 16**,** 203-12.

BASCOUL-COLOMBO, C., GUSCHINA, I. A., MASKREY, B. H., GOOD, M., O'DONNELL, V. B. & HARWOOD, J. L. 2016. Dietary DHA supplementation causes selective changes in phospholipids from different brain regions in both wild type mice and the Tg2576 mouse model of Alzheimer's disease. *Biochim Biophys Acta,* 1861**,** 524-37.

BASHTOVYY, D., JONES, M. K., ANANTHARAMAIAH, G. M. & SEGREST, J. P. 2011. Sequence conservation of apolipoprotein A-I affords novel insights into HDL structure-function. *J Lipid Res,* 52**,** 435-50.

BAXTER, M. G. 2010. "I've seen it all before": explaining age-related impairments in object recognition. Theoretical comment on Burke et al. (2010). *Behav Neurosci,* 124**,** 706-9.

BEAR, M. F., CONNORS, B. W. & PARADISO, M. A. 2006. *Neuroscience: exploring the brain,* Philadelphia, Lippincott Williams and Wilkins.

BENJAMINI, Y. & HOCHBERG, Y. 1995. Controlling the False Discovery Rate: A Practical and Powerful Approach to Multiple Testing. *Journal of the Royal Statistical Society. Series B (Methodological)*

57**,** 289-300.

BERGERON, N. & HAVEL, R. J. 1996. Prolonged postprandial responses of lipids and apolipoproteins in triglyceride-rich lipoproteins of individuals expressing an apolipoprotein epsilon 4 allele. *J Clin Invest,* 97**,** 65-72.

BERLAU, D. J., CORRADA, M. M., HEAD, E. & KAWAS, C. H. 2009. APOE epsilon2 is associated with intact cognition but increased Alzheimer pathology in the oldest old. *Neurology,* 72**,** 829-34.

BEVINS, R. A., BESHEER, J., PALMATIER, M. I., JENSEN, H. C., PICKETT, K. S. & EUREK, S. 2002. Novel-object place conditioning: behavioral and dopaminergic processes in expression of novelty reward. *Behav Brain Res,* 129**,** 41-50.

BEYREUTHER, K. & MASTERS, C. L. 1991. Amyloid precursor protein (APP) and beta A4 amyloid in the etiology of Alzheimer's disease: precursor-product relationships in the derangement of neuronal function. *Brain Pathol,* 1**,** 241-51.

BIRSOY, K., FESTUCCIA, W. T. & LAPLANTE, M. 2013. A comparative perspective on lipid storage in animals. *J Cell Sci,* 126**,** 1541-52.

BJÖRKHEM, I., LÜTJOHANN, D., DICZFALUSY, U., STÅHLE, L., AHLBORG, G. & WAHREN, J. 1998. Cholesterol homeostasis in human brain: turnover of 24S-hydroxycholesterol and evidence for a cerebral origin of most of this oxysterol in the circulation. *J Lipid Res,* 39**,** 1594-600.

BJÖRKQVIST, M., OHLSSON, M., MINTHON, L. & HANSSON, O. 2012. Evaluation of a previously suggested plasma biomarker panel to identify Alzheimer's disease. *PLoS One,* 7**,** e29868.

BLIGH, E. G. & DYER, W. J. 1959. A rapid method of total lipid extraction and purification. *Can J Biochem Physiol,* 37**,** 911-7.

BLISS, T. V. & LOMO, T. 1973. Long-lasting potentiation of synaptic transmission in the dentate area of the anaesthetized rabbit following stimulation of the perforant path. *J Physiol,* 232**,** 331-56.

BLOCK, M. L., ZECCA, L. & HONG, J. S. 2007. Microglia-mediated neurotoxicity: uncovering the molecular mechanisms. *Nat Rev Neurosci,* 8**,** 57-69.

BOCHE, D., PERRY, V. H. & NICOLL, J. A. 2013. Review: activation patterns of microglia and their identification in the human brain. *Neuropathol Appl Neurobiol,* 39**,** 3-18.

BOCHKOV, V., GESSLBAUER, B., MAUERHOFER, C., PHILIPPOVA, M., ERNE, P. & OSKOLKOVA, O. V. 2017. Pleiotropic effects of oxidized phospholipids. *Free Radic Biol Med,* 111**,** 6-24.

BODOVITZ, S. & KLEIN, W. L. 1996. Cholesterol modulates alpha-secretase cleavage of amyloid precursor protein. *J Biol Chem,* 271**,** 4436-40.

BOERWINKLE, E., BROWN, S., SHARRETT, A. R., HEISS, G. & PATSCH, W. 1994. Apolipoprotein E polymorphism influences postprandial retinyl palmitate but not triglyceride concentrations. *Am J Hum Genet,* 54**,** 341-60.

BOIMEL, M., GRIGORIADIS, N., LOURBOPOULOS, A., TOULOUMI, O., ROSENMANN, D., ABRAMSKY, O. & ROSENMANN, H. 2009. Statins reduce the neurofibrillary tangle burden in a mouse model of tauopathy. *J Neuropathol Exp Neurol,* 68**,** 314-25.

BOMBOIS, S., MAURAGE, C. A., GOMPEL, M., DERAMECOURT, V., MACKOWIAK-CORDOLIANI, M. A., BLACK, R. S., LAVIELLE, R., DELACOURTE, A. & PASQUIER, F. 2007. Absence of beta-amyloid deposits after immunization in Alzheimer disease with Lewy body dementia. *Arch Neurol,* 64**,** 583-7.

BOULENOUAR, H., MEDIENE BENCHEKOR, S., MEROUFEL, D. N., LARDJAM HETRAF, S. A., OUHAIBI DJELLOULI, H., HERMANT, X., GRENIER-BOLEY, B., HAMANI MEDJAOUI, I., SAIDI MEHTAR, N., AMOUYEL, P., HOUTI, L., MEIRHAEGHE, A. & GOUMIDI, L. 2013. Impact of APOE gene polymorphisms on the lipid profile in an Algerian population. *Lipids Health Dis,* 12**,** 155.

BOWMAN, G. L., KAYE, J. A. & QUINN, J. F. 2012. Dyslipidemia and blood-brain barrier integrity in Alzheimer's disease. *Curr Gerontol Geriatr Res,* 2012**,** 184042.

BOYLES, J. K., PITAS, R. E., WILSON, E., MAHLEY, R. W. & TAYLOR, J. M. 1985. Apolipoprotein E associated with astrocytic glia of the central nervous system and with nonmyelinating glia of the peripheral nervous system. *J Clin Invest,* 76**,** 1501-13.

BRAAK, H. & BRAAK, E. 1991. Neuropathological stageing of Alzheimer-related changes. *Acta Neuropathol,* 82**,** 239-59.

BRAAK, H., BRAAK, E., GRUNDKE-IQBAL, I. & IQBAL, K. 1986. Occurrence of neuropil threads in the senile human brain and in Alzheimer's disease: a third location of paired helical filaments outside of neurofibrillary tangles and neuritic plaques. *Neurosci Lett,* 65**,** 351-5.

BRADLEY-WHITMAN, M. A. & LOVELL, M. A. 2015. Biomarkers of lipid peroxidation in Alzheimer disease (AD): an update. *Arch Toxicol,* 89**,** 1035-44.

BRANISTE, V., AL-ASMAKH, M., KOWAL, C., ANUAR, F., ABBASPOUR, A., TÓTH, M., KORECKA, A., BAKOCEVIC, N., NG, L. G., GUAN, N. L., KUNDU, P., GULYÁS, B., HALLDIN, C., HULTENBY, K., NILSSON, H., HEBERT, H., VOLPE, B. T., DIAMOND, B. & PETTERSSON, S. 2014. The gut microbiota influences blood-brain barrier permeability in mice. *Sci Transl Med,* 6**,** 263ra158.

BRASH, A. R. 1999. Lipoxygenases: occurrence, functions, catalysis, and acquisition of substrate. *J Biol Chem,* 274**,** 23679-82.

BRIGHTMAN, M. W. & REESE, T. S. 1969. Junctions between intimately apposed cell membranes in the vertebrate brain. *J Cell Biol,* 40**,** 648-77.

BRION, J.-P., PASSARIERO, H., NUNEZ, J. & FLAMENT-DURAND, J. 1985. Mise en évidence immunalogique de la protéine tau au niveau des lésions de dégénérescence neurofibrillaire de la maladie D'ALzheimer. *Biology Archives,* 95**,** 229-235.

BROADWELL, R. D. & SOFRONIEW, M. V. 1993. Serum proteins bypass the blood-brain fluid barriers for extracellular entry to the central nervous system. *Exp Neurol,* 120**,** 245-63.

BRODY, D. L., JIANG, H., WILDBURGER, N. & ESPARZA, T. J. 2017. Non-canonical soluble amyloid-beta aggregates and plaque buffering: controversies and future directions for target discovery in Alzheimer's disease. *Alzheimers Res Ther,* 9**,** 62.

BROWN, A. J. & ROBERTS, D. C. 1991. The effect of fasting triacylglyceride concentration and apolipoprotein E polymorphism on postprandial lipemia. *Arterioscler Thromb,* 11**,** 1737-44.

BROWN, M. W. & AGGLETON, J. P. 2001. Recognition memory: what are the roles of the perirhinal cortex and hippocampus? *Nat Rev Neurosci,* 2**,** 51-61.

BRYANT, C. D. 2011. The blessings and curses of C57BL/6 substrains in mouse genetic studies. *Ann N Y Acad Sci,* 1245**,** 31-3.

BU, G. 2009. Apolipoprotein E and its receptors in Alzheimer's disease: pathways, pathogenesis and therapy. *Nat Rev Neurosci,* 10**,** 333-44.

BUENO-HERNÁNDEZ, N., SIXTOS-ALONSO, M. S., MILKE GARCÍA, M. D. P. & YAMAMOTO-FURUSHO, J. K. 2017. Effect of Cis-palmitoleic acid supplementation on inflammation and expression of HNF4γ, HNF4α and IL6 in patients with ulcerative colitis. *Minerva Gastroenterol Dietol,* 63**,** 257-263.

BURGESS, B. L., MCISAAC, S. A., NAUS, K. E., CHAN, J. Y., TANSLEY, G. H., YANG, J., MIAO, F., ROSS, C. J., VAN ECK, M., HAYDEN, M. R., VAN NOSTRAND, W., ST GEORGE-HYSLOP, P., WESTAWAY, D. & WELLINGTON, C. L. 2006. Elevated plasma triglyceride levels precede amyloid deposition in Alzheimer's disease mouse models with abundant A beta in plasma. *Neurobiol Dis,* 24**,** 114-27.

BURKE, S. N., WALLACE, J. L., NEMATOLLAHI, S., UPRETY, A. R. & BARNES, C. A. 2010. Pattern separation deficits may contribute to age-associated recognition impairments. *Behav Neurosci,* 124**,** 559-73.

BYRDWELL, W. C. 2001. Atmospheric pressure chemical ionization mass spectrometry for analysis of lipids. *Lipids,* 36**,** 327-46.

CAI, X., PERTTULA, K., PAJOUH, S., HUBBARD, A., NOMURA, D. & RAPPAPORT, S. 2014. Untargeted Lipidomic Profiling of Human Plasma Reveals Differences due to Race, Gender and Smoking Status. *Metabolomics:Open Access* [Online], 4.

CANDELA, P., GOSSELET, F., MILLER, F., BUEE-SCHERRER, V., TORPIER, G., CECCHELLI, R. & FENART, L. 2008. Physiological pathway for low-density lipoproteins across the blood-brain barrier: transcytosis through brain capillary endothelial cells in vitro. *Endothelium,* 15**,** 254-64.

CAO, H., GERHOLD, K., MAYERS, J. R., WIEST, M. M., WATKINS, S. M. & HOTAMISLIGIL, G. S. 2008. Identification of a lipokine, a lipid hormone linking adipose tissue to systemic metabolism. *Cell,* 134**,** 933-44.

CARLSSON, C. M., GLEASON, C. E., HESS, T. M., MORELAND, K. A., BLAZEL, H. M., KOSCIK, R. L., SCHREIBER, N. T., JOHNSON, S. C., ATWOOD, C. S., PUGLIELLI, L., HERMANN, B. P.,

MCBRIDE, P. E., STEIN, J. H., SAGER, M. A. & ASTHANA, S. 2008. Effects of simvastatin on cerebrospinal fluid biomarkers and cognition in middle-aged adults at risk for Alzheimer's disease. *J Alzheimers Dis,* 13**,** 187-97.

CARRIÉ, I., CLÉMENT, M., DE JAVEL, D., FRANCÈS, H. & BOURRE, J. M. 2000. Specific phospholipid fatty acid composition of brain regions in mice. Effects of n-3 polyunsaturated fatty acid deficiency and phospholipid supplementation. *J Lipid Res,* 41**,** 465-72.

CASTLE, W. E. & LITTLE, C. C. 1910. ON A MODIFIED MENDELIAN RATIO AMONG YELLOW MICE. *Science,* 32**,** 868-70.

CAVEDO, E., DUBOIS, B., COLLIOT, O., LISTA, S., CROISILE, B., TISSERAND, G. L., TOUCHON, J., BONAFE, A., OUSSET, P. J., ROUAUD, O., RICOLFI, F., VIGHETTO, A., PASQUIER, F., GALLUZZI, S., DELMAIRE, C., CECCALDI, M., GIRARD, N., LEHERICY, S., DUVEAU, F., CHUPIN, M., SARAZIN, M., DORMONT, D., HAMPEL, H. & GROUP, H. S. 2016. Reduced Regional Cortical Thickness Rate of Change in Donepezil-Treated Subjects With Suspected Prodromal Alzheimer's Disease. *J Clin Psychiatry,* 77**,** e1631-e1638.

CAVEDO, E., GROTHE, M. J., COLLIOT, O., LISTA, S., CHUPIN, M., DORMONT, D., HOUOT, M., LEHÉRICY, S., TEIPEL, S., DUBOIS, B., HAMPEL, H. & GROUP, H. S. 2017. Reduced basal forebrain atrophy progression in a randomized Donepezil trial in prodromal Alzheimer's disease. *Sci Rep,* 7**,** 11706.

CHAN, R. B., OLIVEIRA, T. G., CORTES, E. P., HONIG, L. S., DUFF, K. E., SMALL, S. A., WENK, M. R., SHUI, G. & DI PAOLO, G. 2012. Comparative lipidomic analysis of mouse and human brain with Alzheimer disease. *J Biol Chem,* 287**,** 2678-88.

CHATTERJEE, P., LIM, W. L., SHUI, G., GUPTA, V. B., JAMES, I., FAGAN, A. M., XIONG, C., SOHRABI, H. R., TADDEI, K., BROWN, B. M., BENZINGER, T., MASTERS, C., SNOWDEN, S. G., WENK, M. R., BATEMAN, R. J., MORRIS, J. C. & MARTINS, R. N. 2016. Plasma Phospholipid and Sphingolipid Alterations in Presenilin1 Mutation Carriers: A Pilot Study. *J Alzheimers Dis,* 50**,** 887-94.

CHECA, A., BEDIA, C. & JAUMOT, J. 2015. Lipidomic data analysis: tutorial, practical guidelines and applications. *Anal Chim Acta,* 885**,** 1-16.

CHEN, J., KANAI, Y., COWAN, N. J. & HIROKAWA, N. 1992. Projection domains of MAP2 and tau determine spacings between microtubules in dendrites and axons. *Nature,* 360**,** 674-7.

CHEN, J., LI, Q. & WANG, J. 2011. Topology of human apolipoprotein E3 uniquely regulates its diverse biological functions. *Proc Natl Acad Sci U S A,* 108**,** 14813-8.

CHEN, X. S., KURRE, U., JENKINS, N. A., COPELAND, N. G. & FUNK, C. D. 1994. cDNA cloning, expression, mutagenesis of C-terminal isoleucine, genomic structure, and chromosomal localizations of murine 12-lipoxygenases. *J Biol Chem,* 269**,** 13979-87.

CHEN, Y., MA, Z., SHEN, X., LI, L., ZHONG, J., MIN, L. S., XU, L., LI, H., ZHANG, J. & DAI, L. 2018. Serum Lipidomics Profiling to Identify Biomarkers for Non-Small Cell Lung Cancer. *Biomed Res Int,* 2018**,** 5276240.

CHENG, H., WANG, M., LI, J. L., CAIRNS, N. J. & HAN, X. 2013. Specific changes of sulfatide levels in individuals with pre-clinical Alzheimer's disease: an early event in disease pathogenesis. *J Neurochem,* 127**,** 733-8.

CHENG, H., ZHOU, Y., HOLTZMAN, D. M. & HAN, X. 2010. Apolipoprotein E mediates sulfatide depletion in animal models of Alzheimer's disease. *Neurobiol Aging,* 31**,** 1188-96.

CHINNICI, C. M., YAO, Y., DING, T., FUNK, C. D. & PRATICO, D. 2005. Absence of 12/15 lipoxygenase reduces brain oxidative stress in apolipoprotein E-deficient mice. *Am J Pathol,* 167**,** 1371-7.

CHO, B. P., SONG, D. Y., SUGAMA, S., SHIN, D. H., SHIMIZU, Y., KIM, S. S., KIM, Y. S. & JOH, T. H. 2006. Pathological dynamics of activated microglia following medial forebrain bundle transection. *Glia,* 53**,** 92-102.

CHOW, V. W., MATTSON, M. P., WONG, P. C. & GLEICHMANN, M. 2010. An overview of APP processing enzymes and products. *Neuromolecular Med,* 12**,** 1-12.

CHU, C. S., TSENG, P. T., STUBBS, B., CHEN, T. Y., TANG, C. H., LI, D. J., YANG, W. C., CHEN, Y. W., WU, C. K., VERONESE, N., CARVALHO, A. F., FERNANDES, B. S., HERRMANN, N. & LIN, P. Y. 2018. Use of statins and the risk of dementia and mild cognitive impairment: A systematic review and meta-analysis. *Sci Rep,* 8**,** 5804.

CHU, J., LI, J. G., GIANNOPOULOS, P. F., BLASS, B. E., CHILDERS, W., ABOU-GHARBIA, M. & PRATICÒ, D. 2015. Pharmacologic blockade of 12/15-lipoxygenase ameliorates memory deficits, Aβ and tau neuropathology in the triple-transgenic mice. *Mol Psychiatry,* 20**,** 1329-38.

COLEMAN, T., SEIP, R. L., GIMBLE, J. M., LEE, D., MAEDA, N. & SEMENKOVICH, C. F. 1995. COOH-terminal disruption of lipoprotein lipase in mice is lethal in homozygotes, but heterozygotes have elevated triglycerides and impaired enzyme activity. *J Biol Chem,* 270**,** 12518-25.

COLTON, C. A. 2009. Heterogeneity of microglial activation in the innate immune response in the brain. *J Neuroimmune Pharmacol,* 4**,** 399-418.

COLTON, C. A., MOTT, R. T., SHARPE, H., XU, Q., VAN NOSTRAND, W. E. & VITEK, M. P. 2006. Expression profiles for macrophage alternative activation genes in AD and in mouse models of AD. *J Neuroinflammation,* 3**,** 27.

COOPER, J. A., MILLER, G. J. & HUMPHRIES, S. E. 2005. A comparison of the PROCAM and Framingham point-scoring systems for estimation of individual risk of coronary heart disease in the Second Northwick Park Heart Study. *Atherosclerosis,* 181**,** 93-100.

CORDER, E. H., SAUNDERS, A. M., RISCH, N. J., STRITTMATTER, W. J., SCHMECHEL, D. E., GASKELL, P. C., RIMMLER, J. B., LOCKE, P. A., CONNEALLY, P. M. & SCHMADER, K. E. 1994. Protective effect of apolipoprotein E type 2 allele for late onset Alzheimer disease. *Nat Genet,* 7**,** 180-4.

CORDER, E. H., SAUNDERS, A. M., STRITTMATTER, W. J., SCHMECHEL, D. E., GASKELL, P. C., SMALL, G. W., ROSES, A. D., HAINES, J. L. & PERICAK-VANCE, M. A. 1993. Gene dose of apolipoprotein E type 4 allele and the risk of Alzheimer's disease in late onset families. *Science,* 261**,** 921-3.

COREY-BLOOM, J., ANAND, R. & VEACH, J. 1998. A randomized trial evaluating the efficacy and safety of ENA 713 (rivastigmine tartrate), a new acetylcholinesterase inhibitor, in patients with mild to moderately severe Alzheimer's disease. International Journal of Geriatric Psychopharmacology.

COSTANTINI, L. C., BARR, L. J., VOGEL, J. L. & HENDERSON, S. T. 2008. Hypometabolism as a therapeutic target in Alzheimer's disease. *BMC Neurosci,* 9 Suppl 2**,** S16.

COWBURN, R., HARDY, J., ROBERTS, P. & BRIGGS, R. 1988. Regional distribution of pre- and postsynaptic glutamatergic function in Alzheimer's disease. *Brain Res,* 452**,** 403-7.

CRIBBS, D. H., BERCHTOLD, N. C., PERREAU, V., COLEMAN, P. D., ROGERS, J., TENNER, A. J. & COTMAN, C. W. 2012. Extensive innate immune gene activation accompanies brain

aging, increasing vulnerability to cognitive decline and neurodegeneration: a microarray study. *J Neuroinflammation,* 9**,** 179.

CUTLER, R. G., KELLY, J., STORIE, K., PEDERSEN, W. A., TAMMARA, A., HATANPAA, K., TRONCOSO, J. C. & MATTSON, M. P. 2004. Involvement of oxidative stress-induced abnormalities in ceramide and cholesterol metabolism in brain aging and Alzheimer's disease. *Proc Natl Acad Sci U S A,* 101**,** 2070-5.

DALLONGEVILLE, J., LUSSIER-CACAN, S. & DAVIGNON, J. 1992. Modulation of plasma triglyceride levels by apoE phenotype: a meta-analysis. *Journal of Lipid Research,* 33**,** 447-454.

DANI, J. A. 2015. Neuronal Nicotinic Acetylcholine Receptor Structure and Function and Response to Nicotine. *Int Rev Neurobiol,* 124**,** 3-19.

DE ALMEIDA, R. F., FEDOROV, A. & PRIETO, M. 2003. Sphingomyelin/phosphatidylcholine/cholesterol phase diagram: boundaries and composition of lipid rafts. *Biophys J,* 85**,** 2406-16.

DE LEON, M. J., CONVIT, A., WOLF, O. T., TARSHISH, C. Y., DESANTI, S., RUSINEK, H., TSUI, W., KANDIL, E., SCHERER, A. J., ROCHE, A., IMOSSI, A., THORN, E., BOBINSKI, M., CARAOS, C., LESBRE, P., SCHLYER, D., POIRIER, J., REISBERG, B. & FOWLER, J. 2001. Prediction of cognitive decline in normal elderly subjects with 2-[(18)F]fluoro-2-deoxy-D-glucose/poitron-emission tomography (FDG/PET). *Proc Natl Acad Sci U S A,* 98**,** 10966-71.

DE STROOPER, B., SAFTIG, P., CRAESSAERTS, K., VANDERSTICHELE, H., GUHDE, G., ANNAERT, W., VON FIGURA, K. & VAN LEUVEN, F. 1998. Deficiency of presenilin-1 inhibits the normal cleavage of amyloid precursor protein. *Nature,* 391**,** 387-90.

DECOSTANZO, A. J., VOLOSHYNA, I., ROSEN, Z. B., FEINMARK, S. J. & SIEGELBAUM, S. A. 2010. 12-Lipoxygenase regulates hippocampal long-term potentiation by modulating L-type Ca2+ channels. *J Neurosci,* 30**,** 1822-31.

DEHOUCK, B., FENART, L., DEHOUCK, M. P., PIERCE, A., TORPIER, G. & CECCHELLI, R. 1997. A new function for the LDL receptor: transcytosis of LDL across the blood-brain barrier. *J Cell Biol,* 138**,** 877-89.

DELNOMDEDIEU, M., DUVVURI, S., LI, D. J., ATASSI, N., LU, M., BRASHEAR, H. R., LIU, E., NESS, S. & KUPIEC, J. W. 2016. First-In-Human safety and long-term exposure data for AAB-003 (PF-05236812) and biomarkers after intravenous infusions of escalating doses in patients with mild to moderate Alzheimer's disease. *Alzheimers Res Ther,* 8**,** 12.

DI GAUDIO, F., INDELICATO, S., MONASTERO, R., ALTIERI, G. I., FAYER, F., PALESANO, O., FONTANA, M., CEFALÙ, A. B., GRECO, M., BONGIORNO, D., ARONICA, A., NOTO, D. & AVERNA, M. R. 2016. FragClust and TestClust, two informatics tools for chemical structure hierarchical clustering analysis applied to lipidomics. The example of Alzheimer's disease. *Anal Bioanal Chem,* 408**,** 2215-26.

DI MECO, A., LI, J. G., BLASS, B. E., ABOU-GHARBIA, M., LAURETTI, E. & PRATICO, D. 2017. 12/15-Lipoxygenase Inhibition Reverses Cognitive Impairment, Brain Amyloidosis, and Tau Pathology by Stimulating Autophagy in Aged Triple Transgenic Mice. *Biol Psychiatry,* 81**,** 92-100.

DICKSON, D. W., FARLO, J., DAVIES, P., CRYSTAL, H., FULD, P. & YEN, S. H. 1988. Alzheimer's disease. A double-labeling immunohistochemical study of senile plaques. *Am J Pathol,* 132**,** 86-101.

DOBRIAN, A. D., LIEB, D. C., COLE, B. K., TAYLOR-FISHWICK, D. A., CHAKRABARTI, S. K. & NADLER, J. L. 2011. Functional and pathological roles of the 12- and 15-lipoxygenases. *Prog Lipid Res,* 50**,** 115-31.

DONG, Y. & BENVENISTE, E. N. 2001. Immune function of astrocytes. *Glia,* 36**,** 180-90.

DOODY, R. S., THOMAS, R. G., FARLOW, M., IWATSUBO, T., VELLAS, B., JOFFE, S., KIEBURTZ, K., RAMAN, R., SUN, X., AISEN, P. S., SIEMERS, E., LIU-SEIFERT, H., MOHS, R., COMMITTEE, A. S. D. C. S. S. & GROUP, S. S. 2014. Phase 3 trials of solanezumab for mild-to-moderate Alzheimer's disease. *N Engl J Med,* 370**,** 311-21.

DORMAN, R. V., HAMM, T. F., DAMRON, D. S. & FREEMAN, E. J. 1992. Modulation of glutamate release from hippocampal mossy fiber nerve endings by arachidonic acid and eicosanoids. *Adv Exp Med Biol,* 318**,** 121-36.

DREWES, G., TRINCZEK, B., ILLENBERGER, S., BIERNAT, J., SCHMITT-ULMS, G., MEYER, H. E., MANDELKOW, E. M. & MANDELKOW, E. 1995. Microtubule-associated protein/microtubule affinity-regulating kinase (p110mark). A novel protein kinase that regulates tau-microtubule interactions and dynamic instability by phosphorylation at the Alzheimer-specific site serine 262. *J Biol Chem,* 270**,** 7679-88.

DRIN, G. 2014. Topological regulation of lipid balance in cells. *Annu Rev Biochem,* 83**,** 51-77.

DRZEZGA, A., GRIMMER, T., HENRIKSEN, G., MÜHLAU, M., PERNECZKY, R., MIEDERER, I., PRAUS, C., SORG, C., WOHLSCHLÄGER, A., RIEMENSCHNEIDER, M., WESTER, H. J., FOERSTL, H., SCHWAIGER, M. & KURZ, A. 2009. Effect of APOE genotype on amyloid plaque load and gray matter volume in Alzheimer disease. *Neurology,* 72**,** 1487-94.

DUNN, H. C., AGER, R. R., BAGLIETTO-VARGAS, D., CHENG, D., KITAZAWA, M., CRIBBS, D. H. & MEDEIROS, R. 2015. Restoration of lipoxin A4 signaling reduces Alzheimer's disease-like pathology in the 3xTg-AD mouse model. *J Alzheimers Dis,* 43**,** 893-903.

EHEHALT, R., KELLER, P., HAASS, C., THIELE, C. & SIMONS, K. 2003. Amyloidogenic processing of the Alzheimer beta-amyloid precursor protein depends on lipid rafts. *J Cell Biol,* 160**,** 113-23.

EL KHOURY, J. B., MOORE, K. J., MEANS, T. K., LEUNG, J., TERADA, K., TOFT, M., FREEMAN, M. W. & LUSTER, A. D. 2003. CD36 mediates the innate host response to beta-amyloid. *J Exp Med,* 197**,** 1657-66.

EL-AMOURI, S. S., ZHU, H., YU, J., MARR, R., VERMA, I. M. & KINDY, M. S. 2008. Neprilysin: an enzyme candidate to slow the progression of Alzheimer's disease. *Am J Pathol,* 172**,** 1342-54.

ELDER, G. A., GAMA SOSA, M. A. & DE GASPERI, R. 2010. Transgenic mouse models of Alzheimer's disease. *Mt Sinai J Med,* 77**,** 69-81.

ENGELHARDT, B. & RANSOHOFF, R. M. 2012. Capture, crawl, cross: the T cell code to breach the blood-brain barriers. *Trends Immunol,* 33**,** 579-89.

EVANS, K., MITCHESON, J. & LAKER, M. F. 1997. Effect of storage at -70 degrees C on lipid, lipoprotein and apolipoprotein concentrations. *Clin Chim Acta,* 258**,** 219-29.

FAHY, E., ALVAREZ-JARRETA, J., BRASHER, C. J., NGUYEN, A., HAWKSWORTH, J. I., RODRIGUES, P., MECKELMANN, S., ALLEN, S. M. & O'DONNELL, V. B. 2018. LipidFinder on LIPID MAPS: peak filtering, MS searching and statistical analysis for lipidomics. *Bioinformatics*.

FAHY, E., COTTER, D., BYRNES, R., SUD, M., MAER, A., LI, J., NADEAU, D., ZHAU, Y. & SUBRAMANIAM, S. 2007. Bioinformatics for Lipidomics. *In:* BROWN, H. A. (ed.) *Lipidomics and Bioactive Lipids: Mass Spectrometry Based Lipid Analysis.* London, UK: Elsevier Science Publishing Co Inc.

FAHY, E., SUBRAMANIAM, S., BROWN, H. A., GLASS, C. K., MERRILL, A. H., JR., MURPHY, R. C., RAETZ, C. R., RUSSELL, D. W., SEYAMA, Y., SHAW, W., SHIMIZU, T., SPENER, F., VAN MEER, G., VANNIEUWENHZE, M. S., WHITE, S. H., WITZTUM, J. L. & DENNIS, E. A. 2005. A comprehensive classification system for lipids. *J Lipid Res,* 46**,** 839-61.

FAHY, E., SUBRAMANIAM, S., MURPHY, R. C., NISHIJIMA, M., RAETZ, C. R., SHIMIZU, T., SPENER, F., VAN MEER, G., WAKELAM, M. J. & DENNIS, E. A. 2009. Update of the LIPID MAPS comprehensive classification system for lipids. *J Lipid Res,* 50 Suppl**,** S9-14.

FARLOW, M., ARNOLD, S. E., VAN DYCK, C. H., AISEN, P. S., SNIDER, B. J., PORSTEINSSON, A. P., FRIEDRICH, S., DEAN, R. A., GONZALES, C., SETHURAMAN, G., DEMATTOS, R. B., MOHS, R., PAUL, S. M. & SIEMERS, E. R. 2012. Safety and biomarker effects of solanezumab in patients with Alzheimer's disease. *Alzheimers Dement,* 8**,** 261-71.

FASSBENDER, K., SIMONS, M., BERGMANN, C., STROICK, M., LUTJOHANN, D., KELLER, P., RUNZ, H., KUHL, S., BERTSCH, T., VON BERGMANN, K., HENNERICI, M., BEYREUTHER, K. & HARTMANN, T. 2001. Simvastatin strongly reduces levels of Alzheimer's disease beta -amyloid peptides Abeta 42 and Abeta 40 in vitro and in vivo. *Proc Natl Acad Sci U S A,* 98**,** 5856-61.

FEINMARK, S. J., BEGUM, R., TSVETKOV, E., GOUSSAKOV, I., FUNK, C. D., SIEGELBAUM, S. A. & BOLSHAKOV, V. Y. 2003. 12-lipoxygenase metabolites of arachidonic acid mediate metabotropic glutamate receptor-dependent long-term depression at hippocampal CA3-CA1 synapses. *J Neurosci,* 23**,** 11427-35.

FELDMAN, H. H., DOODY, R. S., KIVIPELTO, M., SPARKS, D. L., WATERS, D. D., JONES, R. W., SCHWAM, E., SCHINDLER, R., HEY-HADAVI, J., DEMICCO, D. A., BREAZNA, A. & INVESTIGATORS, L. 2010. Randomized controlled trial of atorvastatin in mild to moderate Alzheimer disease: LEADe. *Neurology,* 74**,** 956-64.

FILIPELLO, F., MORINI, R., CORRADINI, I., ZERBI, V., CANZI, A., MICHALSKI, B., ERRENI, M., MARKICEVIC, M., STARVAGGI-CUCUZZA, C., OTERO, K., PICCIO, L., CIGNARELLA, F., PERRUCCI, F., TAMBORINI, M., GENUA, M., RAJENDRAN, L., MENNA, E., VETRANO, S., FAHNESTOCK, M., PAOLICELLI, R. C. & MATTEOLI, M. 2018. The Microglial Innate Immune Receptor TREM2 Is Required for Synapse Elimination and Normal Brain Connectivity. *Immunity,* 48**,** 979-991.e8.

FLANAGAN, L. A., CUNNINGHAM, C. C., CHEN, J., PRESTWICH, G. D., KOSIK, K. S. & JANMEY, P. A. 1997. The structure of divalent cation-induced aggregates of PIP2 and their alteration by gelsolin and tau. *Biophys J,* 73**,** 1440-7.

FLOEGEL, A., KÜHN, T., SOOKTHAI, D., JOHNSON, T., PREHN, C., ROLLE-KAMPCZYK, U., OTTO, W., WEIKERT, C., ILLIG, T., VON BERGEN, M., ADAMSKI, J., BOEING, H., KAAKS, R. & PISCHON, T. 2018. Serum metabolites and risk of myocardial infarction and ischemic stroke: a targeted metabolomic approach in two German prospective cohorts. *Eur J Epidemiol,* 33**,** 55-66.

FON, E. A. & EDWARDS, R. H. 2001. Molecular mechanisms of neurotransmitter release. *Muscle Nerve,* 24**,** 581-601.

FORD-HUTCHINSON, A. W., BRAY, M. A., DOIG, M. V., SHIPLEY, M. E. & SMITH, M. J. 1980. Leukotriene B, a potent chemokinetic and aggregating substance released from polymorphonuclear leukocytes. *Nature,* 286**,** 264-5.

FRIEDEN, C. 2015. ApoE: the role of conserved residues in defining function. *Protein Sci,* 24**,** 138-44.

FRIEDEN, C., WANG, H. & HO, C. M. W. 2017. A mechanism for lipid binding to apoE and the role of intrinsically disordered regions coupled to domain-domain interactions. *Proc Natl Acad Sci U S A,* 114**,** 6292-6297.

FROST, G. R. & LI, Y. M. 2017. The role of astrocytes in amyloid production and Alzheimer's disease. *Open Biol,* 7.

FUCHS, B., SÜSS, R. & SCHILLER, J. 2010. An update of MALDI-TOF mass spectrometry in lipid research. *Prog Lipid Res,* 49**,** 450-75.

FUENTES, D., FERNÁNDEZ, N., GARCÍA, Y., GARCÍA, T., MORALES, A. R. & MENÉNDEZ, R. 2018. Age-Related Changes in the Behavior of Apolipoprotein E Knockout Mice. *Behav Sci (Basel),* 8.

FUKUMOTO, H., CHEUNG, B. S., HYMAN, B. T. & IRIZARRY, M. C. 2002. Beta-secretase protein and activity are increased in the neocortex in Alzheimer disease. *Arch Neurol,* 59**,** 1381-9.

FURUKAWA, K., SOPHER, B. L., RYDEL, R. E., BEGLEY, J. G., PHAM, D. G., MARTIN, G. M., FOX, M. & MATTSON, M. P. 1996. Increased activity-regulating and neuroprotective efficacy of alpha-secretase-derived secreted amyloid precursor protein conferred by a C-terminal heparin-binding domain. *J Neurochem,* 67**,** 1882-96.

GAO, H. L., ZHANG, A. H., YU, J. B., SUN, H., KONG, L., WANG, X. Q., YAN, G. L., LIU, L. & WANG, X. J. 2018. High-throughput lipidomics characterize key lipid molecules as potential therapeutic targets of Kaixinsan protects against Alzheimer's disease in APP/PS1 transgenic mice. *J Chromatogr B Analyt Technol Biomed Life Sci,* 1092**,** 286-295.

GEIFMAN, N., BRINTON, R. D., KENNEDY, R. E., SCHNEIDER, L. S. & BUTTE, A. J. 2017. Evidence for benefit of statins to modify cognitive decline and risk in Alzheimer's disease. *Alzheimers Res Ther,* 9**,** 10.

GEISTERFER-LOWRANCE, A. A., CHRISTE, M., CONNER, D. A., INGWALL, J. S., SCHOEN, F. J., SEIDMAN, C. E. & SEIDMAN, J. G. 1996. A mouse model of familial hypertrophic cardiomyopathy. *Science,* 272**,** 731-4.

GETZ, G. S. & REARDON, C. A. 2009. Apoprotein E as a lipid transport and signaling protein in the blood, liver, and artery wall. *J Lipid Res,* 50 Suppl**,** S156-61.

GEULA, C., MESULAM, M. M., SAROFF, D. M. & WU, C. K. 1998. Relationship between plaques, tangles, and loss of cortical cholinergic fibers in Alzheimer disease. *J Neuropathol Exp Neurol,* 57**,** 63-75.

GHAYEE, H. K. & AUCHUS, R. J. 2007. Basic concepts and recent developments in human steroid hormone biosynthesis. *Rev Endocr Metab Disord,* 8**,** 289-300.

GIACOBINI, E. 2001. Is anti-cholinesterase therapy of Alzheimer's disease delaying progression? *Aging (Milano),* 13**,** 247-54.

GIANNOPOULOS, P. F., JOSHI, Y. B., CHU, J. & PRATICÒ, D. 2013. The 12-15-lipoxygenase is a modulator of Alzheimer's-related tau pathology in vivo. *Aging Cell,* 12**,** 1082-90.

GILMAN, S., KOLLER, M., BLACK, R. S., JENKINS, L., GRIFFITH, S. G., FOX, N. C., EISNER, L., KIRBY, L., ROVIRA, M. B., FORETTE, F., ORGOGOZO, J. M. & TEAM, A. Q.-.-S. 2005. Clinical effects of Abeta immunization (AN1792) in patients with AD in an interrupted trial. *Neurology,* 64**,** 1553-62.

GLENNER, G. G. & WONG, C. W. 1984. Alzheimer's disease: initial report of the purification and characterization of a novel cerebrovascular amyloid protein. *Biochem Biophys Res Commun,* 120**,** 885-90.

GOATE, A., CHARTIER-HARLIN, M. C., MULLAN, M., BROWN, J., CRAWFORD, F., FIDANI, L., GIUFFRA, L., HAYNES, A., IRVING, N. & JAMES, L. 1991. Segregation of a missense

mutation in the amyloid precursor protein gene with familial Alzheimer's disease. *Nature,* 349**,** 704-6.

GONG, J. S., KOBAYASHI, M., HAYASHI, H., ZOU, K., SAWAMURA, N., FUJITA, S. C., YANAGISAWA, K. & MICHIKAWA, M. 2002. Apolipoprotein E (ApoE) isoform-dependent lipid release from astrocytes prepared from human ApoE3 and ApoE4 knock-in mice. *J Biol Chem,* 277**,** 29919-26.

GONG, Y., CHANG, L., VIOLA, K. L., LACOR, P. N., LAMBERT, M. P., FINCH, C. E., KRAFFT, G. A. & KLEIN, W. L. 2003. Alzheimer's disease-affected brain: presence of oligomeric A beta ligands (ADDLs) suggests a molecular basis for reversible memory loss. *Proc Natl Acad Sci U S A,* 100**,** 10417-22.

GONZÁLEZ-DOMÍNGUEZ, R., GARCÍA-BARRERA, T. & GÓMEZ-ARIZA, J. L. 2014. Metabolomic study of lipids in serum for biomarker discovery in Alzheimer's disease using direct infusion mass spectrometry. *J Pharm Biomed Anal,* 98**,** 321-6.

GORDON, I., GRAUER, E., GENIS, I., SEHAYEK, E. & MICHAELSON, D. M. 1995. Memory deficits and cholinergic impairments in apolipoprotein E-deficient mice. *Neurosci Lett,* 199**,** 1-4.

GORDON, J. W., SCANGOS, G. A., PLOTKIN, D. J., BARBOSA, J. A. & RUDDLE, F. H. 1980. Genetic transformation of mouse embryos by microinjection of purified DNA. *Proc Natl Acad Sci U S A,* 77**,** 7380-4.

GOSSLER, A., DOETSCHMAN, T., KORN, R., SERFLING, E. & KEMLER, R. 1986. Transgenesis by means of blastocyst-derived embryonic stem cell lines. *Proc Natl Acad Sci U S A,* 83**,** 9065-9.

GRANGER, M. W., LIU, H., FOWLER, C. F., BLANCHARD, A. P., TAYLOR, M., SHERMAN, S. P. M., XU, H., LE, W. & BENNETT, S. A. L. 2018. Distinct disruptions in Land's cycle remodeling of glycerophosphocholines in murine cortex mark symptomatic onset and progression in two Alzheimer's Disease mouse models. *J Neurochem*.

GREENAMYRE, J. T., PENNEY, J. B., YOUNG, A. B., D'AMATO, C. J., HICKS, S. P. & SHOULSON, I. 1985. Alterations in L-glutamate binding in Alzheimer's and Huntington's diseases. *Science,* 227**,** 1496-9.

GRIFFIN, W. S., SHENG, J. G., ROBERTS, G. W. & MRAK, R. E. 1995. Interleukin-1 expression in different plaque types in Alzheimer's disease: significance in plaque evolution. *J Neuropathol Exp Neurol,* 54**,** 276-81.

GRIFFIN, W. S., STANLEY, L. C., LING, C., WHITE, L., MACLEOD, V., PERROT, L. J., WHITE, C. L. & ARAOZ, C. 1989. Brain interleukin 1 and S-100 immunoreactivity are elevated in Down syndrome and Alzheimer disease. *Proc Natl Acad Sci U S A,* 86**,** 7611-5.

GRIMM, M. O., GRIMM, H. S., PÄTZOLD, A. J., ZINSER, E. G., HALONEN, R., DUERING, M., TSCHÄPE, J. A., DE STROOPER, B., MÜLLER, U., SHEN, J. & HARTMANN, T. 2005. Regulation of cholesterol and sphingomyelin metabolism by amyloid-beta and presenilin. *Nat Cell Biol,* 7**,** 1118-23.

GROUP, A. S. D. C. 1995. The structure of the presenilin 1 (S182) gene and identification of six novel mutations in early onset AD families. *Nat Genet,* 11**,** 219-22.

GRZYBEK, M., PALLADINI, A., ALEXAKI, V. I., SURMA, M. A., SIMONS, K., CHAVAKIS, T., KLOSE, C. & COSKUN, Ü. 2019. Comprehensive and quantitative analysis of white and brown adipose tissue by shotgun lipidomics. *Mol Metab,* 22**,** 12-20.

GUO, X., LI, H., XU, H., HALIM, V., ZHANG, W., WANG, H., ONG, K. T., WOO, S. L., WALZEM, R. L., MASHEK, D. G., DONG, H., LU, F., WEI, L., HUO, Y. & WU, C. 2012. Palmitoleate

induces hepatic steatosis but suppresses liver inflammatory response in mice. *PLoS One,* 7**,** e39286.
HAMANO, T., YEN, S. H., GENDRON, T., KO, L. W. & KURIYAMA, M. 2012. Pitavastatin decreases tau levels via the inactivation of Rho/ROCK. *Neurobiol Aging,* 33**,** 2306-20.
HAMMAD, S. M., PIERCE, J. S., SOODAVAR, F., SMITH, K. J., AL GADBAN, M. M., REMBIESA, B., KLEIN, R. L., HANNUN, Y. A., BIELAWSKI, J. & BIELAWSKA, A. 2010. Blood sphingolipidomics in healthy humans: impact of sample collection methodology. *J Lipid Res,* 51**,** 3074-87.
HAMOSH, M. & SCOW, R. O. 1973. Lingual lipase and its role in the digestion of dietary lipid. *J Clin Invest,* 52**,** 88-95.
HAN, X. 2007. Potential mechanisms contributing to sulfatide depletion at the earliest clinically recognizable stage of Alzheimer's disease: a tale of shotgun lipidomics. *J Neurochem,* 103 Suppl 1**,** 171-9.
HAN, X. 2010. Multi-dimensional mass spectrometry-based shotgun lipidomics and the altered lipids at the mild cognitive impairment stage of Alzheimer's disease.
HAN, X., M HOLTZMAN, D., MCKEEL, D. W., KELLEY, J. & MORRIS, J. C. 2002a. Substantial sulfatide deficiency and ceramide elevation in very early Alzheimer's disease: potential role in disease pathogenesis. *J Neurochem,* 82**,** 809-18.
HAN, X., M HOLTZMAN, D., MCKEEL, D. W., KELLEY, J. & MORRIS, J. C. 2002b. Substantial sulfatide deficiency and ceramide elevation in very early Alzheimer's disease: potential role in disease pathogenesis. *J Neurochem,* 82**,** 809-18.
HAN, X., ROZEN, S., BOYLE, S. H., HELLEGERS, C., CHENG, H., BURKE, J. R., WELSH-BOHMER, K. A., DORAISWAMY, P. M. & KADDURAH-DAOUK, R. 2011. Metabolomics in early Alzheimer's disease: identification of altered plasma sphingolipidome using shotgun lipidomics. *PLoS One,* 6**,** e21643.
HANCOCK, S. E., FRIEDRICH, M. G., MITCHELL, T. W., TRUSCOTT, R. J. & ELSE, P. L. 2017. The phospholipid composition of the human entorhinal cortex remains relatively stable over 80 years of adult aging. *Geroscience,* 39**,** 73-82.
HANSEN, R. A., GARTLEHNER, G., WEBB, A. P., MORGAN, L. C., MOORE, C. G. & JONAS, D. E. 2008. Efficacy and safety of donepezil, galantamine, and rivastigmine for the treatment of Alzheimer's disease: a systematic review and meta-analysis. *Clin Interv Aging,* 3**,** 211-25.
HARA, A. & RADIN, N. S. 1978. Lipid extraction of tissues with a low-toxicity solvent. *Anal Biochem,* 90**,** 420-6.
HARDY, J. & ALLSOP, D. 1991. Amyloid deposition as the central event in the aetiology of Alzheimer's disease. *Trends Pharmacol Sci,* 12**,** 383-8.
HARVEY, D. J. 1995. Matrix-assisted Laser Desorption/Ionization Mass

Spectrometry of Phospholipids. *Journal of Mass Spectrometry,* 30.
HASHIMOTO, M., KAZUI, H., MATSUMOTO, K., NAKANO, Y., YASUDA, M. & MORI, E. 2005. Does donepezil treatment slow the progression of hippocampal atrophy in patients with Alzheimer's disease? *Am J Psychiatry,* 162**,** 676-82.
HAWE, E., TALMUD, P. J., MILLER, G. J., HUMPHRIES, S. E. & STUDY, S. N. P. H. 2003. Family history is a coronary heart disease risk factor in the Second Northwick Park Heart Study. *Ann Hum Genet,* 67**,** 97-106.
HE, X., HUANG, Y., LI, B., GONG, C. X. & SCHUCHMAN, E. H. 2010. Deregulation of sphingolipid metabolism in Alzheimer's disease. *Neurobiol Aging,* 31**,** 398-408.

HEITMANN, B. L. 1992. The effects of gender and age on associations between blood lipid levels and obesity in Danish men and women aged 35-65 years. *J Clin Epidemiol,* 45**,** 693-702.

HENEKA, M. T., CARSON, M. J., EL KHOURY, J., LANDRETH, G. E., BROSSERON, F., FEINSTEIN, D. L., JACOBS, A. H., WYSS-CORAY, T., VITORICA, J., RANSOHOFF, R. M., HERRUP, K., FRAUTSCHY, S. A., FINSEN, B., BROWN, G. C., VERKHRATSKY, A., YAMANAKA, K., KOISTINAHO, J., LATZ, E., HALLE, A., PETZOLD, G. C., TOWN, T., MORGAN, D., SHINOHARA, M. L., PERRY, V. H., HOLMES, C., BAZAN, N. G., BROOKS, D. J., HUNOT, S., JOSEPH, B., DEIGENDESCH, N., GARASCHUK, O., BODDEKE, E., DINARELLO, C. A., BREITNER, J. C., COLE, G. M., GOLENBOCK, D. T. & KUMMER, M. P. 2015. Neuroinflammation in Alzheimer's disease. *Lancet Neurol,* 14**,** 388-405.

HENSLEY, K. 2010. Neuroinflammation in Alzheimer's disease: mechanisms, pathologic consequences, and potential for therapeutic manipulation. *J Alzheimers Dis,* 21**,** 1-14.

HICKMAN, S. E., ALLISON, E. K. & EL KHOURY, J. 2008. Microglial dysfunction and defective beta-amyloid clearance pathways in aging Alzheimer's disease mice. *J Neurosci,* 28**,** 8354-60.

HIDAKA, H., HANYU, N., SUGANO, M., KAWASAKI, K., YAMAUCHI, K. & KATSUYAMA, T. 2007. Analysis of human serum lipoprotein lipid composition using MALDI-TOF mass spectrometry. *Ann Clin Lab Sci,* 37**,** 213-21.

HIRAI, M., AJITO, S., SATO, S., OHTA, N., IGARASHI, N. & SHIMIZU, N. 2018. Preferential Intercalation of Human Amyloid-β Peptide into Interbilayer Region of Lipid-Raft Membrane in Macromolecular Crowding Environment. *J Phys Chem B,* 122**,** 9482-9489.

HO, C. S., LAM, C. W., CHAN, M. H., CHEUNG, R. C., LAW, L. K., LIT, L. C., NG, K. F., SUEN, M. W. & TAI, H. L. 2003. Electrospray ionisation mass spectrometry: principles and clinical applications. *Clin Biochem Rev,* 24**,** 3-12.

HOKANSON, J. E. & AUSTIN, M. A. 1996. Plasma triglyceride level is a risk factor for cardiovascular disease independent of high-density lipoprotein cholesterol level: a meta-analysis of population-based prospective studies. *J Cardiovasc Risk,* 3**,** 213-9.

HOLMES, C., BOCHE, D., WILKINSON, D., YADEGARFAR, G., HOPKINS, V., BAYER, A., JONES, R. W., BULLOCK, R., LOVE, S., NEAL, J. W., ZOTOVA, E. & NICOLL, J. A. 2008. Long-term effects of Abeta42 immunisation in Alzheimer's disease: follow-up of a randomised, placebo-controlled phase I trial. *Lancet,* 372**,** 216-23.

HOLTZMAN, D. M., HERZ, J. & BU, G. 2012. Apolipoprotein E and apolipoprotein E receptors: normal biology and roles in Alzheimer disease. *Cold Spring Harb Perspect Med,* 2**,** a006312.

HOOVER, B. R., REED, M. N., SU, J., PENROD, R. D., KOTILINEK, L. A., GRANT, M. K., PITSTICK, R., CARLSON, G. A., LANIER, L. M., YUAN, L. L., ASHE, K. H. & LIAO, D. 2010. Tau mislocalization to dendritic spines mediates synaptic dysfunction independently of neurodegeneration. *Neuron,* 68**,** 1067-81.

HORNING, E. C. H., M. G. CARROLL, D. I. DZIDIC, I. STILLWELL, R. N. 1973. New picogram detection system based on a mass spectrometer with an external ionization source at atmospheric pressure. *Analytical Chemistry,* 45**,** 936-943.

HORROCKS, L. A. 1967. Composition of myelin from peripheral and central nervous systems of the squirrel monkey. *J Lipid Res,* 8**,** 569-76.

HOWARD, R. 2011. *Final trial report: Donepezil and memantine in moderate to severe Alzheimer's disease (DOMINO-AD)* [Online]. EU Clinical Trials Register: EU Clinical Trials Register. [Accessed 31st October 2018].

HOWARD, R., MCSHANE, R., LINDESAY, J., RITCHIE, C., BALDWIN, A., BARBER, R., BURNS, A., DENING, T., FINDLAY, D., HOLMES, C., HUGHES, A., JACOBY, R., JONES, R., MCKEITH, I., MACHAROUTHU, A., O'BRIEN, J., PASSMORE, P., SHEEHAN, B., JUSZCZAK, E., KATONA, C., HILLS, R., KNAPP, M., BALLARD, C., BROWN, R., BANERJEE, S., ONIONS, C., GRIFFIN, M., ADAMS, J., GRAY, R., JOHNSON, T., BENTHAM, P. & PHILLIPS, P. 2012. Donepezil and memantine for moderate-to-severe Alzheimer's disease. *N Engl J Med,* 366**,** 893-903.

HSIEH, C. L., KOIKE, M., SPUSTA, S. C., NIEMI, E. C., YENARI, M., NAKAMURA, M. C. & SEAMAN, W. E. 2009. A role for TREM2 ligands in the phagocytosis of apoptotic neuronal cells by microglia. *J Neurochem,* 109**,** 1144-56.

HU, Q., WANG, M., CHO, M. S., WANG, C., NICK, A. M., THIAGARAJAN, P., AUNG, F. M., HAN, X., SOOD, A. K. & AFSHAR-KHARGHAN, V. 2016. Lipid profile of platelets and platelet-derived microparticles in ovarian cancer. *BBA Clin,* 6**,** 76-81.

HUANG, Y., LIU, X. Q., RALL, S. C. & MAHLEY, R. W. 1998. Apolipoprotein E2 reduces the low density lipoprotein level in transgenic mice by impairing lipoprotein lipase-mediated lipolysis of triglyceride-rich lipoproteins. *J Biol Chem,* 273**,** 17483-90.

HUANG, Y. & MAHLEY, R. W. 2014. Apolipoprotein E: Structure and function in lipid metabolism, neurobiology, and Alzheimer's diseases. *Neurobiol Dis*.

HUBERTY, C. J. & MORRIS, J. D. 1989. Multivariate Analysis Versus Multiple Univariate Analyses. *Psychological Bulletin,* 105**,** 302-308.

HUMPHRIES, S. E., COOPER, J. A., TALMUD, P. J. & MILLER, G. J. 2007. Candidate gene genotypes, along with conventional risk factor assessment, improve estimation of coronary heart disease risk in healthy UK men. *Clin Chem,* 53**,** 8-16.

HÄNEL, P., ANDRÉANI, P. & GRÄLER, M. H. 2007. Erythrocytes store and release sphingosine 1-phosphate in blood. *FASEB J,* 21**,** 1202-9.

IFA, D. R., WU, C., OUYANG, Z. & COOKS, R. G. 2010. Desorption electrospray ionization and other ambient ionization methods: current progress and preview. *Analyst,* 135**,** 669-81.

IOFFE, E. & STANLEY, P. 1994. Mice lacking N-acetylglucosaminyltransferase I activity die at mid-gestation, revealing an essential role for complex or hybrid N-linked carbohydrates. *Proc Natl Acad Sci U S A,* 91**,** 728-32.

IQBAL, J., WALSH, M. T., HAMMAD, S. M., CUCHEL, M., TARUGI, P., HEGELE, R. A., DAVIDSON, N. O., RADER, D. J., KLEIN, R. L. & HUSSAIN, M. M. 2015. Microsomal Triglyceride Transfer Protein Transfers and Determines Plasma Concentrations of Ceramide and Sphingomyelin but Not Glycosylceramide. *J Biol Chem,* 290**,** 25863-75.

IQBAL, J., WALSH, M. T., HAMMAD, S. M. & HUSSAIN, M. M. 2017. Sphingolipids and Lipoproteins in Health and Metabolic Disorders. *Trends Endocrinol Metab,* 28**,** 506-518.

ISHII, M. & KURACHI, Y. 2006. Muscarinic acetylcholine receptors. *Curr Pharm Des,* 12**,** 3573-81.

ISHIKAWA, M., MAEKAWA, K., SAITO, K., SENOO, Y., URATA, M., MURAYAMA, M., TAJIMA, Y., KUMAGAI, Y. & SAITO, Y. 2014. Plasma and serum lipidomics of healthy white adults shows characteristic profiles by subjects' gender and age. *PLoS One,* 9**,** e91806.

IWATA, N., MIZUKAMI, H., SHIROTANI, K., TAKAKI, Y., MURAMATSU, S., LU, B., GERARD, N. P., GERARD, C., OZAWA, K. & SAIDO, T. C. 2004. Presynaptic localization of neprilysin contributes to efficient clearance of amyloid-beta peptide in mouse brain. *J Neurosci,* 24**,** 991-8.

IZQUIERDO, I., CAMMAROTA, M., DA SILVA, W. C., BEVILAQUA, L. R., ROSSATO, J. I., BONINI, J. S., MELLO, P., BENETTI, F., COSTA, J. C. & MEDINA, J. H. 2008. The evidence for hippocampal long-term potentiation as a basis of memory for simple tasks. *An Acad Bras Cienc,* 80**,** 115-27.

JAGELS, M. A. & HUGLI, T. E. 1992. Neutrophil chemotactic factors promote leukocytosis. A common mechanism for cellular recruitment from bone marrow. *J Immunol,* 148**,** 1119-28.

JENSEN, P. N., FRETTS, A. M., YU, C., HOOFNAGLE, A. N., UMANS, J. G., HOWARD, B. V., SITLANI, C. M., SISCOVICK, D. S., KING, I. B., SOTOODEHNIA, N., MCKNIGHT, B. & LEMAITRE, R. N. 2019. Circulating sphingolipids, fasting glucose, and impaired fasting glucose: The Strong Heart Family Study. *EBioMedicine,* 41**,** 44-49.

JHA, P., MCDEVITT, M. T., GUPTA, R., QUIROS, P. M., WILLIAMS, E. G., GARIANI, K., SLEIMAN, M. B., DISERENS, L., JOCHEM, A., ULBRICH, A., COON, J. J., AUWERX, J. & PAGLIARINI, D. J. 2018. Systems Analyses Reveal Physiological Roles and Genetic Regulators of Liver Lipid Species. *Cell Syst,* 6**,** 722-733.e6.

JOACHIM, C. L., DUFFY, L. K., MORRIS, J. H. & SELKOE, D. J. 1988. Protein chemical and immunocytochemical studies of meningovascular beta-amyloid protein in Alzheimer's disease and normal aging. *Brain Res,* 474**,** 100-11.

JOHNSON, J. W. & KOTERMANSKI, S. E. 2006. Mechanism of action of memantine. *Curr Opin Pharmacol,* 6**,** 61-7.

JONES, S. R., CARLEY, S. & HARRISON, M. 2003. An introduction to power and sample size estimation. *Emerg Med J,* 20**,** 453-8.

KAABIA, Z., POIRIER, J., MOUGHAIZEL, M., AGUESSE, A., BILLON-CROSSOUARD, S., FALL, F., DURAND, M., DAGHER, E., KREMPF, M. & CROYAL, M. 2018. Plasma lipidomic analysis reveals strong similarities between lipid fingerprints in human, hamster and mouse compared to other animal species. *Sci Rep,* 8**,** 15893.

KAMENETZ, F., TOMITA, T., HSIEH, H., SEABROOK, G., BORCHELT, D., IWATSUBO, T., SISODIA, S. & MALINOW, R. 2003. APP processing and synaptic function. *Neuron,* 37**,** 925-37.

KANAAN, N. M., MORFINI, G. A., LAPOINTE, N. E., PIGINO, G. F., PATTERSON, K. R., SONG, Y., ANDREADIS, A., FU, Y., BRADY, S. T. & BINDER, L. I. 2011. Pathogenic forms of tau inhibit kinesin-dependent axonal transport through a mechanism involving activation of axonal phosphotransferases. *J Neurosci,* 31**,** 9858-68.

KARAS, M., BACHMANN, D., BAHR, U. & HILLENKAMP, F. 1987. Matrix-assisted ultraviolet laser desorption of non-volatile compounds. *International Journal of Mass Spectrometry and Ion Processes,* 78**,** 53-68.

KAWARABAYASHI, T., SHOJI, M., YOUNKIN, L. H., WEN-LANG, L., DICKSON, D. W., MURAKAMI, T., MATSUBARA, E., ABE, K., ASHE, K. H. & YOUNKIN, S. G. 2004. Dimeric amyloid beta protein rapidly accumulates in lipid rafts followed by apolipoprotein E and phosphorylated tau accumulation in the Tg2576 mouse model of Alzheimer's disease. *J Neurosci,* 24**,** 3801-9.

KHRAMEEVA, E., KUROCHKIN, I., BOZEK, K., GIAVALISCO, P. & KHAITOVICH, P. 2018. Lipidome Evolution in Mammalian Tissues. *Mol Biol Evol,* 35**,** 1947-1957.

KIM, M. S., PINTO, S. M., GETNET, D., NIRUJOGI, R. S., MANDA, S. S., CHAERKADY, R., MADUGUNDU, A. K., KELKAR, D. S., ISSERLIN, R., JAIN, S., THOMAS, J. K., MUTHUSAMY, B., LEAL-ROJAS, P., KUMAR, P., SAHASRABUDDHE, N. A., BALAKRISHNAN, L., ADVANI, J., GEORGE, B., RENUSE, S., SELVAN, L. D., PATIL, A. H., NANJAPPA, V., RADHAKRISHNAN, A., PRASAD, S., SUBBANNAYYA, T., RAJU, R., KUMAR, M., SREENIVASAMURTHY, S. K., MARIMUTHU, A., SATHE, G. J., CHAVAN, S., DATTA, K. K., SUBBANNAYYA, Y., SAHU, A., YELAMANCHI, S. D., JAYARAM, S., RAJAGOPALAN, P., SHARMA, J., MURTHY, K. R., SYED, N., GOEL, R., KHAN, A. A., AHMAD, S., DEY, G., MUDGAL, K., CHATTERJEE, A., HUANG, T. C., ZHONG, J., WU, X., SHAW, P. G., FREED, D., ZAHARI, M. S., MUKHERJEE, K. K., SHANKAR, S., MAHADEVAN, A., LAM, H., MITCHELL, C. J., SHANKAR, S. K., SATISHCHANDRA, P., SCHROEDER, J. T., SIRDESHMUKH, R., MAITRA, A., LEACH, S. D., DRAKE, C. G., HALUSHKA, M. K., PRASAD, T. S., HRUBAN, R. H., KERR, C. L., BADER, G. D., IACOBUZIO-DONAHUE, C. A., GOWDA, H. & PANDEY, A. 2014. A draft map of the human proteome. *Nature,* 509**,** 575-81.

KIMOTO, A., OHNUMA, T., TODA, A., TAKEBAYASHI, Y., HIGASHIYAMA, R., TAGATA, Y., ITO, M., OTA, T., SHIBATA, N. & ARAI, H. 2017. Medium-chain triglycerides given in the early stage of mild-to-moderate Alzheimer's disease enhance memory function. *Psychogeriatrics,* 17**,** 520-521.

KING, R., BONFIGLIO, R., FERNANDEZ-METZLER, C., MILLER-STEIN, C. & OLAH, T. 2000. Mechanistic investigation of ionization suppression in electrospray ionization. *J Am Soc Mass Spectrom,* 11**,** 942-50.

KOBAYASHI, A., TAKANEZAWA, Y., HIRATA, T., SHIMIZU, Y., MISASA, K., KIOKA, N., ARAI, H., UEDA, K. & MATSUO, M. 2006. Efflux of sphingomyelin, cholesterol, and phosphatidylcholine by ABCG1. *J Lipid Res,* 47**,** 1791-802.

KOLDAMOVA, R., FITZ, N. F. & LEFTEROV, I. 2014. ATP-binding cassette transporter A1: from metabolism to neurodegeneration. *Neurobiol Dis,* 72 Pt A**,** 13-21.

KOPEIKINA, K. J., HYMAN, B. T. & SPIRES-JONES, T. L. 2012. Soluble forms of tau are toxic in Alzheimer's disease. *Transl Neurosci,* 3**,** 223-233.

KRIMBOU, L., DENIS, M., HAIDAR, B., CARRIER, M., MARCIL, M. & GENEST, J. 2004. Molecular interactions between apoE and ABCA1: impact on apoE lipidation. *J Lipid Res,* 45**,** 839-48.

KRONENBERG, F., LOBENTANZ, E. M., KONIG, P., UTERMANN, G. & DIEPLINGER, H. 1994. Effect of sample storage on the measurement of lipoprotein[a], apolipoproteins B and A-IV, total and high density lipoprotein cholesterol and triglycerides. *J Lipid Res,* 35**,** 1318-28.

KSIEZAK-REDING, H., LIU, W. K. & YEN, S. H. 1992. Phosphate analysis and dephosphorylation of modified tau associated with paired helical filaments. *Brain Res,* 597**,** 209-19.

KSIEZAK-REDING, H., PYO, H. K., FEINSTEIN, B. & PASINETTI, G. M. 2003. Akt/PKB kinase phosphorylates separately Thr212 and Ser214 of tau protein in vitro. *Biochim Biophys Acta,* 1639**,** 159-68.

KSIĄŻEK, M., CHACIŃSKA, M., CHABOWSKI, A. & BARANOWSKI, M. 2015. Sources, metabolism, and regulation of circulating sphingosine-1-phosphate. *J Lipid Res,* 56**,** 1271-81.

KUHN, H., BANTHIYA, S. & VAN LEYEN, K. 2015. Mammalian lipoxygenases and their biological relevance. *Biochim Biophys Acta,* 1851**,** 308-30.

KUMAR-SINGH, S., THEUNS, J., VAN BROECK, B., PIRICI, D., VENNEKENS, K., CORSMIT, E., CRUTS, M., DERMAUT, B., WANG, R. & VAN BROECKHOVEN, C. 2006. Mean age-of-

onset of familial alzheimer disease caused by presenilin mutations correlates with both increased Abeta42 and decreased Abeta40. *Hum Mutat,* 27**,** 686-95.

KUO, Y. M., EMMERLING, M. R., VIGO-PELFREY, C., KASUNIC, T. C., KIRKPATRICK, J. B., MURDOCH, G. H., BALL, M. J. & ROHER, A. E. 1996. Water-soluble Abeta (N-40, N-42) oligomers in normal and Alzheimer disease brains. *J Biol Chem,* 271**,** 4077-81.

KURATA, T., MIYAZAKI, K., KOZUKI, M., PANIN, V. L., MORIMOTO, N., OHTA, Y., NAGAI, M., IKEDA, Y., MATSUURA, T. & ABE, K. 2011. Atorvastatin and pitavastatin improve cognitive function and reduce senile plaque and phosphorylated tau in aged APP mice. *Brain Res,* 1371**,** 161-70.

KÖPKE, E., TUNG, Y. C., SHAIKH, S., ALONSO, A. C., IQBAL, K. & GRUNDKE-IQBAL, I. 1993. Microtubule-associated protein tau. Abnormal phosphorylation of a non-paired helical filament pool in Alzheimer disease. *J Biol Chem,* 268**,** 24374-84.

LAHIRI, S. & FUTERMAN, A. H. 2007. The metabolism and function of sphingolipids and glycosphingolipids. *Cell Mol Life Sci,* 64**,** 2270-84.

LANDER, E. S., LINTON, L. M., BIRREN, B., NUSBAUM, C., ZODY, M. C., BALDWIN, J., DEVON, K., DEWAR, K., DOYLE, M., FITZHUGH, W., FUNKE, R., GAGE, D., HARRIS, K., HEAFORD, A., HOWLAND, J., KANN, L., LEHOCZKY, J., LEVINE, R., MCEWAN, P., MCKERNAN, K., MELDRIM, J., MESIROV, J. P., MIRANDA, C., MORRIS, W., NAYLOR, J., RAYMOND, C., ROSETTI, M., SANTOS, R., SHERIDAN, A., SOUGNEZ, C., STANGE-THOMANN, N., STOJANOVIC, N., SUBRAMANIAN, A., WYMAN, D., ROGERS, J., SULSTON, J., AINSCOUGH, R., BECK, S., BENTLEY, D., BURTON, J., CLEE, C., CARTER, N., COULSON, A., DEADMAN, R., DELOUKAS, P., DUNHAM, A., DUNHAM, I., DURBIN, R., FRENCH, L., GRAFHAM, D., GREGORY, S., HUBBARD, T., HUMPHRAY, S., HUNT, A., JONES, M., LLOYD, C., MCMURRAY, A., MATTHEWS, L., MERCER, S., MILNE, S., MULLIKIN, J. C., MUNGALL, A., PLUMB, R., ROSS, M., SHOWNKEEN, R., SIMS, S., WATERSTON, R. H., WILSON, R. K., HILLIER, L. W., MCPHERSON, J. D., MARRA, M. A., MARDIS, E. R., FULTON, L. A., CHINWALLA, A. T., PEPIN, K. H., GISH, W. R., CHISSOE, S. L., WENDL, M. C., DELEHAUNTY, K. D., MINER, T. L., DELEHAUNTY, A., KRAMER, J. B., COOK, L. L., FULTON, R. S., JOHNSON, D. L., MINX, P. J., CLIFTON, S. W., HAWKINS, T., BRANSCOMB, E., PREDKI, P., RICHARDSON, P., WENNING, S., SLEZAK, T., DOGGETT, N., CHENG, J. F., OLSEN, A., LUCAS, S., ELKIN, C., UBERBACHER, E., FRAZIER, M., et al. 2001. Initial sequencing and analysis of the human genome. *Nature,* 409**,** 860-921.

LAUDER, S. N., TYRRELL, V. J., ALLEN-REDPATH, K., ALDROVANDI, M., GRAY, D., COLLINS, P., JONES, S. A., TAYLOR, P. R. & O'DONNELL, V. 2017. Myeloid 12/15-LOX regulates B cell numbers and innate immune antibody levels. *Wellcome Open Res,* 2**,** 1.

LEBEAU, A., TERRO, F., ROSTENE, W. & PELAPRAT, D. 2004. Blockade of 12-lipoxygenase expression protects cortical neurons from apoptosis induced by beta-amyloid peptide. *Cell Death Differ,* 11**,** 875-84.

LEE, C. Y. & LANDRETH, G. E. 2010. The role of microglia in amyloid clearance from the AD brain. *J Neural Transm (Vienna),* 117**,** 949-60.

LEE, J. Y., HAN, S. H., PARK, M. H., BAEK, B., SONG, I. S., CHOI, M. K., TAKUWA, Y., RYU, H., KIM, S. H., HE, X., SCHUCHMAN, E. H., BAE, J. S. & JIN, H. K. 2018. Neuronal SphK1 acetylates COX2 and contributes to pathogenesis in a model of Alzheimer's Disease. *Nat Commun,* 9**,** 1479.

LEE, L. L., AUNG, H. H., WILSON, D. W., ANDERSON, S. E., RUTLEDGE, J. C. & RUTKOWSKY, J. M. 2017. Triglyceride-rich lipoprotein lipolysis products increase blood-brain barrier

transfer coefficient and induce astrocyte lipid droplets and cell stress. *Am J Physiol Cell Physiol,* 312**,** C500-C516.

LEISSRING, M. A., FARRIS, W., CHANG, A. Y., WALSH, D. M., WU, X., SUN, X., FROSCH, M. P. & SELKOE, D. J. 2003. Enhanced proteolysis of beta-amyloid in APP transgenic mice prevents plaque formation, secondary pathology, and premature death. *Neuron,* 40**,** 1087-93.

LEMAITRE, R. N., YU, C., HOOFNAGLE, A., HARI, N., JENSEN, P. N., FRETTS, A. M., UMANS, J. G., HOWARD, B. V., SITLANI, C. M., SISCOVICK, D. S., KING, I. B., SOTOODEHNIA, N. & MCKNIGHT, B. 2018. Circulating Sphingolipids, Insulin, HOMA-IR, and HOMA-B: The Strong Heart Family Study. *Diabetes,* 67**,** 1663-1672.

LESBURGUERES, E., TSOKAS, P., SACKTOR, T. C. & FENTON, A. A. 2017. The Object Context-place-location Paradigm for Testing Spatial Memory in Mice. *Bio Protoc,* 7.

LEUTHOLD, P., SCHAEFFELER, E., WINTER, S., BÜTTNER, F., HOFMANN, U., MÜRDTER, T. E., RAUSCH, S., SONNTAG, D., WAHRHEIT, J., FEND, F., HENNENLOTTER, J., BEDKE, J., SCHWAB, M. & HAAG, M. 2017. Comprehensive Metabolomic and Lipidomic Profiling of Human Kidney Tissue: A Platform Comparison. *J Proteome Res,* 16**,** 933-944.

LI, G., MAYER, C. L., MORELLI, D., MILLARD, S. P., RASKIND, W. H., PETRIE, E. C., CHERRIER, M., FAGAN, A. M., RASKIND, M. A. & PESKIND, E. R. 2017. Effect of simvastatin on CSF Alzheimer disease biomarkers in cognitively normal adults. *Neurology,* 89**,** 1251-1255.

LI, J., HU, C., ZHAO, X., DAI, W., CHEN, S., LU, X. & XU, G. 2013. Large-scaled human serum sphingolipid profiling by using reversed-phase liquid chromatography coupled with dynamic multiple reaction monitoring of mass spectrometry: method development and application in hepatocellular carcinoma. *J Chromatogr A,* 1320**,** 103-10.

LI, R., XU, D. E. & MA, T. 2015. Lovastatin suppresses the aberrant tau phosphorylation from FTDP-17 mutation and okadaic acid-induction in rat primary neurons. *Neuroscience,* 294**,** 14-20.

LI, Y., MAHER, P. & SCHUBERT, D. 1997. A role for 12-lipoxygenase in nerve cell death caused by glutathione depletion. *Neuron,* 19**,** 453-63.

LIEBLER, D. C. & ZIMMERMAN, L. J. 2013. Targeted quantitation of proteins by mass spectrometry. *Biochemistry,* 52**,** 3797-806.

LILIENFELD, S. 2002. Galantamine--a novel cholinergic drug with a unique dual mode of action for the treatment of patients with Alzheimer's disease. *CNS Drug Rev,* 8**,** 159-76.

LILIENFELD, S. & PARYS, W. 2000. Galantamine: additional benefits to patients with Alzheimer's disease. *Dement Geriatr Cogn Disord,* 11 Suppl 1**,** 19-27.

LISTA, S., KHACHATURIAN, Z. S., RUJESCU, D., GARACI, F., DUBOIS, B. & HAMPEL, H. 2016. Application of Systems Theory in Longitudinal Studies on the Origin and Progression of Alzheimer's Disease. *Methods Mol Biol,* 1303**,** 49-67.

LIU, C., ZONG, W.-J., ZHANG, A.-H., ZHANG, H.-M., LUAN, Y.-H., SUN, H., CAO, H.-X. & WANG, X.-J. 2018. Lipidomic characterisation discovery for coronary heart disease diagnosis based on high-throughput ultra-performance liquid chromatography and mass spectrometry. *Royal Society of Chemistry Advances***,** 647-645.

LIU, X., LI, J., ZHENG, P., ZHAO, X., ZHOU, C., HU, C., HOU, X., WANG, H., XIE, P. & XU, G. 2016. Plasma lipidomics reveals potential lipid markers of major depressive disorder. *Anal Bioanal Chem,* 408**,** 6497-507.

LLADÓ, V., LÓPEZ, D. J., IBARGUREN, M., ALONSO, M., SORIANO, J. B., ESCRIBÁ, P. V. & BUSQUETS, X. 2014. Regulation of the cancer cell membrane lipid composition by

NaCHOleate: effects on cell signaling and therapeutical relevance in glioma. *Biochim Biophys Acta,* 1838**,** 1619-27.

LO SASSO, G., SCHLAGE, W. K., BOUÉ, S., VELJKOVIC, E., PEITSCH, M. C. & HOENG, J. 2016. The Apoe(-/-) mouse model: a suitable model to study cardiovascular and respiratory diseases in the context of cigarette smoke exposure and harm reduction. *J Transl Med,* 14**,** 146.

LOBO, A., LAUNER, L. J., FRATIGLIONI, L., ANDERSEN, K., DI CARLO, A., BRETELER, M. M., COPELAND, J. R., DARTIGUES, J. F., JAGGER, C., MARTINEZ-LAGE, J., SOININEN, H. & HOFMAN, A. 2000. Prevalence of dementia and major subtypes in Europe: A collaborative study of population-based cohorts. Neurologic Diseases in the Elderly Research Group. *Neurology,* 54**,** S4-9.

LU, F., LI, X., SUO, A. Q. & ZHANG, J. W. 2010. Inhibition of tau hyperphosphorylation and beta amyloid production in rat brain by oral administration of atorvastatin. *Chin Med J (Engl),* 123**,** 1864-70.

LU, M.-H., JI, W.-L., XU, D.-E., YAO, P.-P., ZHAO, X.-Y., WANG, Z.-T., FANG, L.-P., HUANG, R., LAN, L.-J., CHEN, J.-B., WANG, T.-H., CHENG, L.-H., XU, R.-X., LIU, C.-F., PUGLIELLI, L. & MA, Q.-H. 2019. Inhibition of sphingomyelin synthase 1 ameliorates alzheimer-like pathology in APP/PS1 transgenic mice through promoting lysosomal degradation of BACE1. *Experimental Neurology,* 311**,** 67-79.

LUC, G., BARD, J. M., ARVEILER, D., EVANS, A., CAMBOU, J. P., BINGHAM, A., AMOUYEL, P., SCHAFFER, P., RUIDAVETS, J. B. & CAMBIEN, F. 1994. Impact of apolipoprotein E polymorphism on lipoproteins and risk of myocardial infarction. The ECTIM Study. *Arterioscler Thromb,* 14**,** 1412-9.

LUE, L. F., KUO, Y. M., ROHER, A. E., BRACHOVA, L., SHEN, Y., SUE, L., BEACH, T., KURTH, J. H., RYDEL, R. E. & ROGERS, J. 1999. Soluble amyloid beta peptide concentration as a predictor of synaptic change in Alzheimer's disease. *Am J Pathol,* 155**,** 853-62.

LÜTJOHANN, D., BREUER, O., AHLBORG, G., NENNESMO, I., SIDÉN, A., DICZFALUSY, U. & BJÖRKHEM, I. 1996. Cholesterol homeostasis in human brain: evidence for an age-dependent flux of 24S-hydroxycholesterol from the brain into the circulation. *Proc Natl Acad Sci U S A,* 93**,** 9799-804.

MACINTOSH, F. C. 1941. The distribution of acetylcholine in the peripheral and the central nervous system. *J Physiol,* 99**,** 436-42.

MAGNANI, E., FAN, J., GASPARINI, L., GOLDING, M., WILLIAMS, M., SCHIAVO, G., GOEDERT, M., AMOS, L. A. & SPILLANTINI, M. G. 2007. Interaction of tau protein with the dynactin complex. *EMBO J,* 26**,** 4546-54.

MAHLEY, R. W. 1988. Apolipoprotein E: cholesterol transport protein with expanding role in cell biology. *Science,* 240**,** 622-30.

MAHLEY, R. W., HUANG, Y. & RALL, S. C. 1999. Pathogenesis of type III hyperlipoproteinemia (dysbetalipoproteinemia). Questions, quandaries, and paradoxes. *J Lipid Res,* 40**,** 1933-49.

MAHLEY, R. W., WEISGRABER, K. H. & HUANG, Y. 2009. Apolipoprotein E: structure determines function, from atherosclerosis to Alzheimer's disease to AIDS. *J Lipid Res,* 50 Suppl**,** S183-8.

MAILE, M. D., STANDIFORD, T. J., ENGOREN, M. C., STRINGER, K. A., JEWELL, E. S., RAJENDIRAN, T. M., SONI, T. & BURANT, C. F. 2018. Associations of the plasma lipidome with mortality in the acute respiratory distress syndrome: a longitudinal cohort study. *Respir Res,* 19**,** 60.

MALGAT, M., MAURICE, A. & BARAUD, J. 1986. Sphingomyelin and ceramide-phosphoethanolamine synthesis by microsomes and plasma membranes from rat liver and brain. *J Lipid Res,* 27**,** 251-60.

MANDREKAR, J. N. 2010. Receiver operating characteristic curve in diagnostic test assessment. *J Thorac Oncol,* 5**,** 1315-6.

MANEV, H., FAVARON, M., GUIDOTTI, A. & COSTA, E. 1989. Delayed increase of Ca2+ influx elicited by glutamate: role in neuronal death. *Mol Pharmacol,* 36**,** 106-12.

MANNI, M. M., TIBERTI, M. L., PAGNOTTA, S., BARELLI, H., GAUTIER, R. & ANTONNY, B. 2018. Acyl chain asymmetry and polyunsaturation of brain phospholipids facilitate membrane vesiculation without leakage. *Elife,* 7.

MANSBACH, C. M. & GORELICK, F. 2007. Development and physiological regulation of intestinal lipid absorption. II. Dietary lipid absorption, complex lipid synthesis, and the intracellular packaging and secretion of chylomicrons. *Am J Physiol Gastrointest Liver Physiol,* 293**,** G645-50.

MARAGOS, W. F., GREENAMYRE, J. T., PENNEY, J. B. & YOUNG, A. B. 1987. Glutamate dysfunction in Alzheimer's disease: an hypothesis. *Trends in Neurosciences,* 10**,** 65-68.

MAROOF, N., RAVIPATI, S., PARDON, M. C., BARRETT, D. A. & KENDALL, D. A. 2014. Reductions in endocannabinoid levels and enhanced coupling of cannabinoid receptors in the striatum are accompanied by cognitive impairments in the AβPPswe/PS1ΔE9 mouse model of Alzheimer's disease. *J Alzheimers Dis,* 42**,** 227-45.

MARQUER, C., LAINE, J., DAUPHINOT, L., HANBOUCH, L., LEMERCIER-NEUILLET, C., PIERROT, N., BOSSERS, K., LE, M., CORLIER, F., BENSTAALI, C., SAUDOU, F., THINAKARAN, G., CARTIER, N., OCTAVE, J. N., DUYCKAERTS, C. & POTIER, M. C. 2014. Increasing membrane cholesterol of neurons in culture recapitulates Alzheimer's disease early phenotypes. *Mol Neurodegener,* 9**,** 60.

MARR, R. A., ROCKENSTEIN, E., MUKHERJEE, A., KINDY, M. S., HERSH, L. B., GAGE, F. H., VERMA, I. M. & MASLIAH, E. 2003. Neprilysin gene transfer reduces human amyloid pathology in transgenic mice. *J Neurosci,* 23**,** 1992-6.

MASKREY, B. H., BERMUDEZ-FAJARDO, A., MORGAN, A. H., STEWART-JONES, E., DIOSZEGHY, V., TAYLOR, G. W., BAKER, P. R., COLES, B., COFFEY, M. J., KUHN, H. & O'DONNELL, V. B. 2007. Activated platelets and monocytes generate four hydroxyphosphatidylethanolamines via lipoxygenase. *J Biol Chem,* 282**,** 20151-63.

MASLIAH, E., MALLORY, M., GE, N., ALFORD, M., VEINBERGS, I. & ROSES, A. D. 1995. Neurodegeneration in the central nervous system of apoE-deficient mice. *Exp Neurol,* 136**,** 107-22.

MATSUO, N., TAKAO, K., NAKANISHI, K., YAMASAKI, N., TANDA, K. & MIYAKAWA, T. 2010. Behavioral profiles of three C57BL/6 substrains. *Front Behav Neurosci,* 4**,** 29.

MATSUZAKI, T., SASAKI, K., HATA, J., HIRAKAWA, Y., FUJIMI, K., NINOMIYA, T., SUZUKI, S. O., KANBA, S., KIYOHARA, Y. & IWAKI, T. 2011. Association of Alzheimer disease pathology with abnormal lipid metabolism: the Hisayama Study. *Neurology,* 77**,** 1068-75.

MATTSON, F. H. & VOLPENHEIN, R. A. 1964. THE DIGESTION AND ABSORPTION OF TRIGLYCERIDES. *J Biol Chem,* 239**,** 2772-7.

MAUE, R. A., BURGESS, R. W., WANG, B., WOOLEY, C. M., SEBURN, K. L., VANIER, M. T., ROGERS, M. A., CHANG, C. C., CHANG, T. Y., HARRIS, B. T., GRABER, D. J., PENATTI, C. A., PORTER, D. M., SZWERGOLD, B. S., HENDERSON, L. P., TOTENHAGEN, J. W., TROUARD, T. P., BORBON, I. A. & ERICKSON, R. P. 2012. A novel mouse model of

Niemann-Pick type C disease carrying a D1005G-Npc1 mutation comparable to commonly observed human mutations. *Hum Mol Genet,* 21**,** 730-50.

MAXWELL, T. J., BALLANTYNE, C. M., CHEVERUD, J. M., GUILD, C. S., NDUMELE, C. E. & BOERWINKLE, E. 2013. APOE modulates the correlation between triglycerides, cholesterol, and CHD through pleiotropy, and gene-by-gene interactions. *Genetics,* 195**,** 1397-405.

MCDONALD, J. G., SMITH, D. D., STILES, A. R. & RUSSELL, D. W. 2012. A comprehensive method for extraction and quantitative analysis of sterols and secosteroids from human plasma. *J Lipid Res,* 53**,** 1399-409.

MCDONALD, J. H. 2014. *Handbook of Biological Statistics,* Baltimore, Maryland, Sparky House Publishing.

MCGEER, P. L., ITAGAKI, S., TAGO, H. & MCGEER, E. G. 1987. Reactive microglia in patients with senile dementia of the Alzheimer type are positive for the histocompatibility glycoprotein HLA-DR. *Neurosci Lett,* 79**,** 195-200.

MCGUINNESS, B., CRAIG, D., BULLOCK, R., MALOUF, R. & PASSMORE, P. 2014. Statins for the treatment of dementia. *Cochrane Database Syst Rev***,** CD007514.

MCNAUGHT, A. D. & WILKINSON, A. 1997. *IUPAC. Compendium of Chemical Terminology,* Oxford, Blackwell Scientific Publications.

MESULAM, M. 1976. A horseradish peroxidase method for the identification of the efferents of acetyl cholinesterase-containing neurons. *J Histochem Cytochem,* 24**,** 1281-5.

MESULAM, M., GUILLOZET, A., SHAW, P. & QUINN, B. 2002. Widely spread butyrylcholinesterase can hydrolyze acetylcholine in the normal and Alzheimer brain. *Neurobiol Dis,* 9**,** 88-93.

METZ, C. E. 1978. Basic principles of ROC analysis. *Semin Nucl Med,* 8**,** 283-98.

MEYER, B. J., MANN, N. J., LEWIS, J. L., MILLIGAN, G. C., SINCLAIR, A. J. & HOWE, P. R. 2003. Dietary intakes and food sources of omega-6 and omega-3 polyunsaturated fatty acids. *Lipids,* 38**,** 391-8.

MICHNO, W., WEHRLI, P. M., ZETTERBERG, H., BLENNOW, K. & HANRIEDER, J. 2018. GM1 locates to mature amyloid structures implicating a prominent role for glycolipid-protein interactions in Alzheimer pathology. *Biochim Biophys Acta Proteins Proteom*.

MIELKE, M. M., BANDARU, V. V., HAUGHEY, N. J., RABINS, P. V., LYKETSOS, C. G. & CARLSON, M. C. 2010. Serum sphingomyelins and ceramides are early predictors of memory impairment. *Neurobiol Aging,* 31**,** 17-24.

MIELKE, M. M., MAETZLER, W., HAUGHEY, N. J., BANDARU, V. V., SAVICA, R., DEUSCHLE, C., GASSER, T., HAUSER, A. K., GRÄBER-SULTAN, S., SCHLEICHER, E., BERG, D. & LIEPELT-SCARFONE, I. 2013. Plasma ceramide and glucosylceramide metabolism is altered in sporadic Parkinson's disease and associated with cognitive impairment: a pilot study. *PLoS One,* 8**,** e73094.

MILLER, G. J., BAUER, K. A., BARZEGAR, S., COOPER, J. A. & ROSENBERG, R. D. 1996. Increased activation of the haemostatic system in men at high risk of fatal coronary heart disease. *Thromb Haemost,* 75**,** 767-71.

MILLER, G. J., BAUER, K. A., BARZEGAR, S., FOLEY, A. J., MITCHELL, J. P., COOPER, J. A. & ROSENBERG, R. D. 1995. The effects of quality and timing of venepuncture on markers of blood coagulation in healthy middle-aged men. *Thromb Haemost,* 73**,** 82-6.

MITCHELL, R. W., ON, N. H., DEL BIGIO, M. R., MILLER, D. W. & HATCH, G. M. 2011. Fatty acid transport protein expression in human brain and potential role in fatty acid transport across human brain microvessel endothelial cells. *J Neurochem,* 117**,** 735-46.

MOCHEL, F. 2018. Lipids and synaptic functions. *J Inherit Metab Dis,* 41**,** 1117-1122.

MOGHADASIAN, M. H., MCMANUS, B. M., NGUYEN, L. B., SHEFER, S., NADJI, M., GODIN, D. V., GREEN, T. J., HILL, J., YANG, Y., SCUDAMORE, C. H. & FROHLICH, J. J. 2001. Pathophysiology of apolipoprotein E deficiency in mice: relevance to apo E-related disorders in humans. *FASEB J,* 15**,** 2623-30.

MONTAGNE, A., ZHAO, Z. & ZLOKOVIC, B. V. 2017. Alzheimer's disease: A matter of blood-brain barrier dysfunction? *J Exp Med,* 214**,** 3151-3169.

MONTEIRO-CARDOSO, V. F., OLIVEIRA, M. M., MELO, T., DOMINGUES, M. R., MOREIRA, P. I., FERREIRO, E., PEIXOTO, F. & VIDEIRA, R. A. 2015. Cardiolipin profile changes are associated to the early synaptic mitochondrial dysfunction in Alzheimer's disease. *J Alzheimers Dis,* 43**,** 1375-92.

MORI, T., PARIS, D., TOWN, T., ROJIANI, A. M., SPARKS, D. L., DELLEDONNE, A., CRAWFORD, F., ABDULLAH, L. I., HUMPHREY, J. A., DICKSON, D. W. & MULLAN, M. J. 2001. Cholesterol accumulates in senile plaques of Alzheimer disease patients and in transgenic APP(SW) mice. *J Neuropathol Exp Neurol,* 60**,** 778-85.

MORRIS, J. C., STORANDT, M., MCKEEL, D. W., RUBIN, E. H., PRICE, J. L., GRANT, E. A. & BERG, L. 1996. Cerebral amyloid deposition and diffuse plaques in "normal" aging: Evidence for presymptomatic and very mild Alzheimer's disease. *Neurology,* 46**,** 707-19.

MORRIS, M., MAEDA, S., VOSSEL, K. & MUCKE, L. 2011. The many faces of tau. *Neuron,* 70**,** 410-26.

MUSUNURU, S., CARPENTER, J. E., SIPPEL, R. S., KUNNIMALAIYAAN, M. & CHEN, H. 2005. A mouse model of carcinoid syndrome and heart disease. *J Surg Res,* 126**,** 102-5.

NAGY, Z., ESIRI, M. M., JOBST, K. A., JOHNSTON, C., LITCHFIELD, S., SIM, E. & SMITH, A. D. 1995. Influence of the apolipoprotein E genotype on amyloid deposition and neurofibrillary tangle formation in Alzheimer's disease. *Neuroscience,* 69**,** 757-61.

NANJEE, M. N. & MILLER, N. E. 1990. Evaluation of long-term frozen storage of plasma for measurement of high-density lipoprotein and its subfractions by precipitation. *Clin Chem,* 36**,** 783-8.

NASARUDDIN, M. L., PAN, X., MCGUINNESS, B., PASSMORE, P., KEHOE, P. G., HÖLSCHER, C., GRAHAM, S. F. & GREEN, B. D. 2018. Evidence That Parietal Lobe Fatty Acids May Be More Profoundly Affected in Moderate Alzheimer's Disease (AD) Pathology Than in Severe AD Pathology. *Metabolites,* 8.

NEWMAN, A. B., FITZPATRICK, A. L., LOPEZ, O., JACKSON, S., LYKETSOS, C., JAGUST, W., IVES, D., DEKOSKY, S. T. & KULLER, L. H. 2005. Dementia and Alzheimer's disease incidence in relationship to cardiovascular disease in the Cardiovascular Health Study cohort. *J Am Geriatr Soc,* 53**,** 1101-7.

NEYMAN, J. & PEARSON, E. S. 1928. <h1 _ngcontent-c18="" class="m-t-0" style="box-sizing: border-box; font-family: sans-serif; margin-right: 0px; margin-bottom: 0px; margin-left: 0px; font-size: 36px; font-weight: 500; line-height: 16px; color: rgb(0, 140, 210); padding: 10px 0px 0px; background-color: rgb(255, 255, 255); margin-top: 0px !important;"> On the use and interpretation of certain test criteria for purposes of statistical inference. *Biometrika,* 20A**,** 175-240.

NG, K. F., ANDERSON, S., MAYO, P., AUNG, H. H., WALTON, J. H. & RUTLEDGE, J. C. 2016. Characterizing blood-brain barrier perturbations after exposure to human triglyceride-rich lipoprotein lipolysis products using MRI in a rat model. *Magn Reson Med,* 76**,** 1246-51.

NG, T. W., OOI, E. M., WATTS, G. F., CHAN, D. C., MEIKLE, P. J. & BARRETT, P. H. 2015. Association of Plasma Ceramides and Sphingomyelin With VLDL apoB-100 Fractional Catabolic Rate Before and After Rosuvastatin Treatment. *J Clin Endocrinol Metab,* 100**,** 2497-501.

NGUYEN, L. N., MA, D., SHUI, G., WONG, P., CAZENAVE-GASSIOT, A., ZHANG, X., WENK, M. R., GOH, E. L. & SILVER, D. L. 2014. Mfsd2a is a transporter for the essential omega-3 fatty acid docosahexaenoic acid. *Nature,* 509**,** 503-6.

NICOLL, J. A., BARTON, E., BOCHE, D., NEAL, J. W., FERRER, I., THOMPSON, P., VLACHOULI, C., WILKINSON, D., BAYER, A., GAMES, D., SEUBERT, P., SCHENK, D. & HOLMES, C. 2006. Abeta species removal after abeta42 immunization. *J Neuropathol Exp Neurol,* 65**,** 1040-8.

NICOLL, J. A., WILKINSON, D., HOLMES, C., STEART, P., MARKHAM, H. & WELLER, R. O. 2003. Neuropathology of human Alzheimer disease after immunization with amyloid-beta peptide: a case report. *Nat Med,* 9**,** 448-52.

NIEWEG, K., SCHALLER, H. & PFRIEGER, F. W. 2009. Marked differences in cholesterol synthesis between neurons and glial cells from postnatal rats. *J Neurochem,* 109**,** 125-34.

NIMMERJAHN, A., KIRCHHOFF, F. & HELMCHEN, F. 2005. Resting microglial cells are highly dynamic surveillants of brain parenchyma in vivo. *Science,* 308**,** 1314-8.

NORMANDIN, M., GAGNÉ, J., BERNARD, J., ELIE, R., MICELI, D., BAUDRY, M. & MASSICOTTE, G. 1996. Involvement of the 12-lipoxygenase pathway of arachidonic acid metabolism in homosynaptic long-term depression of the rat hippocampus. *Brain Res,* 730**,** 40-6.

NÄGGA, K., GUSTAVSSON, A. M., STOMRUD, E., LINDQVIST, D., VAN WESTEN, D., BLENNOW, K., ZETTERBERG, H., MELANDER, O. & HANSSON, O. 2018. Increased midlife triglycerides predict brain β-amyloid and tau pathology 20 years later. *Neurology,* 90**,** e73-e81.

O'CONNOR, A., BRASHER, C. J., SLATTER, D. A., MECKELMANN, S. W., HAWKSWORTH, J. I., ALLEN, S. M. & O'DONNELL, V. B. 2017. LipidFinder: A computational workflow for discovery of lipids identifies eicosanoid-phosphoinositides in platelets. *JCI Insight,* 2**,** e91634.

OITZL, M. S., MULDER, M., LUCASSEN, P. J., HAVEKES, L. M., GROOTENDORST, J. & DE KLOET, E. R. 1997. Severe learning deficits in apolipoprotein E-knockout mice in a water maze task. *Brain Res,* 752**,** 189-96.

OLNEY, J. W. 1969. Brain lesions, obesity, and other disturbances in mice treated with monosodium glutamate. *Science,* 164**,** 719-21.

OLNEY, J. W. & SHARPE, L. G. 1969. Brain lesions in an infant rhesus monkey treated with monsodium glutamate. *Science,* 166**,** 386-8.

ORESIC, M., HÄNNINEN, V. A. & VIDAL-PUIG, A. 2008. Lipidomics: a new window to biomedical frontiers. *Trends Biotechnol,* 26**,** 647-52.

OREŠIČ, M., LÖTJÖNEN, J. & SOININEN, H. 2009. Systems medicine and the integration of bioinformatic tools for the diagnosis of Alzheimer's disease. *Genome Med,* 1**,** 83.

ORGOGOZO, J. M., GILMAN, S., DARTIGUES, J. F., LAURENT, B., PUEL, M., KIRBY, L. C., JOUANNY, P., DUBOIS, B., EISNER, L., FLITMAN, S., MICHEL, B. F., BOADA, M., FRANK, A. & HOCK, C. 2003. Subacute meningoencephalitis in a subset of patients with AD after Abeta42 immunization. *Neurology,* 61**,** 46-54.

OUELLET, M., EMOND, V., CHEN, C. T., JULIEN, C., BOURASSET, F., ODDO, S., LAFERLA, F., BAZINET, R. P. & CALON, F. 2009. Diffusion of docosahexaenoic and eicosapentaenoic

acids through the blood-brain barrier: An in situ cerebral perfusion study. *Neurochem Int,* 55**,** 476-82.

PALLAST, S., ARAI, K., WANG, X., LO, E. H. & VAN LEYEN, K. 2009. 12/15-Lipoxygenase targets neuronal mitochondria under oxidative stress. *J Neurochem,* 111**,** 882-9.

PANCHAL, M., GAUDIN, M., LAZAR, A. N., SALVATI, E., RIVALS, I., AYCIRIEX, S., DAUPHINOT, L., DARGÈRE, D., AUZEIL, N., MASSERINI, M., LAPRÉVOTE, O. & DUYCKAERTS, C. 2014. Ceramides and sphingomyelinases in senile plaques. *Neurobiol Dis,* 65**,** 193-201.

PANZENBOECK, U., BALAZS, Z., SOVIC, A., HRZENJAK, A., LEVAK-FRANK, S., WINTERSPERGER, A., MALLE, E. & SATTLER, W. 2002. ABCA1 and scavenger receptor class B, type I, are modulators of reverse sterol transport at an in vitro blood-brain barrier constituted of porcine brain capillary endothelial cells. *J Biol Chem,* 277**,** 42781-9.

PARDRIDGE, W. M., CONNOR, J. D. & CRAWFORD, I. L. 1975. Permeability changes in the blood-brain barrier: causes and consequences. *CRC Crit Rev Toxicol,* 3**,** 159-99.

PAULING, J. & KLIPP, E. 2016. Computational Lipidomics and Lipid Bioinformatics: Filling In the Blanks. *J Integr Bioinform,* 13**,** 299.

PEARSON, H. A. & PEERS, C. 2006. Physiological roles for amyloid beta peptides. *J Physiol,* 575**,** 5-10.

PEARSON, K. 1901. On lines and planes of closest fit to systems of points in space. *The London, Edinburgh, and Dublin Philosophical Magazine and Journal of Science,* 2**,** 559-572.

PEPE, G., DE MAGLIE, M., MINOLI, L., VILLA, A., MAGGI, A. & VEGETO, E. 2017. Selective proliferative response of microglia to alternative polarization signals. *J Neuroinflammation,* 14**,** 236.

PERRY, E. K., TOMLINSON, B. E., BLESSED, G., BERGMANN, K., GIBSON, P. H. & PERRY, R. H. 1978. Correlation of cholinergic abnormalities with senile plaques and mental test scores in senile dementia. *Br Med J,* 2**,** 1457-9.

PICQ, M., CHEN, P., PEREZ, M., MICHAUD, M., VÉRICEL, E., GUICHARDANT, M. & LAGARDE, M. 2010. DHA metabolism: targeting the brain and lipoxygenation. *Mol Neurobiol,* 42**,** 48-51.

PINTO, S. N., FERNANDES, F., FEDOROV, A., FUTERMAN, A. H., SILVA, L. C. & PRIETO, M. 2013. A combined fluorescence spectroscopy, confocal and 2-photon microscopy approach to re-evaluate the properties of sphingolipid domains. *Biochim Biophys Acta,* 1828**,** 2099-110.

PITAS, R. E., BOYLES, J. K., LEE, S. H., FOSS, D. & MAHLEY, R. W. 1987a. Astrocytes synthesize apolipoprotein E and metabolize apolipoprotein E-containing lipoproteins. *Biochim Biophys Acta,* 917**,** 148-61.

PITAS, R. E., BOYLES, J. K., LEE, S. H., HUI, D. & WEISGRABER, K. H. 1987b. Lipoproteins and their receptors in the central nervous system. Characterization of the lipoproteins in cerebrospinal fluid and identification of apolipoprotein B,E(LDL) receptors in the brain. *J Biol Chem,* 262**,** 14352-60.

POIRIER, R., WOLFER, D. P., WELZL, H., TRACY, J., GALSWORTHY, M. J., NITSCH, R. M. & MOHAJERI, M. H. 2006. Neuronal neprilysin overexpression is associated with attenuation of Abeta-related spatial memory deficit. *Neurobiol Dis,* 24**,** 475-83.

PONOMAREV, E. D., MARESZ, K., TAN, Y. & DITTEL, B. N. 2007. CNS-derived interleukin-4 is essential for the regulation of autoimmune inflammation and induces a state of alternative activation in microglial cells. *J Neurosci,* 27**,** 10714-21.

PORSTEINSSON, A. P., GROSSBERG, G. T., MINTZER, J., OLIN, J. T. & GROUP, M. M.-M.-S. 2008. Memantine treatment in patients with mild to moderate Alzheimer's disease already

receiving a cholinesterase inhibitor: a randomized, double-blind, placebo-controlled trial. *Curr Alzheimer Res,* 5**,** 83-9.

PRADAS, I., HUYNH, K., CABRÉ, R., AYALA, V., MEIKLE, P. J., JOVÉ, M. & PAMPLONA, R. 2018. Lipidomics Reveals a Tissue-Specific Fingerprint. *Front Physiol,* 9**,** 1165.

PRATICÒ, D., ZHUKAREVA, V., YAO, Y., URYU, K., FUNK, C. D., LAWSON, J. A., TROJANOWSKI, J. Q. & LEE, V. M. 2004. 12/15-lipoxygenase is increased in Alzheimer's disease: possible involvement in brain oxidative stress. *Am J Pathol,* 164**,** 1655-62.

PRESEĆKI, P., MÜCK-SELER, D., MIMICA, N., PIVAC, N., MUSTAPIĆ, M., STIPCEVIĆ, T. & SMALC, V. F. 2011. Serum lipid levels in patients with Alzheimer's disease. *Coll Antropol,* 35 Suppl 1**,** 115-20.

PRINCE, M., WIMO, A., GUERCHET, M., ALI, G.-C., WU, Y., PRINA, M., YEE, C. & XIA, Z. 2015. World Alzheimer report 2015 the global impact of dementia. An analysis of prevalence, incidence, cost and trends. London.

PRINS, N. D., VAN DER FLIER, W. A., KNOL, D. L., FOX, N. C., BRASHEAR, H. R., NYE, J. S., BARKHOF, F. & SCHELTENS, P. 2014. The effect of galantamine on brain atrophy rate in subjects with mild cognitive impairment is modified by apolipoprotein E genotype: post-hoc analysis of data from a randomized controlled trial. *Alzheimers Res Ther,* 6**,** 47.

PROITSI, P., KIM, M., WHILEY, L., PRITCHARD, M., LEUNG, R., SOININEN, H., KLOSZEWSKA, I., MECOCCI, P., TSOLAKI, M., VELLAS, B., SHAM, P., LOVESTONE, S., POWELL, J. F., DOBSON, R. J. & LEGIDO-QUIGLEY, C. 2015. Plasma lipidomics analysis finds long chain cholesteryl esters to be associated with Alzheimer's disease. *Transl Psychiatry,* 5**,** e494.

PROITSI, P., KIM, M., WHILEY, L., SIMMONS, A., SATTLECKER, M., VELAYUDHAN, L., LUPTON, M. K., SOININEN, H., KLOSZEWSKA, I., MECOCCI, P., TSOLAKI, M., VELLAS, B., LOVESTONE, S., POWELL, J. F., DOBSON, R. J. & LEGIDO-QUIGLEY, C. 2017. Association of blood lipids with Alzheimer's disease: A comprehensive lipidomics analysis. *Alzheimers Dement,* 13**,** 140-151.

QUAZI, F. & MOLDAY, R. S. 2013. Differential phospholipid substrates and directional transport by ATP-binding cassette proteins ABCA1, ABCA7, and ABCA4 and disease-causing mutants. *J Biol Chem,* 288**,** 34414-26.

QUEHENBERGER, O., ARMANDO, A. M., BROWN, A. H., MILNE, S. B., MYERS, D. S., MERRILL, A. H., BANDYOPADHYAY, S., JONES, K. N., KELLY, S., SHANER, R. L., SULLARDS, C. M., WANG, E., MURPHY, R. C., BARKLEY, R. M., LEIKER, T. J., RAETZ, C. R., GUAN, Z., LAIRD, G. M., SIX, D. A., RUSSELL, D. W., MCDONALD, J. G., SUBRAMANIAM, S., FAHY, E. & DENNIS, E. A. 2010. Lipidomics reveals a remarkable diversity of lipids in human plasma. *J Lipid Res,* 51**,** 3299-305.

RAIVICH, G., BOHATSCHEK, M., KLOSS, C. U., WERNER, A., JONES, L. L. & KREUTZBERG, G. W. 1999. Neuroglial activation repertoire in the injured brain: graded response, molecular mechanisms and cues to physiological function. *Brain Res Brain Res Rev,* 30**,** 77-105.

RAMANAN, V. K., PRZYBELSKI, S. A., GRAFF-RADFORD, J., CASTILLO, A. M., LOWE, V. J., MIELKE, M. M., ROBERTS, R. O., REID, R. I., KNOPMAN, D. S., JACK, C. R., PETERSEN, R. C. & VEMURI, P. 2018. Statins and Brain Health: Alzheimer's Disease and Cerebrovascular Disease Biomarkers in Older Adults. *J Alzheimers Dis*.

RAMDANE, S. & DAOUDI-GUEDDAH, D. 2011. Mild hypercholesterolemia, normal plasma triglycerides, and normal glucose levels across dementia staging in Alzheimer's

disease: a clinical setting-based retrospective study. *Am J Alzheimers Dis Other Demen,* 26**,** 399-405.

REED-GEAGHAN, E. G., SAVAGE, J. C., HISE, A. G. & LANDRETH, G. E. 2009. CD14 and toll-like receptors 2 and 4 are required for fibrillar A{beta}-stimulated microglial activation. *J Neurosci,* 29**,** 11982-92.

REESE, T. S. & KARNOVSKY, M. J. 1967. Fine structural localization of a blood-brain barrier to exogenous peroxidase. *J Cell Biol,* 34**,** 207-17.

REFOLO, L. M., PAPPOLLA, M. A., LAFRANCOIS, J., MALESTER, B., SCHMIDT, S. D., THOMAS-BRYANT, T., TINT, G. S., WANG, R., MERCKEN, M., PETANCESKA, S. S. & DUFF, K. E. 2001. A cholesterol-lowering drug reduces beta-amyloid pathology in a transgenic mouse model of Alzheimer's disease. *Neurobiol Dis,* 8**,** 890-9.

REIS, A., RUDNITSKAYA, A., BLACKBURN, G. J., MOHD FAUZI, N., PITT, A. R. & SPICKETT, C. M. 2013. A comparison of five lipid extraction solvent systems for lipidomic studies of human LDL. *J Lipid Res,* 54**,** 1812-24.

REITZ, C., TANG, M., LUCHSINGER, J. & MAYEUX, R. 2004. Relation of plasma lipids to Alzheimer disease and vascular dementia. *Archives of Neurology,* 61**,** 705-714.

REN, C., LIU, J., ZHOU, J., LIANG, H., WANG, Y., SUN, Y., MA, B. & YIN, Y. 2018. Lipidomic analysis of serum samples from migraine patients. *Lipids Health Dis,* 17**,** 22.

RIEKSE, R. G., LI, G., PETRIE, E. C., LEVERENZ, J. B., VAVREK, D., VULETIC, S., ALBERS, J. J., MONTINE, T. J., LEE, V. M., LEE, M., SEUBERT, P., GALASKO, D., SCHELLENBERG, G. D., HAZZARD, W. R. & PESKIND, E. R. 2006. Effect of statins on Alzheimer's disease biomarkers in cerebrospinal fluid. *J Alzheimers Dis,* 10**,** 399-406.

ROBERTSON, K. S., HAWE, E., MILLER, G. J., TALMUD, P. J., HUMPHRIES, S. E. & II, N. P. H. S. 2003. Human paraoxonase gene cluster polymorphisms as predictors of coronary heart disease risk in the prospective Northwick Park Heart Study II. *Biochim Biophys Acta,* 1639**,** 203-12.

RODRÍGUEZ, E., MATEO, I., INFANTE, J., LLORCA, J., BERCIANO, J. & COMBARROS, O. 2006. Cholesteryl ester transfer protein (CETP) polymorphism modifies the Alzheimer's disease risk associated with APOE epsilon4 allele. *J Neurol,* 253**,** 181-5.

ROGAEV, E. I., SHERRINGTON, R., ROGAEVA, E. A., LEVESQUE, G., IKEDA, M., LIANG, Y., CHI, H., LIN, C., HOLMAN, K. & TSUDA, T. 1995. Familial Alzheimer's disease in kindreds with missense mutations in a gene on chromosome 1 related to the Alzheimer's disease type 3 gene. *Nature,* 376**,** 775-8.

RÖSLER, M., ANAND, R., CICIN-SAIN, A., GAUTHIER, S., AGID, Y., DAL-BIANCO, P., STÄHELIN, H. B., HARTMAN, R. & GHARABAWI, M. 1999. Efficacy and safety of rivastigmine in patients with Alzheimer's disease: international randomised controlled trial. *BMJ,* 318**,** 633-8.

SAITO, H., DHANASEKARAN, P., BALDWIN, F., WEISGRABER, K. H., PHILLIPS, M. C. & LUND-KATZ, S. 2003. Effects of polymorphism on the lipid interaction of human apolipoprotein E. *J Biol Chem,* 278**,** 40723-9.

SALES, S., GRAESSLER, J., CIUCCI, S., AL-ATRIB, R., VIHERVAARA, T., SCHUHMANN, K., KAUHANEN, D., SYSI-AHO, M., BORNSTEIN, S. R., BICKLE, M., CANNISTRACI, C. V., EKROOS, K. & SHEVCHENKO, A. 2016. Gender, Contraceptives and Individual Metabolic Predisposition Shape a Healthy Plasma Lipidome. *Sci Rep,* 6**,** 27710.

SALLOWAY, S., SPERLING, R., FOX, N. C., BLENNOW, K., KLUNK, W., RASKIND, M., SABBAGH, M., HONIG, L. S., PORSTEINSSON, A. P., FERRIS, S., REICHERT, M., KETTER, N., NEJADNIK, B., GUENZLER, V., MILOSLAVSKY, M., WANG, D., LU, Y., LULL, J., TUDOR, I.

C., LIU, E., GRUNDMAN, M., YUEN, E., BLACK, R., BRASHEAR, H. R. & INVESTIGATORS, B. A. C. T. 2014. Two phase 3 trials of bapineuzumab in mild-to-moderate Alzheimer's disease. *N Engl J Med,* 370**,** 322-33.

SALLOWAY, S., SPERLING, R., GILMAN, S., FOX, N. C., BLENNOW, K., RASKIND, M., SABBAGH, M., HONIG, L. S., DOODY, R., VAN DYCK, C. H., MULNARD, R., BARAKOS, J., GREGG, K. M., LIU, E., LIEBERBURG, I., SCHENK, D., BLACK, R., GRUNDMAN, M. & INVESTIGATORS, B. C. T. 2009. A phase 2 multiple ascending dose trial of bapineuzumab in mild to moderate Alzheimer disease. *Neurology,* 73**,** 2061-70.

SANCHEZ-MEJIA, R. O., NEWMAN, J. W., TOH, S., YU, G. Q., ZHOU, Y., HALABISKY, B., CISSÉ, M., SCEARCE-LEVIE, K., CHENG, I. H., GAN, L., PALOP, J. J., BONVENTRE, J. V. & MUCKE, L. 2008. Phospholipase A2 reduction ameliorates cognitive deficits in a mouse model of Alzheimer's disease. *Nat Neurosci,* 11**,** 1311-8.

SANDERSON, K. J., VAN RIJ, A. M., WADE, C. R. & SUTHERLAND, W. H. 1995. Lipid peroxidation of circulating low density lipoproteins with age, smoking and in peripheral vascular disease. *Atherosclerosis,* 118**,** 45-51.

SANGO, K., YAMANAKA, S., HOFFMANN, A., OKUDA, Y., GRINBERG, A., WESTPHAL, H., MCDONALD, M. P., CRAWLEY, J. N., SANDHOFF, K., SUZUKI, K. & PROIA, R. L. 1995. Mouse models of Tay-Sachs and Sandhoff diseases differ in neurologic phenotype and ganglioside metabolism. *Nat Genet,* 11**,** 170-6.

SANO, M., BELL, K. L., GALASKO, D., GALVIN, J. E., THOMAS, R. G., VAN DYCK, C. H. & AISEN, P. S. 2011. A randomized, double-blind, placebo-controlled trial of simvastatin to treat Alzheimer disease. *Neurology,* 77**,** 556-63.

SANTACRUZ, K., LEWIS, J., SPIRES, T., PAULSON, J., KOTILINEK, L., INGELSSON, M., GUIMARAES, A., DETURE, M., RAMSDEN, M., MCGOWAN, E., FORSTER, C., YUE, M., ORNE, J., JANUS, C., MARIASH, A., KUSKOWSKI, M., HYMAN, B., HUTTON, M. & ASHE, K. H. 2005. Tau suppression in a neurodegenerative mouse model improves memory function. *Science,* 309**,** 476-81.

SANTIAGO, A. R., BERNARDINO, L., AGUDO-BARRIUSO, M. & GONÇALVES, J. 2017. Microglia in Health and Disease: A Double-Edged Sword. *Mediators Inflamm,* 2017**,** 7034143.

SASSIN, I., SCHULTZ, C., THAL, D. R., RÜB, U., ARAI, K., BRAAK, E. & BRAAK, H. 2000. Evolution of Alzheimer's disease-related cytoskeletal changes in the basal nucleus of Meynert. *Acta Neuropathol,* 100**,** 259-69.

SAVICA, R., MURRAY, M. E., PERSSON, X. M., KANTARCI, K., PARISI, J. E., DICKSON, D. W., PETERSEN, R. C., FERMAN, T. J., BOEVE, B. F. & MIELKE, M. M. 2016. Plasma sphingolipid changes with autopsy-confirmed Lewy Body or Alzheimer's pathology. *Alzheimers Dement (Amst),* 3**,** 43-50.

SAWADA, M., SUZUMURA, A., HOSOYA, H., MARUNOUCHI, T. & NAGATSU, T. 1999. Interleukin-10 inhibits both production of cytokines and expression of cytokine receptors in microglia. *J Neurochem,* 72**,** 1466-71.

SCHEUNER, D., ECKMAN, C., JENSEN, M., SONG, X., CITRON, M., SUZUKI, N., BIRD, T. D., HARDY, J., HUTTON, M., KUKULL, W., LARSON, E., LEVY-LAHAD, E., VIITANEN, M., PESKIND, E., POORKAJ, P., SCHELLENBERG, G., TANZI, R., WASCO, W., LANNFELT, L., SELKOE, D. & YOUNKIN, S. 1996. Secreted amyloid beta-protein similar to that in the senile plaques of Alzheimer's disease is increased in vivo by the presenilin 1 and 2 and APP mutations linked to familial Alzheimer's disease. *Nat Med,* 2**,** 864-70.

SCHIFFERER, R., LIEBISCH, G., BANDULIK, S., LANGMANN, T., DADA, A. & SCHMITZ, G. 2007. ApoA-I induces a preferential efflux of monounsaturated phosphatidylcholine and

medium chain sphingomyelin species from a cellular pool distinct from HDL(3) mediated phospholipid efflux. *Biochim Biophys Acta,* 1771**,** 853-63.

SCHILLER, J., SÜSS, R., ARNHOLD, J., FUCHS, B., LESSIG, J., MÜLLER, M., PETKOVIĆ, M., SPALTEHOLZ, H., ZSCHÖRNIG, O. & ARNOLD, K. 2004. Matrix-assisted laser desorption and ionization time-of-flight (MALDI-TOF) mass spectrometry in lipid and phospholipid research. *Prog Lipid Res,* 43**,** 449-88.

SCHNEIDER, L. S., DAGERMAN, K. S., HIGGINS, J. P. & MCSHANE, R. 2011. Lack of evidence for the efficacy of memantine in mild Alzheimer disease. *Arch Neurol,* 68**,** 991-8.

SCHØNHEYDER, F. & VOLQVARTZ, K. 1946. The gastric lipase in man. *Acta Physiologica,* 11**,** 349-89.

SEGREST, J. P., JONES, M. K., MISHRA, V. K., PIEROTTI, V., YOUNG, S. H., BORÉN, J., INNERARITY, T. L. & DASHTI, N. 1998. Apolipoprotein B-100: conservation of lipid-associating amphipathic secondary structural motifs in nine species of vertebrates. *J Lipid Res,* 39**,** 85-102.

SENGUPTA, A., KABAT, J., NOVAK, M., WU, Q., GRUNDKE-IQBAL, I. & IQBAL, K. 1998. Phosphorylation of tau at both Thr 231 and Ser 262 is required for maximal inhibition of its binding to microtubules. *Arch Biochem Biophys,* 357**,** 299-309.

SERHAN, C. N. 2014. Pro-resolving lipid mediators are leads for resolution physiology. *Nature,* 510**,** 92-101.

SERHAN, C. N., HONG, S., GRONERT, K., COLGAN, S. P., DEVCHAND, P. R., MIRICK, G. & MOUSSIGNAC, R. L. 2002. Resolvins: a family of bioactive products of omega-3 fatty acid transformation circuits initiated by aspirin treatment that counter proinflammation signals. *J Exp Med,* 196**,** 1025-37.

SERHAN, C. N. & PETASIS, N. A. 2011. Resolvins and protectins in inflammation resolution. *Chem Rev,* 111**,** 5922-43.

SERRANO-POZO, A., VEGA, G. L., LÜTJOHANN, D., LOCASCIO, J. J., TENNIS, M. K., DENG, A., ATRI, A., HYMAN, B. T., IRIZARRY, M. C. & GROWDON, J. H. 2010. Effects of simvastatin on cholesterol metabolism and Alzheimer disease biomarkers. *Alzheimer Dis Assoc Disord,* 24**,** 220-6.

SEVIGNY, J., CHIAO, P., BUSSIÈRE, T., WEINREB, P. H., WILLIAMS, L., MAIER, M., DUNSTAN, R., SALLOWAY, S., CHEN, T., LING, Y., O'GORMAN, J., QIAN, F., ARASTU, M., LI, M., CHOLLATE, S., BRENNAN, M. S., QUINTERO-MONZON, O., SCANNEVIN, R. H., ARNOLD, H. M., ENGBER, T., RHODES, K., FERRERO, J., HANG, Y., MIKULSKIS, A., GRIMM, J., HOCK, C., NITSCH, R. M. & SANDROCK, A. 2016. The antibody aducanumab reduces Aβ plaques in Alzheimer's disease. *Nature,* 537**,** 50-6.

SHAH, D. J., ROHLFING, F., ANAND, S., JOHNSON, W. E., ALVAREZ, M. T., COBELL, J., KING, J., YOUNG, S. A., KAUWE, J. S. & GRAVES, S. W. 2016. Discovery and Subsequent Confirmation of Novel Serum Biomarkers Diagnosing Alzheimer's Disease. *J Alzheimers Dis,* 49**,** 317-27.

SHAHID, S. U., , S., COOPER, J. A., BEANEY, K. E., LI, K., REHMAN, A. & HUMPHRIES, S. E. 2016. Effect of SORT1, APOB and APOE polymorphisms on LDL-C and coronary heart disease in Pakistani subjects and their comparison with Northwick Park Heart Study II. *Lipids Health Dis,* 15**,** 83.

SHALINI, S. M., HO, C. F., NG, Y. K., TONG, J. X., ONG, E. S., HERR, D. R., DAWE, G. S. & ONG, W. Y. 2018. Distribution of Alox15 in the Rat Brain and Its Role in Prefrontal Cortical Resolvin D1 Formation and Spatial Working Memory. *Mol Neurobiol,* 55**,** 1537-1550.

SHANKAR, G. M., LI, S., MEHTA, T. H., GARCIA-MUNOZ, A., SHEPARDSON, N. E., SMITH, I., BRETT, F. M., FARRELL, M. A., ROWAN, M. J., LEMERE, C. A., REGAN, C. M., WALSH, D. M., SABATINI, B. L. & SELKOE, D. J. 2008. Amyloid-beta protein dimers isolated directly from Alzheimer's brains impair synaptic plasticity and memory. *Nat Med,* 14**,** 837-42.

SHARMA, A., BEMIS, M. & DESILETS, A. R. 2014. Role of Medium Chain Triglycerides (Axona®) in the Treatment of Mild to Moderate Alzheimer's Disease. *Am J Alzheimers Dis Other Demen,* 29**,** 409-14.

SHARMAN, M. J., SHUI, G., FERNANDIS, A. Z., LIM, W. L., BERGER, T., HONE, E., TADDEI, K., MARTINS, I. J., GHISO, J., BUXBAUM, J. D., GANDY, S., WENK, M. R. & MARTINS, R. N. 2010. Profiling brain and plasma lipids in human APOE epsilon2, epsilon3, and epsilon4 knock-in mice using electrospray ionization mass spectrometry. *J Alzheimers Dis,* 20**,** 105-11.

SHENG, J. G., MRAK, R. E. & GRIFFIN, W. S. 1997a. Glial-neuronal interactions in Alzheimer disease: progressive association of IL-1alpha+ microglia and S100beta+ astrocytes with neurofibrillary tangle stages. *J Neuropathol Exp Neurol,* 56**,** 285-90.

SHENG, J. G., MRAK, R. E. & GRIFFIN, W. S. 1997b. Neuritic plaque evolution in Alzheimer's disease is accompanied by transition of activated microglia from primed to enlarged to phagocytic forms. *Acta Neuropathol,* 94**,** 1-5.

SHENG, M., SABATINI, B. L. & SÜDHOF, T. C. 2012. Synapses and Alzheimer's disease. *Cold Spring Harb Perspect Biol,* 4.

SHERRINGTON, R., ROGAEV, E. I., LIANG, Y., ROGAEVA, E. A., LEVESQUE, G., IKEDA, M., CHI, H., LIN, C., LI, G., HOLMAN, K., TSUDA, T., MAR, L., FONCIN, J. F., BRUNI, A. C., MONTESI, M. P., SORBI, S., RAINERO, I., PINESSI, L., NEE, L., CHUMAKOV, I., POLLEN, D., BROOKES, A., SANSEAU, P., POLINSKY, R. J., WASCO, W., DA SILVA, H. A., HAINES, J. L., PERKICAK-VANCE, M. A., TANZI, R. E., ROSES, A. D., FRASER, P. E., ROMMENS, J. M. & ST GEORGE-HYSLOP, P. H. 1995. Cloning of a gene bearing missense mutations in early-onset familial Alzheimer's disease. *Nature,* 375**,** 754-60.

SHEVCHENKO, A. & SIMONS, K. 2010. Lipidomics: coming to grips with lipid diversity. *Nat Rev Mol Cell Biol,* 11**,** 593-8.

SHUNMOOGAM, N., NAIDOO, P. & CHILTON, R. 2018. Paraoxonase (PON)-1: a brief overview on genetics, structure, polymorphisms and clinical relevance. *Vasc Health Risk Manag,* 14**,** 137-143.

SIERRA, S., RAMOS, M. C., MOLINA, P., ESTEO, C., VÁZQUEZ, J. A. & BURGOS, J. S. 2011. Statins as neuroprotectants: a comparative in vitro study of lipophilicity, blood-brain-barrier penetration, lowering of brain cholesterol, and decrease of neuron cell death. *J Alzheimers Dis,* 23**,** 307-18.

SILVA, L. C., DE ALMEIDA, R. F., CASTRO, B. M., FEDOROV, A. & PRIETO, M. 2007. Ceramide-domain formation and collapse in lipid rafts: membrane reorganization by an apoptotic lipid. *Biophys J,* 92**,** 502-16.

SIMARD, A. R. & RIVEST, S. 2006. Neuroprotective properties of the innate immune system and bone marrow stem cells in Alzheimer's disease. *Mol Psychiatry,* 11**,** 327-35.

SIMARD, A. R., SOULET, D., GOWING, G., JULIEN, J. P. & RIVEST, S. 2006. Bone marrow-derived microglia play a critical role in restricting senile plaque formation in Alzheimer's disease. *Neuron,* 49**,** 489-502.

SIMON, M. M., GREENAWAY, S., WHITE, J. K., FUCHS, H., GAILUS-DURNER, V., WELLS, S., SORG, T., WONG, K., BEDU, E., CARTWRIGHT, E. J., DACQUIN, R., DJEBALI, S., ESTABEL, J., GRAW, J., INGHAM, N. J., JACKSON, I. J., LENGELING, A., MANDILLO, S., MARVEL, J.,

MEZIANE, H., PREITNER, F., PUK, O., ROUX, M., ADAMS, D. J., ATKINS, S., AYADI, A., BECKER, L., BLAKE, A., BROOKER, D., CATER, H., CHAMPY, M. F., COMBE, R., DANECEK, P., DI FENZA, A., GATES, H., GERDIN, A. K., GOLINI, E., HANCOCK, J. M., HANS, W., HÖLTER, S. M., HOUGH, T., JURDIC, P., KEANE, T. M., MORGAN, H., MÜLLER, W., NEFF, F., NICHOLSON, G., PASCHE, B., ROBERSON, L. A., ROZMAN, J., SANDERSON, M., SANTOS, L., SELLOUM, M., SHANNON, C., SOUTHWELL, A., TOCCHINI-VALENTINI, G. P., VANCOLLIE, V. E., WESTERBERG, H., WURST, W., ZI, M., YALCIN, B., RAMIREZ-SOLIS, R., STEEL, K. P., MALLON, A. M., DE ANGELIS, M. H., HERAULT, Y. & BROWN, S. D. 2013. A comparative phenotypic and genomic analysis of C57BL/6J and C57BL/6N mouse strains. *Genome Biol,* 14**,** R82.

SIMONS, K. & TOOMRE, D. 2000. Lipid rafts and signal transduction. *Nat Rev Mol Cell Biol,* 1**,** 31-9.

SIMONS, M., KELLER, P., DE STROOPER, B., BEYREUTHER, K., DOTTI, C. G. & SIMONS, K. 1998. Cholesterol depletion inhibits the generation of beta-amyloid in hippocampal neurons. *Proc Natl Acad Sci U S A,* 95**,** 6460-4.

SIMONS, M., SCHWÄRZLER, F., LÜTJOHANN, D., VON BERGMANN, K., BEYREUTHER, K., DICHGANS, J., WORMSTALL, H., HARTMANN, T. & SCHULZ, J. B. 2002. Treatment with simvastatin in normocholesterolemic patients with Alzheimer's disease: A 26-week randomized, placebo-controlled, double-blind trial. *Ann Neurol,* 52**,** 346-50.

SING, C. F. & DAVIGNON, J. 1985. Role of the apolipoprotein E polymorphism in determining normal plasma lipid and lipoprotein variation. *Am J Hum Genet,* 37**,** 268-85.

SITTIWET, C., SIMONEN, P., NISSINEN, M. J., GYLLING, H. & STRANDBERG, T. E. 2018. Serum noncholesterol sterols in Alzheimer's disease: the Helsinki Businessmen Study. *Transl Res*.

SKIPSKI, V. P., BARCLAY, M., BARCLAY, R. K., FETZER, V. A., GOOD, J. J. & ARCHIBALD, F. M. 1967. Lipid composition of human serum lipoproteins. *Biochem J,* 104**,** 340-52.

SLATTER, D. A., ALDROVANDI, M., O'CONNOR, A., ALLEN, S. M., BRASHER, C. J., MURPHY, R. C., MECKLEMANN, S., RAVI, S., DARLEY-USMAR, V. & O'DONNELL, V. B. 2016. Mapping the Human Platelet Lipidome Reveals Cytosolic Phospholipase A2 as a Regulator of Mitochondrial Bioenergetics during Activation. *Cell Metab,* 23**,** 930-44.

SMALL, G. W., MAZZIOTTA, J. C., COLLINS, M. T., BAXTER, L. R., PHELPS, M. E., MANDELKERN, M. A., KAPLAN, A., LA RUE, A., ADAMSON, C. F. & CHANG, L. 1995. Apolipoprotein E type 4 allele and cerebral glucose metabolism in relatives at risk for familial Alzheimer disease. *JAMA,* 273**,** 942-7.

SMITH, C. A., WANT, E. J., O'MAILLE, G., ABAGYAN, R. & SIUZDAK, G. 2006. XCMS: processing mass spectrometry data for metabolite profiling using nonlinear peak alignment, matching, and identification. *Anal Chem,* 78**,** 779-87.

SMITH, C. C., BOWEN, D. M., FRANCIS, P. T., SNOWDEN, J. S. & NEARY, D. 1985. Putative amino acid transmitters in lumbar cerebrospinal fluid of patients with histologically verified Alzheimer's dementia. *J Neurol Neurosurg Psychiatry,* 48**,** 469-71.

SMITH, J. A., DAS, A., RAY, S. K. & BANIK, N. L. 2012. Role of pro-inflammatory cytokines released from microglia in neurodegenerative diseases. *Brain Res Bull,* 87**,** 10-20.

SNIEDER, H., VAN DOORNEN, L. J. & BOOMSMA, D. I. 1997. The age dependency of gene expression for plasma lipids, lipoproteins, and apolipoproteins. *Am J Hum Genet,* 60**,** 638-50.

SOUÊTRE, E., THWAITES, R. M. & YEARDLEY, H. L. 1999. Economic impact of Alzheimer's disease in the United Kingdom. Cost of care and disease severity for non-institutionalised patients with Alzheimer's disease. *Br J Psychiatry,* 174**,** 51-5.

SPARKS, D. L., SABBAGH, M. N., CONNOR, D. J., LOPEZ, J., LAUNER, L. J., BROWNE, P., WASSER, D., JOHNSON-TRAVER, S., LOCHHEAD, J. & ZIOLWOLSKI, C. 2005. Atorvastatin for the treatment of mild to moderate Alzheimer disease: preliminary results. *Arch Neurol,* 62**,** 753-7.

STANCU, C. & SIMA, A. 2001. Statins: mechanism of action and effects. *J Cell Mol Med,* 5**,** 378-87.

STERNICZUK, R., DYCK, R. H., LAFERLA, F. M. & ANTLE, M. C. 2010. Characterization of the 3xTg-AD mouse model of Alzheimer's disease: part 1. Circadian changes. *Brain Res,* 1348**,** 139-48.

STEWART, C. R., STUART, L. M., WILKINSON, K., VAN GILS, J. M., DENG, J., HALLE, A., RAYNER, K. J., BOYER, L., ZHONG, R., FRAZIER, W. A., LACY-HULBERT, A., EL KHOURY, J., GOLENBOCK, D. T. & MOORE, K. J. 2010. CD36 ligands promote sterile inflammation through assembly of a Toll-like receptor 4 and 6 heterodimer. *Nat Immunol,* 11**,** 155-61.

STURCHLER-PIERRAT, C., ABRAMOWSKI, D., DUKE, M., WIEDERHOLD, K. H., MISTL, C., ROTHACHER, S., LEDERMANN, B., BÜRKI, K., FREY, P., PAGANETTI, P. A., WARIDEL, C., CALHOUN, M. E., JUCKER, M., PROBST, A., STAUFENBIEL, M. & SOMMER, B. 1997. Two amyloid precursor protein transgenic mouse models with Alzheimer disease-like pathology. *Proc Natl Acad Sci U S A,* 94**,** 13287-92.

SUCCOL, F. & PRATICO, D. 2007. A role for 12/15 lipoxygenase in the amyloid beta precursor protein metabolism. *J Neurochem,* 103**,** 380-7.

SUCCOL, F. & PRATICÒ, D. 2007. A role for 12/15 lipoxygenase in the amyloid beta precursor protein metabolism. *J Neurochem,* 103**,** 380-7.

SUD, M., FAHY, E., COTTER, D., BROWN, A., DENNIS, E. A., GLASS, C. K., MERRILL, A. H., MURPHY, R. C., RAETZ, C. R., RUSSELL, D. W. & SUBRAMANIAM, S. 2007. LMSD: LIPID MAPS structure database. *Nucleic Acids Res,* 35**,** D527-32.

SUDDUTH, T. L., SCHMITT, F. A., NELSON, P. T. & WILCOCK, D. M. 2013. Neuroinflammatory phenotype in early Alzheimer's disease. *Neurobiol Aging,* 34**,** 1051-9.

SUI, H. J., ZHANG, L. L., LIU, Z. & JIN, Y. 2015. Atorvastatin prevents Aβ oligomer-induced neurotoxicity in cultured rat hippocampal neurons by inhibiting Tau cleavage. *Acta Pharmacol Sin,* 36**,** 553-64.

SULLIVAN, P. M., MEZDOUR, H., QUARFORDT, S. H. & MAEDA, N. 1998. Type III hyperlipoproteinemia and spontaneous atherosclerosis in mice resulting from gene replacement of mouse Apoe with human Apoe*2. *J Clin Invest,* 102**,** 130-5.

SUMMERS, W. K., MAJOVSKI, L. V., MARSH, G. M., TACHIKI, K. & KLING, A. 1986. Oral tetrahydroaminoacridine in long-term treatment of senile dementia, Alzheimer type. *N Engl J Med,* 315**,** 1241-5.

SURMA, M. A., HERZOG, R., VASILJ, A., KLOSE, C., CHRISTINAT, N., MORIN-RIVRON, D., SIMONS, K., MASOODI, M. & SAMPAIO, J. L. 2015. An automated shotgun lipidomics platform for high throughput, comprehensive, and quantitative analysis of blood plasma intact lipids. *Eur J Lipid Sci Technol,* 117**,** 1540-1549.

SURRIDGE, C. D. & BURNS, R. G. 1994. The difference in the binding of phosphatidylinositol distinguishes MAP2 from MAP2C and Tau. *Biochemistry,* 33**,** 8051-7.

SUVITAIVAL, T., BONDIA-PONS, I., YETUKURI, L., PÖHÖ, P., NOLAN, J. J., HYÖTYLÄINEN, T., KUUSISTO, J. & OREŠIČ, M. 2018. Lipidome as a predictive tool in progression to type 2 diabetes in Finnish men. *Metabolism,* 78**,** 1-12.

SWEENEY, M. D., SAGARE, A. P. & ZLOKOVIC, B. V. 2018. Blood-brain barrier breakdown in Alzheimer disease and other neurodegenerative disorders. *Nat Rev Neurol,* 14**,** 133-150.

TAKI, T. 2012. An approach to glycobiology from glycolipidomics: ganglioside molecular scanning in the brains of patients with Alzheimer's disease by TLC-blot/matrix assisted laser desorption/ionization-time of flight MS. *Biol Pharm Bull,* 35**,** 1642-7.

TAKÁTS, Z., WISEMAN, J. M., GOLOGAN, B. & COOKS, R. G. 2004. Mass spectrometry sampling under ambient conditions with desorption electrospray ionization. *Science,* 306**,** 471-3.

TAMAOKA, A., SAWAMURA, N., FUKUSHIMA, T., SHOJI, S., MATSUBARA, E., SHOJI, M., HIRAI, S., FURIYA, Y., ENDOH, R. & MORI, H. 1997. Amyloid beta protein 42(43) in cerebrospinal fluid of patients with Alzheimer's disease. *J Neurol Sci,* 148**,** 41-5.

TANG, L. & KEBARLE, P. 1993. Dependence of ion intensity in electrospray mass spectrometry on the concentration of the analytes in the electrosprayed solution. *Analytical Chemistry,* 64**,** 3654–3668.

TANG, Y. & LE, W. 2016. Differential Roles of M1 and M2 Microglia in Neurodegenerative Diseases. *Mol Neurobiol,* 53**,** 1181-94.

TARIOT, P. N., FARLOW, M. R., GROSSBERG, G. T., GRAHAM, S. M., MCDONALD, S., GERGEL, I. & GROUP, M. S. 2004. Memantine treatment in patients with moderate to severe Alzheimer disease already receiving donepezil: a randomized controlled trial. *JAMA,* 291**,** 317-24.

TARIOT, P. N., SOLOMON, P. R., MORRIS, J. C., KERSHAW, P., LILIENFELD, S. & DING, C. 2000. A 5-month, randomized, placebo-controlled trial of galantamine in AD. The Galantamine USA-10 Study Group. *Neurology,* 54**,** 2269-76.

TAYLOR, P. J. 2005. Matrix effects: the Achilles heel of quantitative high-performance liquid chromatography-electrospray-tandem mass spectrometry. *Clin Biochem,* 38**,** 328-34.

TIRABOSCHI, P., HANSEN, L. A., MASLIAH, E., ALFORD, M., THAL, L. J. & COREY-BLOOM, J. 2004. Impact of APOE genotype on neuropathologic and neurochemical markers of Alzheimer disease. *Neurology,* 62**,** 1977-83.

TOMITA, T., MARUYAMA, K., SAIDO, T. C., KUME, H., SHINOZAKI, K., TOKUHIRO, S., CAPELL, A., WALTER, J., GRÜNBERG, J., HAASS, C., IWATSUBO, T. & OBATA, K. 1997. The presenilin 2 mutation (N141I) linked to familial Alzheimer disease (Volga German families) increases the secretion of amyloid beta protein ending at the 42nd (or 43rd) residue. *Proc Natl Acad Sci U S A,* 94**,** 2025-30.

TRACEY, T. J., STEYN, F. J., WOLVETANG, E. J. & NGO, S. T. 2018. Neuronal Lipid Metabolism: Multiple Pathways Driving Functional Outcomes in Health and Disease. *Front Mol Neurosci,* 11**,** 10.

TROJANOWSKI, J. Q., SCHUCK, T., SCHMIDT, M. L. & LEE, V. M. 1989. Distribution of tau proteins in the normal human central and peripheral nervous system. *J Histochem Cytochem,* 37**,** 209-15.

UPENDER, M. B. & NAEGELE, J. R. 1999. Activation of microglia during developmentally regulated cell death in the cerebral cortex. *Dev Neurosci,* 21**,** 491-505.

VAN LEYEN, K., ARAI, K., JIN, G., KENYON, V., GERSTNER, B., ROSENBERG, P. A., HOLMAN, T. R. & LO, E. H. 2008. Novel lipoxygenase inhibitors as neuroprotective reagents. *J Neurosci Res,* 86**,** 904-9.

VAN LEYEN, K., KIM, H. Y., LEE, S. R., JIN, G., ARAI, K. & LO, E. H. 2006. Baicalein and 12/15-lipoxygenase in the ischemic brain. *Stroke,* 37**,** 3014-8.

VAN ROSSUM, G. & DRAKE JR, F. L. 1995. *Python tutorial,* The Netherlands, Centrum voor Wiskunde en Informatica Amsterdam.

VANCE, J. E. 1990. Lipoproteins secreted by cultured rat hepatocytes contain the antioxidant 1-alk-1-enyl-2-acylglycerophosphoethanolamine. *Biochim Biophys Acta,* 1045**,** 128-34.

VEINBERGS, I., JUNG, M. W., YOUNG, S. J., VAN UDEN, E., GROVES, P. M. & MASLIAH, E. 1998. Altered long-term potentiation in the hippocampus of apolipoprotein E-deficient mice. *Neurosci Lett,* 249**,** 71-4.

WALTER, S., LETIEMBRE, M., LIU, Y., HEINE, H., PENKE, B., HAO, W., BODE, B., MANIETTA, N., WALTER, J., SCHULZ-SCHUFFER, W. & FASSBENDER, K. 2007. Role of the toll-like receptor 4 in neuroinflammation in Alzheimer's disease. *Cell Physiol Biochem,* 20**,** 947-56.

WANG, C., KONG, H., GUAN, Y., YANG, J., GU, J., YANG, S. & XU, G. 2005. Plasma phospholipid metabolic profiling and biomarkers of type 2 diabetes mellitus based on high-performance liquid chromatography/electrospray mass spectrometry and multivariate statistical analysis. *Anal Chem,* 77**,** 4108-16.

WANG, H., LI, J., FOLLETT, P. L., ZHANG, Y., COTANCHE, D. A., JENSEN, F. E., VOLPE, J. J. & ROSENBERG, P. A. 2004. 12-Lipoxygenase plays a key role in cell death caused by glutathione depletion and arachidonic acid in rat oligodendrocytes. *Eur J Neurosci,* 20**,** 2049-58.

WANG, N., LAN, D., GERBOD-GIANNONE, M., LINSEL-NITSCHKE, P., JEHLE, A. W., CHEN, W., MARTINEZ, L. O. & TALL, A. R. 2003. ATP-binding cassette transporter A7 (ABCA7) binds apolipoprotein A-I and mediates cellular phospholipid but not cholesterol efflux. *J Biol Chem,* 278**,** 42906-12.

WANG, X., ZHU, M., HJORTH, E., CORTÉS-TORO, V., EYJOLFSDOTTIR, H., GRAFF, C., NENNESMO, I., PALMBLAD, J., ERIKSDOTTER, M., SAMBAMURTI, K., FITZGERALD, J. M., SERHAN, C. N., GRANHOLM, A. C. & SCHULTZBERG, M. 2015. Resolution of inflammation is altered in Alzheimer's disease. *Alzheimers Dement,* 11**,** 40-50.e1-2.

WATERSTON, R. H., LINDBLAD-TOH, K., BIRNEY, E., ROGERS, J., ABRIL, J. F., AGARWAL, P., AGARWALA, R., AINSCOUGH, R., ALEXANDERSSON, M., AN, P., ANTONARAKIS, S. E., ATTWOOD, J., BAERTSCH, R., BAILEY, J., BARLOW, K., BECK, S., BERRY, E., BIRREN, B., BLOOM, T., BORK, P., BOTCHERBY, M., BRAY, N., BRENT, M. R., BROWN, D. G., BROWN, S. D., BULT, C., BURTON, J., BUTLER, J., CAMPBELL, R. D., CARNINCI, P., CAWLEY, S., CHIAROMONTE, F., CHINWALLA, A. T., CHURCH, D. M., CLAMP, M., CLEE, C., COLLINS, F. S., COOK, L. L., COPLEY, R. R., COULSON, A., COURONNE, O., CUFF, J., CURWEN, V., CUTTS, T., DALY, M., DAVID, R., DAVIES, J., DELEHAUNTY, K. D., DERI, J., DERMITZAKIS, E. T., DEWEY, C., DICKENS, N. J., DIEKHANS, M., DODGE, S., DUBCHAK, I., DUNN, D. M., EDDY, S. R., ELNITSKI, L., EMES, R. D., ESWARA, P., EYRAS, E., FELSENFELD, A., FEWELL, G. A., FLICEK, P., FOLEY, K., FRANKEL, W. N., FULTON, L. A., FULTON, R. S., FUREY, T. S., GAGE, D., GIBBS, R. A., GLUSMAN, G., GNERRE, S., GOLDMAN, N., GOODSTADT, L., GRAFHAM, D., GRAVES, T. A., GREEN, E. D., GREGORY, S., GUIGÓ, R., GUYER, M., HARDISON, R. C., HAUSSLER, D., HAYASHIZAKI, Y., HILLIER, L. W., HINRICHS, A.,

HLAVINA, W., HOLZER, T., HSU, F., HUA, A., HUBBARD, T., HUNT, A., JACKSON, I., JAFFE, D. B., JOHNSON, L. S., JONES, M., JONES, T. A., JOY, A., KAMAL, M., KARLSSON, E. K., et al. 2002. Initial sequencing and comparative analysis of the mouse genome. *Nature,* 420**,** 520-62.

WEBSTER, S. J., BACHSTETTER, A. D., NELSON, P. T., SCHMITT, F. A. & VAN ELDIK, L. J. 2014. Using mice to model Alzheimer's dementia: an overview of the clinical disease and the preclinical behavioral changes in 10 mouse models. *Front Genet,* 5**,** 88.

WEINTRAUB, M. S., EISENBERG, S. & BRESLOW, J. L. 1987. Dietary fat clearance in normal subjects is regulated by genetic variation in apolipoprotein E. *J Clin Invest,* 80**,** 1571-7.

WEINTRAUB, S., WICKLUND, A. H. & SALMON, D. P. 2012. The neuropsychological profile of Alzheimer disease. *Cold Spring Harb Perspect Med,* 2**,** a006171.

WEISGRABER, K. H., INNERARITY, T. L. & MAHLEY, R. W. 1982. Abnormal lipoprotein receptor-binding activity of the human E apoprotein due to cysteine-arginine interchange at a single site. *J Biol Chem,* 257**,** 2518-21.

WEISGRABER, K. H., RALL, S. C. & MAHLEY, R. W. 1981. Human E apoprotein heterogeneity. Cysteine-arginine interchanges in the amino acid sequence of the apo-E isoforms. *J Biol Chem,* 256**,** 9077-83.

WHITEHOUSE, C. M., DREYER, R. N., YAMASHITA, M. & FENN, J. B. 1985. Electrospray interface for liquid chromatographs and mass spectrometers. *Anal Chem,* 57**,** 675-9.

WHITEHOUSE, P. J., PRICE, D. L., CLARK, A. W., COYLE, J. T. & DELONG, M. R. 1981. Alzheimer disease: evidence for selective loss of cholinergic neurons in the nucleus basalis. *Ann Neurol,* 10**,** 122-6.

WHITMER, R. A., SIDNEY, S., SELBY, J., JOHNSTON, S. C. & YAFFE, K. 2005. Midlife cardiovascular risk factors and risk of dementia in late life. *Neurology,* 64**,** 277-81.

WILCOCK, G. K., GAUTHIER, S., FRISONI, G. B., JIA, J., HARDLUND, J. H., MOEBIUS, H. J., BENTHAM, P., KOOK, K. A., SCHELTER, B. O., WISCHIK, D. J., DAVIS, C. S., STAFF, R. T., VUKSANOVIC, V., AHEARN, T., BRACOUD, L., SHAMSI, K., MAREK, K., SEIBYL, J., RIEDEL, G., STOREY, J. M. D., HARRINGTON, C. R. & WISCHIK, C. M. 2018. Potential of Low Dose Leuco-Methylthioninium Bis(Hydromethanesulphonate) (LMTM) Monotherapy for Treatment of Mild Alzheimer's Disease: Cohort Analysis as Modified Primary Outcome in a Phase III Clinical Trial. *J Alzheimers Dis,* 61**,** 435-457.

WILCOCK, G. K., LILIENFELD, S. & GAENS, E. 2000. Efficacy and safety of galantamine in patients with mild to moderate Alzheimer's disease: multicentre randomised controlled trial. Galantamine International-1 Study Group. *BMJ,* 321**,** 1445-9.

WILCOX, H. G., DAVIS, D. C. & HEIMBERG, M. 1971. The isolation of lipoproteins from human plasma by ultracentrifugation in zonal rotors. *J Lipid Res,* 12**,** 160-72.

WOLFE, M. S., XIA, W., OSTASZEWSKI, B. L., DIEHL, T. S., KIMBERLY, W. T. & SELKOE, D. J. 1999. Two transmembrane aspartates in presenilin-1 required for presenilin endoproteolysis and gamma-secretase activity. *Nature,* 398**,** 513-7.

WOLFF, M. M. & STEPHENS, W. E. 1953. A Pulsed Mass Spectrometer with Time Dispersion. *Review of Scientific Instruments,* 24**,** 616-617.

WOLOZIN, B., KELLMAN, W., RUOSSEAU, P., CELESIA, G. G. & SIEGEL, G. 2000. Decreased prevalence of Alzheimer disease associated with 3-hydroxy-3-methyglutaryl coenzyme A reductase inhibitors. *Arch Neurol,* 57**,** 1439-43.

WONG, C. W., QUARANTA, V. & GLENNER, G. G. 1985. Neuritic plaques and cerebrovascular amyloid in Alzheimer disease are antigenically related. *Proc Natl Acad Sci U S A,* 82**,** 8729-32.

WOOD, P. L., BARNETTE, B. L., KAYE, J. A., QUINN, J. F. & WOLTJER, R. L. 2015a. Non-targeted lipidomics of CSF and frontal cortex grey and white matter in control, mild cognitive impairment, and Alzheimer's disease subjects. *Acta Neuropsychiatr,* 27**,** 270-8.

WOOD, P. L., CEBAK, J. E. & WOLTJER, R. L. 2018. Diacylglycerols as biomarkers of sustained immune activation in Proteinopathies associated with dementia. *Clin Chim Acta,* 476**,** 107-110.

WOOD, P. L., LOCKE, V. A., HERLING, P., PASSARO, A., VIGNA, G. B., VOLPATO, S., VALACCHI, G., CERVELLATI, C. & ZULIANI, G. 2016. Targeted lipidomics distinguishes patient subgroups in mild cognitive impairment (MCI) and late onset Alzheimer's disease (LOAD). *BBA Clin,* 5**,** 25-8.

WOOD, P. L., MEDICHERLA, S., SHEIKH, N., TERRY, B., PHILLIPPS, A., KAYE, J. A., QUINN, J. F. & WOLTJER, R. L. 2015b. Targeted Lipidomics of Fontal Cortex and Plasma Diacylglycerols (DAG) in Mild Cognitive Impairment and Alzheimer's Disease: Validation of DAG Accumulation Early in the Pathophysiology of Alzheimer's Disease. *J Alzheimers Dis,* 48**,** 537-46.

WOOD, P. L. & WOLTJER, R. L. 2018. CSF Lipidomics Analysis: High-Resolution Mass Spectrometry Analytical Platform. *Methods Mol Biol,* 1750**,** 69-74.

WORLEY, B. & POWERS, R. 2013. Multivariate Analysis in Metabolomics. *Curr Metabolomics,* 1**,** 92-107.

WUBBOLTS, R., LECKIE, R. S., VEENHUIZEN, P. T., SCHWARZMANN, G., MÖBIUS, W., HOERNSCHEMEYER, J., SLOT, J. W., GEUZE, H. J. & STOORVOGEL, W. 2003. Proteomic and biochemical analyses of human B cell-derived exosomes. Potential implications for their function and multivesicular body formation. *J Biol Chem,* 278**,** 10963-72.

YANG, H., ZHUO, J. M., CHU, J., CHINNICI, C. & PRATICÒ, D. 2010. Amelioration of the Alzheimer's disease phenotype by absence of 12/15-lipoxygenase. *Biol Psychiatry,* 68**,** 922-9.

YANG, K. & HAN, X. 2016. Lipidomics: Techniques, Applications, and Outcomes Related to Biomedical Sciences. *Trends Biochem Sci,* 41**,** 954-969.

YAO, Y., CLARK, C. M., TROJANOWSKI, J. Q., LEE, V. M. & PRATICÒ, D. 2005. Elevation of 12/15 lipoxygenase products in AD and mild cognitive impairment. *Ann Neurol,* 58**,** 623-6.

YATOMI, Y., OZAKI, Y., OHMORI, T. & IGARASHI, Y. 2001. Sphingosine 1-phosphate: synthesis and release. *Prostaglandins Other Lipid Mediat,* 64**,** 107-22.

YU, Z., CHEN, H., AI, J., ZHU, Y., LI, Y., BORGIA, J. A., YANG, J. S., ZHANG, J., JIANG, B., GU, W. & DENG, Y. 2017. Global lipidomics identified plasma lipids as novel biomarkers for early detection of lung cancer. *Oncotarget,* 8**,** 107899-107906.

ZAMRINI, E., MCGWIN, G. & ROSEMAN, J. M. 2004. Association between statin use and Alzheimer's disease. *Neuroepidemiology,* 23**,** 94-8.

ZHANG, J. & LIU, Q. 2015. Cholesterol metabolism and homeostasis in the brain. *Protein Cell,* 6**,** 254-64.

ZHANG, S. H., REDDICK, R. L., PIEDRAHITA, J. A. & MAEDA, N. 1992. Spontaneous hypercholesterolemia and arterial lesions in mice lacking apolipoprotein E. *Science,* 258**,** 468-71.

ZHONG, F., XU, M., BRUNO, R. S., BALLARD, K. D. & ZHU, J. 2017. Targeted High Performance Liquid Chromatography Tandem Mass Spectrometry-based Metabolomics differentiates metabolic syndrome from obesity. *Exp Biol Med (Maywood),* 242**,** 773-780.

ZHOU, D., LIU, H., LI, C., WANG, F., SHI, Y., LIU, L., ZHAO, X., LIU, A., ZHANG, J., WANG, C. & CHEN, Z. 2016. Atorvastatin ameliorates cognitive impairment, Aβ1-42 production and Tau hyperphosphorylation in APP/PS1 transgenic mice. *Metab Brain Dis,* 31**,** 693-703.

ZHU, X. C., TAN, L., WANG, H. F., JIANG, T., CAO, L., WANG, C., WANG, J., TAN, C. C., MENG, X. F. & YU, J. T. 2015. Rate of early onset Alzheimer's disease: a systematic review and meta-analysis. *Ann Transl Med,* 3**,** 38.

ZIVKOVIC, A. M., WIEST, M. M., NGUYEN, U. T., DAVIS, R., WATKINS, S. M. & GERMAN, J. B. 2009. Effects of sample handling and storage on quantitative lipid analysis in human serum. *Metabolomics,* 5**,** 507-516.

ZLOKOVIC, B. V. 2008. The blood-brain barrier in health and chronic neurodegenerative disorders. *Neuron,* 57**,** 178-201.

ZULIANI, G., DONNORSO, M. P., BOSI, C., PASSARO, A., DALLA NORA, E., ZURLO, A., BONETTI, F., MOZZI, A. F. & CORTESE, C. 2011. Plasma 24S-hydroxycholesterol levels in elderly subjects with late onset Alzheimer's disease or vascular dementia: a case-control study. *BMC Neurol,* 11**,** 121.